STATUS OF THESIS

Title of thesis	NUMERICAL INVESTIGATION AND OPTIMIZATION OF THE CRANK-ROCKER ENGINE IGNITION TIMING BASED ON PERFORMANCE AND COMBUSTION CHARACTERISTICS

I MILAD FAKOURDABBAGHI

hereby allow my thesis to be placed at the Information Resource Center (IRC) of Universiti Teknologi PETRONAS (UTP) with the following conditions:

1. The thesis becomes the property of UTP.
2. The IRC of UTP may make copies of the thesis for academic purposes only.
3. This thesis is classified as

☐ Confidential

☐ Non-confidential

If this thesis is confidential, please state the reason:

___

___

___

The contents of the thesis will remain confidential for ________ years.

Remarks on disclosure:

___

___

___

Signature of Author

Permanent Address:

B-18-07, Residensi Vogue One

KL Eco City 59200, Malaysia,

Date: 27/05/2022

Endorsed by:

Assoc Prof Ir Dr Masri Baharom
Mechanical Engineering Department
Universiti Teknologi PETRONAS

Signature of Supervisor

Name of Supervisor:

Assoc. Prof. Ir Dr Masri bin Baharom

Date: 27/05/2022

UNIVERSITI TEKNOLOGI PETRONAS

NUMERICAL INVESTIGATION AND OPTIMIZATION OF THE CRANK-ROCKER ENGINE IGNITION TIMING BASED ON PERFORMANCE AND COMBUSTION CHARACTERISTICS

by

MILAD FAKOURDABBAGHI

The undersigned certify that they have read, and recommend to the Postgraduate Studies Programme for acceptance of this thesis for the fulfilment of the requirements for the degree stated.

Assoc Prof Ir Dr Masri Baharom
Mechanical Engineering Department
Universiti Teknologi PETRONAS

Signature: ______________________

Main Supervisor: Assoc. Prof. Ir Dr Masri bin Baharom

Dr Zainal Ambri Bin Abdul Karim
Associate Professor
Mechanical Engineering Department
Universiti Teknologi PETRONAS
Bandar Seri Iskandar, 31750, Tronoh
Perak, Malaysia.

Signature: ______________________

Co-Supervisor: Assoc. Prof. Dr Zainal Ambri bin Abdul Karim

ASSOC. PROF. DR. MASDI BIN MUHAMMAD
Chair
Mechanical Engineering Department
Universiti Teknologi PETRONAS
32610 Seri Iskandar
Perak Darul Ridzuan, Malaysia

Signature: ______________________

Head of Department: Assoc. Prof. Dr Masdi bin Muhammad

Date: 27/5/2022

NUMERICAL INVESTIGATION AND OPTIMIZATION OF THE
CRANK-ROCKER ENGINE IGNITION TIMING BASED ON PERFORMANCE
AND COMBUSTION CHARACTERISTICS

by

MILAD FAKOURDABBAGHI

A Thesis
Submitted to the Postgraduate Studies Programme
as a Requirement for the Degree of

MASTER OF SCIENCE
MECHANICAL DEPARTMENT
UNIVERSITI TEKNOLOGI PETRONAS
BANDAR SERI ISKANDAR
PERAK

June 2022

DECLARATION OF THESIS

Title of thesis	NUMERICAL INVESTIGATION AND OPTIMIZATION OF THE CRANK-ROCKER ENGINE IGNITION TIMING BASED ON PERFORMANCE AND COMBUSTION CHARACTERISTICS

I MILAD FAKOURDABBAGHI

hereby declare that the thesis is based on my original work except for quotations and citations which have been duly acknowledged. I also declare that it has not been previously or concurrently submitted for any other degree at UTP or other institutions.

Witnessed by

Assoc Prof Ir Dr Masri Baharom
Mechanical Engineering Department
Universiti Teknologi PETRONAS

Signature of Author

Permanent Address:

B-18-07, Residensi Vogue One

KL Eco City 59200, Malaysia,

Date: 27/05/2022

Signature of Supervisor

Name of Supervisor:

Assoc. Prof. Ir Dr Masri bin Baharom

Date: 27/05/2022

DEDICATION

To my beloved parents for their endless love, support, and encouragement.

ACKNOWLEDGEMENTS

First of all, I would like to state my extreme appreciation to my supportive supervisor, Ap. Ir. Dr Masri Bin Baharom for his ultimate guidance and valuable advises throughout this journey.His comments and suggestions helped me to improve the quality of the project and motivated me to work towards the infinity.

Furthermore, I would like to express my deepest gratitude to Dr. Salah Eldin Mohammed Elfakki for his endless support who without his extreme experience and knowledge this project would not be a success. His counseling and recommendations have been always a platform to improve the process of the project and assist me to achieve beyond the scope.

Lastly, thanks should go to my colleagues, all PhD students and also together with all MSc student at the Center for Automotive Research and Electric Mobility (CAREM) in Mechanical Engineering Department, UTP for their help and assistance.

ABSTRACT

Crank-rocker (CR) engine is a newly developed combustion engine based on a combination of the conventional and toroidal engine with a curved-cylinder combustion chamber. The fundamental of the CR engine has been obtained from a four-bar mechanism. The engine is significantly required to be optimized in terms of ignition timing. Meanwhile, the detailed characteristics of the performance with respect to the optimum ignition timing for the CR engine are still undetermined. Thus, this research aimed to investigate the effect of varying the spark timing on the performance characteristics of the CR engine while predicting the ignition timing for the best performance using mathematical modeling. For these purposes, a four-stage methodology was designed to perform the investigations. These include modification of the CR engine combustion model, heat transfer correlations evaluation, and optimization process of CR engine in terms of performance characteristics under various operating parameters and predicting the optimum condition. Then, the results were analyzed and compared with experimental data at each stage. The accuracy of the modified combustion model increased once a sub-model of the specific heat ratio was included. Comparing various heat transfer correlations and their influence on the accuracy of the prediction led to concluding that Annand's model is the best choice for heat transfer modeling. The developed models in the optimization process shed light on the effects of various parameters that led to the modification of the optimization model. The results were compared with the benchmarked engine (Modenas ACE115) and showed a good match in terms of performance. In conclusion, the optimum timing for the CR engine was determined to be at 24° CA BTDC, which resulted in the best performance characteristics with the maximum values for the brake torque, brake power, and brake thermal efficiency of 8.9 Nm, 8 kW, and 32% respectively.

ABSTRAK

Enjin engkol-jumpelang ialah enjin pembakaran dalam yang baru dibangunkan berdasarkan gabungan enjin konvensional dan toroidal dengan kebuk pembakaran silinder melengkung. Asas enjin CR telah diperoleh daripada mekanisme empat bar. Enjin ini amat diperlukan untuk dioptimumkan dari segi pemasaan pencucuhan. Sementara itu, ciri terperinci prestasi berkenaan dengan pemasaan pencucuhan optimum untuk enjin CR masih belum pernah ditentukan. Oleh itu, penyelidikan ini bertujuan untuk mengkaji kesan mempelbagaikan pemasaan percikan ke atas ciri prestasi enjin CR untuk meramalkan pemasaan pencucuhan untuk prestasi terbaik dengan menggunakan pemodelan matematik. Untuk tujuan ini, metodologi empat peringkat telah dikemukakan untuk melaksanakan pengkajian. Ini termasuk pengubahsuaian model pembakaran enjin CR, penilaian korelasi pemindahan haba, dan proses pengoptimuman enjin CR dari segi ciri prestasi di bawah pelbagai parameter operasi dan meramalkan keadaan optimum. Kemudian, keputusan dianalisis dan dibandingkan dengan data eksperimen pada setiap peringkat. Ketepatan model pembakaran yang diubah suai meningkat sebaik sahaja submodel nisbah haba tertentu dimasukkan. Membandingkan pelbagai korelasi pemindahan haba dan pengaruhnya terhadap ketepatan ramalan membawa kepada kesimpulan bahawa model Annand adalah pilihan terbaik untuk pemodelan pemindahan haba. Model yang dibangunkan dengan menggunakan proses pengoptimuman memberi penerangan tentang kesan pelbagai parameter yang membawa kepada pengubahsuaian model pengoptimuman. Hasilnya dibandingkan dengan enjin penanda aras (Modenas ACE115) dan menunjukkan persetujuan yang baik dari segi prestasi. Kesimpulannya, pemasaan optimum untuk enjin CR ditentukan pada 24° CA BTDC, yang menghasilkan ciri prestasi terbaik dengan nilai maksimum untuk daya kilas brek, kuasa brek, dan kecekapan haba brek masing-masing 8.9 Nm, 8 kW, dan 32 %.

TABLE OF CONTENTS

ABSTRACT Vii
ABSTRAK Viii
LIST OF TABLES Xiv
LIST OF FIGURES Xv
ABBREVIATIONS Xvii
NOMENCLATURE Xix
CHAPTER 1 INTRODUCTION 1
1.1 Overview 1
1.2 Research Background 3
1.3 Problem Statement 5
1.4 Research Question and Hypothesis 7
1.5 Research Objectives 8
1.6 Scope of Study 8
CHAPTER 2 LITERATURE REVIEW 10
2.1 Overview 10
2.2 New Technologies and Mechanisms 11
2.2.1 Some New Technologies 11
2.2.2 New Mechanisms 12
2.3 The Fundamental Concept and Operating Principle of CR Engine 14
2.4 Engine Optimization 17
2.4.1 Spark Ignition System Optimization 18
2.4.2 Ignition Timing and Its Influence on SI Engines 20
2.5 Simulation Models for Internal Combustion Engines 21
2.5.1 Numerical Simulation Classification 22
2.5.1.1 Mean Value Model 22
2.5.1.2 Zero-dimensional Model 22

2.5.1.3 Quasi-dimensional Model 23
2.5.1.4 Multi-dimensional Model 23
2.5.1.5 Single-Zone and Multi-Zone Models 24
2.6 Heat-Release Models and Their Fundamentals 26
2.6.1 Rassweiler - Withrow Model 27
2.6.2 Krieger – Borman Model 27
2.6.3 Gatowski et al. Model 28
2.6.4 Comparison of Heat-Release Traces 29
2.7 Specific Heat Ratio Models 30
2.7.1 Linear Model by Gatowskie et al. 32
2.7.2 Segment Linear Model by Chun and Heywood 32
2.7.3 Polynomial Model by Krieger and Borman 33
2.8 Heat Transfer Model and The Correlations 33
2.8.1 Woschni's Correlation 35
2.8.2 Hohenberg's Correlation 36
2.8.3 Sitkei's Correlation 36
2.8.4 Annand's Correlation 37
2.8.5 Notes on Other Heat Transfer Correlations 38
2.9 Literature Review Summary 39
CHAPTER 3 METHODOLOGY 40
3.1 Overview 40
3.2 Stage One: Modified Combustion Model 44
3.2.1 Model Integration 45
3.2.2 Output Parameters 47
3.3 Stage Two: Heat Transfer Comparison and Evaluation 47
3.3.1 Model Integration 48
3.4 Stage Three: Optimization Part I 49
3.4.1 Model Integration 51
3.4.2 Output Parameters 54
3.5 Stage Four: Optimization Part II 56
3.5.1 Model Integration 58

3.5.2 Output Parameters 59
3.6 Summary 60
CHAPTER 4 Results and Discussion 61
4.1 Overview 61
4.2 Stage I and II: Modified Combustion Model and Comparative Evaluation of The Heat Transfer Coefficient Correlations 62
4.2.1 Validation of In-Cylinder Pressure Trends 62
4.2.2 Simulated In-cylinder Temperature 65
4.2.3 Heat Transfer Correlations and Parameter Estimation Analysis . 67
4.2.4 Heat Transfer Correlation Choice Optimization 71
4.3 Stage III: Optimization Part One 73
4.3.1 In-Cylinder Pressure Trends Under Various Engine Speed 73
4.3.2 Optimization Process of the CR Engine 76
4.3.2.1 Experimental and Simulated Torque Trends 76
4.3.3 Case-Scenarios: Influence of Assumed Maximum Combustion Efficiency and Combustion Duration 78
4.3.3.1 Case-Scenario One: Maximum Combustion Efficiency Variation 78
4.3.3.2 Case-Scenario Two: Combustion Duration Variation . 80
4.3.3.3 Case-Scenario Three: Maximum Combustion Efficiency and Combustion Duration Variation 82
4.4 Stage IV: Optimization Part Two 83
4.4.1 The Optimum Ignition Timing 84
4.4.2 The Optimum Engine Speed 86
4.4.3 Benchmarking Analysis 90
4.4.4 Comparison Between The Cases 91
4.5 Summary 94
CHAPTER 5 Conclusions and Future Directions 96
5.1 Overview 96
5.2 Conclusions 99
5.3 Recommendations and Future work 101

REFERENCES 102
APPENDICES 115

LIST OF TABLES

Table 2.1 Main literature review summary of toroidal engine 13

Table 2.2 Summary of previous development on CR mechanisms 15

Table 2.3 Summary of previous works on ignition timing 19

Table 2.4 Summary of some previous works using numerical investigation . . 25

Table 2.5 Heat release model comparison by Klein 30

Table 3.1 Input data for modified CR model 45

Table 3.2 Optimization part I - the case scenarios variations 50

Table 3.3 Optimization part II - the case scenarios variations 57

Table 4.1 Final correlations comparison 72

Table 4.2 The CR engine pressure data under various speed 75

Table 4.3 The CR engine torque data under various spark ignition 77

Table 4.4 Engines specification comparison 90

Table 4.5 Engines performance comparison 90

Table 4.6 MBT variation at different case scenarios 92

Table 4.7 The brake torque variation at different case scenarios 92

Table 4.8 The brake power variation at different case scenarios 93

Table 4.9 The BSFC variation at different case scenarios 93

Table 4.10 The BTE variation at different case scenarios 94

Table E.1 Woschni C_1 and C_2 value 212

Table E.2 Coefficient values 216

LIST OF FIGURES

Figure 1.1	A curve cylinder geometry engine	3
Figure 1.2	CR mechanism with an extended rocker arm	4
Figure 2.1	Crank-rocker engine prototype and basic geometry	14
Figure 2.2	Piston motion profile comparison between CR and slider-crank	17
Figure 2.3	Heat release model comparison by Klein	29
Figure 2.4	First CR engine combustion model pressure data	31
Figure 3.1	Project activities flowchart	43
Figure 3.2	Modified combustion model flowchart	44
Figure 3.3	Heat transfer evaluation of different correlations	48
Figure 3.4	Optimization part I - initial process flowchart	52
Figure 3.5	The model algorithm for optimization part I	53
Figure 3.6	The combustion efficiency vs. fuel equivalence ratio	57
Figure 4.1	(a-b) In-cylinder pressure variation at full load	63
Figure 4.2	(a-e) In-cylinder pressure variation at different engine loads	64
Figure 4.3	(a-d) Temperature vs. crank angle variation at 100% - 25% load	66
Figure 4.4	(a-d) Maximum temperature for different correlations	67
Figure 4.5	(a-d) The heat transfer coefficients comparison	68
Figure 4.6	(a-d) Net heat transfer and heat loss variation for various correlations	70
Figure 4.7	(a-f) Validation of in-cylinder pressure trends from 1800-2800 rpm	74
Figure 4.8	Brake torque comparison under various ignition timing	77
Figure 4.9	Case scenario I - (a) Brake torque (b) power vs spark ignition	79
Figure 4.10	Case scenario II - (a) Brake torque (b) power vs spark ignition	81
Figure 4.11	Case scenario III - (a) Brake torque (b) power vs spark ignition	83
Figure 4.12	3D plot of (a) brake torque (b) brake power variation	84
Figure 4.13	A contour representation of brake torque variation	86

Figure 4.14 (a) Brake torque and power (b) BSFC and BTE at optimum 87
Figure 4.15 3D plot of (a) BSFC (b) BTE variation 87
Figure 4.16 (a-d) Combustion characteristics of the CR engine at optimum . . . 89

Figure A.1 3D plot of (a) brake torque (b) brake power variation (case 2) . . . 115
Figure A.2 3D plot of (a) brake torque (b) brake power variation (case 3) . . . 115
Figure A.3 3D plot of (a) brake torque (b) brake power variation (case 4) . . . 116
Figure A.4 3D plot of (a) brake torque (b) brake power variation (case 5) . . . 116
Figure A.5 3D plot of (a) brake torque (b) brake power variation (case 6) . . . 116
Figure A.6 A contour representation of brake torque variation (case 2) 117
Figure A.7 A contour representation of brake torque variation (case 3) 117
Figure A.8 A contour representation of brake torque variation (case 4) 118
Figure A.9 A contour representation of brake torque variation (case 5) 118
Figure A.10 A contour representation of brake torque variation (case 6) 119
Figure A.11 (a-b) Performance characteristics at optimum (case 2) 119
Figure A.12 (a-b) Performance characteristics at optimum (case 3) 120
Figure A.13 (a-b) Performance characteristics at optimum (case 4) 120
Figure A.14 (a-b) Performance characteristics at optimum (case 5) 121
Figure A.15 (a-b) Performance characteristics at optimum (case 6) 121
Figure A.16 3D plot of (a) BSFC (b) BTE variation (case 2) 122
Figure A.17 3D plot of (a) BSFC (b) BTE variation (case 3) 122
Figure A.18 3D plot of (a) BSFC (b) BTE variation (case 4) 123
Figure A.19 3D plot of (a) BSFC (b) BTE variation (case 5) 123
Figure A.20 3D plot of (a) BSFC (b) BTE variation (case 6) 124
Figure A.21 (a-d) Combustion characteristics of the CR engine (Case 2) 124
Figure A.22 (a-d) Combustion characteristics of the CR engine (Case 3) 125
Figure A.23 (a-d) Combustion characteristics of the CR engine (Case 4) 125
Figure A.24 (a-d) Combustion characteristics of the CR engine (Case 5) 126
Figure A.25 (a-d) Combustion characteristics of the CR engine (Case 6) 126

Figure E.1 Crank-Rocker Engine Mechanism 199
Figure E.2 The torus geometry of the crank-rocker cylinder. 202

ABBREVIATIONS

AFR	Air-Fuel Ratio
ATDC	After Top-Dead-Center
BDC	Bottom-Dead-Center
BMEP	Brake Mean Effective Pressure
BSFC	Brake Specific Fuel Consumption
BTDC	Before Top-Dead-Center
BTE	Brake Thermal Efficiency
CA	Crank Angle
CAREM	Center for Automotive Research and Electric Mobility
CI	Compression-Ignition
CNG	Compressed Natural Gas
CR	Crank-Rocker
DoE	Design of Experiment
EGR	Exhaust Gas Recirculation
EVO	Exhaust Valve Opening
HCCI	Homogeneous Charge Compression Ignition
FMEP	Friction-Mean-Effective-Pressure
IVC	Inlet Valve Closing
ICE	Internal Combustion Engine
LHV	Lower Heating Value
LPG	Liquefied Petroleum Gas
MFB	Mass Fraction Burned
MBT	Maximum Brake Torque
MSVVTL	Multi-Stage Variable Valve Timing and Lift
RPM	Revolution Per Minute
SI	Spark-Ignition
TDC	Top-Dead-Center

UTP	Universiti Teknologi PETRONAS
VTEC	Valve Timing Electronic Control
VVT	Variable Valve Timing
WOT	Wide Open Throttle

NOMENCLATURE

A	Instantaneous Heat Transfer Area
AF	Air-Fuel Ratio
$\mathrm{AF}_{\mathrm{ac}}$	Actual Air-Fuel Ratio
$\mathrm{AF}_{\mathrm{stoich}}$	Stoichiometric Air-Fuel Ratio
B	Engine Bore
CA	Crank Angle
C_8H_{18}	Octane
CO_2	Carbon Dioxide
$comb$	Combustion
$comp$	Compression
Cr	Compression Ratio
Cp	Constant Pressure Specific Heat
Cv	Constant Volume Specific Heat
$fmeh$	Friction-Mean-Effective-Pressure
h_c	Convective Heat Transfer Coefficient
h_g	Instantaneous Heat Transfer Coefficient
h_r	Radiation Heat Transfer Coefficient
k_{gas}	The Thermal Conductivity of the Cylinder Gas
m	cylinder Mass
m_a	Mass of Air
m_b	Burned Mass
m_c	Mass of Combustion
m_f	Mass of Fuel
NO_x	Nitrogen Oxides
Nu	Nusselt Number
L_2	The Crank Radius Length
L_3	The Connecting Rod Length

L_4	The Rocker Length
L_{41}	The Extended Rocker Length
P	Pressure
$\mathrm{P_{atm}}$	Atmospheric Pressure
$\mathrm{P_e}$	Exhaust Gas Pressure
$\mathrm{P_i}$	Inlet Gas Pressure
$\mathrm{P_m}$	Motored Cylinder Pressure
$\mathrm{P_r}$	Reference Pressure
ΔP_c	Pressure Rise Due to Combustion
ΔP_v	Pressure Rise Due to Volumetric Expansion
Q	Chemical Heat Released
$\mathrm{Q_{ch,fuel}}$	Chemical Heat Release from Fuel
$\mathrm{Q_{ht}}$	Heat Transfer Through The Walls
$\mathrm{R, R_{air}}$	Universal Gas Constant
Re	Reynolds Number
rpm	Revolution Per Minute
$\mathrm{S, S_{rocker}}$	Stroke Length
T	Temperature
$\mathrm{T_{atm}}$	Atmospheric Temperature
$\mathrm{T_e}$	Exhaust Gas Temperature
$\mathrm{T_i}$	Inlet Gas Temperature
$\mathrm{T_g}$	Temperature of Gas
$\mathrm{T_r}$	Reference Temperature
$\mathrm{T_w}$	Temperature of Cylinder Wall
U	Internal Energy
$\mathrm{U_p}$	Mean Piston velocity
$\mathrm{U_s}$	Sensible Energy
V	Volume
$\mathrm{V_c}$	Clearance Volume
$\mathrm{V_d}$	Displaced Volume
$\mathrm{V_r}$	Reference Volume

W	Work Energy Transfer
$\mathrm{X_b}$	Mass Fraction Burned
x_{rocker}	Piston Displacement
γ	Specific Heat Ratio (Gamma)
θ	Crank Angle (Theta)
θ_b, θ_d	Combustion Duration
θ_s	Spark Timing)
$\theta_\circ$	Ignition Timing
λ	The Air-Fuel Ratio, Lambda Number
Φ	Swing Angle
ϕ	Fuel Equivalent Ratio
ω	Average Gas Velocity (Omega)

CHAPTER 1

INTRODUCTION

1.1 Overview

The revolution of the internal combustion engine (ICE) began in the years 1867 and 1892 when Nicolaus August Otto and Rudolph Diesel developed a spark-ignition (SI) and compression-ignition (CI) engine, respectively. Henceforth, the process of innovation and development of ICEs have become important in the automotive sector. As our limited knowledge began to expand in this sector, new technologies have been developed and became available. That leads to incremental environment interference and disturbance due to higher demand for new kinds.

Sustaining a clean environment has become an important aspect in industrialized societies. Environmental pollution and the problems associated with them are the major concerns against internal combustion engines [1]. For instance, the performance and emission of ICEs have become essential due to the depletion of oil reserves and global warming. Therefore, developing innovative technologies and finding futuristic solutions become a major priority for researchers and scientists. The main intention, thus, is to increase engine efficiency while reducing the possible emissions.

Nowadays, humankind has gained significant interest in finding sustainable energy sources. From available alternative sources, those produced from renewable and environmentally friendly sources like green energies are preferred. For example, the use of biofuels in combustion engines can be regarded as a potential approach for the reduction in emissions and a prospective substitution for fuels such as gasoline and diesel due to their advantage in reducing the emission level [2, 3].

There are, however, numerous downsides affiliated with biofuels that are caused due to their low energy density. These include decrements in performance rate and efficiency when compared to unblended diesel and gasoline fuels [4–6]. Several adjustments to current conventional engines are necessary for the improvement of the biofuel combustion quality, while maintaining the engine performance without degrading it. Although numerous methods and approaches have been adopted to improve the current conventional engines, including fuel direct-injection, turbocharged direct-injection system, valve timing, engine downsizing, valve lift, etc., these technologies are still considered complex, and exorbitant systems [7–9].

Over the years, the method of enhancing SI engine characteristics has evolved significantly. The primary objectives in the early years were to overcome the instability and low capacity of an engine by conducting modifications on the engine power and improving its operational reliability. However, throughout the years, the principal focus has been remarkably shifted to maximizing and stabilizing the engine performance, while reducing its emission [10, 11].

Among the efforts brought forth by researchers are development of a novel engine with alternative configurations to significantly increase the performance and the power. This might, however, be a solution to remarkably improve the efficiency of these novel engines compared to the conventional engines. An engine with a curved-cylinder geometry (Figure 1.1) is one example of a novel alternative engine design that can improve the air-fuel mixing quality and hence raise the combustion efficiency of fossil fuel or biofuel [12]. Other engine designs such as rotary (Wankel), opposed-piston, duke, radial, and toroidal engines have all been considered and developed as alternatives to traditional reciprocating ICEs in the past [13–15].

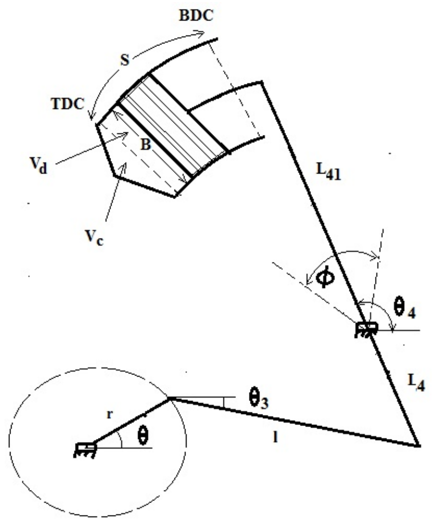

Figure 1.1: A curve cylinder geometry engine [12].

On the contrary, to improve the engine in terms of economic, effectiveness, and practicality, every factor must be addressed and investigated, which involves a comprehensive set of engine testing. As a result, computer models are frequently used to evaluate initial concepts due to their low cost. Hence, engine modeling codes are regarded as important tools for optimizing and analyzing the performance of an engine.

1.2 Research Background

Nowadays, the idea of toroidal engines has become the center of attention for both academia and industrial researchers, even though the concept of a curved piston oscillating in a curved cylinder block has been there for two centuries [12]. The toroidal engines can be widely categorized based on their designs and developments. This categorization can be formed mainly based on the mechanisms that incorporate the piston movements, which might be either oscillating piston or rotating piston mechanisms. Previously, researchers suggested different forms of toroidal engines that used various mechanisms. There are several improved configurations of toroidal engines that have been proposed based on a four-bar mechanism or known as crank-rocker (CR) mechanism (Figure 1.2) [16–18].

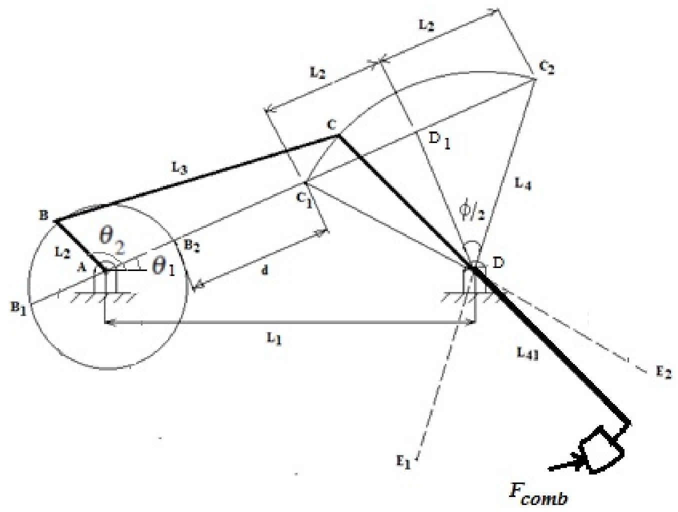

Figure 1.2: CR mechanism with an extended rocker arm [12].

While some engine developers are enticed by toroidal engine advantages and the CR mechanism, a group of researchers at Universiti Teknologi PETRONAS (UTP) presented a novel engine design [18]. They developed an alternative way of producing a crank output motion with oscillating curved-piston through utilizing a crank-rocker mechanism. The engine is known as a single-curved cylinder SI CR engine, and it is integrated from conventional and toroidal engines. It is believed that the difference in engine geometry could improve the thermodynamic cycles and functioning as an alternative engine from the performance perspective. Various analyses have been conducted to study its behavior, while finding alternatives ways to improve its performance.

There are, however, many cooperative elements that could influence the SI engines in the enhancement of their performance. One of the most crucial factors is ignition timing. To be precise on the meaning of ignition timing, it is the time setting process when ignition or spark will occur in the cylinder according to piston position and crankshaft angular velocity. Any key change or upgrades in the engine would involve some modification to the ignition time setting. Thus, engine ignition timing is considered as one of the major parameters for engine optimization due to availability and adaptable flexibility.

Numerous studies have been performed experimentally and theoretically to optimize ignition timing based on performance and emission characteristics. According to Salah E. Mohammed [19], one of the most common techniques that have been used broadly is Design of Experiment (DoE) [20, 21]. The concept of this method is to allow the researchers to find the most optimum timing based on the higher output torque by using a trial-error approach. Furthermore, this experiment could be extended to obtain the optimum timing under various operating conditions to find the Maximum Brake Torque (MBT).

The purpose of the optimization is not only to boost the engine performance; in fact, the optimal ignition timing has drawn much attention in order to shed light on exhaust gas reduction. To achieve such terms, the fuel must be ignited at the most precise moment at which the maximum efficiency and performance could be obtained, while the emission rate would be dropped to the lowest possible point. Moreover, igniting the fuel at the earliest point would slow the piston from rising to the top dead center; meanwhile, late ignition would decrease the piston speed towards the bottom dead center. The untimely spark ignition could lead to excessive engine vibrations and cause severe damages such as sluggish acceleration, hard starting, backfiring, pinging, and knocking. Nevertheless, to find the optimum point of the engine design and operative variables, researchers need to conduct extensive engine testing that could be costly due to the damages caused. For this matter, engine modeling codes are generally more preferred for initial observations and optimization.

1.3 Problem Statement

Based on the previous section, there is a significant need to optimize the engine performance associated with emissions. As one of the main parameters of engine operation, spark timing influences the combustion mechanism of the chamber that has an impact on engine performance and fuel consumption. This element plays an important role in the performance and efficiency optimization, permitting combustion engines to conform to future emission targets and standards. For this reason, it is crucial to define and set the correct ignition timing for better performance.

Meanwhile, the majority of the studies on the influences of ignition timing are conducted based on various engine types. Most of the researchers performed their theoretical and experimental investigations on conventional engines such as gasoline and Diesel engines. Investigations on the toroidal engine, however, can be rarely found either experimentally or theoretically.

Furthermore, several investigations have been conducted to study the behavior and the enhancement of CR engine performance developed by the Center for Automotive Research and Electric Mobility (CAREM) after fabrication. Mohammed et al. [18] conducted a combustion characteristics analysis and performance comparison between the crank-rocker and conventional slider-crank engines experimentally. According to their results, the CR engine has higher indicated torque, power, and thermal efficiency. Modeling the combustion characteristics [22], the effect of engine throttle position fitted with a conventional cylinder head [23], thermodynamic analysis [24], and effects of five different ignition timings on the performance and emissions characteristics [19] are some examples of previous experimental and theoretical observation that have been conducted.

Despite the fact that several studies have been conducted on the CR engine; the detailed and accurate characteristics of performance with respect to the ignition timing and the optimum timing are still unknown. Therefore, a theoretical investigation is needed more than any time to examine the influence of the ignition timing on CR engine performance and defining the optimum operating conditions.

Nevertheless, the currently available combustion model developed by [22] does not include all aspects of the investigation. For instance, the specific heat ratios are highly desired for modeling an ICE, and the accuracy of these models are highly dependent on the complexity of the corresponding computation [25]. In the previous developed model by [22], the specific heat ratio was considered as a constant value. However, by including such sub-model in to the heat release model of the engine will improve the accuracy of the simulation. In addition, the author [22] adopted a single heat transfer correlation while the influence of implementing other correlations has not been discussed.

With regard to the study of five different ignition timings on the performance and emissions characteristics of the developed CR engine by CAREM [19], it is clear that there is lack of experimental data on the ignition timing for performance evaluation. Therefore, majority of the optimization methods that utilize experimental data to predict the hidden performance parameters of a system cannot be used.

Besides optimization approaches that relies on tremendous amount of accessible experimental data, using numerical modeling to predict the behavior of an engine in terms of performance and by utilizing the obtained data for defining an optimum condition can be considered as another approach towards optimization. Thus, it is essential to estimate using numerical investigations for CR engine ignition timing optimization due to eliminating the experimental work related costs. Under such circumstances, the unavailability of the optimization model along with sub-model for prediction, concerning ignition timing for performance evaluation on CR engine is considered as an inspiration for conducting this research.

1.4 Research Question and Hypothesis

The research questions for this study are:

1. What are the effects of varying the ignition timing on the performance characteristics of the CR engine?

2. How to develop a model to investigate the performance characteristics of the CR engine?

3. What type of models and approaches can be used to simulate the performance of the CR engine with respect to timing?

1.5 Research Objectives

Based on the given problem statement and the research questions, the main objective of this research is to investigate the effect of varying the ignition timing on the performance characteristics and to predict the ignition timing for the best performance of the crank-rocker engine using mathematical modeling. To achieve this objective, the following sub-objectives are required:

1. To investigate the effect of various heat transfer correlations and to provide an optimized choice for a more convenient modified combustion model in the case of a crank rocker engine using a mathematical modeling.

2. To investigate the influence of various operating parameters on a single curved-cylinder crank-rocker engine optimization based on performance characteristics by varying the ignition timing.

3. To numerically determine the best timing which yields the optimum operating condition based on performance characteristics under different operating conditions and to compare with a benchmark engine.

1.6 Scope of Study

This research focuses on the CR engine that uses gasoline as a working fluid. In order to investigate the influence of different ignition timing and to predict the optimum condition, necessary calculations and modeling were required. The research objectives and the tasks were unexpectedly increasing; thus, several boundaries and scopes were defined to avoid this.

A mathematical model established by Mohammed et al. [22] has been adopted. This model was developed from a simple ideal gas model to evaluate the combustion characteristics of the CR engine; therefore, several modifications and amendments have been conducted. In addition, the developed model in this research used a zero-dimensional (single-zone) approach for modeling the combustion chamber using heat release modeling. To improve the CR model, the effect of various heat transfer correlations was investigated, and the optimum choice for a more accurate combustion model was selected. In addition, the main aims in this research are developing a model with a high accuracy predictability and optimization of CR engine ignition timing based on performance and combustion characteristics only. Therefore, emission characteristics of CR engine are not considered in this study. Hence, including the crevices effect and considering development of a two-zone model for combustion is not required.

This research used MATLAB (R2019a) environment to develop the CR engine in-cylinder process model. All the experimental data in this study were obtained from CAREM, UTP for comparison and validation purposes. Thus, design or set-up an experimental was not within the scope of study.

With regards to the experimental data used in this study for validation purposes, the source of these data are from three main published work by Mohammed et al. [18, 19, 22]. In a nutshell, the experiments were conducted at six different engine speeds ranging from 1800 to 2800 rpm with ignition timing set at 8.6° CA BTDC at Wide Open Throttle (WOT) and full load condition [18].

Although the CR engine operating condition that is investigated numerically in this study is not limited as above. The engine speed and ignition timing examined are varied from 1000 rpm to 13000 rpm with increment of 100 rpm and 50° CA BTDC to 10° CA ATDC at various engine load. However, there are several limitation such as the turbulence and combustion duration are not modeled. Moreover, due to the different limited experimental data available for each stage of the research validation, the maximum combustion efficiency and combustion duration was not set identical for all the simulations. Hence, the optimization of ignition timing was carried out at six different assumed combustion efficiency considering the air-fuel ratio was varied as rich, stoichiometric, and lean conditions.

CHAPTER 2

LITERATURE REVIEW

2.1 Overview

In this chapter, a detailed description of basic principles and essential concepts of ICEs concerning the optimization and improvement of ICEs are presented. Chapter two consists of nine different sections that each section provides required fundamental knowledge, formulations, and all the works and techniques that had been done. In addition, all these works that had been conducted to improve the performance and efficiency of the ICE in terms of optimization have been reviewed.

In furtherance of maximizing performance while minimizing fuel consumption as well as emission, some researchers started to develop new technologies, mechanisms, and novel configurations for ICEs (section 2.2). Among those developments, the CR engine was developed with its novel configuration (section 2.3). Once the fundamental concept and operating principle of the CR engine were known, the importance of the optimization process begins (section 2.4).

Once the optimization of ignition timing becomes essential, it is a matter of using which approach and methods to achieve the goals. In section 2.5, simulation models for ICE and their classifications are presented along with relevant literature sources and reviews. In terms of the structure of the selected model, different developed heat-release models and their derivation were described in section 2.6. To improve the accuracy of the prediction, careful selection of the specific heat ratio and heat transfer model becomes essential. In sections 2.7 and 2.8, the most commonly used models for specific heat ratios and heat transfer have been presented, respectively.

2.2 New Technologies and Mechanisms

2.2.1 Some New Technologies

As mentioned earlier, there are many research works conducted that may increase the efficiency of the engines in terms of performance and emission. In the furtherance of maximizing performance while minimizing the consumption of fuel along with its emission, several technologies have been developed and evaluated for these purposes. Among these, there are various strategies for fuel combustion, port fuel injection, direct fuel injection, turbocharging with a direct injection system, variable displacement engine, variable valve timing, and lift [24].

In the early 20^{th} century, some new technologies had been launched in production vehicles such as variable valve timing. Ronald [26] proposed the variable valve actuation concept to anticipate the result of current variable valve timing for a cam-less valve actuation that results in an efficiency upgrade. Furthermore, variable compression and displacement engines are two different factors that have been addressed by researchers and automobile manufacturers [27–29].

In addition to the new technologies, Honda employs variable Valve Timing Electronic Control (VTEC) to their engines to improve their volumetric efficiency. This system can switch the timing and lift the intake and exhaust valves simultaneously. This improvement results in reducing fuel usage at a lower engine speed while increasing efficiency at high speed [30].

Another example work is a developed novel Variable Valve Timing (VVT) and life mechanism by Khan and Ayyappath [31]. The developed VVT model implemented Multi-Stage Variable Valve Timing and Lift (MSVVTL) mechanism. The system is used on smaller scaled engines to improve performance parameters such as volumetric efficiency, torque, brake power, and reduction in Brake Specific Fuel Consumption (BSFC) [31].

2.2.2 New Mechanisms

In general, majority of research works are concentrating on the optimization of engine parameters by utilizing different technologies and various approaches on the conventional engines. However, there was a limited number of researchers who looked into alternative configurations and mechanisms besides the conventional slider-crank engine. Even though there are few in numbers, some researchers proposed and developed new engine configurations such as radial, opposed-piston, duke, rotary, and toroidal engines.

The main aim of developing a new engine with an alternative configuration was to convert the reciprocating motion of the piston into the rotational motion of a crankshaft. The attempt to design an engine incorporating oscillating curved pistons led engineers to patent some of their works. For instance, the Wankel engine was proposed to be a substitution for a conventional engine. In conjunction with powerful performance and completely new configuration, a high incidence of sealing loss led to high emission for this engine [18, 32].

Predominantly, the inventors desired to increase the efficiency of the engines by remodeling and redesigning the mechanisms leading to entirely changing engine configurations. There are, however, potential problems associated with the complexity of those mechanisms. Another developed design was presented by Hüttlin [33]. He developed an oscillating curved cylinder engine with an opposed piston. Although it is believed that this design comes with many positive benefits; nevertheless, it is considered a complex design with several defects such as limited speed up to 3000 rpm and a low power density [34].

Several designers and researchers proposed designs and configurations to substitute the conventional engines with curved pistons that rotate or oscillate within a cylinder block. Meanwhile, most of the information on this technology is available informs of pattern documents. There are several excellent reviews conducted on toroidal engines focused on the design techniques, development, and operation, which can be found in the work of Salah Eldin Mohammed Elfakki Hassan [12], Murphy [35] and Hanis [36]. With reference to Salah work, whose Ph.D. was focused on the development, performance, and emission assessment of a single-cylinder air-cooled gasoline CR engine; it can be considered the initial work for the CR engine developed by CAREM [12]. The following Tables 2.1 highlights some main literature review summary of the alternative mechanism for ICE which was presented in his thesis [12].

Table 2.1: Main literature review summary of toroidal engine [12]

<table>
<tr><th>Year</th><th>Author (s)</th><th>Type</th><th>Features</th><th>Limitations</th></tr>
<tr><td>2005</td><td>Hoose [14]</td><td rowspan="3">Toroidal
(Rotating)</td><td rowspan="3">Completely balanced
Fewer components
Less weight
Higher torque output</td><td rowspan="3">Sealing issues
Low thermal efficiency
Low power density
Complex configuration</td></tr>
<tr><td>2007</td><td>Morgado [37]</td></tr>
<tr><td>2008</td><td>Hüttlin [33]</td></tr>
<tr><td>1913</td><td>Beck [38]</td><td>Toroidal
(Oscillating)</td><td>Lower piston friction
Higher torque output</td><td>Extra linkages
Excessive components
High loss
Complicated design</td></tr>
<tr><td>1955</td><td>Granville [35]</td><td>Toroidal
(Oscillating)</td><td>Completely balanced
Performs at high RPM
Low inertial loadings
Produces high power.</td><td>Bulky
Complex in design
Expensive
Commercially unsuitable</td></tr>
</table>

With reference to the Table 2.1, the concept of toroidal engines has gained the attention of researchers [12, 35, 36]. There are various proposed types utilizing different mechanisms; however, in this study, the focus is on the crank-rocker mechanism and the CR engine developed by CAREM, UTP.

2.3 The Fundamental Concept and Operating Principle of CR Engine

As mentioned earlier, the researchers at the CAREM, UTP developed a novel engine known as the CR engine. They have patented a design and conducted various experimental investigations on a single-curved cylinder four-stroke CR engine [18]. This engine produces the crank output motion with oscillating curved-piston utilizing a CR mechanism that the concept is integrated from the toroidal and conventional combustion engine. Inside the engine, the output bar is a crank, which is the shortest bar, whereas the input bar is a rocker. With reference to Figure 2.1, by using the connecting rod that is located between the crank and rocker, the energy can be transmitted through the input and output bar. The engine is utilized to transform the oscillating motion of the curve-piston caused by the combustion force to the crankshaft's rotary motion.

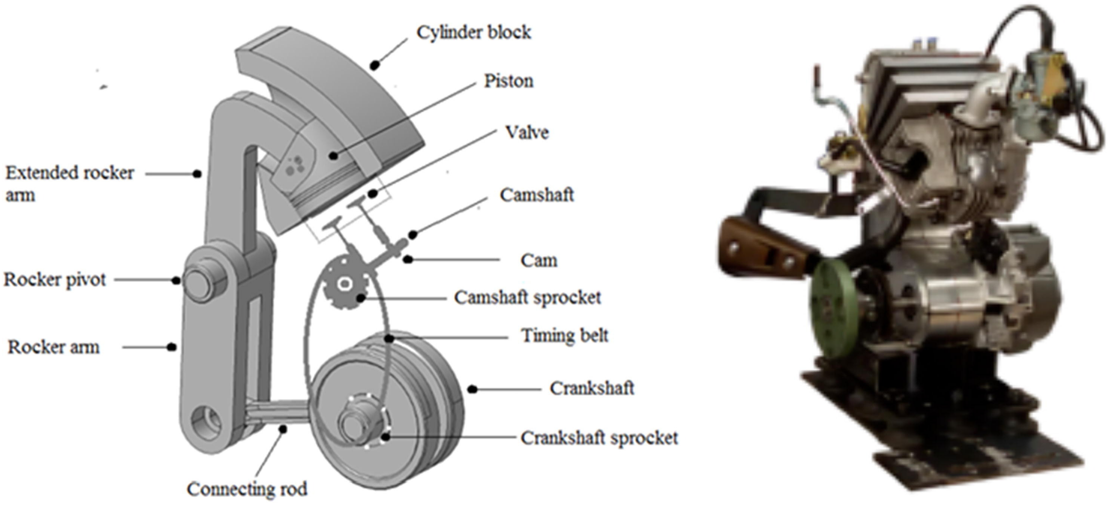

Figure 2.1: CR engine prototype (right), basic CR geometry (left) [18, 22]

Powell, Wolff, and others proposed using the CR mechanism, often known as the 4-bar mechanism, in ICEs between 1925 and 1930 [12, 39, 40]. Taurozzi [17] used the concept of the CR mechanism to develop a pendulum engine (toroidal) in 2002. Meanwhile, Hanis [36] proposed a two-stroke CR gasoline engine which he performed the required preliminary works that include concept validation. In Table 2.2, a summary of previous development on crank-rocker mechanisms and their features and limitations is presented from [12].

Table 2.2: Summary of previous development on CR mechanisms and their features [12]

Author (s)	Type	Features	Limitations
Powell [39] (1925)	Crank-rocker (Sliding)	Improved combustion The stroke length varies (without altering the radius)	High friction loss Low efficiency
Szymkowiak [41] (2012)	Crank-rocker (Sliding)	High efficiency High power density Less fuel consumption	Complex configuration Costly Only for two-stroke engine Need extra compressor
Szwaja [16] (2012)	Crank-rocker (Sliding)	Faster piston movment Reduced thermal losses Reduced frictional losses Improved efficiency	High inertia forces Complex construction
Wolff [40] (1931)	Crank-rocker (Oscillating)	High torque output Less piston friction	Heavy weight Lubrication problem
Taurozzi [17] (2002)	Crank-rocker (Oscillating)	Fully balanced	Complicated concept Low efficiency
Hanis [36] (2013)	Crank-rocker (Oscillating)	Less components High torque output	High friction losses Low efficiency

The CR engines possess numerous fundamental advantages compared to conventional ICEs [41]. In curved cylinder engines, the crank radius can be changed without altering the stroke length, while this is impossible in slider-crank due to the dependency of the stroke on the crank size [36, 41]. In addition, in slider-crank engines, the piston strikes and slaps against the cylinder wall that can cause friction losses. Meanwhile, the friction between the curved cylinder wall and the piston can be reduced in the CR engine. This is due to the rigid connection of the piston and rocker arm by utilizing a bolt. As a result, this prevents the deflection and slapping of the piston against the cylinder wall during the operation. However, the only interaction is within the ring and the cylinder liner [18]. Moreover, the CR engine can dwell longer at the Top-Dead-Center (TDC) comparing to the slider-crank engines. This is mainly due to its kinematics configuration that retracts faster after a certain degree, whereas the maximum pressure force also can be obtained at TDC [18, 36].

The main reason for introducing the concept of toroidal engines with a crank-rocker mechanism is to improve the packaging and increasing engine efficiency. Moreover, this engine has the capability of being adjusted to use or operate under various working fluids such as compressed natural gas (CNG), hydrogen, ethanol. With certain design modifications, it can be operative on renewable energies such as biodiesel that can be used as an alternative fuel for the engine.

One of the great features of the CR engine is that the thermodynamic cycle of the engine can be improved by optimizing the piston motion profile to expand faster from TDC. In Figure 2.2, the piston motion profiles comparison of the developed CR engine by Szymkowiak [41] and the conventional slider engine is given. It can be observed that during the power stroke, the top-left piston for the CR engine travels faster than the conventional slider engine that leads to the reduction in the combustion temperature. The lower temperature in the combustion leads to much lesser heat transfer to the cylinder liner. Therefore, the engine's overall efficiency will improve while NO_x emission is reduced consequently.

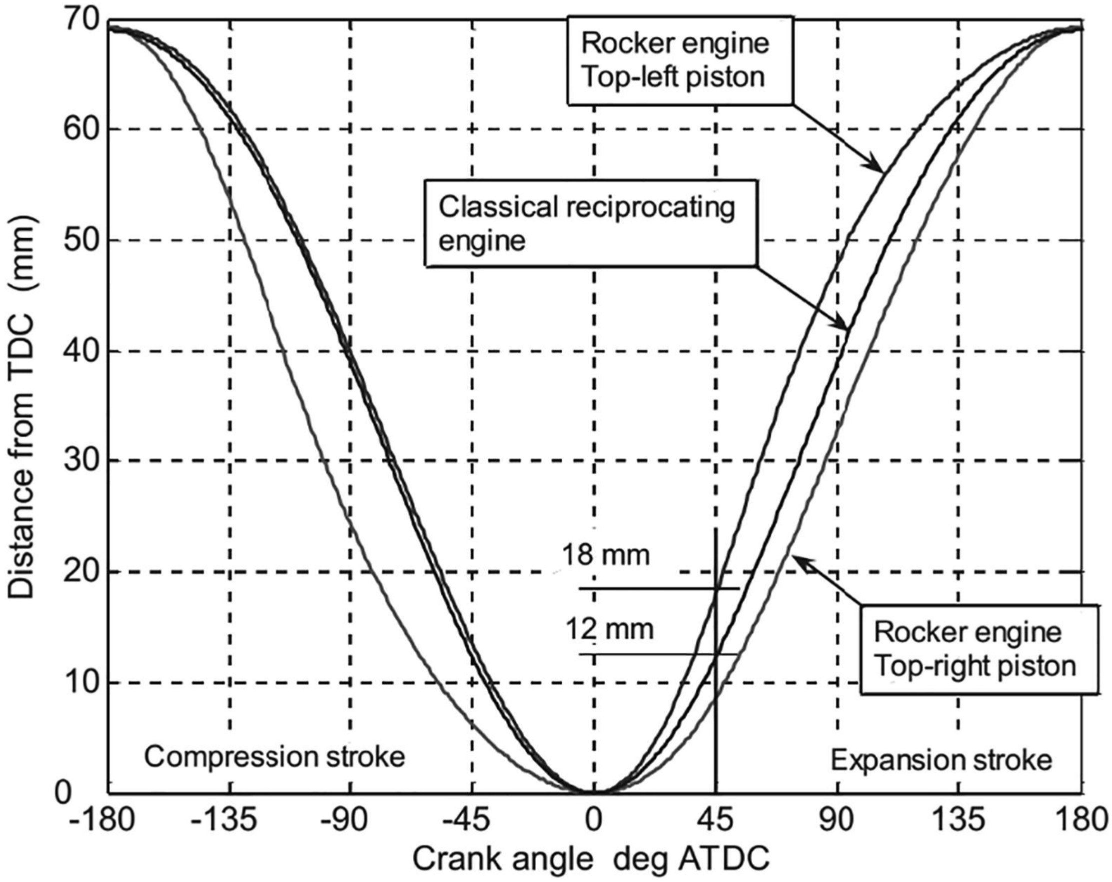

Figure 2.2: Piston motion profile comparison between crank-rocker and slider-crank engines [41]

2.4 Engine Optimization

According to Heywood [42], there are important factors to engine users over the operating range of an engine. These factors are the performance, fuel consumption, noises and air pollutant emissions, reliability and durability, maintenance, and the overall cost of fuels and operation of an engine. Under such given circumstances, obtaining the best results is essential for developers. To achieve this ultimate goal means to minimize the drawbacks while maximizing the desired benefits of their designs. Thus, the optimization process begins with the design, construction, or maintenance of any engineering system.

In general, the definition of the optimization process is to find a set of data for a vector of design variables which leads to an optimum value of the objective or cost function [43]. Various optimization methods have been adopted to improve the performances and emissions characteristics of ICEs such as numerical investigation and modelling, polynomial neural networks, artificial neural networks, response surface methodology, group method of data handling. There are many well optimization approaches that are well documented in [43]. These methods were mainly used to optimize the operating conditions of engines, namely ignition timing, injection timing, intake valve timing, exhaust valve timing, engine speed, load, compression, and air-fuel ratios. The majority of studies were implemented on various types of engines under different operating conditions especially with alternative fuels and different methodology [43–50]. However, majority where conducted experimentally or the adopted approach was dependent on availability of various experimental data or a huge data set. Meanwhile, the current research mainly focuses on the optimization of SI engine ignition timing based on their performance parameters under various operating conditions such as different speeds, loads, lean and rich mixtures using numerical modeling due to unavailability of the experimental data on the developed CR engine by CAREM.

2.4.1 Spark Ignition System Optimization

The ignition system of the SI engine is a critical factor for the optimization of the performance and emission to achieve the highest efficiency. The combustion process, power output, and emissions performance of an engine are highly influenced by this system [51]. The main reason is due to the initial time of the combustion reaction that is precisely controlled by this system. Moreover, this system is an essential feature for flame propagation inside the combustion chamber and the entire combustion operation due to the same precise control [52].

It is important to know that three main elements significantly affect the ignition process of an engine. These elements are the primary energy of the ignition, the location of the ignition, and the timing of the ignition. Many scholars studied the influences of these elements on engine performance. For instance, Xie et al. [53] worked on a SI engine fueled with methanol to control the load by using Exhaust Gas Recirculation (EGR) and igniting timing. They concluded that the optimum engine performance could be obtained by properly adjusting the spark timing. In another study, Daniel et al. [54] conducted a comparative evaluation on ignition timing sensitivities of oxygenated biofuels that have been compared to gasoline in a direct-injection SI engine. In their observations, they summarized that the igniting timing sensitivity of the biofuels was much superior compared to gasoline. In terms of the location, Wang et al. [55] carried out a numerical analysis that studies the effects of the fuel injection timing and ignition position in a direct-injection natural gas engine. Others such as Erkus et al. [56] and Yasin et al. [57] applied a liquefied petroleum gas (LPG) and hydrogen fuel to their investigation, respectively. Similarly, both investigation results showed that it is possible for ignition timing to improve the performance and to obtain a higher exergy efficiency with optimum timing, correspondingly.

Table 2.3: Summary of previous works on ignition timing

Source	Methode	Major Highlights
Xie et al. [53]	Experimental	Concluded that the optimum engine performance could be obtained by properly adjusting the spark timing
Daniel et al. [54]	Experimental	Summarized that the igniting timing sensitivity of the biofuels was much superior compared to gasoline
Wang et al. [55]	Numerical Large-eddy	The ignition location affects engine combustion in engine through two mechanisms. The ignition location determines the space for flame development
Erkus et al. [56]	Experimental	It is possible for ignition timing to improve the performance with optimum timing
Yasin et al. [57]	Experimental	It is possible for ignition timing to obtain a higher exergy efficiency with optimum timing

2.4.2 Ignition Timing and Its Influence on SI Engines

The crucial operating factor that can affect spark-ignition engine performance, efficiency, and emission at any given load and speed is spark timing. As discussed before, it is foremost to define the best ignition timing for an engine for a significant combustion process. The untimely combustion could lead to inefficient engine performance. For a better illustration, if the combustion begins in advance, the work, which moves from the piston to the gases in the cylinder at the end of the compression stroke, would be extremely massive. However, if the combustion begins with a significant delay, the peak cylinder pressure would be decreased along with the power output during the expansion [42].

Furthermore, parameters such as maximum brake power, maximum brake torque, minimum brake specific fuel consumption could be acquired by defining the optimal level of ignition timing. Spark timing also has an impact on peak cylinder pressure which affects the peak unburned and burned gas temperatures. The delay of spark timing minimizes these factors and is occasionally applied for NO_x emission control to avoid knock. Ignition timing also influences the exhaust temperature that increases due to the delay of MBT and resulting in engine efficiency drop [42].

As ignition timing has been interrogated whether it can improve engine performance and reduce CO_2 emission, several efforts have been carried out experimentally and theoretically. These investigations have been conducted to study the effects of ignition timing on engine performance and emissions. Roussos et al. [58] investigated the influence of ignition timing on the performance and emission characteristics of a light-duty engine under three different fuel operating modes. Their results revealed that with optimum ignition timing together with an alternative fuel, the performance and emission characteristics of the engine could be improved. Shojaeefard et.al [59] studied the impact of ignition timing on the exergy of linear four-cylinder SI engine using a three-dimensional numerical simulation. Kale et.al [60] conducted experiments to investigate the relationship between advanced angle and ignition timing by varying the ignition timing to improve engine performance. They claimed that the ignition angle could be a parameter for controlling engine performance relative to engine speed. Zareei and Kakaee [61] researched the influence of ignition timing on the performance of the Peugeot 206 TU3A engine, numerically and experimentally. In their experimental works, various ignition timing (in the range of 10° ATDC to 41° BTDC at 3400 rpm and wide-open throttle) were tested.

In summary, the above works indicate that the ignition system elements are highly indispensable and have an undeniable influence on the engine combustion and performance characteristics. To significantly improve these characteristics of an engine, it is important to define their optimum points for an engine [44]. Thus, this research will mainly focus on optimizing the ignition timing for crank-rocker engine.

2.5 Simulation Models for Internal Combustion Engines

Once the optimization of ignition timing becomes essential to developers and researchers, various approaches have been used to achieve such a goal. For optimization purposes, precise observation and accurate prediction of an ICE performance are required. To obtain such highly detailed outcomes, practical approaches like simulation modeling frequently have been used. These methods are extremely beneficial when it comes to evaluating various operating parameters extensively. These models are often implemented during initial assessments on the ICEs performance to acquire their possible limitations without the necessity of the extreme operating conditions of real engine testing that could be cost-intensive [42, 62].

There are many different frameworks of models that have been used for the prediction of the engine performance parameters under various operating conditions for both CI and SI engines. One of the most commonly used approaches is through utilizing the first law of thermodynamic. This law mostly has been used for combustion modeling and it is considered an essential method and obliging in investigating different parameters of ICEs [42, 62–64]. This allows researchers to numerically model and develop the working process of an engine in various approaches.

Under these circumstances, these methods could be broadly categorized into four main branches [65]:

1. Mean Value Model
2. Zero-dimensional Model
3. Quasi-dimensional Model
4. Multi-dimensional Model

2.5.1 Numerical Simulation Classification

2.5.1.1 Mean Value Model

The mean value cylinder engine modeling mainly focuses on the approach that a comprehensive engine model could be simplified into a mean value engine model. Generally, this not only utilizes a simplified neural network-based cylinder but also a simplified intake and exhaust system. The aim of using the mean value model is not mainly for engine development, but also it is useful and suitable for integrated system research. Therefore, huge amount of engine experimental data is required and the ability of prediction is not a property of the mean value model [66, 67].

2.5.1.2 Zero-dimensional Model

With regards to zero-dimensional, this model is considered as one of the simplest numerical model with only one independent variable. In general, this variable is either time or crank angle in terms of ICEs. Moreover, a heat transfer model is usually implemented for improvement of the accuracy. The main advantages of a zero-dimensional is that they are computationally effective due to the low time consumption of simulation. Thus, a zero-dimensional model can be used for immediate application and considered as a practical tool for the design and development of an engine. For example, when using the experimental engine data to develop an experimental model, the obtained model could be applied to new engines as long as they have a similar and comparable design parameters to give the qualitative trends in a predictive manner [68].

2.5.1.3 Quasi-dimensional Model

Besides the zero-dimensional models, new alternative models with higher accuracy and flexibility (for such complicated events as the formation of nitric oxide and soot in engine cylinder) have been developed due to the urge and importance of investigating the performance of ICEs to control the pollutant emission [69]. These new models are categorized as quasi models [69, 70].

In terms of quasi-dimensional model, this model attempt to estimate the burn rate information by considering a spherical flame front geometry [69]. This model utilizes a separate turbulent sub-model to derive a heat release model, while gathering turbulent combustion information to be used as an input [69].

Both zero-dimensional and quasi-dimensional models can be used for predicting the efficiency, performance and emissions of ICEs [69]. These models are easily integrated into complete engine models. However, there is no direct link with the cylinder geometry. Subsequently, these models are only suitable for parametric investigations related to engine development [69].

2.5.1.4 Multi-dimensional Model

Several researchers aimed to obtain additional details of in-cylinder parameters compared to those obtained through utilizing zero or quasi-dimensional models by developing a more advanced model for engine flows and combustion processes. For this purpose, they utilize a more complex method for their investigation that is known as multi-dimensional modeling. In particular, these models provide comprehensive information regarding fuel-air distribution that allows researchers to calculate the exhaust gas composition more precisely.

Furthermore, a multi-dimensional model not only solves the equations for mass and energy conservation but also momentum and species conservation in different dimensions to predict the flame propagation. This is mainly due to the aim of this model to obtain more accurate results at the expense of resources and computational time [69].

Meanwhile, there are two common approaches to multi-dimensional modelling which known as multi-zone models and computational fluid dynamic (CFD). With regards to time consumption, a multi-zone model has considerably a lower computational time compare to a CFD model. CFD models resolve extremely at a small-scale zones by transforming of domain into a discrete form (small control volumes). Once the discretization of domain is completed, the CFD method will solve all the governing equations in all direction. Thus, it can produces result with a higher accuracy due to more efficient solving of the boundary layer or the turbulent effects.

2.5.1.5 Single-Zone and Multi-Zone Models

There are several approaches to zero, quasi, and multi-dimensional modeling. The most common methods are single-zone or multi-zone models. In terms of single-zone models, they are accounting for the basic features of engine operation whereby the cylinder contents are treated as a uniform mixture or as one homogenous block. These models are highly preferred due to their simplicity and reasonable accuracy that come with the lowest time consumption of computation in engine combustion process modeling [11].

Meanwhile, in multi-zone models, the cylinder contents are broken down into different zones depending on the engine type. In each zone, specific physical and chemical processes are analyzed. The main reason is that each zone acts as an individual thermodynamic system with energy and mass interactions within themselves along with their common surroundings [71].

In multi-zone modeling of SI engines, the zone is started from the heat source that is located from the spark plug and propagated according to the flame front motion. A two-zone combustion model could be considered one of the most commonly multi-zone modeling approaches. This model divides the cylinder section into two separate zones, namely the burned and unburned zones. The burned zone consists of equilibrium products of combustion; meanwhile, the unburned zone comprises a homogeneous mixture of air, fuel, and residual gas [69–71].

Regardless of the incompetence to forecast high accuracy, they are recognized as suitable primary tools for investigations. However, this is highly dependent on how appropriate they are constructed. The advantages of the two-zone model are similar to the single-zone model that come with a lower computational cost; however, the prediction rate is significantly more accurate than the single-zone model due to the cylinder separation.

Nevertheless, various authors conducted comparison investigations between single-zone, multi-zone, and multi-dimensional models [25, 63, 72–75]. While the computational factors consumed by the multi-dimensional model are significantly higher compared to the others, the variation in results is inconsiderable for a preliminary evaluation [76]. Thus, single-zone and two-zone models are still preferred due to their benefits of simplicity and reasonable computational cost [61].

Table 2.4: Summary of some previous works using numerical investigation.

Source	Scope	Method	Models Included
S. Mohammed [24]	Thermodynamic analysis of CR engine	single-zone, two-zone	1st law, apparent heat release, heat transfer (Woschni)
S. Mohammed [22]	Combustion modeling of CR engine	single-zone	1st law , apparent heat release, heat transfer (Woschni)
J. Cuddihy [25]	Predicting SI engine performance and emissions characteristics	single-zone, two-zone	1st law, apparent heat release, heat transfer (Woschni, Annand)
H. Shapiro [70]	Second law analysis of ICE	two-zone	2nd law , combustion modeling
M. Klein [77]	A specific heat ratio model and compression ratio estimation	single-zone, two-zone	1st law, heat release
M. Reyes [78]	Characterization of the combustion process and cycle-to-cycle variations	two-zone	Thermodynamic combustion diagnosis model

2.6 Heat-Release Models and Their Fundamentals

The fundamentals of the ICE performance are the processes that occurred in the cylinder. The goal of combustion analysis of a SI engine is to generate a curve associating mass fraction burned, while for the case of a diesel engine is to obtain cumulative heat release versus time or crank angle. The application of heat release and combustion models are distinct and could be described into two different alternatives [70, 79]:

- To estimate the pressure trends of the cylinder as a function of crank angle by applying an empirical heat release or mass burned profile.
- To obtain the rate of heat release versus the crank angle by inferring from pressure data in a cylinder that is obtained experimentally.

The in-cylinder pressure of an ICE has always been an essential experimental diagnostic in the research and development of automotive when it comes to analysis. The main reason is due to its direct and close relation to the combustion and work production process [80, 81]. This parameter reflects the process of combustion, produced piston work on the gas (caused by variation of the cylinder volume), and transferred heat to the cylinder wall.

In addition, the in-cylinder pressure indicates the rate of mass flow in and out of the crevices regions within the piston, rings, and cylinder liner. Consequently, if highly precise and accurate information regarding the propagation of the combustion process in the cylinder is required, each of these processes should be indicated by in-cylinder pressure; thus, the combustion process could be distinguished.

The substitution of some parameters such as volume variation, heat transfer, and mass loss from the combustion chamber pressure during the closed system of the engine cycle (intake and exhaust valves closed) is known as heat-release analysis. This analysis is done within the framework of the thermodynamic first law that could be implemented by utilizing zero-dimensional, quasi-dimensional, or multi-dimensional modeling. Although the simplest approach is to adopt zero-dimensional, single-zone modeling due to the explained reason in the previous section (refer to section 2.5.1); the heat transfer and crevice effect could be included to increase the accuracy. The heat release model basis and their assumptions can be found in Appendix (E.3). In the next subsections, only three different models developed by Rassweiler and Withrow [82], Krieger and Borman [83], and Gatowski et al. [84] will be discussed while related equations are presented in Appendix (E.3).

2.6.1 Rassweiler - Withrow Model

In this section, one of the first-ever zone-based models developed is presented. Rassweiler-Withrow [82], formulated a single-zone model that corresponded to the measured pressure traces with a polytropic behavior. This method is used to calculate mass-fraction-burned (MFB) that can be seen as a normalized version of the heat release trace with the assumed interval values of (0,1). The developed model is considered to be one of the simplest and computationally efficient models for MFB calculation by normalizing the burned mass using the total charge mass [77, 82]. The corresponding relationship between the quantity of the burned mass fraction and the amount of heat released can be explained by the fact that these two parameters are connected proportionally. The fundamental principle for the Rassweiler and Withrow method is that there could be a polytropic relation within pressure and volume data [77, 82]. Polytropic assumptions and the quantified pressure indications were used to detect the change in combustion and volumetric pressure. To extract the MFB profile, the ratio of accumulated pressure to the total change of combustion pressure and the assumption of the corresponding relationship between the change of combustion pressure and the amount of energy released from fuel burned was applied [77]. The related equations are presented in Appendix (E.3.1).

2.6.2 Krieger – Borman Model

One of the most frequently used heat release models is the model developed by Krieger and Borman between 1966 till 1967 [83]. This model is known as the computation of apparent heat release or net heat release. This approach takes neither crevice nor heat transfer into account.

There are some similarities between the Krieger-Borman and the Rassweiler-Withrow model in terms of net heat release trace and MFB profile. Klein [77], claimed that the accuracy of burn profile predictions on a specific engine could significantly be improved by careful selection of the specific heat ratio.

Despite more reliability in providing an accurate result, careful selection of the ratio of specific heats obtained more precise outcomes compared to the basic polytropic model. However, many researchers preferred to derive a more accurate estimation of this preferred model. Thus, the heat transfer model and crevice effects have been included in a model developed by Gatowski et al. [84] to increase the accuracy of the heat release model. The related equations can be found in Appendix (E.3.2).

2.6.3 Gatowski et al. Model

In terms of heat release models, there is a more complex model that has been developed by Gatowski et al. [84]. This model incorporates various subsidiary models, including heat transfer, crevices effects, and specific heat ratios, into the main heat release equation (E.19). This model has been implemented on three different types of engines, including the SI engine in 1984.

The first subsidiary model is the heat transfer model that has been added. The heat transfer model and the correlation models rely upon Newton's law of cooling. This particular topic has completely been covered in section 2.8. In terms of the Gatowski et al. model, the Woschni correlation has been used (sub-section 2.8.1).

The second sub-model that has been included by Gatowski et al. is the influence of the crevices. In a brief discussion, crevices are the small, narrow volumes on the piston in a cylinder. During the compression stroke, some of the fuel mixtures fall into the crevices. Some of these charges usually would return to the cylinder during the expansion stroke, while a small amount of them would blow due to the top ring during the combustion phase. This phenomenon is known as blow-by, which results end up in the crank-case [42].

According to Gatowski et al. [84], the crevice volumes could constitute about one to two percent of the clearance volume in size. In the model, they made few assumptions, such as all crevices could be modeled based on a single aggregate constant volume, similar temperature as the cylinder wall, and same pressure rate as in-cylinder pressure. Lastly, they modeled the ratio of the specific heat as a linear function of temperature. In other words, the specific heat ratio varies as temperature varies and the internal energy varies with it. In section 2.7, the topic of specific heat ratio has been discussed by introducing the three most common models, including the Gatowski et al. model.

2.6.4 Comparison of Heat-Release Traces

Klein [77] conducted a comparison study of heat release trace based on the previously described models (Figure 2.3). As he expected, the Gatowski model obtained higher heat release trace mainly due to the heat transfer and crevices effects that have been taken into account. Meanwhile, Klein concluded that the other two models are computationally more efficient compared to the Gatowski model.

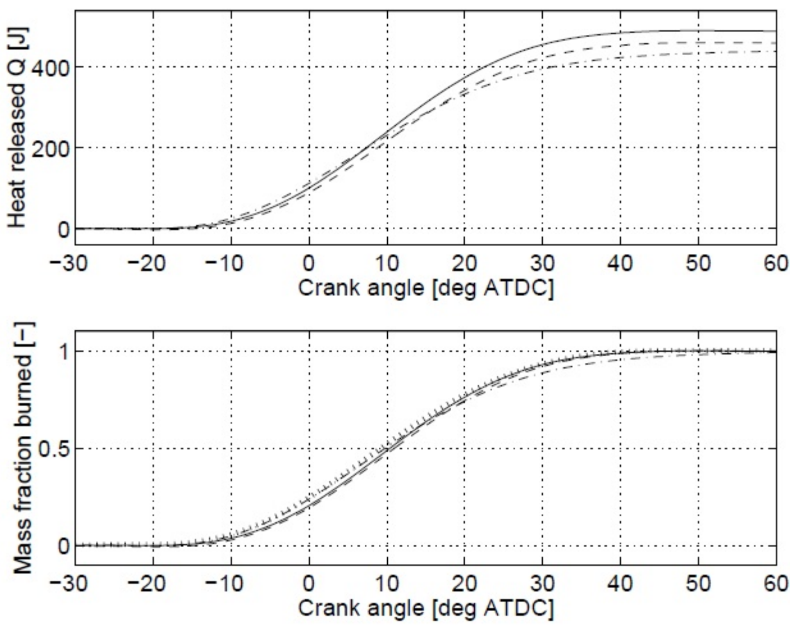

Figure 2.3: Calculated heat release trace (upper) and mass fraction burned trace (lower), Gatowski (solid), Krieger - Borman (dashed), and Rassweiler-Withrow (dash dotted) methods [77]

According to Table 2.5, it showed that the accuracy of burn profile predictions on a specific engine can be improved significantly by careful selection of the specific heat ratio [77].

Table 2.5: Heat release model comparison by Klein [77]

Heat Release Model	θ_{10}	θ_{50}	θ_{85}	θ_b
Rassweiler-Withrow	-4.5	9.8	25.2	29.8
Krieger-Borman	-6.4	11	26.9	33.3
Gatowski et al.	-5.1	10.4	24.4	29.5

2.7 Specific Heat Ratio Models

Several studies have been conducted by researchers to calculate the heat release rate and MFB by proposing different approaches, such as developing a single-zone model or two-zone model for both CI and SI engines [25, 72, 77, 80, 85–87]. It is essential that all engine variables be taken into account when modeling an engine.

According to Lounici et al. [68], the relevancy of the simulations relies on how accurate the heat release and heat transfer models are. In terms of heat release analysis, numerous researchers have investigated the influences of different parameters, mainly specific heat ratio, and choice of heat transfer correlation on combustion characteristics of various engines [68, 87–89].

The accuracy of the combustion modeling and heat release analysis is highly dependent on how precisely the internal energy variation of the cylinder is calculated. Based on the descriptions provided in the previous section, the ratio of the specific heat is extremely influential in improving the prediction of combustion characteristics in heat release models.

As mentioned before, Mohammed et al.[22], have developed the first combustion model for the CR engine, and the results obtained from the model are presented in the Figure 2.4. The graphs illustrate the predicted in-cylinder pressure data based on the initial combustion model and then compared with the obtained experimental data. Even though the simulated results demonstrate a good match with experimental data required for the competency on the scope [22]; during the compression phase, in-cylinder pressure values are much lower than those obtained experimentally. The maximum relative error of these data was calculated slightly above 15 percent [22]. It was concluded that assuming the specific heat ratio as a constant value was one of the main reasons for such inaccuracy [22].

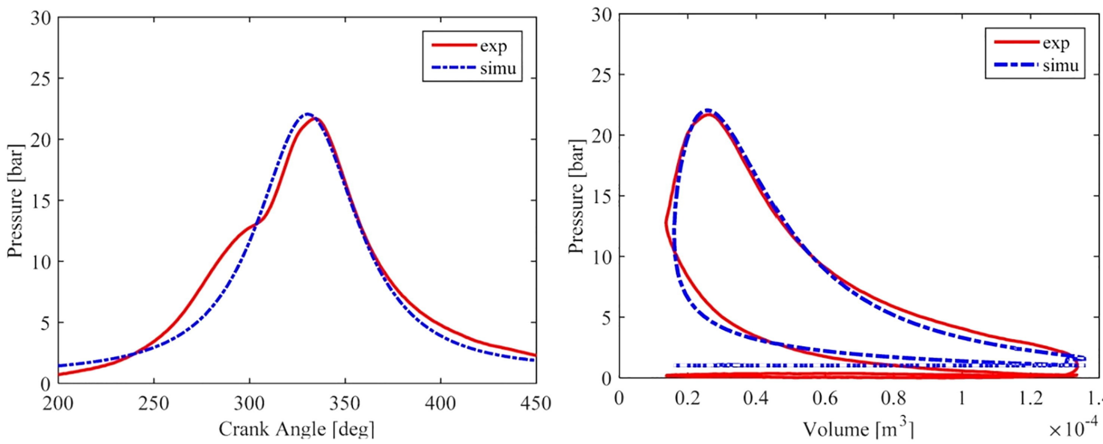

Figure 2.4: First CR engine combustion model data; Pressure vs CA (left), P-V Diagram (right) [22].

Therefore, the aim of this section is to study the previously developed models and provide a sufficient explanation of the existing models for the ratio of the specific heat while selecting the most reasonable model for CR engine combustion modeling.

Among the existing models of γ, there are three main well-known models such as the linear model in T by [84], Segment linear model in T by [80], and the Polynomial model in P and T by [83]. In this sub-section, a brief description is provided for each of the mentioned models. This section of the literature review is taken from Klein [77, 88], who conducted an investigation on specific heat ratio models for single-zone heat release models.

2.7.1 Linear Model by Gatowskie et al.

In Gatowskie et al. [84], the ratio of specific heat is modeled as a linear function of temperature (please refer to Appendix E.6.1). This is an important component that shows the relationship between internal energy and temperature. The value of gamma is most frequently have been modeled as either a constant value or as a linear function of temperature when the system is in a closed cycle. According to Gatowskie et al. [84], this is an approximation that is consistent with other approximations in the heat release models. In terms of temperature region, Klein [77] stated that this limitation could be avoided if a more complex model and a second or even higher order of polynomial is used.

2.7.2 Segment Linear Model by Chun and Heywood

While some researchers claimed that gamma could be a constant value or a linear mean temperature dependent, others like Chun and Heywood [80] believed this commonly made assumption is not accurately sufficient. Under these circumstances, they developed a new model based on the different segments of an engine. They proposed a segmentation approach towards the engine during the closed cycle part, where the intake and exhaust valves are closed. Chun and Heywood [80], divided the system into three different segments, namely, compression, combustion, and post-combustion (expansion stroke), by only considering the close cycle part (please refer to Appendix E.6.2). For these three classifications, the MFB value has been utilized to classify each segment. According to Klein [77], this model comes with a limitation and could cause a systematic problem during the estimation phase. The main cause for this is due to the discontinuities of the model during switching within the phases.

2.7.3 Polynomial Model by Krieger and Borman

The third model that has been developed to increase the accuracy of the heat release model was the Polynomial model. This model was developed by Krieger and Borman [83] in 1967 to compute the specific heat ratio. The polynomial model determines the internal energy variations by utilizing various correction factors that are corresponding to the temperature variations compared to a reference point. The internal energy of the combustion products can be described through this polynomial model, especially for those involving hydrocarbon fuels. All the required numerical descriptions of this particular approach can be found in Appendix (E.6.3).

2.8 Heat Transfer Model and The Correlations

As mentioned in section 2.6, the relevancy and accuracy of the simulation models are highly dependent on the heat release and combustion models in terms of prediction. Some researchers have mainly investigated different parameters, including specific heat ratios to increase the accuracy of the heat release models, while others focused on the choice of heat transfer model and its correlations.

In balancing the combustion chamber energy, heat transfer has been considered a significant and critical factor. Based on some engines, the gas temperature and the heat flux could often be extremely high. The temperature can be increased by about 2800 K and high amount of heat flux in $\frac{MW}{m^2}$ [90]. Moreover, heat transfers play a key role in combustion chamber heat analysis. They constitute between thirty to forty percent of all the energies [90]. For instance, it has been discovered by Franco [91] that nearly one-half of the fuel energy is converted to heat loss in a small-scale 125 cm^3 two-stroke SI engine. Hence, it is highly important to include the heat transfer analysis to increase the accuracy of the modeling.

Although there are numerous studies that have been carried out to investigate the single-zone combustion models for SI and CI engines; only a few numbers of them deliberated on utilizing various correlations and their influences on the accuracy of the model prediction. With regard to modeling and analyses of toroidal engines, they can be rarely found while mostly are limited to patent documents only [18].

Various research works have been published on the evaluation of the processes in heat transfer and the instantaneous heat transfer coefficient. These works mainly suggested utilizing different correlations such as Woschni [92], Hohenberg [93], Sitkei [94], and Annand [95]. these correlations have been used widely in heat transfer calculations. For example, Mohammed et al. [22] used a single heat transfer correlation for a CR engine combustion model that is a single-zone. Although they included the heat transfer analysis in their combustion modeling, the effectiveness of implementing various correlations has not been discussed. Thus, this research aimed to include a comparative evaluation of various heat transfer correlations on the CR engine. The main reason is to study the influence of various correlations and to provide an optimum choice to significantly increase the accuracy of the CR combustion model.

In this section, the importance of the heat transfer model and the four most commonly used correlations for it have been explained and discussed theoretically and numerically. According to Klein [77], heat transfer consumes about twenty up to thirty-five percent of overall energy while passes it to the coolant. The overall heat transfer in the engine consists of one-half of the in-cylinder heat transfer, while the other potion comes from the exhaust port.

The in-cylinder heat transfer comprises convection and radiation, where the convection composes the majority[77]. Meanwhile, the amount of radiation can approximately be around twenty percent in SI engines; however, this amount is significantly lower in the in-cylinder heat transfer [92]. Even though it is considerably low, radiation is often included in the correlation for convective heat transfer [25, 88]. While the fact that a significant part of in-cylinder heat transfer originates from convection for the SI engine, the heat transfer in CI engines is mainly from radiation which can reach a maximum of forty percent [42] and has to be considered explicitly [95].

Over the years, the importance of heat transfer coefficient led to several investigations that have been carried out experimentally and theoretically. There are several correlations that have been proposed for both SI and CI engines [92, 93, 95–97].

In terms of classification, the heat transfer correlations can be classified based on the origin of the heat transfer and the retrained assumptions. According to these two factors, the correlations are divided into natural or forced convection assumptions. Those correlations that are developed based on natural assumptions are unreliable and not applicable to every engine type due to their insufficient assumptions [68]. For evaluation purposes, only forced convection-based correlations are selected due to their realistic assumptions. This is because the fluid flows in-cylinder are the result of external mechanical actions in the chamber [68].

This comparative evaluation was inspired by similar work that Louini et al. [68] and Fagundez et al. [98] conducted. To obtain a higher effective model, Lounici [68] carried out a comparative analysis on heat transfer correlations for a two-zone combustion model for the case of SI engines that used natural gas as their fuel. Similarly, Fagundez [98] investigated the case of a spark-ignition engine using wet ethanol as their fuel.

2.8.1 Woschni's Correlation

Woschni's correlation [92] is a set of empirical equations obtained through experiments that have been used to predict the heat transfer coefficient within gasses and walls inside combustion chamber. This correlation is widely recognized and frequently have been implemented on various SI and CI engines. Woshchni included a term for the average gas velocity which separated the gas velocity into the unfired and time-dependent, combustion-induced gas velocity. Woschni modified the average gas velocity by considering the changes in density during combustion and expansion strokes. In addition, he included the motored pressure term and taking the pressure changes (due to combustion) into account. In other correlations, the gas velocity is considered as a time-averaged parameter that is proportional to the mean piston speed during the engine cycle, while the gas velocity in Woschni's correlation is considered to grow during the combustion process [92]. The numerical description of this correlation has been individually described in Appendix (E.4.1).

2.8.2 Hohenberg's Correlation

According to Hohenberg [93], Woschni correlation comes with some limitations in terms of accuracy. Based on him, the heat transfer coefficient is underestimated and overestimated during compression and combustion processes, respectively. These inaccuracies result in the exaggeration of the average heat flux throughout the cycle. In addition, it has been highlighted that Woschni correlation is complicated in terms of usage. Thus, Hohenberg has developed a new correlation shown below [93]:

$$h_g = C_1 \times V_c^{-0.06} \times P^{0.8} \times T^{-0.4} \left(C_2 + \bar{U}_p\right)^{0.8} \tag{2.1}$$

The cylinder volume is denoted by V_c, P is the instantaneous pressure calculated in unite bar, $\bar{U}_p$ is the mean piston speed, and T stands for mean gas temperature. C_1 and C_2 are the two constants that their values were obtained by utilizing detailed and precise calculations of heat balance, heat flux, and component temperatures on various Dl-diesel engines. Respectively, the values of 130 for C_1 and 1.4 for C_2 were obtained. Regardless of the engine type, while their combustion are similar, Hohenberg discovered that the variation of heat transfer for these engines is about 10 percent. Meanwhile, the variation can rise to twenty percent.

2.8.3 Sitkei's Correlation

Another correlation namely Sitkei's correlation has been developed, which is consistent with Woschni and Hohenberg's correlations. Similarly, this correlation has been established based on the experimental data of a diesel engine [94] and shown below:

$$h_g = \text{ Const. } (1+b) \frac{P^{0.7} \times \bar{U}_p^{0.7}}{T^{0.2} \times d_e^{0.3}} \tag{2.2}$$

Sitkei provided the following values of constants for b variation [94]:

- Direct combustion chamber (0 – 0.03)
- Piston Chamber (0.05 – 0.1)
- Swirl Chamber (0.15 – 0.25)
- Pre-combustion Chamber (0.25 – 0.35)

2.8.4 Annand's Correlation

The last correlation covered in this chapter belongs to a researcher who developed it in 1963. Annand [95] developed a model for heat transfer prediction by utilizing the Newtonian equation (see equation E.41), the N$\ddot{u}$sselt number as well as Reynolds. In contrast, the instantaneous heat transfer coefficient in Annand model has been divided into the convective and radiation . Thus, the coefficient can be stated as follows [95]:

$$h_g = h_c + h_r \tag{2.3}$$

The convective heat transfer coefficient is denoted by h_c, and presented as below:

$$h_c = \frac{k_{gas} Nu}{B} \tag{2.4}$$

In equation (2.4), the N$\ddot{u}$sselt number is represented by $Nu = aRe^{0.7}$, B stands for the cylinder bore, and the thermal conductivity of the cylinder gas is denoted by k_{gas} where it is modeled using a polynomial curve-fitting of the experimental data. Based on Blair [99], the gas thermal conductivity of the cylinder can be obtained using an iterative solver. Accordingly, the expression is represented in equation (2.5).

$$k_{\text{gas}} = 6.1944 \times 10^{-3} + 7.3814 \times 10^{-5} T[k] - 1.2491 \times 10^{-8} T[k]^2 \tag{2.5}$$

On the other hand, the radiation heat transfer coefficient can be modeled as follows:

$$h_r = a \times \frac{k_g}{B} Re^b + c.\sigma \frac{(T^4 - T_w^4)}{(T - T_w)} \tag{2.6}$$

Where a and b are constant values, and vary according to engine geometry and cylinder charge motion. The value of a is between 0.35 and 0.8 during normal combustion (standard operating condition). The value of a rises in the considered region with an increment of the charge motion intensity. In terms of the four-stroke engine, $a = 0.49$. The other parameters in equation (2.6) are b that is equivalent to 0.7, $C = 0.075$ during combustion and expansion strokes (for SI engines) while $C = 0$ during compression, and lastly $\sigma = 5.67$.

2.8.5 Notes on Other Heat Transfer Correlations

The correlations mentioned in sections 2.8.1 - 2.8.3 are developed based on experiments that had been carried out on diesel engines. Undoubtedly, there are some enormous differences between CI and SI engines in terms of principles and the range of operations. Thus, correlations such as Woschni, Hohenberg, and Sitkei are not fully desirable to be utilized for modeling an in-cylinder heat transfer process of SI engines, theoretically. They can, however, be considered as alternatives options for such purposes. For instance, Soylu and Gerpan [11] studied the influence of various parameters such as the composition of fuel, ignition timing, and equivalence ratio on the burning rate of a natural gas engine. They developed a model based on Annand's correlation for heat transfer rate. Zareei and Kakaee [10] studied the influence of spark timing on the performance and emission characteristics of a gasoline SI engine. In their model, they adopted Woschni's correlation to model the engine heat transfer process. Similarly, Chan and Zhu [100] utilized Woschni's correlation to model a gasoline engine in-cylinder thermodynamics that goes under high values of retarded ignition timings. Oguri [101] estimated the rate of heat transfer for a SI engine using Eichelberg's correlation model. The results provided by the model were as expected and aligned with the experimental data during the expansion stroke. Meanwhile, the obtained results during the compression phase did not match with the experimental findings. it should be noted that Eichelberg's correlation model was not described in the previous section due to its category (natural convection assumption).

Even though there are few correlations developed based on SI engines [68], Trapy's correlation [102] could be considered in this category. This correlation is unlike those presented in the previous sections. According to Louini et al. [68], this correlation is lack of universal characteristics and the uniqueness of constant coefficients in each engine differs from one to another. The only developed correlation that has been derived from both CI and SI is the correlation modeled by Annand (see section 2.8.4).

2.9 Literature Review Summary

The literature review advocates that several researchers have combined efforts to contribute to the development of new alternative mechanisms to solve the problems associated with the performance and emission of ICEs. According to section 2.4, different optimization methods were used for the improvement of performances and emissions characteristics of ICEs. Various researchers focused on optimizing the operating conditions of engines, while implemented on various types of engines under different operating conditions, and fuels. Due to the main focus of this study, ignition timing becomes the main key for investigation. Furthermore, in order to conduct the optimization process, a precise and accurate combustion model is required. Based on the explanation given in section 2.5, a single-zone combustion model is decided to be developed based on zero-dimensional modelling due to its reasonable accuracy and low computational time.

With regard to the accuracy of the heat release model, three main developed models were described and the comparison by Klein [77] was presented. Based on his conclusion, the Apparent heat release model developed by Krieger and Borman was selected (see section 2.6.4). Moreover, To increase the accuracy of the heat release model and the combustion prediction, it was recommended to develop a model for specific heat ratio instead of considering it as linear or different constant values. Similarly, three well known previously developed models were introduced in section 2.7 and the most promising model must be selected to be used in CR engine modeling.

Furthermore, it was also important to include the heat transfer model to obtain the result with higher accuracy. However, during the literature search, it was observed that the heat transfer coefficient plays an important role in the modeling of in-cylinder heat transfer. There are various developed correlations to describe this parameter (see section 2.8). For this reason, the most commonly used correlation for both SI and CI engines were selected. In contrast with heat release or specific heat ratio models, there was not enough evidence to support any of the correlations as a suitable match for the CR engine. Thus, it was decided to conduct a comparative study to investigate the influence of each correlation on the CR engine combustion characteristics prediction.

CHAPTER 3

METHODOLOGY

3.1 Overview

In this chapter, the methods, designs, and developments procedure that has been done to achieve the research objectives are described. According to section 1.5, the main aims of this research are to investigate the influence of different ignition timing on the performance characteristics while predicting it for the best performance of the CR engine. In addition, to numerically determine the best timing which yields the optimum operating condition based on performance characteristics under different operating conditions. In order to obtain such goals, several tasks were required to be considered, and this chapter is separated accordingly.

The theoretical investigation carried out in this project mainly consists of thermodynamic analysis, which includes heat release and combustion analysis. These analyses are developed based on the 1^{st} law of thermodynamics, mass and energy conservations, and ideal gas laws. The combustion process and characteristics of an engine can be well understood after determining parameters such as rate of heat-release, combustion rate, the cylinder gas pressure, and the rate of pressure rise in the cylinder leads to a better discernment of the combustion process.

There are always several losses like friction, in-cylinder mass, and heat losses that can influence the performance of the engine. To obtain more accurate and precise results and the fact that total energy can be neither created nor destroyed, other critical factors such as heat transfer investigation should be comprised. Thus, it should be taken into consideration when modeling an engine.

Once the background studies and previous works have been reviewed, it was determined that several measures in terms of methodology must be taken into account. In general, this research was structured around four deliverables. Each one of them was discussed separately in the following sections of this chapter. A brief project research description, including model integration, output parameters, has been discussed in detail for each of them. Thus, the main activities of this research can be listed as follows:

1. Modification and improvement of the developed combustion model of the CR engine (section 3.2).

    (a) Develop a single-zone combustion model based on the selected heat release model in MATLAB ®.

    (b) Investigate different developed models for gamma and adopt the most suitable one based on the previous works done.

    (c) Develop a polynomial model of the internal energy for the combustion products in MATLAB ®.

    (d) Thermodynamic formulation of specific heat ratio model in MATLAB ® for modified CR model.

    (e) Conduct the required corrections on previously developed combustion model for CR engine, including reconsideration of some assumptions.

2. Investigation on the effect of various heat transfer correlations and providing an optimized choice for a more convenient modified combustion model in the case of CR engine using mathematical modeling (section 3.3).

    (a) Select various developed correlations for heat transfer calculation.

    (b) Develop four different models from modified CR model based on each heat transfer correlation.

(c) Evaluate and compare the selected correlations based on their prediction of combustion characteristics of the CR engine.

(d) Select the best correlation based on the results comparison.

3. Investigate the effects of various operating parameters on the CR engine optimization based on performance characteristics by varying the ignition timing (Optimization part I - section 3.4).

   (a) Develop a model for optimization of CR engine based on its performance characteristics.

   (b) Evaluate the influence of the given operating conditions and assumptions on the accuracy of the model prediction.

   (c) Compare the simulation results with those obtained experimentally for validation purposes.

   (d) Conduct the required corrections based on the results comparison.

4. Develop a model to predict the ignition timing for the best performance of the CR engine by varying the speed and spark timing (Optimization part II - section 3.5).

   (a) Modify the developed optimization model based on the out come of the case studies.

   (b) Develop a user-friendly optimization model for other users to conduct a similar evaluation based on their preferred operating conditions and assumptions.

   (c) Conduct a simulation under six different operation conditions for general optimization purposes.

   (d) Evaluate and select the optimum ignition timing and the optimum speed based on the obtained data.

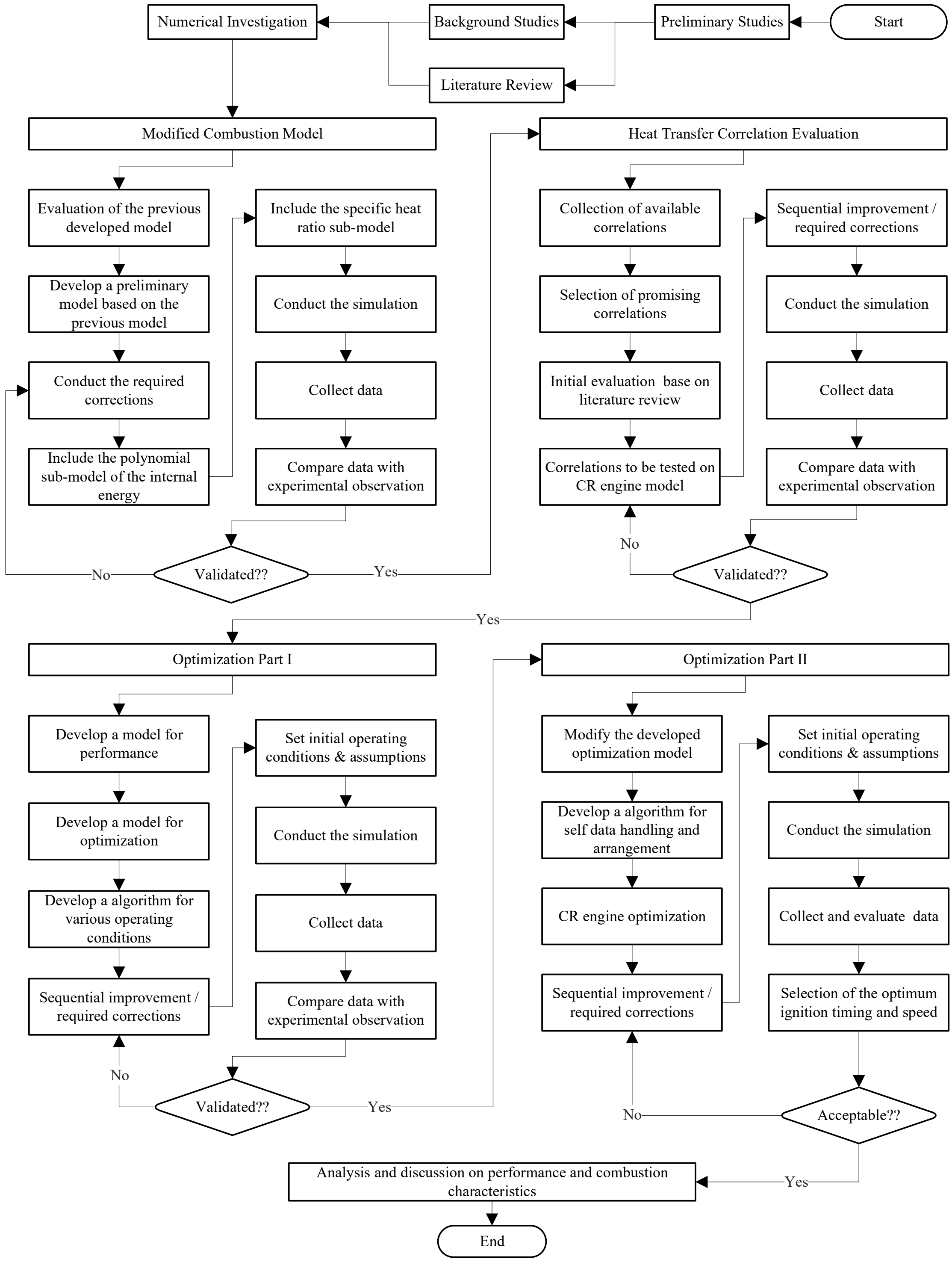

Figure 3.1: Project activities flowchart.

3.2 Stage One: Modified Combustion Model

The methodology adopted to improve and modify the previously developed CR combustion engine is described in this section. The main aims of stage one are listed in section 3.1. In the first stage of this research, a single-zone model was developed based on the model selections in the literature review section. This modified model includes the polynomial model of the internal energy for the combustion products and the specific heat ratio model. A brief model description and main output parameters are provided in the sections 3.2.1 and 3.2.2, respectively. Meanwhile, the modified combustion model process flowchart is illustrated in Figure 3.2.

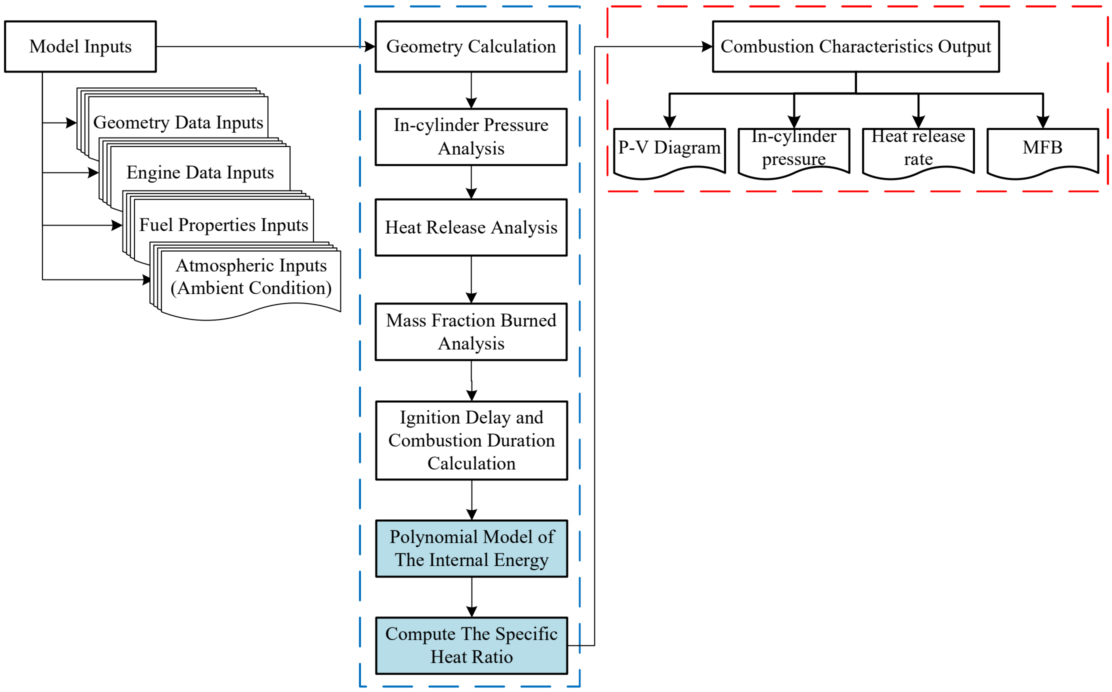

Figure 3.2: Modified combustion model flowchart.

3.2.1 Model Integration

First of all, the MATLAB script model code specified the input variables for the CR engine. The input variables include the geometry data of the CR engine, such as crank radius, connecting rod, rocker, and extended rocker lengths. Other input variables used to develop the model are CR engine specifications and fuel input data. The next step was to determine the atmospheric temperature and pressure, lower heating value, and assumed combustion efficiency variables according to the region and conditions of the engine. For more details, refer to Table 3.1.

Table 3.1: Input data for modified CR model.

Name	Variable	Value	Unit
INPUT #1: Crank-Rocker Engine Geometry and Specification Data			
The Crank Radius Length	L2	0.0253	[m]
The Connecting Rod Length	L3	0.1	[m]
The Rocker Length	L4	0.1388	[m]
The Extended Rocker Length	L41	0.1381	[m]
Swing Angle	PHI	21	[degree]
Engine Bore	B	0.055	[m]
Number of Cylinder	N_cyl	1	-
Number of Rev/Stroke	N_r	2	-
Compression Ratio	C_r	8.5	-
Intake Valve Closes	IVC	0	[degrees]
Exhaust Valve Opens	EXO	540	[degrees]
Combustion Duration	theta_b	vary	[degrees]
Engine Load	Load	vary	[%]
Engine Speed	RPM	vary	[rpm]
Ignition Timing	theta_0	vary	[degrees]
INPUT #2: Fuel Input Data			
Gravimetric Air Fuel Ratio (Stoich)	AF_ratio_stoich	15.09	
Molar Air Fuel Ratio (Stoich)	AF_ratio_mol_sotich	14.7	
Excess Air Coefficient	lambda	1	
Lower Heating Value	LHV	4.73E+07	[J/kg]
Gas Constant for Air	R_air	287	[J/kg-K]
INPUT #3: Ambient Conditions			
Atmospheric Pressure	P_atm	101325	[Pa]
Atmospheric Temperature	T_atym	290	[K]
INPUT #4: Assumptions			
Assumed Maximum Combustion Efficiency	eta_combmaX	vary	[%]
Assumed Wall Temperature	T_W	490	[K]
Preallocate Gamma Array (sets initial value)	gamma(1:720)	1.34	

Once the required inputs were included, the computational calculations of the cylinder head area, engine displacement, clearance volume, average piston speed, and piston cross-sectional area were determined. The computation continues with determination of the engine stroke, which the MATLAB script relied on the swing angle, and the rocker extended arm. Meanwhile, to obtain the friction losses of the engine, Blair's equation was used, depending on the speed and stroke according to section E.7. In order to calculate the overall volume of the CR engine cylinder, various computations such as piston displacement, transmission angle, crank angle, swing angle were needed, which have been discussed in section E.2 of this thesis. Moreover, these variables and equations can be found in the works of Mohammed et al. [22].

It should be noted that the calculation of all the magnitudes of engine inputs such as transmission angle, cylinder volume, piston position, etc. are highly dependent on the crank angle. Furthermore, the MFB curve was used to calculate and predict the combustion characteristic while the in-cylinder fuel mass and the Weibe function were derived in MATLAB. Lambda (λ) reading, a stoichiometric reaction within air and fuel, and balanced equations were utilized to compute the AFR [24]. In terms of other aspects of the model, such as the heat release calculation, in-cylinder pressure trends, and temperature estimations, all were modeled while MATLAB scripts were used to program these parameters. The numerical method used to solve the differential equations for pressure and temperature is based on backward Euler method known as implicit Euler method. The residual gas fraction was modeled from polytropic relationships to represent the mass fraction burned analysis implementation. It should be mentioned that the temperature trends have been corrected from the ratios between the volumetric residual and inlet gases at each crank angle. Furthermore, the model included the computation of variable specific heat ratios, as it was discussed in the literature review section. Lastly, the final model that consists of all sub-models is referred to as the Modified CR Model. This model does not include the heat transfer calculation since the heat transfer evaluation based on the different correlations is carried out separately.

3.2.2 Output Parameters

With the aids of predicted combustion characteristics, most of the validation procedures were carried out. The main output parameters for a combustion model can be expressed as the pressure trends, temperature trends, P-V diagram, the rate of heat release, and the MFB profile. Moreover, an engine can results in failure when it is constantly subjected to high thermal load and mechanical stresses. The accuracy of prediction for this risk, therefore, is highly crucial. Thus, further analysis of the maximum pressure and temperature is needed.

The in-cylinder pressure trends and temperature are the two primary parameters in modeling an engine in terms of combustion analysis. This is highly due to their role as the starting point of other performance parameters computation. For this purpose, the in-cylinder pressure and temperature data as a function of crank angle are considered as the main outputs for this research. These data are obtained and discussed in the next chapter.

3.3 Stage Two: Heat Transfer Comparison and Evaluation

In this section, the main approaches to conducting a comparative evaluation of various heat transfer correlations on CR engine modeling are explained. In Figure 3.3, a simplified block diagram of implementing the heat transfer evaluation of various correlations is presented. In order to conduct the simulation, MATLAB code scripts of each correlation described in section 2.8.1 - 2.8.4 were developed and presented in section 3.3.1 along with a brief integration description.

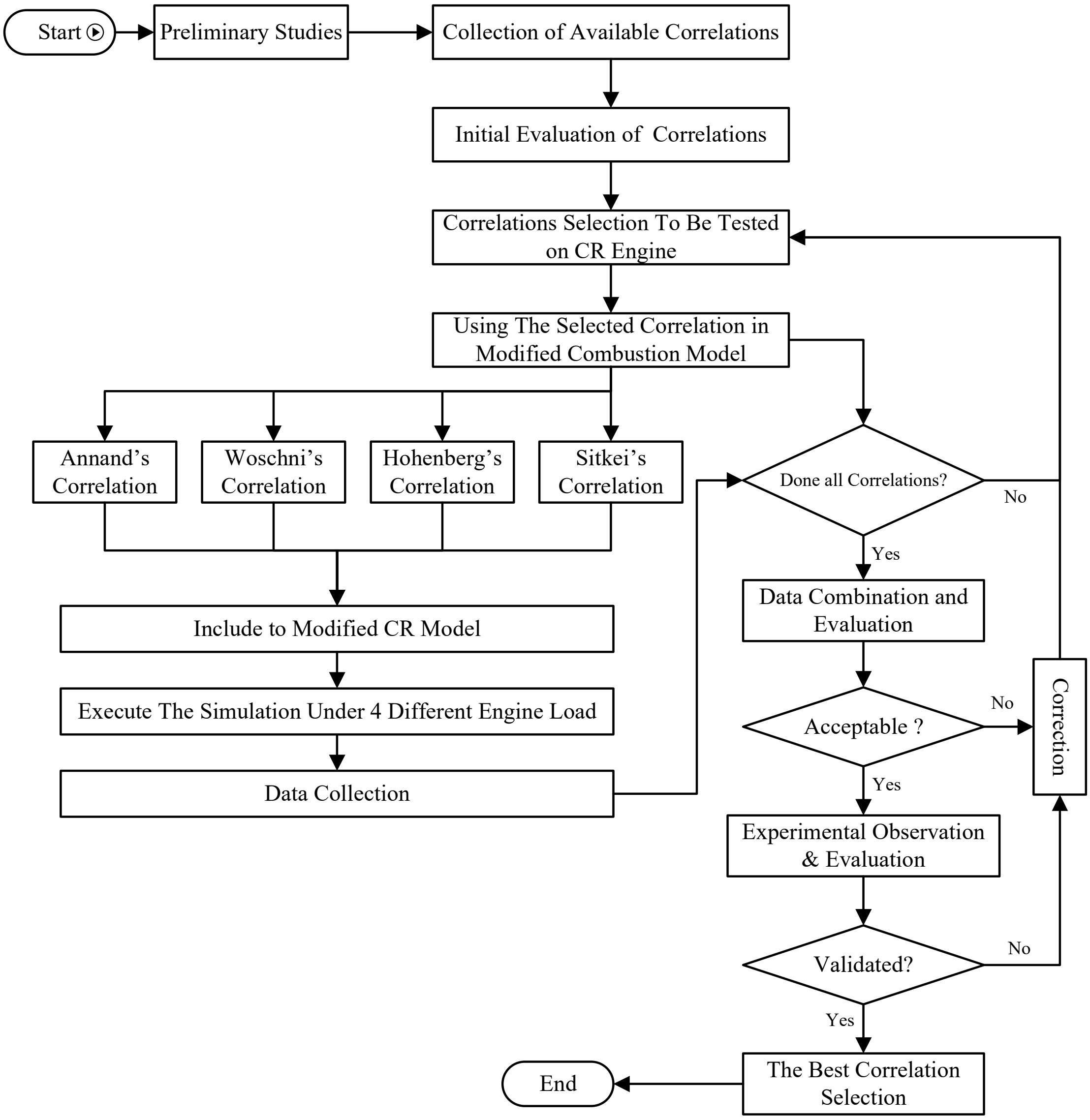

Figure 3.3: Heat transfer evaluation of different correlations.

3.3.1 Model Integration

With reference to the literature review section, it was decided to investigate the influence of different heat transfer correlations on the prediction accuracy of the model while providing an optimized choice for a more convenient modified CR model. According to section 3.1, three main tasks were required to be attended. The first step was to conduct preliminary studies on the topic and collecting the most common and available correlations. After the selection of the four correlations, developing their models and including them in the modified CR model separately were the second main steps. Lastly, conducting the simulation and obtaining the required data for evaluation and comparison while selecting the optimum choice.

Moreover, to investigate the characteristics of the model outputs under various operating conditions, further simulations were executed. The increase in the engine load while running under steady speed features a considerable impact on the maximum values of the heat flux and heat transfer coefficient [103]. Based on Sanli's [103] observations, while a gradual rise occurs to the engine load at the constant speed, the amount of variation between the maximum values of the heat flux and heat transfer coefficient decreases significantly. Therefore, it was decided to conduct the investigation under four different engine loads with the increment of twenty-five percent. Unfortunately, the only available experimental data for CR engine was at full load (100%); thus, the simulation for the four models have been carried out at 25%, 50%, and 75% additionally for further investigation and prediction. Meanwhile, both experimental and theoretical results at 100% were used for validation purposes.

3.4 Stage Three: Optimization Part I

Once the modified CR model was developed with the optimum heat transfer correlation selected, the model was capable of predicting the combustion characteristics of the engine during the combustion phase without any issue. However, this model was lack of particular parameters and aspects to be utilized for the optimization process. To conduct the optimization for ignition timing based on performance characteristics, developing a new model was required to be combined with the modified combustion model. This was for obtaining results with higher accuracy and also the ability to predict several performance parameters. Thus, the following activities were conducted.

1. Develop a model including performance parameters calculations.

2. Combine the new model with the modified combustion model.

3. Create a function in MATLAB from the combination of the models.

4. Develop a model based on variable ignition timing, engine speed, and load while utilizing the created function for simulation.

5. Validate the obtained performance parameters with experimental data.

However, the above tasks were not specifically designed for optimization part I. The optimization process was supposed to be only a single part; however, during the validation process of the obtained results, it was found out that some of the assumed parameters have a high impact on the model prediction of performance parameters. There are several parameters in the model that have been assumed. Meanwhile, the two parameters, namely, maximum combustion efficiency and the combustion duration, had the most influence on simulated results. Therefore, further investigations and analysis of these parameters were required. It should be noted that all information regarding the results and validations are provided in the next chapter, while the methodology and how the optimization process leading to this analysis are discussed in this section.

Under such circumstances, the optimization process for the CR engine was divided into two parts. In part one, the combined CR model has been used to conduct the performance evaluation based on various ignition timing and further study of combustion duration and assumed maximum combustion efficiency effects. In a real engine test, these parameters can vary based on the engine performance and influence the main output parameters, such as torque and power. For this reason, three different case scenarios have been considered to define the possible influences and effects (Please refer to the Table 3.2).

Table 3.2: Optimization part I - the case scenarios variations

Scenario	Maximum Combustion Efficiency	Combustion Duration	Ignition Timing
# 1	45% - 85%	40° CA	310°-360° CA
# 2	72%	30°-85° CA	310°-360° CA
# 3	30%-80%	30°-80° CA	310°-360° CA

Under these three scenarios, the model works with a similar operation condition as the experimental operating condition. Similarly, the engine speed is set at 2000 rpm, under full load condition with a compression ratio of 8.5. However, the following parameters have been varied with the increment of five percent and 5° CA for maximum combustion efficiency and combustion duration, respectively. According to Table 3.2, the lower and upper range of investigated ignition timing is adjusted at 310° CA (equivalent to 50° CA BTDC) and 360° CA (at TDC), respectively. In the next sub-section, a brief model integrations for each scenario is provided.

3.4.1 Model Integration

The first optimization model was developed based on the modified CR model and the performance model. These two models were combined and have been set as a CR combined model. Using the function format of MATLAB, the CR combined model was called by the program at which the engine speed, load, and ignition timings are varied according to the given range. Firstly, it was required to set the initial conditions and define the upper and lower range of the speed, load, and ignition timing while a pre-allocation should have been defined for each parameter.

The investigation range of the parameters that require optimization has been defined previously. It was decided to vary the engine speed from 1000 to 10000 rpm while for each speed, the load varies from forty percent to one-hundred percent (full load). Meanwhile, at each engine speed and engine load, the crank angle for ignition is varied from 310° CA (equivalent to 50° CA BTDC) to 360° CA (at TDC). In other words, three main For-Loops were developed to conduct the simulation and collect the data. These loops produced huge amounts of data for investigation at which the selection of the optimum ignition timing and the speed for the CR engine would be carried out.

Once everything was set, the simulation started. Upon extraction and validation stage, it was found out that the results were highly influenced by the range of assumptions made for maximum combustion efficiency and combustion duration, and additional analysis is required to predefine them more accurately. The process flowchart of the first optimization model is presented in Figure 3.4.

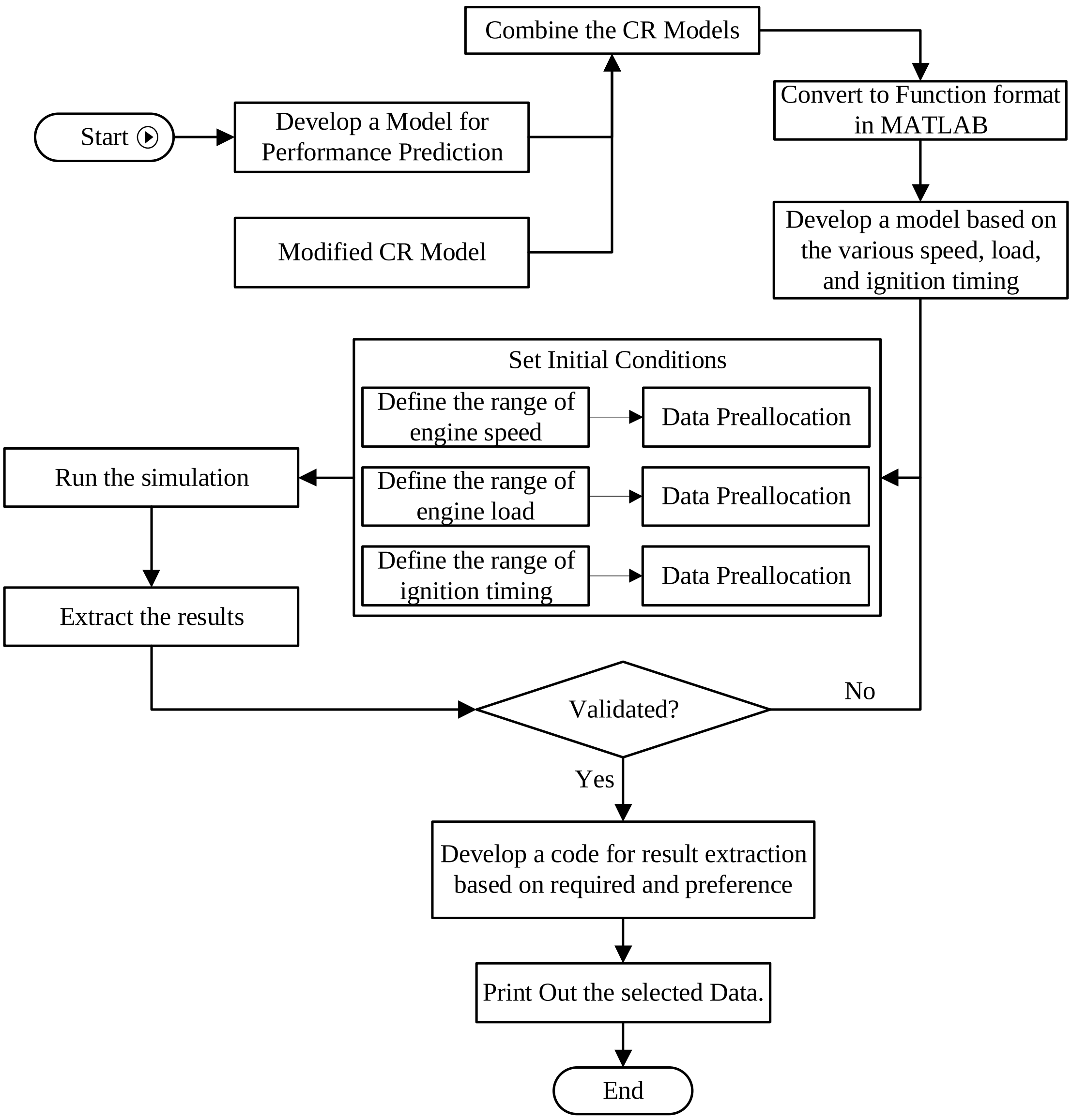

Figure 3.4: Optimization part I - Initial process flowchart.

For a better illustration of the For-Loops used in the model, the following algorithm is presented (please refer to Figure 3.5). The increment for engine speed is set at100 rpm, 10 percent increment for load, and 1° CA for ignition timing.

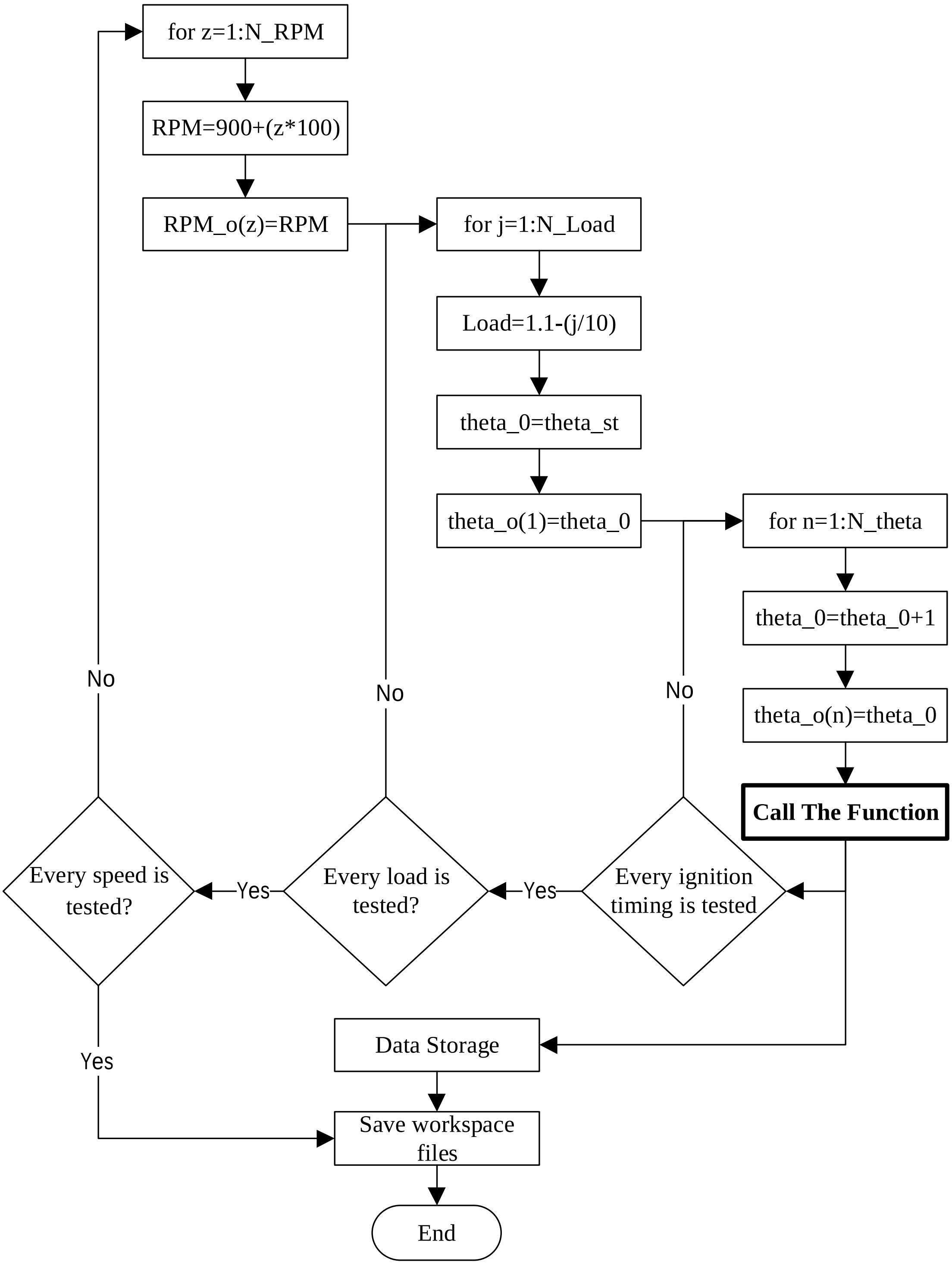

Figure 3.5: The model algorithm for optimization part I.

In terms of the additional analysis (case scenarios), the model algorithm was required to be changed according to each case scenario. In these investigations, the engine speed was set at 2000 rpm, and only the mentioned parameter in Table 3.2 was varied in the loops. The first scenario is considered a fixed combustion duration while the combustion efficiency varied from forty percent to eighty-five percent with an increment of five percent. During the second scenario, the efficiency is set as a constant value, whereas the combustion duration decreased from 85° CA to 30° CA with the decrement of 5° CA. Lastly, scenario three is a combination of scenarios one and two to study the influence of assumed maximum combustion efficiency and combustion duration on model prediction.

3.4.2 Output Parameters

The in-cylinder pressure data and temperature are the two prime parameters in combustion modeling since they serve as the starting points for the computation of other engine performance parameters. However, to finalize the optimum ignition timing for CR engines, the finishing points for the performance parameters are the brake torque and brake power. Therefore, the main outputs for this stage are pressure, brake torque and brake power as a function of crank angle.

In case of validations, there were two validation process. The first validation was based on the obtained pressure data from the model at different engine speed by utilizing the first optimization model. The experimental data for this validation was obtained from [18] and the operating condition of the engine for simulation was matched with the carried out experiment. The second validation in this stage used the brake torque and brake power outputs as the main parameters. The experimental data for this validation was adopted from [19]. Similar to the first validation, the simulation operating conditions were set according to the experimental condition in Mohammed et al. study of igniting timing [19]. In the second validation, a fix engine speed at 2000 rpm and the variation of brake torque and brake power versus ignition timing at WOT was considered.

The simulations have been carried out by adopting two different methodologies to predict the brake torque. In the first method, the combined CR model assumed a fixed value of combustion duration at 2000 rpm for all the ignition timings. Meanwhile, the assumed maximum combustion efficiency has been varied in a manner of curve fitting at each ignition timing.

In contrast, both values of combustion duration and maximum combustion efficiency have been set at fixed values during the second simulation. Due to the significant amount of error and difference between the two methods, the influence of the two mentioned assumed parameters become a question. The validation of these parameters leaded to the additional studies known as the case scenarios. For this reason, the three case scenarios have been developed, and further investigation on combustion duration and maximum combustion efficiency effect on the main optimization output have been carried out.

Based on the results discussed in the next chapter, the brake torque and brake power are not only influenced by engine speed and load but also the combustion efficiency of the engine and duration of the combustion. It was realized that these two parameters should be varied accordingly along with the engine load and speed during the optimization process that leads to defining the optimum spark ignition and speed for the CR engine. Thus, these required several modifications to the combined CR model function and the optimization program. Therefore, optimization part II was needed.

3.5 Stage Four: Optimization Part II

In optimization of part II, developing a model to predict the ignition timing for the best performance of the CR engine by varying the speed and ignition timing was the prime objective. The first step towards this objective was to conduct some modifications to the model after the case scenarios studies. These modifications were implemented to improve the capability of the optimization model that the model could be run on various operating conditions, assumptions, engine speed, load, and ignition timing. Other modifications such as improving the user interface, data handling, and selection were implemented on the model. Please refer to Figure 3.1 for the process flowchart of the stage.

Once the required modifications were applied to the optimization model, it was used to conduct simulations under different operating conditions. According to Pulkrabek [104], the combustion efficiency in SI engines is commonly ranged between 95 to 98 percent for those with a lean mixture, while the range for a rich mixture is lower. Figure 3.6 shows the combustion efficiency varies based on the fuel equivalence ratio. Based on the plot, the combustion efficiency for engines operating under lean conditions has been extensively obtained around ninety-eight percent; however, when an engine is operating under rich conditions, the combustion efficiency will drop due to the lack of oxygen to react with all the fuel. Thus, an SI engine will be more efficient when the mixture is at stoichiometric level or slightly lean; to avoid a misfire and incomplete combustion caused by a highly lean mixture or insufficient amount of oxygen, respectively [42, 104].

Therefore, the ideal operating condition for the CR engine simulation was selected at a full load and a lean mixture condition where the combustion efficiency was assumed at ninety-eight percent. The other scenarios were selected for additional analysis and prediction purposes (please refer to the Table 3.3). In each case scenario, the engine speed varies from 1000 rpm up to 13000 rpm while the ignition timing change from 310° CA (50° CA BTDC) to 370° CA (10° CA ATDC).

Table 3.3: Optimization part II - the case scenarios variations.

<table>
<tr><th>Case Scenario</th><th colspan="2">Engine Load</th><th>Mixture</th><th>Combustion Efficiency</th><th>Lambda</th></tr>
<tr><td>#1</td><td rowspan="3">Full Load</td><td rowspan="3">100%</td><td>Lean</td><td>98%</td><td>1.2</td></tr>
<tr><td>#2</td><td>stoichiometric</td><td>95%</td><td>1</td></tr>
<tr><td>#3</td><td>Rich</td><td>85%</td><td>0.8</td></tr>
<tr><td>#4</td><td rowspan="3">Partial Load</td><td rowspan="3">50%</td><td>Lean</td><td>98%</td><td>1.2</td></tr>
<tr><td>#5</td><td>stoichiometric</td><td>95%</td><td>1</td></tr>
<tr><td>#6</td><td>Rich</td><td>85%</td><td>0.8</td></tr>
</table>

The value of lambda varies according to the value of fuel equivalence ratio, $(\lambda = \phi^{-1})$. According to heywood [42], if $\phi < 1$ and $\lambda > 1$, the engine is running lean. Meanwhile, if $\phi > 1$ and $\lambda < 1$, the engine is running rich.

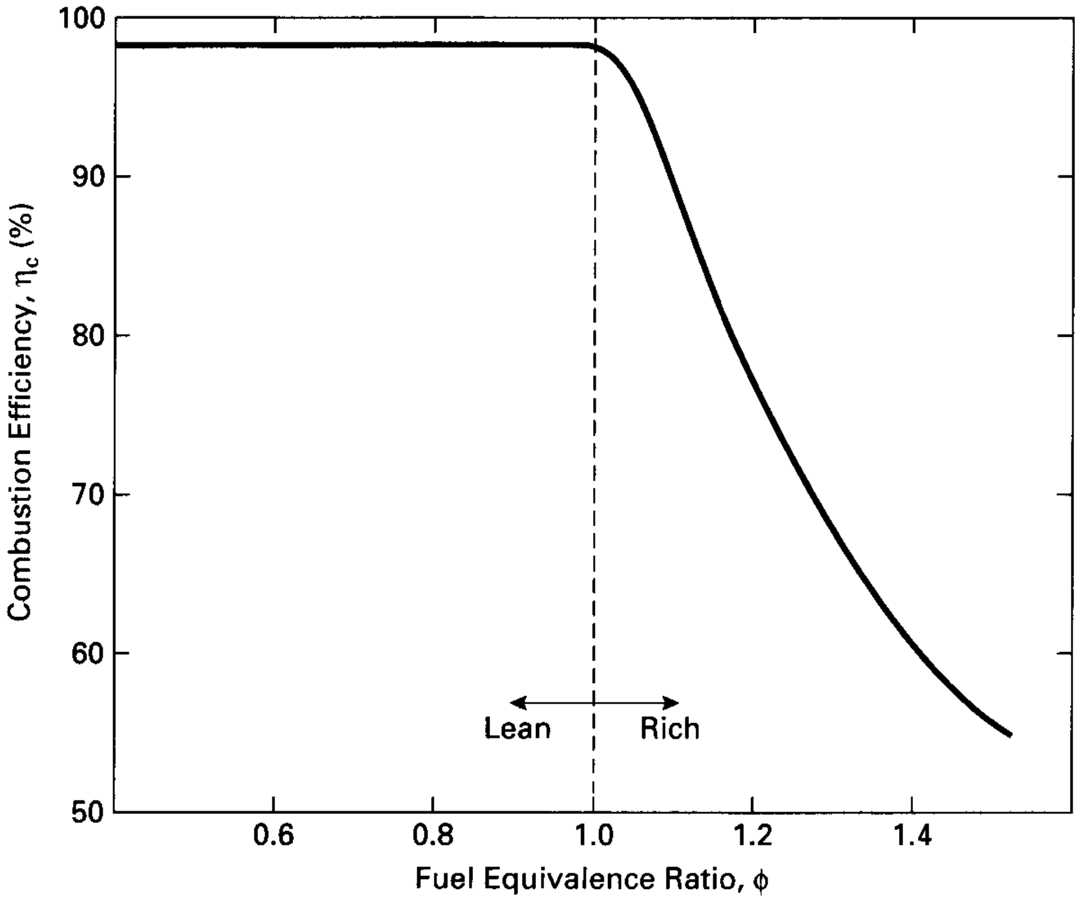

Figure 3.6: The combustion efficiency vs. fuel equivalence ratio [104]

3.5.1 Model Integration

In this model, the program will ask various questions before starting the simulation due to the implemented modification. The answer to those questions will be used as the main inputs for the optimization, which indicates the following parameters respectively.

1. The engine load $[\%]$.

2. The engine assumed maximum combustion efficiency $[\%]$.

3. The engine speed starting point $[rpm]$.

4. The engine speed finishing point $[rpm]$.

5. The increment of engine speed $[rpm]$.

6. The lower range of guessed ignition timing in $[deg]$ with 360° CA being at TDC.

7. The upper range of guessed ignition timing in $[deg]$ with 360° CA being at TDC.

8. The increment of crank angle for ignition timing in $[deg]$.

Once the above information is provided to the model, the model will start the initial calculations to obtain the number of speeds and ignition timing inputs that are being investigated. These calculations are necessary, and they will allow the program to pre-allocate the outputs. Then, the program will reach a point where similar main For-loops in Figure 3.5 have been developed. The differences are only in the range of the parameters. In the previous model, the range and the amount of increment were fixed, while in the modified optimization model, the starting, finishing, and increment ranges are requested as inputs for the main parameters. Moreover, the For-loop developed for the load was deleted, and it is required to be entered as an input.

Similarl to before, the model will call on the combined model that has been converted in the form of a MATLAB function for each iteration based on the allocated speed, ignition timing, and other inputs. these process will continue and each time the data will be stored in MATLAB memory. Lastly, the main results can be extracted once they are sorted and arranged according to the pre-allocation defined. There are various code lines in the program, which generate the required graphs spontaneously.

3.5.2 Output Parameters

In this stage, the main outputs are the same as in the previous section. The brake torque and brake power are the key parameters in defining the optimum ignition timing and optimum speed of the engine. However, other performance parameters have been extracted at each iteration for further investigation, such as brake specific fuel consumption and brake thermal efficiency (BTE).

In addition, the combustion characteristics of the case scenarios based on the optimum ignition timing and optimum speed have been extracted, which includes the following parameters:

- In-cylinder Pressure
- Heat Release Rate
- Mass Fraction Burn
- In-cylinder Temperature

3.6 Summary

In this chapter, the main methodology adopted to conduct the numerical investigation and optimization of the CR engine ignition timing based on performance and combustion characteristics are described. This chapter consists of four main sections that describe the major stages in the process of this research. In stage one (section 3.2), the previously developed combustion modeling of the CR engine was adopted, while based on the literature review section, several modifications were implemented to modify the model. In stage two of the methodology (section 3.3), the modified CR model was used to numerically investigate and compare the influence of the other developed heat transfer correlations on the prediction of the model that could lead to selecting the most optimum choice of correlation.

In stage three of this research (section 3.4), the main objective was to conduct the optimization process for the CR engine based on the combined CR model; during the validation process, the influence of two assumed parameters became a question. The significant amount of error and difference between the obtained data led to further investigation of their influence on the model. Lastly, in stage four (section 3.5), the optimization model for the CR engine was developed and modified based on the findings in stage three. Not only the modifications were implemented to increase the model predictability but also to improve the user interface of the model.

According to the scopes of study (section 1.6), conducting experimental investigations is not part of this research. All the experimental data used in this study for validations were obtained from previously obtained data experimentally by the researcher from CAREM. The information regarding the experimental set-up, tools, and methods can be found in Mohammed et al.'s published papers [18, 19].

CHAPTER 4

RESULTS AND DISCUSSION

4.1 Overview

This chapter discusses the results obtained from each stage of the methodology. Accordingly, there are four main sections based on the research methodology that each illustrates the relevant results. The main results related to stage I and stage II are provided in section 4.2. This section focuses on the modified combustion model theoretical and experimental results and the comparative evaluation of the heat transfer coefficient correlations. At the end of this section, the most optimum choice of the heat transfer correlations has been selected. The optimization part one consists of several investigations and validation processes in terms of performance. In section 4.3, the related results are displayed and discussed that include validation in terms of in-cylinder pressure and brake torque under different operating conditions. Moreover, this section provides information on the influence of maximum combustion efficiency and combustion duration on the developed CR model under three case scenarios. Finally, in section 4.4, the results regarding stage IV (Optimization part two) are presented. The required information regarding the optimum ignition timing, optimum engine speed, and benchmarking analysis of the CR engine are given. In addition, a comparison between six different case scenarios based on the information provided in Table 3.3 has been conducted.

4.2 Stage I and II: Modified Combustion Model and Comparative Evaluation of The Heat Transfer Coefficient Correlations

In order to validate the results that are obtained through the modified CR model, the in-cylinder pressure versus crank angles from the experimental observation under full load condition is compared with the simulation data. The charts in Figure 4.1 (a-b) (see section 4.2.1) illustrate the indicated cylinder pressure versus crank angle of four different models developed based on various correlations. Meanwhile, Figure 4.2 (a-f) provides similar information for other operating conditions under different load percentages. Overall, the Annand model has obtained the lowest maximum pressure, while the Hohenberg model acquired the highest maximum amount. In terms of the Sitkei and Woschni models, the results showed similar trends within each other.

4.2.1 Validation of In-Cylinder Pressure Trends

Figure 4.1 (a) and (b) show the predicted in-cylinder pressure trends versus crank angle and the maximum obtained pressure by each correlation, respectively. These data are compared with the experimental data obtained by Mohammed et al. [22] that was conducted at an engine speed of 2000 rpm, the ignition timing of 8.60° CA BTDC, full load, and WOT condition. The simulated results have been acquired in a similar operating condition. The relative errors with reference to the experimental observation of pressure [22] for different correlations are 0.09 %, 17.07%, 19.33%, and 35.15% for Annand, Woschni, Sitkei, and Hohenberg, respectively. It should be mentioned that the above error calculation is based on the peak in-cylinder pressure using the bar chart at Figure 4.1 (b).

Based on the Figure 4.1 (a), it can be noted that the Annand heat transfer correlation model has the lowest relative error that matches the actual experimental results. Since one of the models is capable of producing the results with the lowest possible error; thus, it can be deduced that the modified CR model developed in stage one is valid to be utilized for further investigations and simulation analysis. However, the most accurate model is the one embedded with the Annand heat transfer correlation.

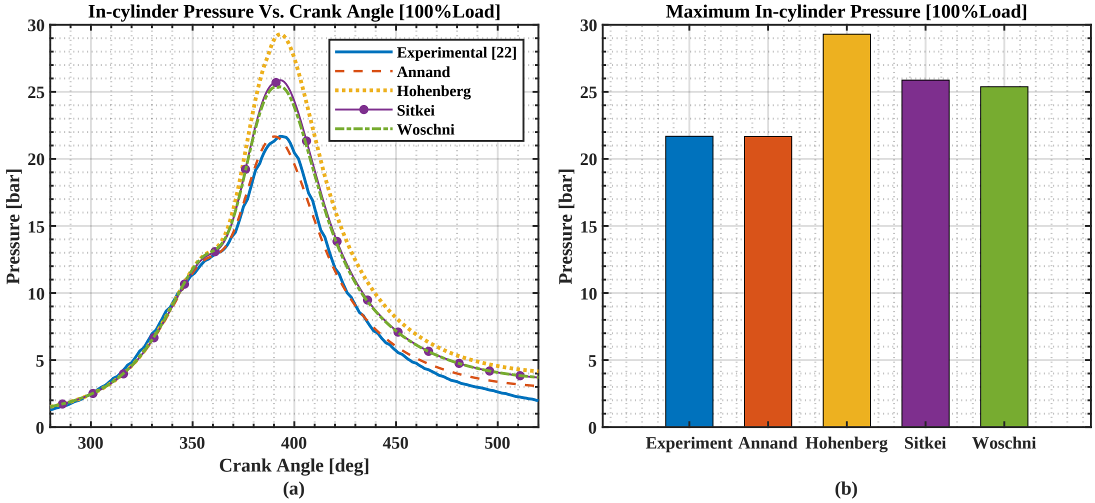

Figure 4.1: (a) Pressure vs. CA (b) Maximum pressure variation at full load.

In terms of full load condition (100 % load), the Hohenberg correlation has predicted the highest peak pressure, i.e., just slightly over 28.0 bar. Meanwhile, the Annand correlation obtained the lowest maximum pressure, i.e., at 21.6 bar. Most of the correlations predicted the peak pressure higher than the one obtained experimentally, except for the Annand model. These occurred due to their derivations that are based on CI engines specifications. It is clear that in CI engines, the heat release starts with a high value at the beginning of the process but decays in the cycle later on.

Figure 4.2 (a-f) show the simulated characteristics of in-cylinder pressure for different engine loads. In terms of Sitkei and Woschni models, the model based on Sitkei's correlation has predicted the peak pressure slightly higher than the model based on Woschni correlation by about 0.5 bar at full load. Meanwhile, based on Figure 4.2 (a-b), these two models have yielded almost the same amount of peak pressure at 75% load. However, once the engine load decreased to 50% and 25%, the peak pressure obtained by Sitkei's model dropped relatively to Woschni (please refer to Figure 4.2 (c-d) and (e-f), respectively).

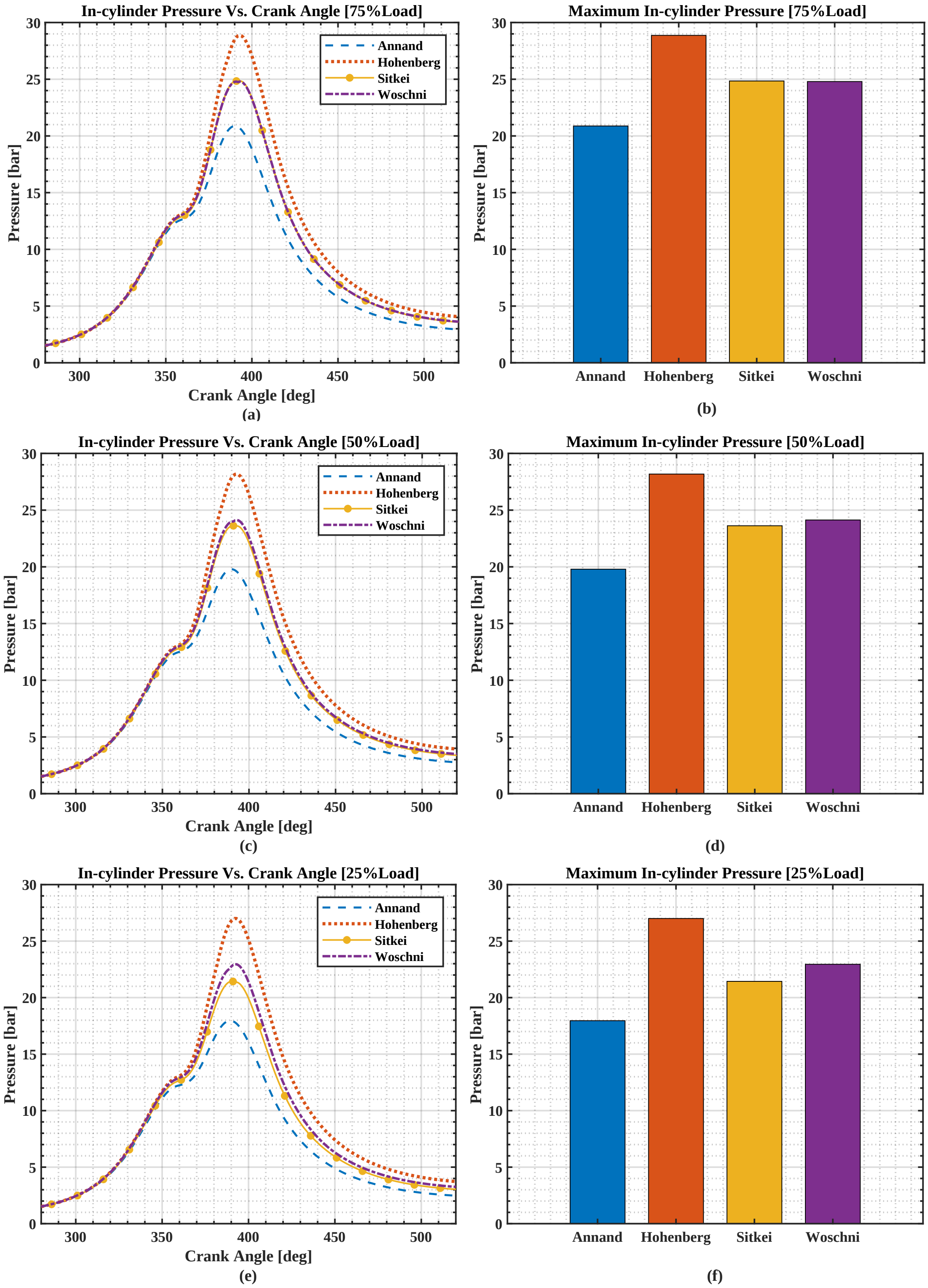

Figure 4.2: In-cylinder pressure variation at (a-b) 75%, (c-d) 50%, (e-f) 25% engine load.

Based on all the sub-figures in Figures 4.1 and 4.2, for all the cases in terms of engine loads and used correlations, it is visible that the pressure trends dropped with the decreases in the engine load. This phenomenon can be explained in terms of Brake Mean Effective Pressure (BMEP). Generally, if the engine load reduces, the bmep rate drops as well; and this causes the in-cylinder pressure to consequently decrease. By evaluating the results, an over-prediction of the in-cylinder pressure data can be noted in the CR engine modeled by Hohenberg, Woschni, and Sitkei. This over-prediction is mainly caused due to the under-prediction of the heat transfer coefficient in an engine by these models. Thus, the over-estimated pressure trends caused by these correlations are due to the fact that they reflected a lower amount of heat transfer coefficient and heat flux to the cylinder walls in the whole cycle of the engine through computation.

4.2.2 Simulated In-cylinder Temperature

The given charts in Figure 4.3 (a-d) illustrate the in-cylinder temperature versus crank angle by each model under four different engine loads. Meanwhile, in Figure 4.4 (a-d) the maximum in-cylinder temperatures are presented in form of bar chart for a better illustration purposes. Similar to the in-cylinder pressure trends, the Hohenberg based model obtained the highest prediction rate of in-cylinder temperature compared to the other correlations used in this study. With reference to Figure 4.4 (a), under the full load condition of the CR engine, the Hohenberg model estimated the maximum temperature exactly 1776 K, while this value decreased slightly to 1748 K under 25% engine load in Figure 4.4 (d). Meanwhile, the lowest predicted amount of maximum temperature is yielded by Annand's model about 1735 K and 1716 k at 100% and 25% engine load, respectively.

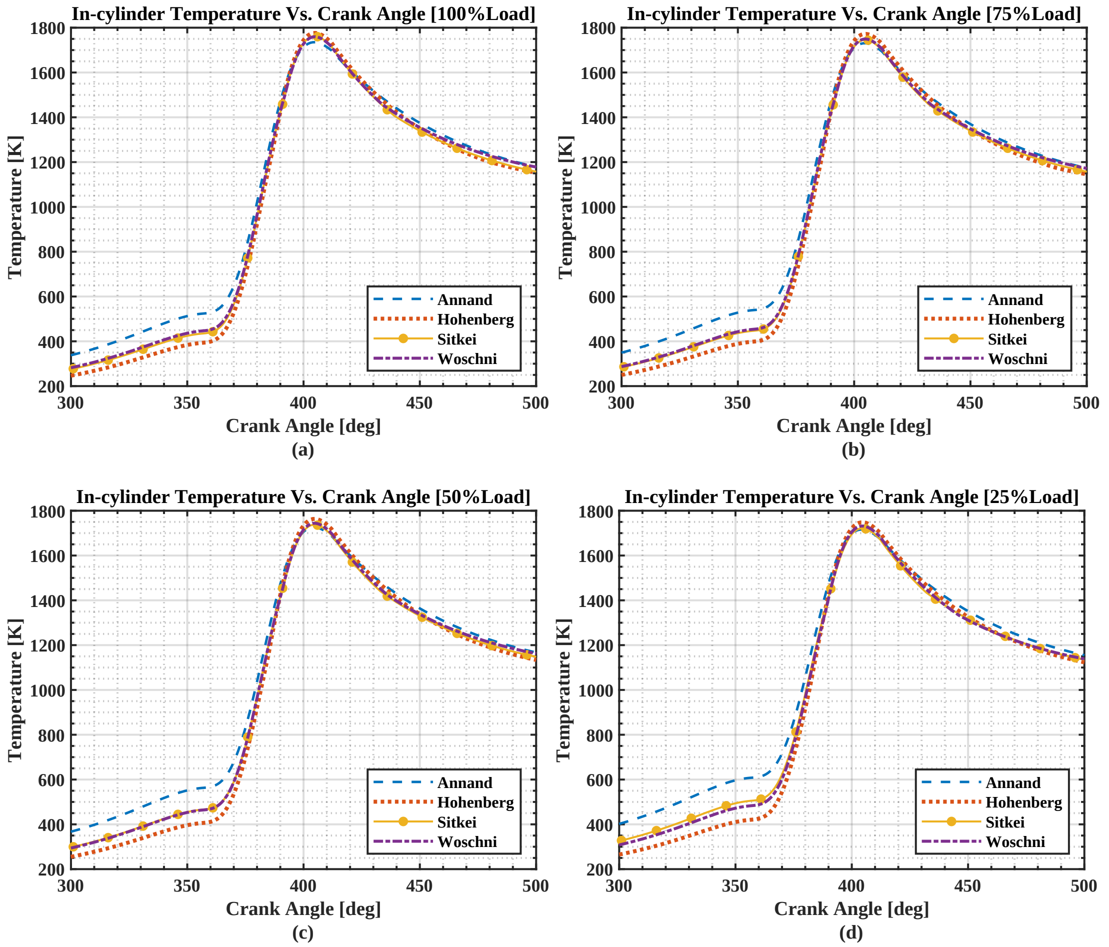

Figure 4.3: Temperature vs. crank angle at (a) 100% (b) 75% (c) 50% (d) 25% load for different correlations.

According to the bar charts in Figure 4.4, it was noted that the maximum temperature of the CR engine elevated as the engine load increases toward the full load condition. In the case of Sitkei and Woschni, the model based on the Sitkei correlation has obtained a higher rate during the full load condition, i.e., at 1761 K (sub-figure (a) in Figure 4.4). Meanwhile, the maximum temperature prediction rate by Woschni started to increase compare to the Sitkei once the engine loads were reduced. Initially, the difference between the obtained maximum temperatures by Woschni and Sitkei was only at 2 K. As engine load decreased and maximum temperate reduced, the difference between these two correlations prediction rate increased up to 10 K at 25% engine load. Based on Figures 4.4 (c) and (d), Woschni predicted the maximum temperature approximately at 1750 K and 1745 K during 75% and partial load (50% engine load), respectively.

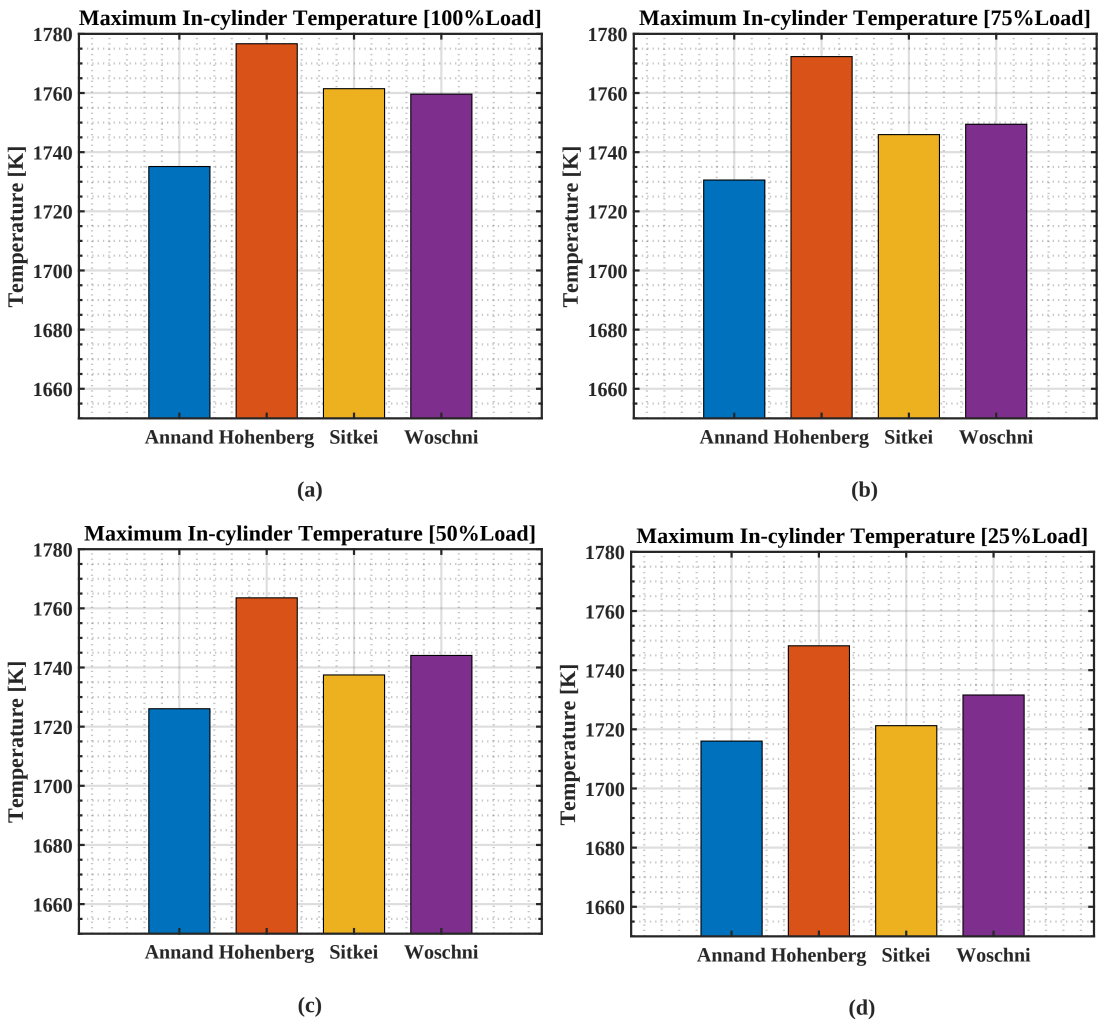

Figure 4.4: Maximum temperature at (a) 100% (b) 75% (c) 50% (d) 25% load for different correlations.

4.2.3 Heat Transfer Correlations and Parameter Estimation Analysis

Figure 4.5 (a-d) illustrates the comparison of heat transfer coefficients between four different developed models under full and partial engine loads. Overall, the highest heat transfer coefficient has been predicted using the Annand correlation, while the minimum amount is acquired by Sitkei's and Hohenberg's models. Meantime, the modified CR model based on the Woschni correlation predicted the second-highest value in both 100 % and 50 % engine loads.

In Figure 4.5 (a), in terms of full load condition, the modified CR model based on Annand correlation predicted the maximum value of the coefficient, which is approximately around $820\frac{W}{m^2 \cdot K}$. Meanwhile, the lowest value of this parameter is obtained by the Sitkei and the Hohenberg models with almost a similar value of $640\frac{W}{m^2 \cdot K}$. During the partial load of the engine, in Figure 4.5 (b), the Hohenberg model estimated the coefficient value slightly higher than Sitkei, with a difference of about $20\frac{W}{m^2 \cdot K}$. Woschni correlation predicted the coefficient of heat transfer around $740\frac{W}{m^2 \cdot K}$ and $720\frac{W}{m^2 \cdot K}$ under full and partial engine load, respectively. Moreover, the tuning coefficient is believed to have a significant impact on the heat transfer coefficient, and the reason for such fluctuation within the predicted values can be explained and traced back to the constant coefficients, such as "a", "C," and exponent indices "b" in the main equation of each correlation.

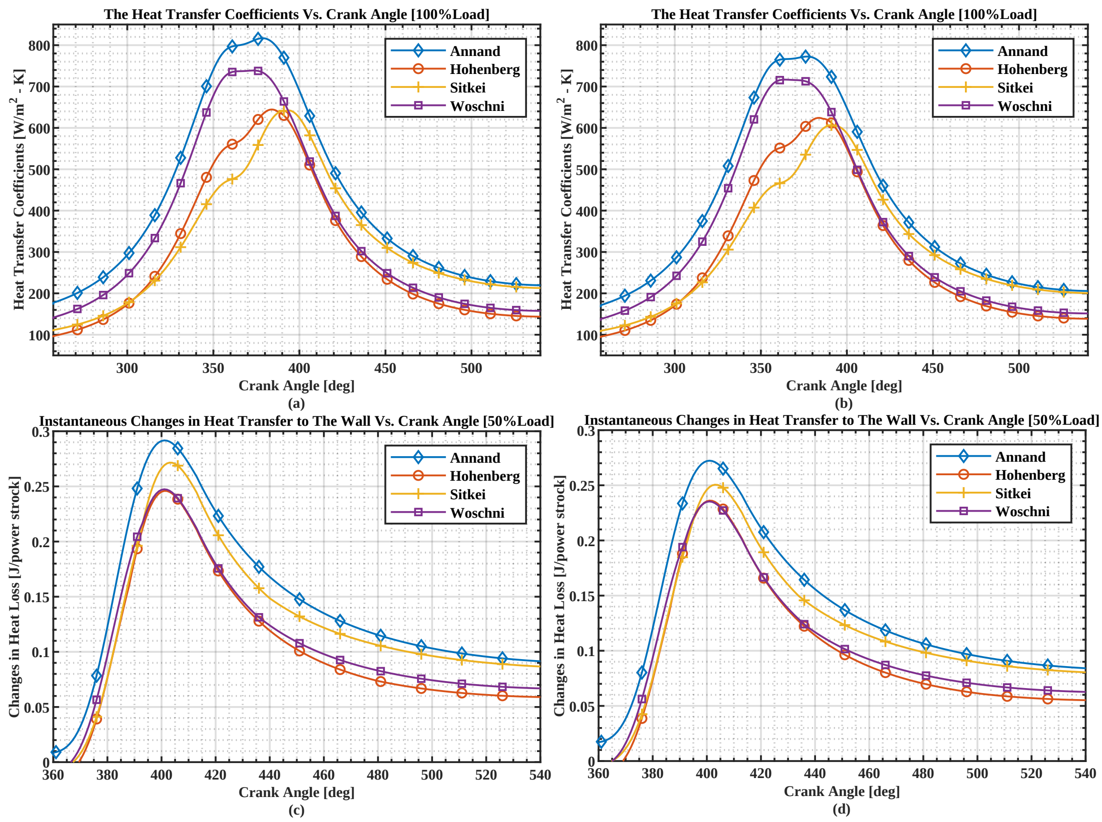

Figure 4.5: (a-b) The heat transfer coefficients comparison (c-d) The heat transfer to the wall comparison, for various correlations within two cases.

The heat transfer rate to the walls throughout the engine compression and expansion strokes reaches its highest value, while heat flux variations are almost at negative values during intake and exhaust strokes of an engine. These fluctuations are significantly affected by gas temperature and pressure [103]. Moreover, other factors affect heat transfer rates and heat flux changes as well. Soyhan et al. [105] carried out an evaluation study to compare various correlations for an HCCI engine. They reduced the correlation to a single generic form and presented the impact of length scale, pressure, velocity, and temperature on the magnitude of the correlations. For example, if the temperature of the correlation has a high value of power, the suppression of the heat transfer coefficient peak will be stronger. The reason is due to the variation of the power within correlations which significantly impacts the level of heat transfer coefficient.

Based on Soyhan et al. [105] findings, temperature power has an influence only on the magnitude of the correlations. Meanwhile, the length scale factors influence not only the magnitude of the correlations but also their shape. To emphasize more, consider the two correlations developed by Woschni and Hohenberg. For instance, Woshcni's expression utilizes the cylinder bore as a length scale, while Hohenberg uses the instantaneous volume of the cylinder as a length scale in his correlation. Thus, the prediction of the heat transfer coefficient is highly dependent on length scale factors; in terms of sensitivity, the variety in both magnitude and shapes.

The net heat transfer plots in Figure 4.6 (a) and (b) present the combination of heat transfer into and convective losses transferred out of the system. Overall, the highest and the lowest net heat transfer and heat loss are predicted by Hohenberg and Annand correlations, respectively. In terms of a full engine load condition, Woschni and Sitkei have almost identical values till the net heat transfer values of the Sitkei correlation-based model slightly dropped with the crank angle at partial load.

A similar observation can be noticed in the case of heat loss, as illustrated in Figures 4.6 (c) and (d). There have been slight convective gains or losses during the intake and compression strokes of the engine. However, the plots exhibited a steep increase in overall heat transfer once the ignition occurred. This swift expansion is the result of the combustion process in the engine. When the air-fuel mixture is entirely burned inside the cylinder, a considerable fall can be noted that represents the convective losses caused by the combustion temperature and gas flow increments.

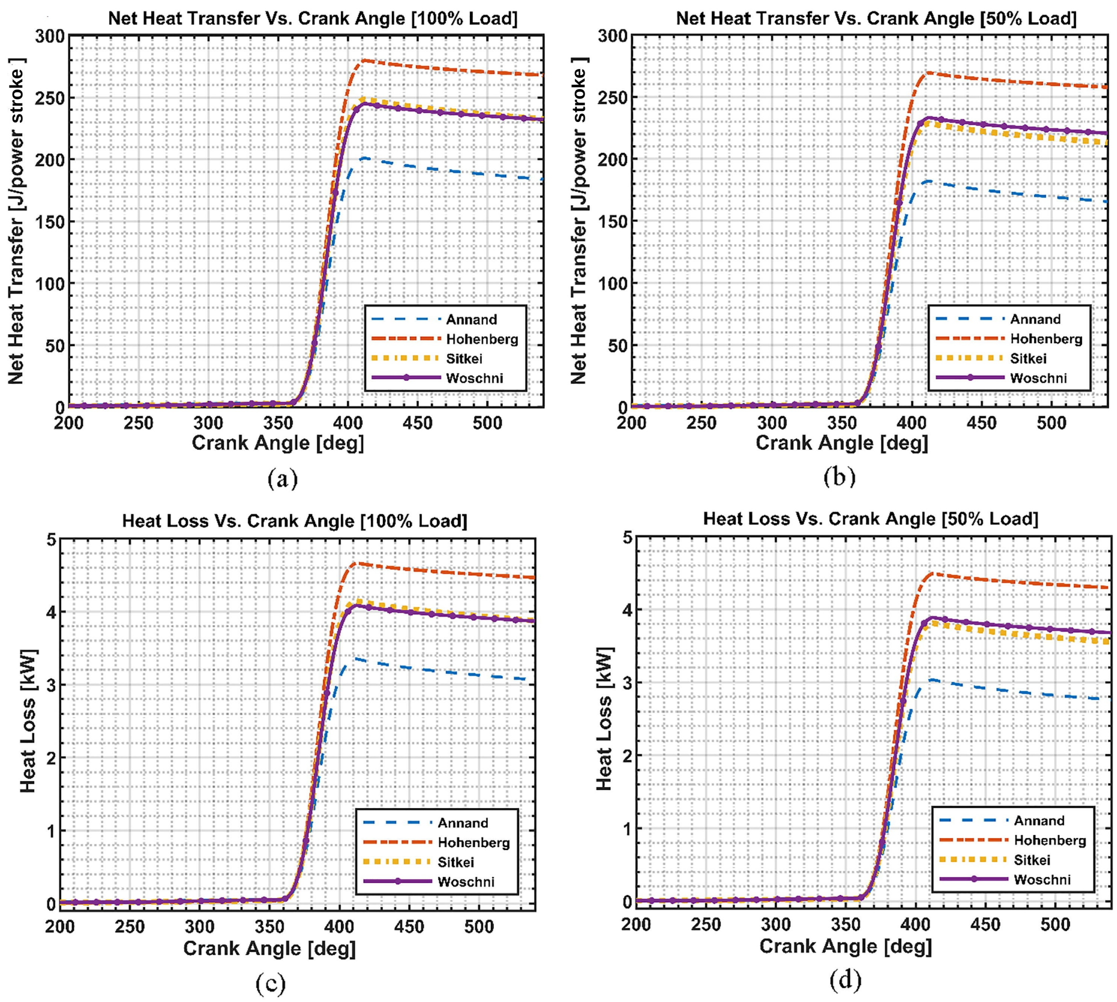

Figure 4.6: (a-b) Net heat transfer vs. crank angle (c-d) Heat loss vs. crank angle, for various correlations within two cases.

4.2.4 Heat Transfer Correlation Choice Optimization

The accuracy of the results obtained by all correlations must be considered to select an optimum correlation choice for a modified single-zone combustion model. Not only the prediction accuracy is an essential factor for the selection process, but also it is inevitably required to consider other factors such as the computational time and practical convenience of the correlations.

The prediction of the in-cylinder pressure of an engine is based on the projection of the rates of heat transferred and the heat released when the same operating conditions and design parameters are used. According to Hohenberg [93], the developed correlation by Woschni overestimates the coefficient of heat transfer upon combustion stroke while underestimating it during the compression phase.

Nevertheless, the Woschni correlation influence on the cycle performance can be stated as insignificant. The developed correlation by Woschni separates the referenced gas velocity into two different parts, including the unfired gas and induced gas velocity. It was previously mentioned that the unfired gas velocity is in proportion to the mean piston speed. Meanwhile, the combustion induced-gas velocity is the time dependence. It is a function of the distinction between two types of pressure known as the motoring and firing pressures. In addition, the Woschni correlation is hard to be implemented since the pressure is required to be tracked spontaneously. It requires more computational time for correlation to be applied compared to the other correlations.

According to the literature review section 2.8.2, Hohenberg proposed that his correlation is a modified and improved version of Woschni's correlation that diminishes several flaws and inadequacies [68]. Besides these, the computational time for this correlation is at its minimal. Moreover, the implementation of this correlation was simple compared with the rest of the correlations compared in this study. However, the accuracy of Hohenberg's correlation in terms of the predicted in-cylinder pressure trend was not acceptable as the model overestimated these data for the CR engine.

In terms of the modified model based on Sitkei's correlation, a similar statement as Hohenberg's can be stated, owning to the underestimation of the coefficient of the heat transfer while exceeding the performance cycle. However, the modified model based on Annand's correlation managed to predict the closest outcomes to the obtained experimental data among all the tested correlations. Thus, the decision on the effectiveness of applying the four different heat transfer models has been tabulated in Table 4.1 based on the previous findings and analysis.

From Table 4.1, it can be concluded that the model based on Annand's correlation offers the best heat transfer model to achieve high accuracy of results for the CR engine combustion modeling. Moreover, besides taking overall criteria in terms of accuracy, Annand's model computational time and usage perspective were at a satisfying level.

Furthermore, if the relative error of less than 20% is acceptable for other users, both Woschni and Sitkei correlation can be used for modeling. However, it should be considered that due to the high computational time and difficulty of implementing, Sitkei correlation comes as the second-best choice. Thus, the least preferable correlation in this study is Hohenberg, which is due to the lowest achieved accuracy.

Table 4.1: Final correlations comparison.

Correlation	**Accuracy**	**Computational Time**	**Usage**
Woschni	Moderate	More	Hard
Hohenberg	Low	Good	Easy
Sitkei	Moderate	Good	Easy
Annand	High	Good	Medium

4.3 Stage III: Optimization Part One

4.3.1 In-Cylinder Pressure Trends Under Various Engine Speed

The in-cylinder pressure data as a function of the crank angle for the CR engine are plotted in Figure 4.7 (a-f). These results are obtained under various engine speeds starting at 1800 rpm up to 2800 rpm with an increment of 200 rpm under 100% load experimentally and numerically. The experimental data used in this section are gathered from Mohammed et al. [18] study. A similar operating condition as the experiment was selected for the simulation where the ignition timing was set at 8.60 CA BTDC, full engine load, and WOT condition. With reference to the published work [18], the air-fuel ratio during the experiment was varied as rich, stoichiometric, and lean conditions.

According to the Figure 4.7, it can be noted that the peak pressure is increased and moved closer to TDC (360° CA) with the increment in the engine speed for all the cases. The maximum peak pressure is obtained at a higher crank angle due to the CR engine configuration at every engine speed. Mohammed et al. [18] compared the CR engine pressure data and conventional slider-crank engine and explained that the difference in the configuration causes dwelling effects in the CR engine.

Figure 4.7 (a) illustrates the initial tested engine speed at 1800 rpm. Both simulation and experimental data are almost well aligned. Similarly, Figure 4.7 (b) shows a good match between predicted in-cylinder pressure at 2000 with the experimental pressure. However, the program began to gradually over-predict the pressure once the engine speed increased to 2200 rpm onwards. These trends can be noted in 4.7 (c), (d), (e), and (f). These slight inaccuracies in the simulated results are due to the turbulence, which is not considered in the model. Moreover, the difficulty in assuming a more accurate combustion efficiency and combustion duration for the simulation is another reason for over prediction of the peak pressure. In Table 4.2, these trends are further explained.

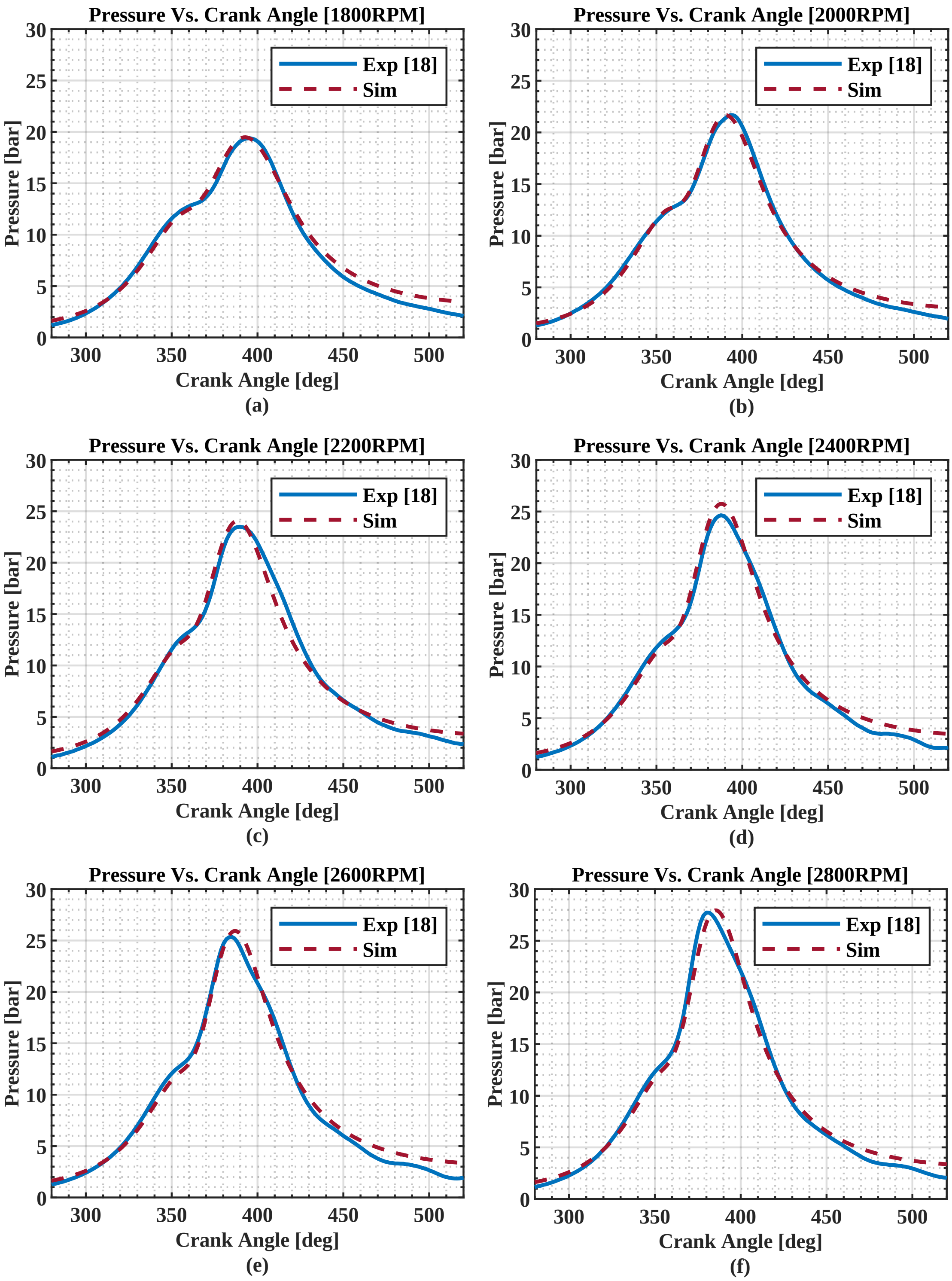

Figure 4.7: (a-f) Validation of in-cylinder pressure trends at 1800-2800 rpm.

Table 4.2: The CR engine pressure data under various speed.

	Peak Pressure [bar]		**Crank Angle at Peak [deg]**		**Relative Error [%]**	
EngineSpeed	Experiment [18]	Simulation	Experiment [18]	Simulation	Pressure	Crank Angle
1800RPM	19.38	19.48	395.81	393.00	0.50	0.72
2000RPM	21.69	21.67	393.21	390.00	0.08	0.82
2200RPM	23.49	24.08	389.74	388.00	2.45	0.45
2400RPM	24.64	25.75	387.52	388.00	4.32	0.12
2600RPM	25.36	25.93	384.99	387.00	2.22	0.52
2800RPM	27.73	27.94	379.95	385.00	0.75	1.31

According to Table 4.2, the highest relative error based on the peak pressure is obtained slightly above 4.3% during the engine speed of 2400 rpm, where the acquired pressures are 24.64 and 25.75 bar through experiment and simulation, respectively. Meanwhile, the lowest pressure error estimated under 2000 rpm is about 0.08 percent. All the simulation results have been obtained under similar operating conditions as the experiment carried out. However, parameters such as maximum combustion efficiency and combustion duration of the simulation data have been assumed for each engine speed test. These values have been varied to minimize the error percentage based on the trial-error approach accordingly.

The lowest maximum cylinder pressure for both experimental and simulation data occurred at 1800 rpm of the engine speed. Similar to the experimental data, the combustion process of the CR engine was slow because of the assumed combustion duration, which happened due to less turbulence, and a high heat transfer rate towards the chamber wall resulted in a decrease in engine performance. Moreover, the rate of combustion and performance in the engine have been improved. This is due to the provided additional time by the piston that stays longer at TDC, which allows the air and fuel to blend perfectly. Thus, based on the first validation of the obtained pressure data throughout the experiment and simulations, it can be said the combined CR model development is well accepted for further investigation, specifically in terms of the optimization process.

4.3.2 Optimization Process of the CR Engine

According to the explanation in the methodology chapter, the optimal ignition timing can be found through varying the spark ignition of the engine and observing the effect on predicted parameters such as engine torque and power. The influences of changing the ignition timing on the performance characteristics have been experimentally and theoretically investigated. The previous section was dedicated to the first validation of the optimization process stage (III), which utilized the pressure data for such purposes. Meanwhile, the second validation for this stage is to compare the obtained brake torque through simulation using the combined CR model and experimental observations. This parameter is a function of engine speed; however, in the second validation, a fixed engine speed at 2000 rpm and the variation of brake torque versus ignition timing at WOT is considered. The experimental data used in this section are gathered from Mohammed et al. [19] study. According to [19], the experiments were carried out at five different ignition timings at WOT and engine speed of 2000 rpm. The selected ignition timings were at 6.5°, 8.5°, 10.5°, 12.5°, and 14.5° CA BTDC for the experimental tests. Similarly, the exact operating condition as the experiment was selected for the simulation in order to carry out the second validation. The main reason for the selection of 2000 rpm is that the experimental data on torque and power variation of CR engine is limited. Thus far, [19] is the only available experimental investigation on developed CR engine at CAREM that focused on the variation of different ignition timing (limited to 5 only).

4.3.2.1 Experimental and Simulated Torque Trends

With regards to section 3.4, the simulation has been carried out by adopting two different methods to predict the brake torque. In the first method, a fixed duration of the combustion was assumed for the model. Meanwhile, the efficiency was changing in a manner of curve fitting at each ignition timing. In contrast, both parameters were set at fixed values during the second method. The range of the combustion efficiency changes is between 55 and 75 percent. This random selection is mainly due to the unavailability of experimental data on operating lambda or AFR in [19] study.

In Table 4.3, the CR engine brake torque data obtained under various ignition timings are presented. Based on the provided table, for both methods, the maximum error percentage was obtained at 6.5° CA BTDC, which is equivalent to 353.5° CA, with TDC being at 360° CA. While the calculated maximum error is at 353.5° CA, the highest amount of brake torque acquired at 349.5° and 351.5° CA about 5.05 N.m for method one and 5.017 N.m for method two, respectively. (Please refer to Figure 4.8)

Table 4.3: The CR engine torque data under various spark ignition.

Ignition Timing	Torque [N.m]			Error	
CA BTDC	Experimental [19]	Simulation (Method 1)	Simulation (Method 2)	(Method 1)	(Method 2)
14.50 °	4.87	4.86	4.985	0.17%	2.49%
12.50 °	4.95	4.95	5.006	0.08%	1.12%
10.50 °	5.06	5.05	5.016	0.16%	0.83%
8.50 °	4.12	4.12	5.017	0.11%	17.79%
6.50 °	3.97	3.94	5.009	0.62%	21.23%

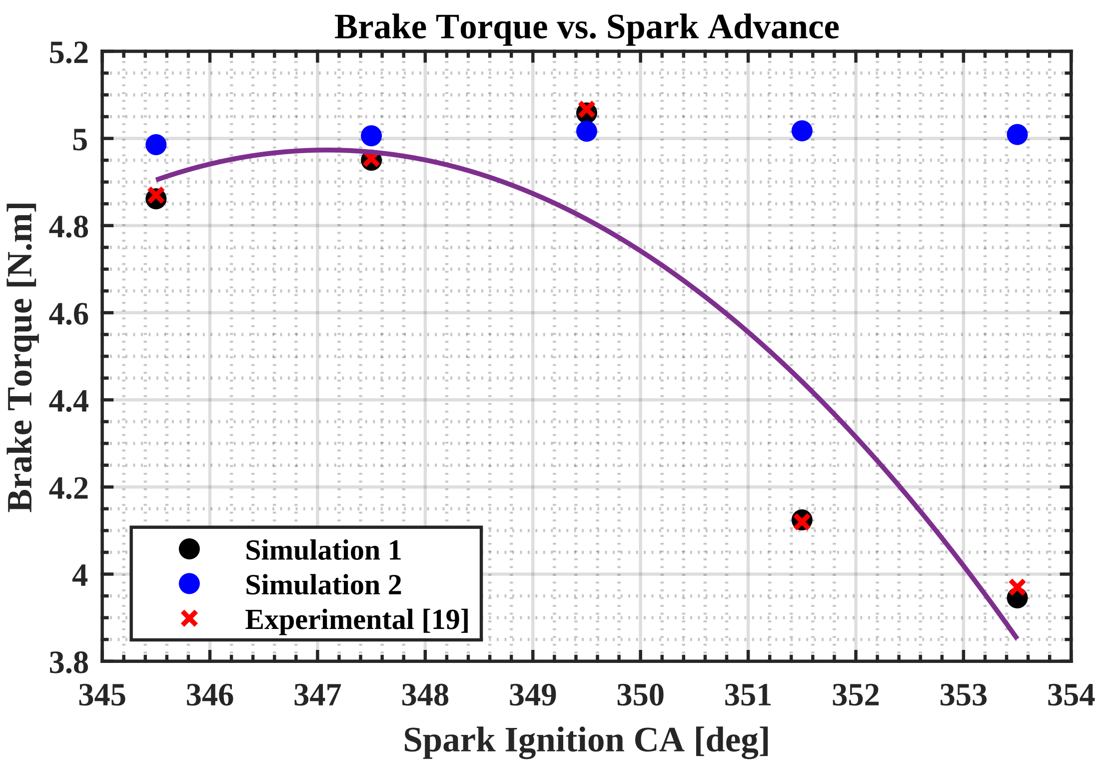

Figure 4.8: Brake torque comparison under various ignition timing.

According to the acquired results, it can be noticed that the error percentage of the first method is significantly lower than those obtained during the second method. Due to the significant amount of error and difference between the two method, the influence of the two mentioned parameters become a question. Theoretically, the difference between each obtained brake torque should not be a considerable amount. For further explanation, the obtained torque will normally vary at a fixed engine speed, while the ignition timing is changing; although the differences will not be at a high value. However, there is a tremendous drop of brake torque from 5.06 N.m to 3.97 N.m at the experimental result with ignition timing varying from 349.5° CA up to 353.5° CA with an increment of 2° CA only. Thus, three case-scenarios have been developed and, further investigation on combustion duration and maximum combustion efficiency effects on the main optimization output have been carried out.

4.3.3 Case-Scenarios: Influence of Assumed Maximum Combustion Efficiency and Combustion Duration

As mentioned in section 3.4, three case-scenarios have been developed based on similar operating conditions. The first scenario considered a fixed combustion duration while the combustion efficiency is varied. In contrast, the maximum combustion efficiency was defined as a constant value, whereas the combustion duration changed at each iteration during the second scenario. Lastly, scenario three was designed to illustrate the combination of scenario one and two to study the influence of assumed maximum combustion efficiency and combustion duration on the developed CR model.

4.3.3.1 Case-Scenario One: Maximum Combustion Efficiency Variation

In this scenario, the ignition timing varied from 310° CA to 360° CA, while for each ignition, various efficiency for combustion has been assumed. The maximum combustion efficiency is increased from 45% up to 85% with an increment of 5%. It can be noticed that by increasing the assumed combustion efficiency in a combined CR engine, the values of brake torque and power increase accordingly. Due to the huge set of data, the results from 340° CA to 360° CA for scenario one is only illustrated. (Please refer to Figure 4.9)

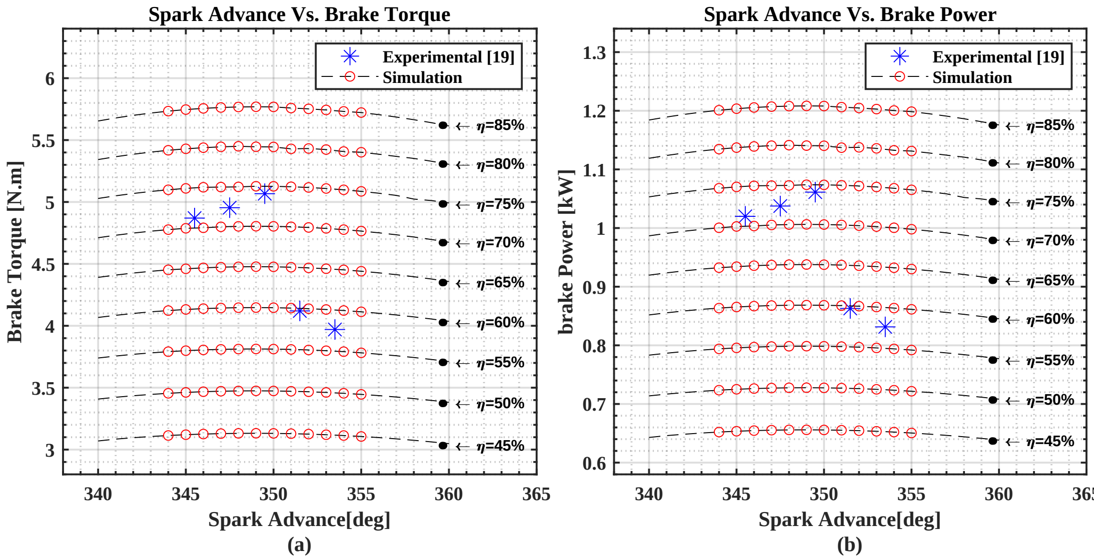

Figure 4.9: Case scenario I - (a) Brake torque (b) Brake power vs spark ignition.

Figure 4.9 (a) shows the highest experimental brake torque, approximately 5.0 N.m at 10.5° CA BTDC, while in Figure 4.9 (b), the maximum experimental brake power is obtained slightly above 1 kW at the same ignition timing. With reference to [19], the brake torque and power rise when the spark ignition increases. This is due to the fact that the in-cylinder pressure increases; therefore, additional work is generated by the engine piston [19]. Hence, by further advancing the spark timing, ignition occurs at early stage before the engine piston reaches the TDC [19]. Under these circumstances, the peak pressure is achieved while the engine piston is still moving up [19]. Consequently, the produced work to push the piston down is dropped and thus reducing the engine performance [19].

Based on the findings in this section, the main reason for a high percentage of error between method one and method two in Table 4.3 can be perfectly explained by the fact that the combustion efficiency in method one was not selected at a fixed value for every ignition timing. Meanwhile, the maximum combustion efficiency in method two was fixed at 73% only. In fact, for method one the efficiency values were set at 77%, 79.5%, 82.5%, 67.5%, 65.5% for 14.50 °, 12.5 °, 10.5 °, 8.5 °, 6.5 ° CA BTDC respectively. This was done to increase the accuracy while minimizing the relative error based on trial-error approach.

According to the experimental data plotted in Figure 4.9, the final two ignition timing points are between 55 percent and 60 percent of maximum combustion efficiency, which differ from the previously mentioned 67.5% and 65.5% values. The explanation is that in scenario one the combustion duration was considered a shorter value compared to the combustion duration defined in methods one and two of the second validation process. This is one of the main reasons for such differences in obtained results; thus, case-scenario two was developed for further study of the combustion duration effects.

Based on the explanation in section 3.5, SI engines have a combustion efficiency between 95% to 98% for lean mixtures and lower values for rich mixtures. According to the Figure 4.9, it is visible that the efficiency of the experimental data is within 55 percent to 75 percent which varied at each ignition timing. These data are indicating that the CR engine was operating under fuel-rich conditions during the experiment. Based on the published results in [19], there are not any available experimental data shows the operating lambda or AFR on the developed CR engine of CAREM. Therefore, it can be assumed that incomplete combustion frequently occurred due to an insufficient amount of oxygen in the mixture which caused a reduction in combustion efficiency during the experiment. This assumption can be varied once further experimental investigations are carried out and thus for future work they are recommended.

4.3.3.2 Case-Scenario Two: Combustion Duration Variation

The case-scenario two was run under WOT 2000 rpm at a fix assumed combustion efficiency of 72 % while the combustion duration and ignition timing varied from 30° CA to 85° CA and 310° CA to 360° CA, respectively. One of the outcomes of this study was to understand the influence of the combustion duration on the brake torque obtained at different ignition timing.

In Figure 4.10 (a), the red circles illustrate the maximum torque obtained at the specific combustion duration. It can be noted that the lower combustion duration causes the peak torque to be closer to the TDC, and by increasing the combustion duration, the peak torque not only decreases compared to the previous duration but also it gets further from the TDC. For instance, at combustion duration 30 ° CA, the peak torque occurred at 355 ° CA for about 5 N.m while at combustion duration 85 ° CA, the peak torque obtained at 325 ° CA around 4.7 N.m which is 30° CA more advanced. The ignition timing will need to become increasingly advanced (relative to TDC) as the engine speed increases; thus, the air-fuel mixture has the correct sufficient amount of time to be completely burned. As the engine speed rises, the time available to burn the mixture reduces.

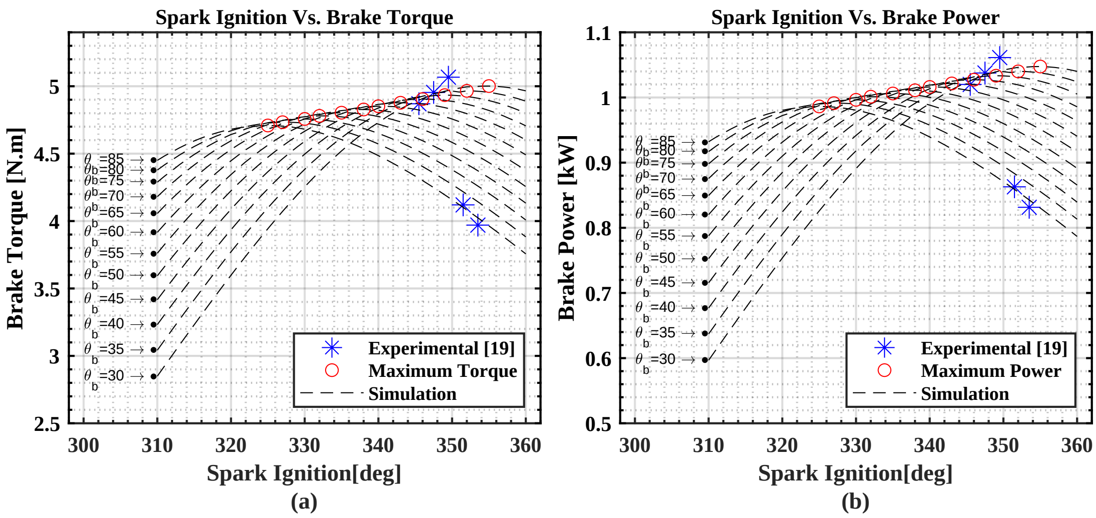

Figure 4.10: Case scenario II - (a) Brake torque (b) Brake power vs spark ignition.

Furthermore, the maximum value of torque at each combustion efficiency has an exact igniting timing in terms of case-scenario one; while in terms of scenario two, the maximum torque occurred at a different crank angle once a different combustion duration was set at a fixed amount of combustion efficiency for each iteration of the simulation. It is well known that the optimum timing which provides the maximum brake torque is highly dependent on various factors including, the combustion duration.

Based on Heywood [42], the combined period of the flame development of an engine and its propagation process is often from 30° CA - 90° CA, and the length, the details of the termination, and the traveled path of the flame across the cylinder will highly influence the optimum spark setting. Moreover, these depend on other factors such as engine design, operating conditions, and the properties of the fuel, air, and mixtures.

Based on the uncertainty in the results of scenario one and scenario two, it is extremely important to develop a proper model for combustion duration in terms of optimization as the burning rate of the mixture is strongly influenced by the speed of the engine. Based on some investigations, researchers believed that as engine speed increases, the combustion duration would either increase [25] or decrease [106] because the combustion process is much faster due to the higher turbulence inside the cylinder [106]. Thus, the statement by Heywood [42], which stated that the flame development and its propagation vary cycle-by-cycle and cylinder-by-cylinder, can be applied here. Therefore, a simple assumption of increasing or decreasing will not be sufficient for such a highly influential parameter. It is required to make assumptions and modeling relative to the laminar flame, turbulence flame, engine speed, configuration, and other key design parameters while considering the fuel and the mixture being either rich or lean. Therefore, developing a combustion duration model is highly recommended for future works on this topic.

4.3.3.3 Case-Scenario Three: Maximum Combustion Efficiency and Combustion Duration Variation

For a better illustration of case-scenario one and two, case-scenario three was developed. This scenario consists of three loops of combustion efficiency, duration, and spark ignition varied from 30% - 80%, 30° CA - 80° CA, and 310° CA - 360° CA, respectively. In Figure 4.11 (a-b), the maximum combustion efficiencies are indicated by different colors, while at each color, each line indicates a different combustion duration similar to the plotted figures in case-scenario two for brake torque and power.

According to Figure 4.11 (a-b), the experimental data for brake torque and power falls between 80 % and 60 %, which this value can vary based on the assumed combustion duration. By analyzing the figures, it can be noted that the combustion duration can completely influence the results; thus, proper modeling of this parameter is essential. However, due to the complicated process of modeling this parameter, and since this modeling was not included in the scope of studies, it is highly recommended to be considered for further work to increase the accuracy of the prediction.

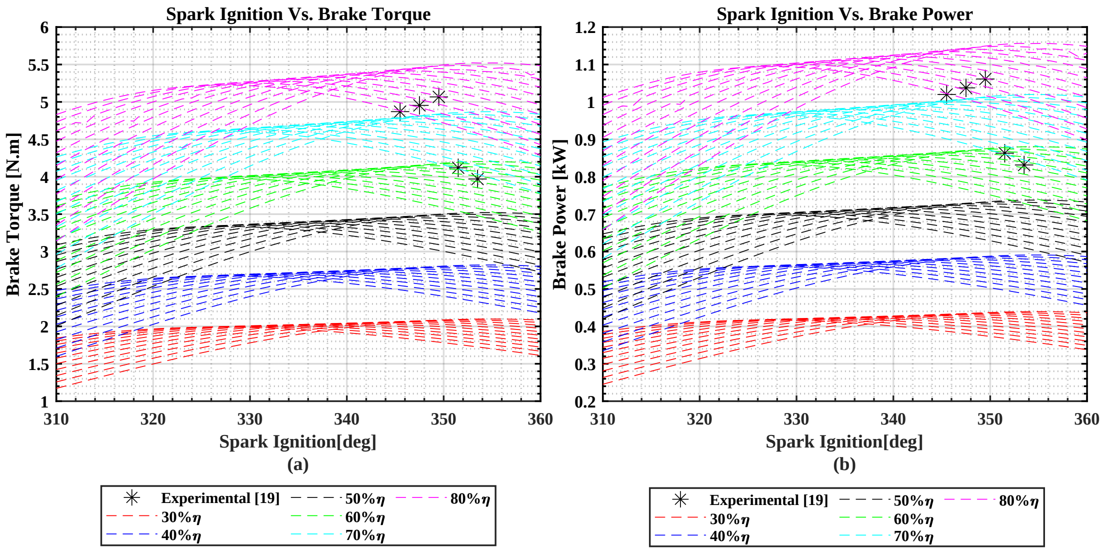

Figure 4.11: Case scenario III - (a) Brake torque (b) Brake power vs spark ignition.

4.4 Stage IV: Optimization Part Two

In this study, the optimization of the CR engine is considered the action of predicting the optimum spark ignition timing and the optimum engine speed. According to section 4.3.3.3, the maximum combustion efficiency of the CR engine was assumed during this process. The assumptions were made according to the condition of the mixture, such as lean, stoichiometric, and rich condition. Thus, six different case scenarios were developed based on the mixture type and the engine load (see section 3.5). In the following sections, only the selected ideal case scenario is shown and discussed. In terms of other case scenarios, their analyses are presented in the Appendices (please refer to section A).

4.4.1 The Optimum Ignition Timing

A simulation under various engine speeds with varying engine ignition timing at each speed was conducted to define the best ignition timing for the CR engine. Meanwhile, the mixture of the fuel was assumed lean (ideal conditions) at full engine load (please refer to Table 3.3). The brake torque and brake power variations were recorded and presented in Figure 4.12 (a) and (b), respectively. The overall shape of the plots indicates that the brake power and torque increased with the advance of spark ignition and then decreased slightly when the ignition timing was advanced further.

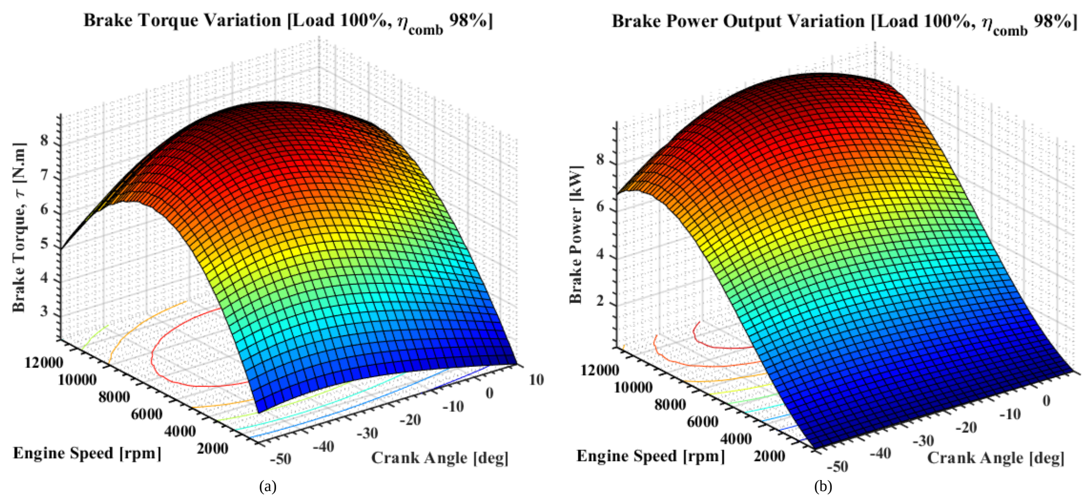

Figure 4.12: 3D plot of (a) brake torque (b) brake power variation of the CR engine.

Figure 4.12 (b), present the brake power output variation as the engine increased and igniting timing varied accordingly at each speed. Based on the figure, the lowest values of engine power were obtained at the early stage of simulation, where the CR engine speed was initiated at 1000 rpm and increased up to 5000 rpm. However, there was a gradual growth in the brake power during the beginning of the simulation till this moderated climb became a considerable rise at 6000 rpm. In fact, the highest brake power outputs were recorded when the engine was running between 7000 rpm till 11500 rpm while the spark ignition was set between 10° CA BTDC and 30° CA BTDC caused by the reduction of heat transfer per cycle due to the increment in engine speed. Moreover, a slight decrement of power output can be detected when the engine speed passes 12000 rpm. This reduction continued till the final tested engine speed, which is at 13000 rpm.

Figure 4.12 (a) illustrate the brake torque variation where the engine speed increased from 1000 rpm to 13000 rpm while at each engine speed, the ignition timing changed from 50° CA BTDC to 10° CA ATDC. By utilizing the jet color-map illustration, it can be noted that the higher brake torques are obtained between 7000 rpm and 11000 rpm while the ignition timing was set between 36° CA BTDC and 12° CA BTDC. Based on the given data, the engine brake torque increased as the ignition became more advance, and the speed raised almost up to 9000 rpm. Then, this parameter decreased slightly when the ignition timing was advanced further, and the engine speed increased between 9000 rpm till 13000 rpm.

According to Figure 4.12 (b), the highest power output was obtained at 9.8388 kW when the CR engine was running at 12000 while the ignition occurred at 342° CA (18° CA BTDC). Meanwhile, the lowest values of this parameter were obtained at the early stage of simulation, where the CR engine speed was started (from 1000 rpm till 5000 rpm). The minimum brake power value is 0.24367 kW, and the ignition timing was 370° CA, equivalent to 10° CA ATDC. In addition, the maximum brake torque value is obtained at 8.9144 N.m during the simulated engine speeds and spark timings. To be precise, this maximum value was obtained when the ignition was set at 336° CA, which is equivalent to 24° CA BTDC, and it is achieved at 8800 rpm. Meanwhile, the lowest brake torque was recorded around 2.3 N.m during the initial engine speed at 1000 rpm. This value was acquired when the engine ignition timing was set at 10° CA ATDC.

For a better illustration, a contour representation was used in Figure 4.13 to show the variation of CR engine brake torque at different speeds and ignition timings under full engine load conditions. To determine the optimum ignition timing, it is required to observe and obtain the MBT. The brake torque increases to the highest possible value then decreases while advancing the engine spark from an initial retarded setting at each engine speed. To maintain the optimum timing and engine performance, the ignition timing must be advanced every time the engine speed increases due to the influences on the combustion process, which causes the increment of its duration. Thus, the value of MBT is highly dependent on the engine speed.

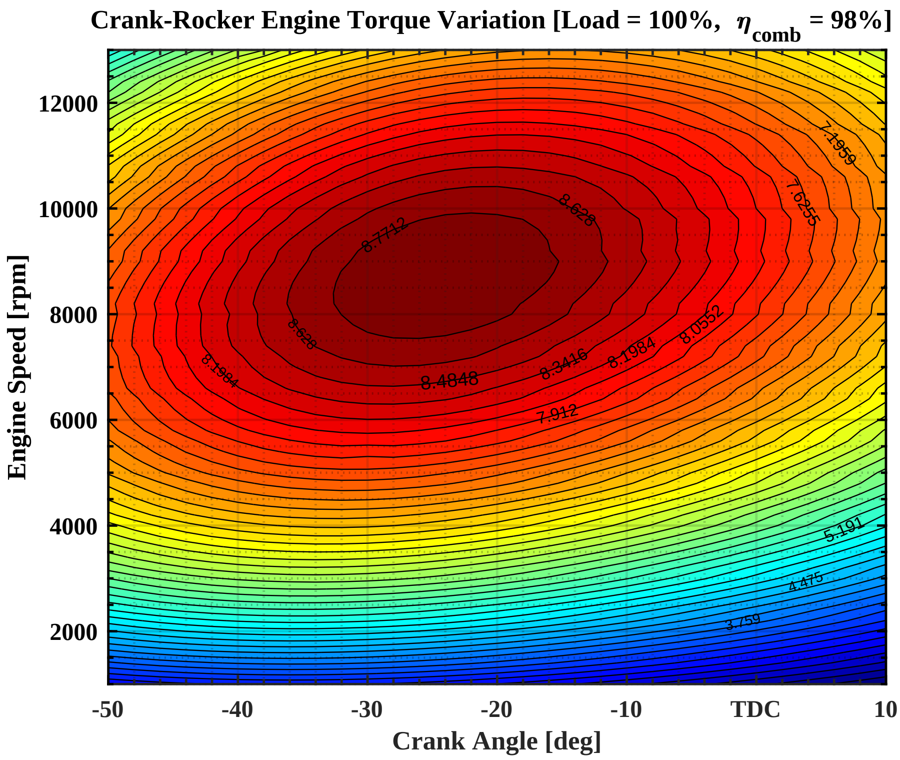

Figure 4.13: A contour representation of brake torque variation of the CR engine.

Moreover, the brake torque and power rise when the spark timing increases (advanced from 5° CA BTDC till 24° CA BTDC) resulting from the growth of the in-cylinder pressure, which causes the piston to produce more work. However, if the spark ignition timing is further advanced, the peak pressure is obtained while the piston is still in motion due to the ignition that occurred before the piston reached the TDC (its maximum point). Under these circumstances, the produced work by the gas would be decreased, thus reducing the engine performance capability.

4.4.2 The Optimum Engine Speed

To define the optimum ignition timing, the advanced spark that MBT has been obtained is selected. With reference to Figures 4.12 (a) and 4.13, the MBT was obtained at 8.9144 N.m while the spark occurred at 24° CA BTDC. However, to determine the optimum speed of the CR engine, the obtained brake torque and power during the optimum ignition timing have been used. These data are presented in Figures 4.14 (a) together with the acquired BSFC and BTE data 4.14 (b). A 3D representation of BSFC and BTE are provided in Figure 4.15 (a-b).

The brake torque and power variation of the CR engine at different speeds, while the optimum ignition timing was chosen at 24° CA BTDC, are shown in Figure 4.14 (a). Meanwhile, the BTE and BSFC variations are presented in sub-figure (b). Overall, The CR engine brake torque increased quickly and reduced right after MBT as the engine speed raised gradually. However, the brake power continued its significant increment. In terms of BSFC, the fuel consumption during the initial engine speed was higher than the finishing point, while the initial BTE was lower than the one recorded at the final engine speed.

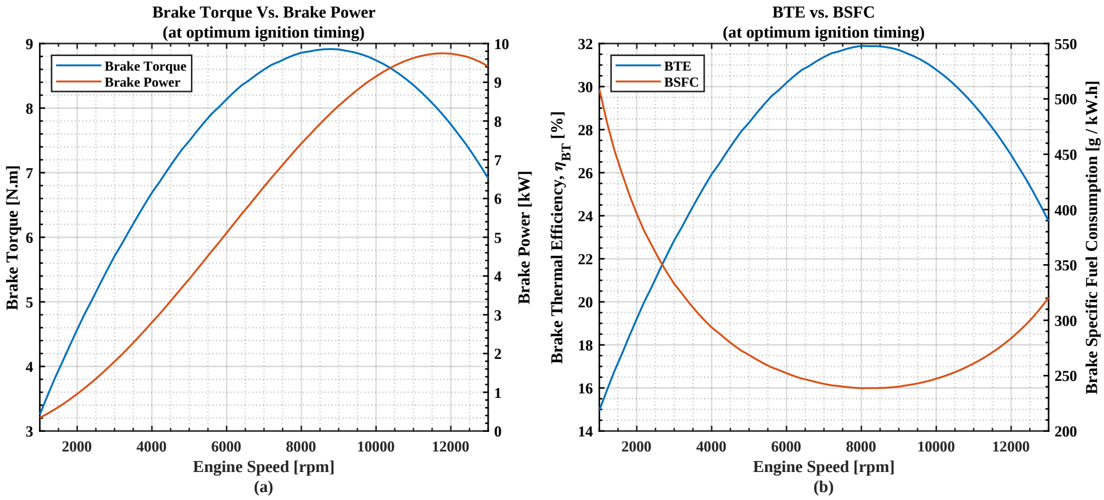

Figure 4.14: (a) Brake torque and brake power (b) BSFC and BTE vs engine speed at optimum ignition timing.

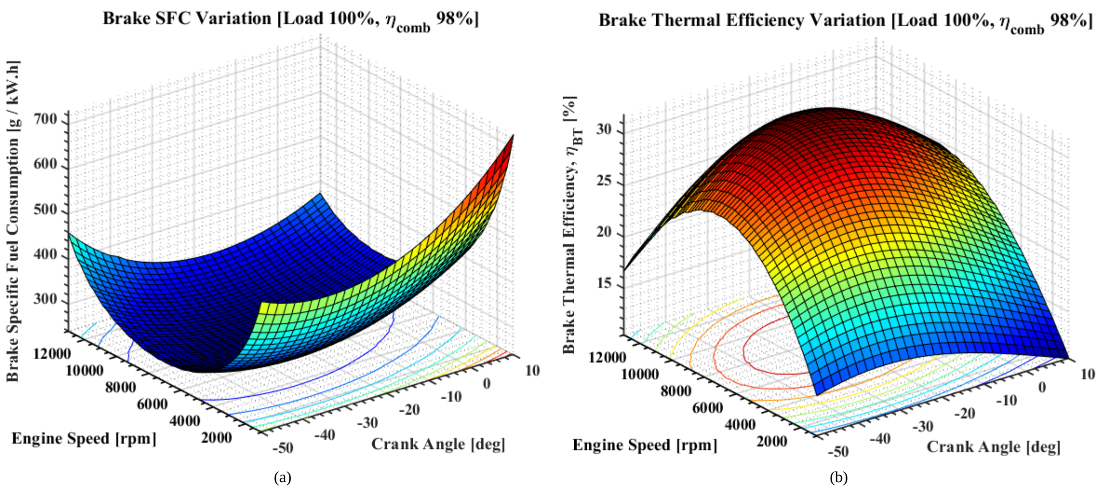

Figure 4.15: 3D plot of (a) BSFC (b) BTE variation of the CR engine.

With reference to the brake torque and power plots in in Figure 4.14 (a), the maximum brake power was obtained at 9.75 kW when the engine was running at 11800 rpm. However, the MBT at optimum ignition timing occurred at 8800 rpm, which the corresponding brake power was obtained slightly above 8 kW. Based on the given data, the maximum rate of reduction in CR engine brake torque happened at 10000 rpm (i.e., 8.7 Nm), which can be justified by the fact that the volumetric efficiency of the CR engine is decreased resulting from the increment of the engine speed. This phenomenon has happened because it becomes significantly difficult to fill the curved cylinder with the air-fuel mixture. In addition, there is not an adequate amount of time for the mixture to completely burn because of the fast rotation in the engine. However, it burns at a higher rate than any other point of air-fuel equivalence ratio, which causes the mixture temperature to increase, which results in higher in-cylinder pressure. As a result of the increased pressure inside the cylinder, the engine can provide higher torque and power due to the higher discharged force on the piston.

In Figure 4.14 (b), the BSFC as a function of engine speed at optimum ignition timing is illustrated. It is found that the BSFC reduced as the CR engine speed increased about 8500 rpm and then began to rise once the engine speed exceeded 9000 rpm. Higher BSFC has been found due to incomplete combustion, heat losses, and friction losses. The lowest BSFC is obtained, around 238.66 g/kWh, which occurred at 8000 rpm. The difference between the minimum and the obtained BSFC at MBT is only 0.75 g/kWh which occurred when the engine was running at 8800 rpm with BSFC recorded at 239.41 g/kWh. According to Heywood [42], the specific fuel consumption of an engine increases during three stages. Firstly, at a low compression ratio because of low thermal efficiency, at a higher engine speed where the friction and pumping losses are increased, and during lower engine speed, that engine has a higher rate of heat loss. In terms of BTE, it can be noted that the BTE increases with the engine speed increased up to 8500 rpm with a maximum value of around 32% and then slightly decreased only about 0.02% at the MBT while it fell in to decline once the engine speed passed 9000 rpm.

In Figure 4.16 (a-d), the combustion characteristics of the CR engine at optimum speed and ignition timing is illustrated. These results are the prediction of combustion parameters such as 4.16 (a) in-cylinder pressure, 4.16 (b) heat transfer rate, 4.16 (c) mass fraction burn, and 4.16 (d) temperature variations within the cycle. The maximum in-cylinder pressure was obtained at 48.75 bar, while the peak is close to the TDC at 376 ° CA equivalent to 16° ATDC. One reason for predicting a high in-cylinder pressure is that the piston of CR engine tends to stay longer at TDC. This allows the air-fuel mixture to burn completely which not only improves the combustion rate but also the engine performance will be increased. Meanwhile, the highest heat release rate recorded at 367° CA equals to 7° CA ATDC about 11.1 $\times 10^{-3}$ $\frac{kJ}{CA}$.

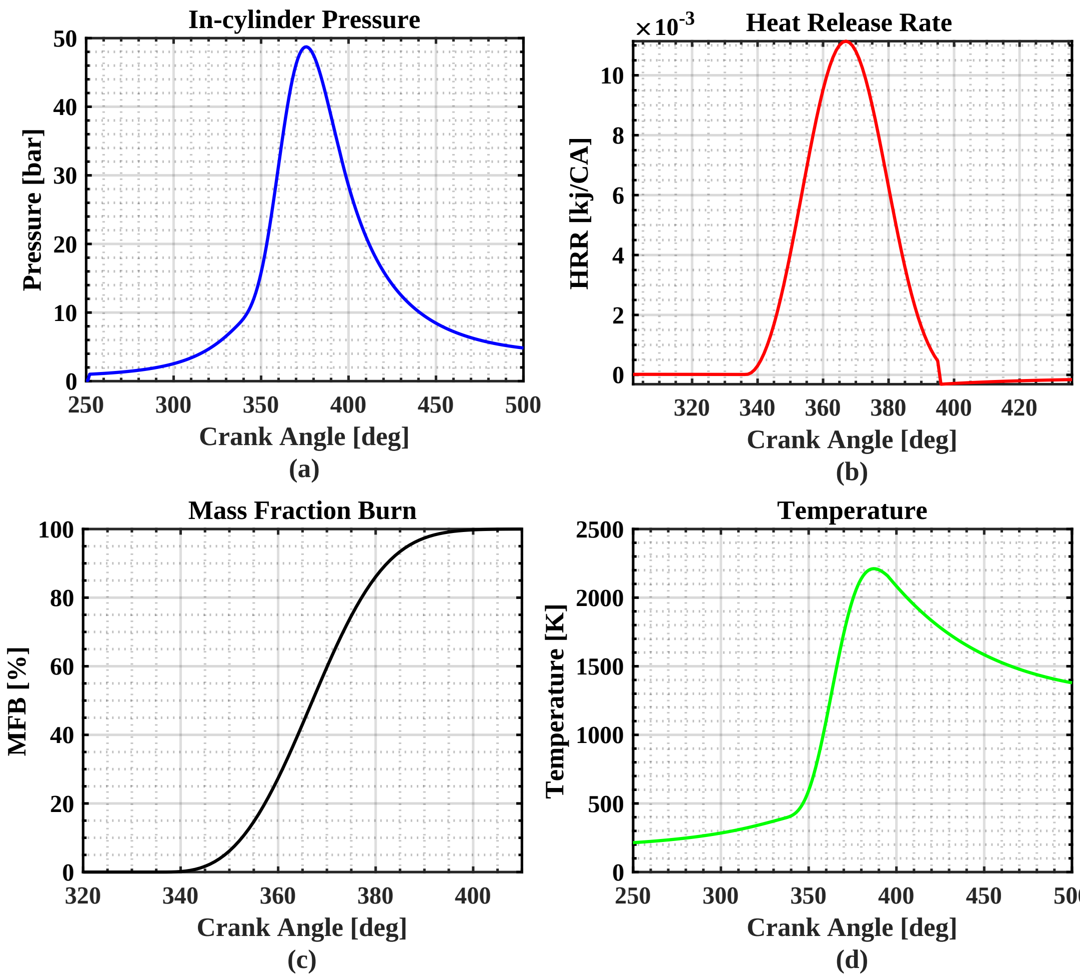

Figure 4.16: (a) In-cylinder pressure (b) Heat release (c) MFB (d) Temperature of the CR engine at optimum speed and ignition timing.

4.4.3 Benchmarking Analysis

In order to compare the predicted CR engine performance parameters with an existing conventional model, a benchmark analysis has been conducted. The purpose of this analysis is to shed light on the difference between CR engine and Modenas - ACE115 (motorcycle engine) performance parameters as selected benchmark. This engine was used for benchmarking in [12, 18]. Since this research is a continue work of the mentioned studies, thus, this comparison with Modenas engine is required for future development and improvement on CR engine. The engine specification and performance parameters comparison of these two engines are provided in Table 4.4 and Table 4.5, respectively.

Table 4.4: Engines specification comparison.

No.	**Parameters**	**Modenas-ACE115**	**CAREM CR Engine**
1	Displacement (cm3)	120	120
2	Number of Strokes	4	4
3	Number of Cylinder	1	1
4	Bore $\times$ Stroke (mm)	55 $\times$ 50.60	55 $\times$ 50.60
5	Compression Ratio	9:8:1	8:1

Table 4.5: Engines performance comparison.

No.	Parameters	Modenas - ACE115	CAREM CR Engine	Difference	Relative Error Percentage
1	Maximum Brake Torque (N.m)	9.10	8.91	0.19	2.04
3	Maximum Brake Power (kW)	7.30	9.75	2.45	33.56
5	Brake Mean Effective Pressure (bar)	9.5	9.3	0.19	2.04

According to Table 4.4, the Modenas - ACE115 engine size is 120 cc with bore and stroke of 55 mm and 50.60 mm, sequentially. With regards to Table 4.5, the main performance parameters are recorded; whereas the maximum brake torque is slightly above 9 N.m, and brake power of 7.3 kW is obtained. However, the maximum brake torque for the CR engine was obtained slightly lower than ACE115 with difference of approximately 0.2 N.m only. In terms of power, the Modenas engine power is stated exactly 7.3 kW which is slightly lower than the CR engine by 2.45 kW. Base on the data, the CR engine performance characteristics show a good match with Modenas - ACE115 in terms of MBT, while the CR engine has a higher rate in term of power. According to the third row of Table 4.5, the brake mean effective pressure is calculated around 9.5 bar and 9.3 bar for ACE115 and CR engine, respectively.

4.4.4 Comparison Between The Cases

According to Table 3.3, the optimization part II was conducted under six different case scenarios. One of these scenarios was selected as the ideal case that has been discussed in the previous sections. In terms of other conditions, summary tables have been presented to illustrate the variation of the primary output data such as MBT, optimum ignition, optimum speed, brake torque, brake power, BSFC, and brake thermal efficiency while the figures are shown in Appendix A.

In Table 4.6, the MBT variations at different case scenarios are presented. In terms of the full engine load, it can be noted that the value of MBT increased as the mixture became richer while the MBT occurred at 24° CA BTDC. Thus, the ignition timing that MBT has achieved is considered as optimum timing, and the given brake torque from other timing that is advanced or retarded from the optimum is lower. Meanwhile, in terms of the partial load, the ignition timing decreased to 22° CA and 20° CA BTDC. Based on Heywood [42], the optimum timing is highly dependent on the combustion duration primary parameters such as flame development rate, the rate of propagation, the distance traveled by the flame throughout the cylinder, and the flame termination process details right after reaching the cylinder wall. Therefore, it is important to further modify the mode by including the combustion duration modeling in the developed model, as was recommended previously.

Table 4.6: MBT variation at different case scenarios.

Case Scenario	Engine Load	Mixture	Combustion Efficiency	Lambda	MBT		
					Value [N.m]	Ignition Timing	Speed [rpm]
#1	Full Load	Lean	98%	1.2	8.9144	24 deg BTDC	8800
#2		Stoichiometric	95%	1	12.0389	24 deg BTDC	8750
#3		Rich	85%	0.8	13.2325	24 deg BTDC	9000
#4	Partial Load	Lean	98%	1.2	8.11626	22 deg BTDC	8800
#5		Stoichiometric	95%	1	11.0338	20 deg BTDC	9000
#6		Rich	85%	0.8	11.1805	20 deg BTDC	9000

Furthermore, the minimum and maximum obtained brake torque and power can be found in Tables 4.7 and 4.8. The engine speeds that MBT has obtained are recorded between 8750 rpm to 9000 rpm. The highest brake torque is about 13.23 N.m under this condition which belongs to the case scenario 3, where the engine mixture was rich at full engine load. The minimum values of both parameters are obtained at 1000 rpm engine speed while the values slightly increased as the mixture became richer and the combustion efficiency reduced. Moreover, the brake power at MBT reduced when the engine load became half (50 % load). During full load condition, the brake power at MBT was recorded at 8.21 kW, 11.03 kW, and 12.47 kW when the mixture was assumed lean, stoichiometric, and rich, respectively. However, these values reduced by 0.73 kW, 0.63 kW, and 1.93 kW at partial engine load in that order.

Table 4.7: The brake torque variation at different case scenarios.

Case Scenario	Ignition Timing	Brake Torque			
		Min. Value [N.m]	Speed [rpm]	Max. Value [N.m]	Speed [rpm]
#1	24 deg BTDC	3.25	1000	8.91	8800
#2	24 deg BTDC	4.31	1000	12.04	8750
#3	24 deg BTDC	4.73	1000	13.23	9000
#4	22 deg BTDC	2.88	1000	8.12	8800
#5	20 deg BTDC	3.80	1000	11.03	9000
#6	20 deg BTDC	3.86	1000	11.18	9000

Table 4.8: The brake power variation at different case scenarios.

Case Scenario	Ignition Timing	Brake Power					
		Min. Value [kW]	Speed [rpm]	Max. Value [kW]	Speed [rpm]	Value [kW] at MBT	Speed [rpm]
#1	24 deg BTDC	0.34	1000	9.75	11800	8.21	8800
#2	24 deg BTDC	0.45	1000	13.36	12000	11.03	8750
#3	24 deg BTDC	0.50	1000	14.72	12000	12.47	9000
#4	22 deg BTDC	0.30	1000	8.85	11800	7.48	8800
#5	20 deg BTDC	0.40	1000	12.30	12000	10.40	9000
#6	20 deg BTDC	0.40	1000	12.46	12000	10.54	9000

Table 4.9 and 4.10 provides information on the variation of the BSFC and BTE during optimization process II. Overall, the BSFC and BTE are increased and decreased accordingly as the engine mixture varied from lean to rich. Based on the Figure (ref), the BSFC as a function of ignition timing and engine speed decreased as the engine speed increased and the spark timing advanced further. However, this decrement started to become an increment when the simulation passed the MBT point. Regarding Table 4.9, there are insignificant differences between the minimum obtained BSFC values and that others acquired at MBT. At 100 percent engine load, the lowest BSFC recorded slightly above 238.5 g/kWh when the mixture is assumed lean, and the highest BSFC belongs to the third scenario at about 361 g/kWh, where the mixture was set at rich condition. As the engine load reduced by half, the BSFC trends showed a similar path; the value of each scenario raised slightly at this condition where the highest and lowest value was recorded, about 314 g/kWh and 243 g/kWh, respectively. In terms of BTE, the thermal efficiency of the CR engine dropped as the mixture changed from lean to rich, while the difference during the full load and partial load is insignificant. Under the six scenarios, the first and second highest BTE obtained around 32 % and 31 % during the first and the fourth scenario, respectively.

Table 4.9: The BSFC variation at different case scenarios.

Case Scenario	Ignition Timing	Brake Specific Fuel Consumption					
		Min. Value [g/kWh]	Speed [rpm]	Max. Value [g/kWh]	Speed [rpm]	Value [g/kWh] at MBT	Speed [rpm]
#1	24 deg BTDC	238.66	8000	508.88	1000	239.41	8800
#2	24 deg BTDC	254.52	8250	553.90	1000	254.83	8750
#3	24 deg BTDC	361.30	8400	789.29	1000	362.60	9000
#4	22 deg BTDC	243.34	8200	521.35	1000	244.35	8800
#5	20 deg BTDC	258.27	8400	569.60	1000	259.19	9000
#6	20 deg BTDC	314.44	8500	693.63	1000	315.68	9000

Table 4.10: The BTE variation at different case scenarios.

Case Scenario	Ignition Timing	Brake Thermal Efficiency					
		Min. Value [%]	Speed [rpm]	Max. Value [%]	Speed [rpm]	Value [%] at MBT	Speed [rpm]
#1	24 deg BTDC	14.96	1000	31.89	8000	31.79	8800
#2	24 deg BTDC	13.74	1000	29.90	8250	29.87	8750
#3	24 deg BTDC	9.64	1000	21.07	8400	20.99	9000
#4	22 deg BTDC	14.60	1000	31.28	8200	31.15	8800
#5	20 deg BTDC	13.36	1000	29.47	8400	29.37	9000
#6	20 deg BTDC	10.97	1000	24.20	8500	24.11	9000

4.5 Summary

In this chapter, the results and related discussions for numerical investigation and optimization of the CR engine ignition timing based on performance and combustion characteristics are provided. In section 4.2, the validation of the modified combustion model has been discussed using in-cylinder pressure data obtained experimentally and theoretically while theoretically comparing the accuracy of the proposed correlation for heat transfer prediction. In general, the Annand model has obtained the lowest maximum pressure with the highest accuracy and a reasonable commutating time compared to the other three correlations. Thus, it was decided to continue the investigation and optimization part one using Annand as a prospective heat transfer correlation model for the modified combustion model.

In section 4.3, the results for optimization part one are presented. The experimental data were compared with simulation acquired data in terms of in-cylinder pressure and brake torque at different ignition timing and speed. The purpose of the first validation of stage III is to evaluate the pressure data in section 4.3.1, while the second validation is to compare the obtained braked torque and power in section 4.3.2. According to the first validation of stage III, it was concluded that the combined CR model development is well accepted for further investigation, specifically in terms of the optimization process where the engine speed and ignition timing varied. Two methods of the simulation were carried out during the second validation. In the first one, a fixed combustion duration was assumed while the combustion efficiency was varied, and the second method considered both parameters as a fixed value. As a result of a significant amount of error in the prediction of brake torque, the influence of the combustion duration and assumed combustion efficiency led to the three case-scenario studies for further investigating the effects of these parameters on the main optimization output (see section 4.3.2.1).

With reference to section 4.3.3, the influence of assumed maximum combustion efficiency and combustion duration have been discussed. Based on the first case scenario's result (see section 4.3.3.1), the CR engine was operating under fuel-rich conditions during the experiment; thus, the simulation and experimental results were obtained at a high error percentage during the second validation of stage III. Moreover, this was further justified by the fact that incomplete combustion frequently occurred resulting from an insufficient amount of oxygen in the mixture that caused the efficiency of combustion to drop. During case scenario two investigation (see section 4.3.3.2), it was concluded that the uncertainty in the result due to the combustion duration is high; therefore, it is highly important to develop a model for combustion duration in terms of optimization. This conclusion was made due to the strong influence of the engine speed on the burning rate of a mixture.

The optimization part two of this research was considered as a prediction of the optimum timing and speed. The result and discussion of this topic can be found in section 4.4, where main output parameters such as brake torque, brake power, BSFC, and BTE are presented. In sections 4.4.1 and 4.4.2, a detailed analysis of these parameters is provided. Based on the obtained data in section 4.4.4, the optimum timing and optimum speed of the CR engine were predicted at 24° CA BTDC while the optimum speed that MBT occurred varied from 8750 rpm to 9000 rpm. A benchmark comparison is provided in section 4.4.3, where the results of the CR engine are compared with a conventional model known as Modenas- Kriss (motorcycle engine).

CHAPTER 5

CONCLUSIONS AND FUTURE DIRECTIONS

5.1 Overview

In this research, a newly developed ICE with a curved-cylinder combustion chamber known as Crank-Rocker was investigated and optimized numerically in terms of ignition timing based on its performance and combustion characteristics. This engine was developed based on an alternative way of producing a crank output motion with oscillating curved-piston by using a four-bar mechanism. It is believed that it could enhance the thermodynamic cycles and function as an alternative engine in terms of performance due to its unique geometry.

Several studies have been conducted to investigate the CR engine behavior while finding alternative methods to improve its performance. There was a significant need to optimize the CR engine in terms of the ignition timing while increasing the performance. However, the majority of the previously done investigation on ignition timing was conducted based on other conventional engine types. Thus, investigation regarding the toroidal engine could be rarely found. Several studies have been carried out based on the combustion and performance characteristics of the CR engine. However, the detailed investigation of these characteristics with respect to the ignition timing was still unknown. Therefore, this research aimed to study the influence of changing the ignition timing on performance characteristics while defining the best timing for the full-load performance of the engine using numerical modeling. In addition, this work intended to numerically select the optimum timing that yields the optimum operating condition under various engine operating conditions.

Various tasks were required to be undertaken to obtain the above objectives. It was essential to take several measures in terms of methodology, such as thermodynamic analysis, heat release analysis, and combustion analysis. These analyses were developed according to the first law of thermodynamic, mass and energy conservation, and ideal gas law. Moreover, several losses were considered that could influence the performance of an engine including, friction losses, in-cylinder mass, and heat losses. Thus, the objectives could be achieved with high accuracy. In general, four main stages structured the methodology of this research. The works that have been done are summarized as follows:

1. Stage I: Modified Combustion Model

    - This section focused on conducting various modifications and improvements on the previously developed combustion model. These modifications and improvements include developing a single-zone combustion model based on the developed heat released by Krieger and Borman. In addition, investigating various developed models for gamma and adopting the most suitable one based on the previous literature works. Then, developing a polynomial model of the internal energy for the combustion product and thermodynamic formulation of a specific heat ratio model was considered as further actions. Lastly, conducting the required correction on the previously developed combustion model for the CR engine, including reconsidering some essential assumptions, were part of this stage activities. It should be mentioned that all the above developments were done in MATLAB ®.

2. Stage II: Heat Transfer Comparison and Evaluation

   - This stage has studied the implementation of different heat transfer coefficient correlations to provide the most accurate single-zone combustion model for the CR engine by selecting the optimal choice for the heat transfer model. For this purpose, the previously developed modified CR combustion model was adopted, and four different models have been established based on the selected correlations for heat transfer calculation. The incorporated correlations are namely known as Woschni, Hohenberg, Annand, and Sitkei.

3. Stage III: Optimization Part I

   - This part of the research has investigated the influence of various parameters including, different ignition timing, engine speed, and engine load on CR engine optimization based on performance characteristics. Moreover, it was found out that there are mainly two assumed parameters in the modified CR model that influence the results during the validation. For this reason, three case scenarios were developed, and the effects of each parameter have been studied.

4. Stage IV: Optimization Part II

   - The effects of varying the ignition timing and engine speed on the performance characteristics of the CR engine were investigated right after developing a model for such purposes. This development was included the modification of the optimization model based on the outcomes of stage three (optimization part I). In addition, the modified optimization model was developed in a way that is more user-friendly in terms of various operating conditions, assumptions setting, data handling, evaluation, selections of the key parameters, and plotting. Then, the simulation was conducted under six different case scenarios in terms of operating conditions to define the optimum ignition timing at each.

5.2 Conclusions

The following conclusions are made based on the research outcome of each stage:

1. In terms of stage I and II, further simulations were conducted to investigate the characteristics of model outputs under various operating conditions upon model validation by a comparison study between the results obtained experimentally and theoretically. These analyses include study the pressure and temperature trends for all the correlations. Based on the results, it was found out that the models developed by Hohenberg and Annand predicted the highest maximum pressure and temperature, respectively. In order to compare the accuracy of the prediction, the recorded in-cylinder pressure data was compared with those obtained experimentally at a constant engine speed of 2000 rpm at full load condition. Based on this comparison, it was found out that Annand obtained the lowest error ad matched well with the experimental data while others such as Woschni, Hohenberg, and Sitkei overestimated. Thus, the heat transfer correlation developed by Annand was considered as the best and optimum option for CR engine combustion modelling. This conclusion was also made based on other criteria such as the limit of acceptable error, computational time, and usage. With these additional criteria for consideration, the second most preferable correlation is Sitkei followed by Woschni and Hohenberg.

2. The influence of various parameters on CR engine optimization based on performance characteristics by varying the ignition timing has been investigated in stage III. According to the first validation of this stage, it was concluded that the combined CR model development is well acceptable for the optimization process. However, during the second validation, due to the high error percentage between simulation and experiment data, the influence of combustion duration and assumed maximum combustion efficiency on prediction of the model is high, which led to the three case scenarios studies. Based on the results, the torque and power are not only influenced by engine speed and load but also by the combustion efficiency and combustion duration of the engine. After further investigation, it was concluded that the experimental data of brake torque and

power were obtained while the engine was operating under fuel-rich conditions. Thus, incomplete combustion frequently occurred because of an insufficient amount of oxygen in the mixture that caused the efficiency to drop. Moreover, based on the uncertainty in the results of case scenario one and two, it was concluded that the model needs to be further modified in terms of combustion duration. This parameter should be varied as well as engine load and speed during the optimization process to define the maximum brake torque and optimum spark ignition. A simple assumption of increasing or decreasing the combustion duration based on the variation of the engine speed is not sufficient for such a highly influential parameter. Therefore, it was recommended to further modify the model in terms of the combustion duration modeling for future works on this topic.

3. The effects of varying the ignition timing on the performance characteristics of a crank rocker engine were investigated through simulations in stage IV. Six different case scenarios were assumed based on the mixture variation and the engine load. The ideal case scenario was selected at the lean condition with a combustion efficiency of 98% and engine load of 100%. Based on the investigation, it was found that the maximum values for the brake torque, power, and thermal efficiency were 8.9 Nm, 8 kW, and 32%, respectively, while ignition timing was adjusted to 24° CA BTDC for the ideal condition. From the simulation results, it is found that the BSFC decreases as the spark timing increases up to 24° CA BTDC and starts to increase when the ignition timing exceeds 24° CA BTDC. According to the comparison with benchmark data, the CR engine performance characteristics have a good match in terms of MBT by relative error percentage of 2.04%. Regarding other case scenarios, the MBT for three out of six scenarios was obtained at 24° CA BTDC. However, once the engine load was reduced, the optimum ignition timing dropped between 22° CA BTDC and 20° CA BTDC. Thus, the optimum spark ignition timing for the CR engine was at 336° CA, which has a better impact and is considered the best choice.

5.3 Recommendations and Future work

The present study has made contribution towards improving the CR engine characteristics by numerically optimizing the ignition timing. However, further research work is still required to achieve further improvements in terms of efficiency and performance of this novel engine. Therefore, the following recommendations are presented:

1. One of the main recommendations for future work is to further improve this study by including the emission prediction to the model and conducting the optimization based on performance and emission characteristics.

2. It is required to further improve the thermodynamic model by assuming two-zone combustion to include the emission prediction. Thus, it is highly recommended to further advance the combustion model of the CR engine by considering the quasi-dimensional modeling.

3. It is essential to develop a model for combustion duration calculation and prediction. The optimum ignition timing is highly dependent on the flame propagation and development rate, the flame length that passes through the cylinder, and the detailed calculation of the flame termination process once it reaches the cylinder wall. Thus, developing such a model and being included in the optimization model will increase the rate of accuracy.

4. The CR engine model can be further improved by including a model for intake and exhaust valves. This sub-model can include the related calculations of fluid and gas dynamics through the valves to predict precisely and obtain results with higher accuracy.

5. A general recommendation for this topic can be developing a graphical user interface for the developed model, which allows the users to specify the exact inputs and extract the required outputs without going through hundreds of code lines. Preparing a graphical user interface will also protect the lines of MATLAB codes from being deleted by accident during other investigations.

REFERENCES

[1] Venkata K.K. Upadhyayula, Abhijeet G. Parvatker, Anju Baroth, and Kavitha Shanmugam. Lightweighting and electrification strategies for improving environmental performance of passenger cars in india by 2030: A critical perspective based on life cycle assessment. *Journal of Cleaner Production*, 209:1604–1613, 2019.

[2] Choongsik Bae and Jaeheun Kim. Alternative fuels for internal combustion engines. *Proceedings of the Combustion Institute*, 36(3):3389–3413, 2017.

[3] Dheeraj Rathore, Abdul-Sattar Nizami, Anoop Singh, and Deepak Pant. Key issues in estimating energy and greenhouse gas savings of biofuels: challenges and perspectives. *Biofuel Research Journal*, 3(2):380–393, 2016.

[4] İlker Yilmaz and Murat Taştan. Investigation of hydrogen addition to methanol-gasoline blends in an si engine. *International Journal of Hydrogen Energy*, 43(44):20252–20261, 2018. The International Advanced Researches and Engineering Congress-2017 (IAREC 2017), 16-18 November 2017, Osmaniye, Turkey.

[5] Gvidonas Labeckas, Stasys Slavinskas, and Marius Mažeika. The effect of ethanol–diesel–biodiesel blends on combustion, performance and emissions of a direct injection diesel engine. *Energy Conversion and Management*, 79:698–720, 2014.

[6] J.W.G. Turner, R.J. Pearson, E. Dekker, B. Iosefa, K. Johansson, and K. ac Bergström. Extending the role of alcohols as transport fuels using iso-stoichiometric ternary blends of gasoline, ethanol and methanol. *Applied Energy*, 102:72–86, 2013. Special Issue on Advances in sustainable biofuel production

and use - XIX International Symposium on Alcohol Fuels - ISAF.

[7] Corey E Weaver. Advanced gasoline turbocharged direct injection (gtdi) engine development. *2011 DOE Vehicle Technologies Program Review*, 2011.

[8] Tim Lake, John Stokes, Richard Murphy, Richard Osborne, and Andreas Schamel. Turbocharging concepts for downsized di gasoline engines. Technical report, SAE Technical Paper, 2004.

[9] C Stan and S Taeubert. Analysis of engine performances improvement by down sizing in relationship with super-and turbocharging, adapted scavenging and direct injection. Technical report, SAE Technical Paper, 2009.

[10] Javad Zareei and AH Kakaee. Study and the effects of ignition timing on gasoline engine performance and emissions. *European Transport Research Review*, 5(2):109–116, 2013.

[11] Seref Soylu and Jon Van Gerpen. Development of empirically based burning rate sub-models for a natural gas engine. *Energy Conversion and Management*, 45(4):467–481, 2004.

[12] Salah E. Mohammed. *Development, Performance and Emission Assessment of a Single-cylinder Air-cooled Gasoline Crank-Rocker Engine*. PhD thesis, Universiti Teknologi PETRONAS, 2018.

[13] F. Amrouche, P. Erickson, J. Park, and S. Varnhagen. An experimental investigation of hydrogen-enriched gasoline in a wankel rotary engine. *International Journal of Hydrogen Energy*, 39(16):8525–8534, 2014.

[14] Karl V Hoose. Toroidal internal combustion engine, April 19 2005. US Patent 6,880,494 B2.

[15] Ronald A Holland. Opposed piston engine, October 22 2015. US Patent 2015/0300241 A1.

[16] Mirosław Szymkowiak and Stanislaw Szwaja. New concept of a rocker engine-kinematic analysis. *Journal of KONES*, 19:443–449, 2012.

[17] Eduardo Taurozzi. Balanced modular pendulum mechanism, May 7 2002. US Patent 6,382,143.

[18] Salah E Mohammed, MB Baharom, and A Rashid A Aziz. Performance and combustion characteristics of a novel crank-rocker engine. *Journal of Mechanical Science and Technology*, 31(7):3563–3571, 2017.

[19] Salah E Mohammed, MB Baharom, A Rashid A Aziz, A Ezrann Z Zainal, and F Firmansyah. Experimental investigation of ignition timing on the performance and emission characteristics of a crank-rocker engine. *International Journal of Vehicle Structures Systems (IJVSS)*, 10(2), 2018.

[20] K Roepke, A Rosenek, M Fischer, and PEP Pep. Practical application of doe methods in the development of production internal combustion engines. In *International Conference on Statistics and Analytical Methods in Automotive Engineering, London, England*, pages 105–115, 2002.

[21] Mark Guerrier and Paul Cawsey. The development of model based methodologies for gasoline ic engine calibration. Technical report, SAE technical paper, 2004.

[22] Salah E. Mohammed, M. B. Baharom, A. Rashid A. Aziz, and Ezrann Z. Zainal A. Modelling of combustion characteristics of a single curved-cylinder spark-ignition crank-rocker engine. *Energies*, 12(17), 2019.

[23] Ramtin. Kardan, M. B. Baharom, Salah E. Mohammed, A. Rashid A. Aziz, Ezrann Z. Zainal A., and Firmansyah. The effect of engine throttle position on the performance characteristics of a crank-rocker engine fitted with a conventional cylinder head. *AIP Conference Proceedings*, 2035(1):020001, 2018.

[24] Salah E Mohammed, MB Baharom, and A Rashid A Aziz. Thermodynamic analysis of a single cylinder crank-rocker engine. *ARPN J. Eng. Appl. Sci*,

11:12239–12246, 2016.

[25] Jeremy L Cuddihy. *A user-friendly, two-zone heat release model for predicting spark-ignition engine performance and emissions*. PhD thesis, University of Idaho, 2014.

[26] Ronald J Pierik and James F Burkhard. Design and development of a mechanical variable valve actuation system. Technical report, SAE Technical Paper, 2000.

[27] W. H. Adams, H. G. Hinrichs, F. F. Pischinger, P. Adamis, V. Schumacher, and P. Walzer. Analysis of the combustion process of a spark ignition engine with a variable compression ratio. *SAE Transactions*, 96:749–757, 1987.

[28] Hakan Ozcan and Jehad A.A. Yamin. Performance and emission characteristics of lpg powered four stroke si engine under variable stroke length and compression ratio. *Energy Conversion and Management*, 49(5):1193–1201, 2008.

[29] Jehad A.A. Yamin and Mohammad H. Dado. Performance simulation of a four-stroke engine with variable stroke-length and compression ratio. *Applied Energy*, 77(4):447–463, 2004.

[30] Takefumi Hosaka and Minoru Hamazaki. Development of the variable valve timing and lift (vtec) engine for the honda nsx. *SAE transactions*, 100(3):1–7, 1991.

[31] Shahnawaz Ahmed Khan and Prajod Ayyappath. Design and development of variable valve timing and lift mechanism for improving the performance of single cylinder two wheeler gasoline engine. Technical report, SAE Technical Paper, 2014.

[32] Gregory J Thompson, Zenovy S Wowczuk, and James E Smith. Rotary engines–a concept review. 2003.

[33] H Hüttlin. Oscillating piston machine. *United State Patent Office*, 20, 2008. US

Patent 7,435,064,.

[34] L Giurca. Hybrid opposite piston engine-hope & portable range extender. *Powertrain Tech*, 2013.

[35] Braden A Murphy, Erica A Fraser, and Darrel A Doman. Review of recent toroidal rotary engine patents. *Recent Patents on Mechanical Engineering*, 6(1):26–36, 2013.

[36] S. Hanis. Development of crank-rocker mechanism in an internal combustion engine. Master's thesis, Universiti Teknologi PETRONAS, Malaysia, 2013.

[37] Ralph Morgado. Internal combustion engine and method, August 30 2007. US Patent 2007/0199537 A1.

[38] Frederic Beck. Rotary explosion-motor, November 29 1910. US Patent 977,260.

[39] Alvah L Powell. Internal-combustion engine, December 29 1925. US Patent 1,567,172.

[40] Louis J Wolff. Internal-combustion engine, June 9 1931. US Patent 1,809,577.

[41] M. Szymkowiak and S. Szwaja. New concept of a rocker engine - kinematic analysis. *Journal of KONES*, Vol. 19, No. 3:443–449, 2012.

[42] John B Heywood. *Internal combustion engine fundamentals*. McGraw-Hill Education, 2018.

[43] K. Atashkari, N. Nariman-Zadeh, M. Gölcü, A. Khalkhali, and A. Jamali. Modelling and multi-objective optimization of a variable valve-timing spark-ignition engine using polynomial neural networks and evolutionary algorithms. *Energy Conversion and Management*, 48(3):1029–1041, 2007.

[44] Wei Chen, Jianfeng Pan, Wenming Yang, Yangxian Liu, Baowei Fan, Yao Lu, and Peter Otchere. Stratified combustion characteristics analysis and assisted-ignition strategy optimization in a natural gas blended diesel wankel engine.

Fuel, 292:120192, 2021.

[45] Omar I. Awad, R. Mamat, Obed M. Ali, W.H. Azmi, K. Kadirgama, I.M. Yusri, A.M. Leman, and T. Yusaf. Response surface methodology (rsm) based multi-objective optimization of fusel oil -gasoline blends at different water content in si engine. *Energy Conversion and Management*, 150:222–241, 2017.

[46] Tetsuya Nakayasu, Hajime Yamada, Toshikazu Suda, Noritoshi Iwase, and Kyo Takahashi. Intake and exhaust systems equipped with a variable valve control device for enhancing of engine power. *SAE Transactions*, 110:166–173, 2001.

[47] Mustafa Gölcü, Yakup Sekmen, Perihan Erduranlı, and M. Sahir Salman. Artificial neural-network based modeling of variable valve-timing in a spark-ignition engine. *Applied Energy*, 81(2):187–197, 2005.

[48] I.M. Yusri, R. Mamat, W.H. Azmi, A.I. Omar, M.A. Obed, and A.I.M. Shaiful. Application of response surface methodology in optimization of performance and exhaust emissions of secondary butyl alcohol-gasoline blends in si engine. *Energy Conversion and Management*, 133:178–195, 2017.

[49] Jun Li, Chao Guo, Wenbin Wang, and Zhuojian Wu. Optimal mixture ratios of biodiesel ethanol diesel for diesel engines. *Energy and Power Engineering*, 3(5), 2011.

[50] Xun Shen, Yahui Zhang, Tielong Shen, and Chanyut Khajorntraidet. Spark advance self-optimization with knock probability threshold for lean-burn operation mode of si engine. *Energy*, 122:1–10, 2017.

[51] Seima Tsuboi, Shinji Miyokawa, Masayoshi Matsuda, Takeshi Yokomori, and Norimasa Iida. Influence of spark discharge characteristics on ignition and combustion process and the lean operation limit in a spark ignition engine. *Applied Energy*, 250:617–632, 2019.

[52] Naoto Hayashi, Akimitsu Sugiura, Yuya Abe, and Kotaro Suzuki. Development of ignition technology for dilute combustion engines. *SAE International Journal*

of Engines, 10(3):984–994, 2017.

[53] Fang-Xi Xie, Xiao-Ping Li, Xin-Chao Wang, Yan Su, and Wei Hong. Research on using egr and ignition timing to control load of a spark-ignition engine fueled with methanol. *Applied Thermal Engineering*, 50(1):1084–1091, 2013.

[54] Ritchie Daniel, Guohong Tian, Hongming Xu, and Shijin Shuai. Ignition timing sensitivities of oxygenated biofuels compared to gasoline in a direct-injection si engine. *Fuel*, 99:72–82, 2012.

[55] Tao Wang, Xin Zhang, Jibao Zhang, and Xiaosen Hou. Numerical analysis of the influence of the fuel injection timing and ignition position in a direct-injection natural gas engine. *Energy Conversion and Management*, 149:748–759, 2017.

[56] Barış Erkuş, M. İhsan Karamangil, and Ali Sürmen. Enhancing the heavy load performance of a gasoline engine converted for lpg use by modifying the ignition timings. *Applied Thermal Engineering*, 85:188–194, 2015.

[57] Yasin Şöhret, Habib Gürbüz, and İsmail Hakkı Akçay. Energy and exergy analyses of a hydrogen fueled si engine: Effect of ignition timing and compression ratio. *Energy*, 175:410–422, 2019.

[58] Roussos G. Papagiannakis, Dimitrios C. Rakopoulos, and Constantine D. Rakopoulos. Theoretical study of the effects of spark timing on the performance and emissions of a light-duty spark ignited engine running under either gasoline or ethanol or butanol fuel operating modes. *Energies*, 10(8), 2017.

[59] Mohamadhasan Shojaeefard, Keayvan Keramati, Mojtaba Tahani, and Alireza Veisi. *3D Numerical Investigation of Ignition Timing Effects on the SI Engine Exergy*, pages 1123–1137. Springer International Publishing, Cham, 2018.

[60] Aditya Balkrishna Kale, Jyoti Madhav Phate, Prashant Sarjerao Munfan, and Yogesh Suresh Chavan. Investigation of relation between ignition timing and advance angle to improve engine performance. In U. Chandrasekhar, Lung-Jieh Yang, and S. Gowthaman, editors, *Innovative Design, Analysis and Development*

Practices in Aerospace and Automotive Engineering (I-DAD 2018), pages 33–39, Singapore, 2019. Springer Singapore.

[61] A. H. Kakaee and J. Zareei. Influence of varying timing angle on performance of an si engine: An experimental and numerical study. *Journal of Computational and Applied Research in Mechanical Engineering (JCARME)*, 2(2):33–43, 2013.

[62] Colin R Ferguson and Allan T Kirkpatrick. *Internal combustion engines: applied thermosciences*. John Wiley & Sons, 2015.

[63] Jeremy Worm Jeffrey Naber Yeliana Y, Christopher Cooney. The calculation of mass fraction burn of ethanol-gasoline blended fuels using single and two-zone models. Technical report, SAE Technical Paper, 2008.

[64] Gholamreza Abbaszadehmosayebi. *Diesel engine heat release analysis by using newly defined dimensionless parameters*. PhD thesis, 2014.

[65] Francesco Baldi, Gerasimos Theotokatos, and Karin Andersson. Development of a combined mean value–zero dimensional model and application for a large marine four-stroke diesel engine simulation. *Applied Energy*, 154:402–415, 2015.

[66] Yu Ding, Douwe Stapersma, and Hugo Grimmelius. Using parametrized finite combustion stage models to characterize combustion in diesel engines. *Energy & Fuels*, 26(12):7099–7106, 2012.

[67] Congbiao Sui, Enzhe Song, Douwe Stapersma, and Yu Ding. Mean value modelling of diesel engine combustion based on parameterized finite stage cylinder process. *Ocean Engineering*, 136:218–232, 2017.

[68] Mohand Said Lounici, Khaled Loubar, Mourad Balistrou, and Mohand Tazerout. Investigation on heat transfer evaluation for a more efficient two-zone combustion model in the case of natural gas si engines. *Applied Thermal Engineering*, 31(2):319–328, 2011.

[69] Richard Stone. *Introduction to internal combustion engines*. Macmillan International Higher Education, 2012.

[70] C.D. Rakopoulos and E.G. Giakoumis. Second-law analyses applied to internal combustion engines operation. *Progress in Energy and Combustion Science*, 32(1):2–47, 2006.

[71] La Xiang, Enzhe Song, and Yu Ding. A two-zone combustion model for knocking prediction of marine natural gas si engines. *Energies*, 11(3), 2018.

[72] C.D. Rakopoulos, D.C. Rakopoulos, and D.C. Kyritsis. Development and validation of a comprehensive two-zone model for combustion and emissions formation in a di diesel engine. *International Journal of Energy Research*, 27(14):1221–1249, 2003.

[73] A Agarwal, Z. S. Filipi, D. N. Assanis, and D. M. Baker. Assessment of single- and two-zone turbulence formulations for quasi-dimensional modeling of spark-ignition engine combustion. *Combustion Science and Technology*, 136(1-6):13–39, 1998.

[74] Hai-Wen Ge, Harmit Juneja, Yu Shi, Shiyou Yang, and Rolf D Reitz. A two-zone multigrid model for si engine combustion simulation using detailed chemistry. *Journal of Combustion*, 2010, 2010.

[75] C.D. Rakopoulos and C.N. Michos. Development and validation of a multi-zone combustion model for performance and nitric oxide formation in syngas fueled spark ignition engine. *Energy Conversion and Management*, 49(10):2924–2938, 2008.

[76] E.G. Pariotis, G.M. Kosmadakis, and C.D. Rakopoulos. Comparative analysis of three simulation models applied on a motored internal combustion engine. *Energy Conversion and Management*, 60:45–55, 2012. Special issue of Energy Conversion and Management dedicated to ECOS 2011 - the 24th International Conference on Efficiency, Costs, Optimization, Simulation and Environmental

Impact of Energy Systems.

[77] Marcus Klein. *A specific heat ratio model and compression ratio estimation*. PhD thesis, Division of Vehicular Systems, Department of Electrical Engineering, Linköping University, 2004.

[78] M. Reyes, F.V. Tinaut, A. Melgar, and A. Pérez. Characterization of the combustion process and cycle-to-cycle variations in a spark ignition engine fuelled with natural gas/hydrogen mixtures. *International Journal of Hydrogen Energy*, 41(3):2064–2074, 2016.

[79] C. D. Rakopoulos, D. T. Hountalas, D. C. Rakopoulos, and E. G. Giakoumis. Experimental heat release rate analysis in both chambers of an indirect injection turbocharged diesel engine at various load and speed conditions. *SAE Transactions*, 114:867–882, 2005.

[80] KWANG MIN CHUN and JOHN B. HEYWOOD. Estimating heat-release and mass-of-mixture burned from spark-ignition engine pressure data. *Combustion Science and Technology*, 54(1-6):133–143, 1987.

[81] Hon M. Cheung and John B. Heywood. Evaluation of a one-zone burn-rate analysis procedure using production si engine pressure data. *SAE Transactions*, 102:2292–2303, 1993.

[82] Gerald M. Rassweiler and Lloyd Withrow. Motion pictures of engine flames correlated with pressure cards. *SAE Transactions*, 33:185–204, 1938.

[83] R. B. Krieger and Borman G. L. The computation of apparent heat release for internal combustion engines. *ASME Paper 66-WA/DGP-4*, 1967.

[84] J. A. Gatowski, E. N. Balles, K. M. Chun, F. E. Nelson, J. A. Ekchian, and John B. Heywood. Heat release analysis of engine pressure data. In *1984 SAE International Fall Fuels and Lubricants Meeting and Exhibition*. SAE International, oct 1984.

[85] Yeliana, C. Cooney, J. Worm, D. Michalek, and J. Naber. Wiebe function parameter determination for mass fraction burn calculation in an ethanol-gasoline fuelled si engine. *Journal of KONES*, Vol. 15, No. 3:567–574, 2008.

[86] M.A. Ceviz and İ. Kaymaz. Temperature and air–fuel ratio dependent specific heat ratio functions for lean burned and unburned mixture. *Energy Conversion and Management*, 46(15):2387–2404, 2005.

[87] Yann G. Guezennec and Wajdi Hamama. Two-zone heat release analysis of combustion data and calibration of heat transfer correlation in an i. c. engine. In *International Congress & Exposition*. SAE International, mar 1999.

[88] Marcus Klein, Lars Eriksson, and Jan Åslund. Compression ratio estimation based on cylinder pressure data. *Control Engineering Practice*, 14(3):197–211, 2006. Advances in Automotive Control (AC'04).

[89] R. Ebrahimi. Effect of specific heat ratio on heat release analysis in a spark ignition engine. *Scientia Iranica*, 18(6):1231–1236, 2011.

[90] Ph Guibert. Modeling of the engine cycle. zero-dimensional approach; modelisation du cycle moteur. approche zerodimensionnelle.

[91] Alessandro Franco and Luigi Martorano. Evaluations on the heat transfer in the small two-stroke engines. *SAE Transactions*, 107:978–993, 1998.

[92] G. Woschni. A universally applicable equation for the instantaneous heat transfer coefficient in the internal combustion engine. In *National Fuels and Lubricants, Powerplants, Transportation Meetings*. SAE International, feb 1967.

[93] Günter F. Hohenberg. Advanced approaches for heat transfer calculations. *SAE Transactions*, 88:2788–2806, 1979.

[94] G. Sitkei and G. V. Ramanaiah. A rational approach for calculation of heat transfer in diesel engines. *SAE Transactions*, 81:165–174, 1972.

[95] W. J. D. Annand. Heat transfer in the cylinders of reciprocating internal

combustion engines. *Proceedings of the Institution of Mechanical Engineers*, 177(1):973–996, 1963.

[96] G. Eichelberg. Some new investigations on old combustion engine problems. *Engineering*, 148:463–547, 1939.

[97] Gary Borman and Kazuie Nishiwaki. Internal-combustion engine heat transfer. *Progress in Energy and Combustion Science*, 13(1):1–46, 1987.

[98] J.L.S. Fagundez, R.L. Sari, M.E.S. Martins, and N.P.G. Salau. Comparative analysis of different heat transfer correlations in a two-zone combustion model applied on a si engine fueled with wet ethanol. *Applied Thermal Engineering*, 115:22–32, 2017.

[99] Gordon P. Blair. *Design and Simulation of Four-Stroke Engines*. SAE International, aug 1999.

[100] Siew Hwa Chan and J. Zhu. Modelling of engine in-cylinder thermodynamics under high values of ignition retard. *International Journal of Thermal Sciences*, 40(1):94–103, 2001.

[101] Tatsu OGURI. On the coefficient of heat transfer between gases and cylinder walls of the spark-ignition engine. *Bulletin of JSME*, 3(11):363–369, 1960.

[102] J. Trapy. Measurement and modeling of heat transfer at walls in internal combustion engines. [transferts thermiques dans les moteurs a combustion interne. mesure et modelisation.]. *Revue generale de thermique*, 20(233):385–390, 1981. cited By 5.

[103] Ali Sanli, Ahmet N. Ozsezen, Ibrahim Kilicaslan, and Mustafa Canakci. The influence of engine speed and load on the heat transfer between gases and in-cylinder walls at fired and motored conditions of an idi diesel engine. *Applied Thermal Engineering*, 28(11):1395–1404, 2008.

[104] Willard W. Pulkrabek. Engineering Fundamentals of the Internal Combustion

Engine, 2nd Ed. *Journal of Engineering for Gas Turbines and Power*, 126(1):198–198, 03 2004.

[105] H.S. Soyhan, H. Yasar, H. Walmsley, B. Head, G.T. Kalghatgi, and C. Sorusbay. Evaluation of heat transfer correlations for hcci engine modeling. *Applied Thermal Engineering*, 29(2):541–549, 2009.

[106] Jehad AA Yamin, HN Gupta, and BB Bansal. The effect of combustion duration on the performance and emission characteristics of propane-fueled 4-stroke si engines. *Emirates Journal for Engineering Research*, 8(1):1–14, 2003.

[107] Michael L Monaghan. Engine friction—a change in emphasis: A new approach which may result in significant fuel consumption gains. *Industrial Lubrication and Tribology*, 1988.

APPENDIX A

OPTIMIZATION PART II - CASE SCENARIOS RESULTS

A.1 Brake Torque and Brake Power Variation

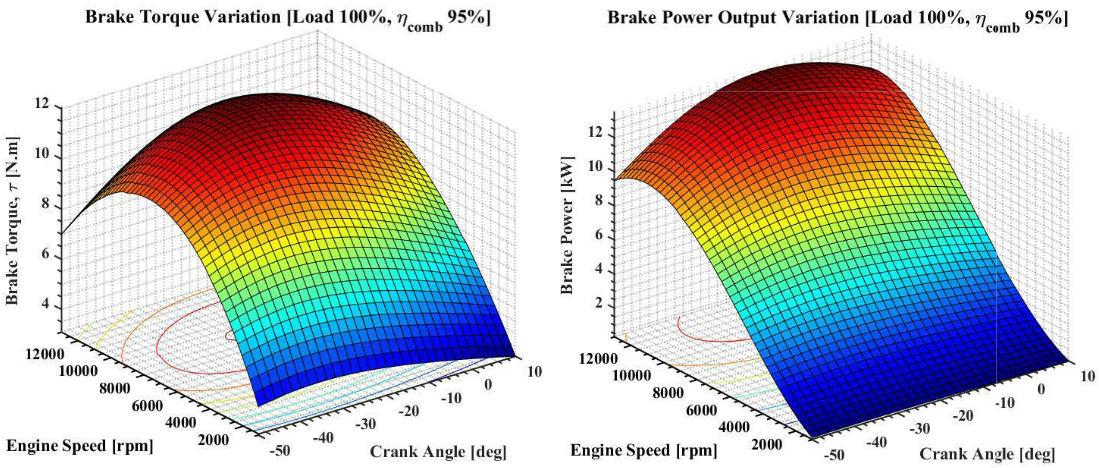

Figure A.1: Optimization Part II - Case scenario (2) - 3D Plot of Brake Torque and Brake Power Variation of The CR Engine

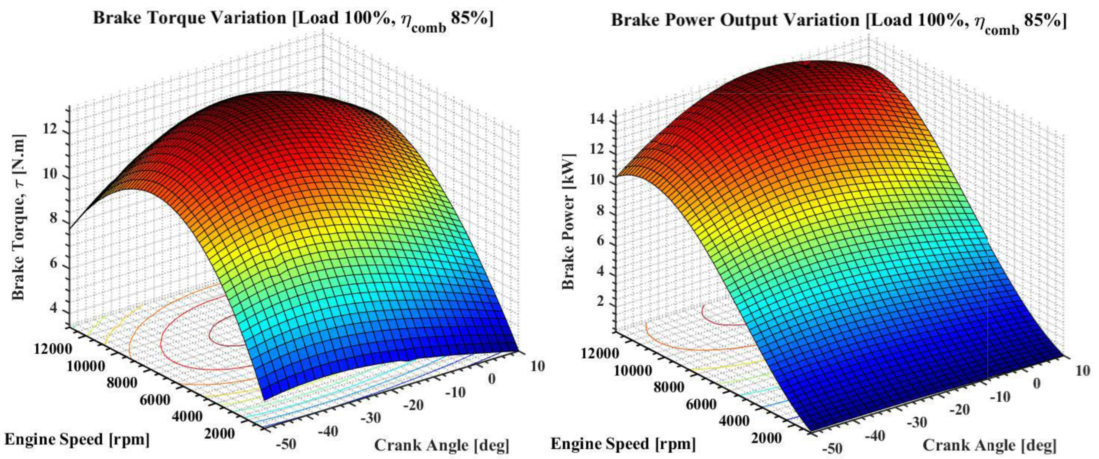

Figure A.2: Optimization Part II - Case scenario (3) - 3D Plot of Brake Torque and Brake Power Variation of The CR Engine

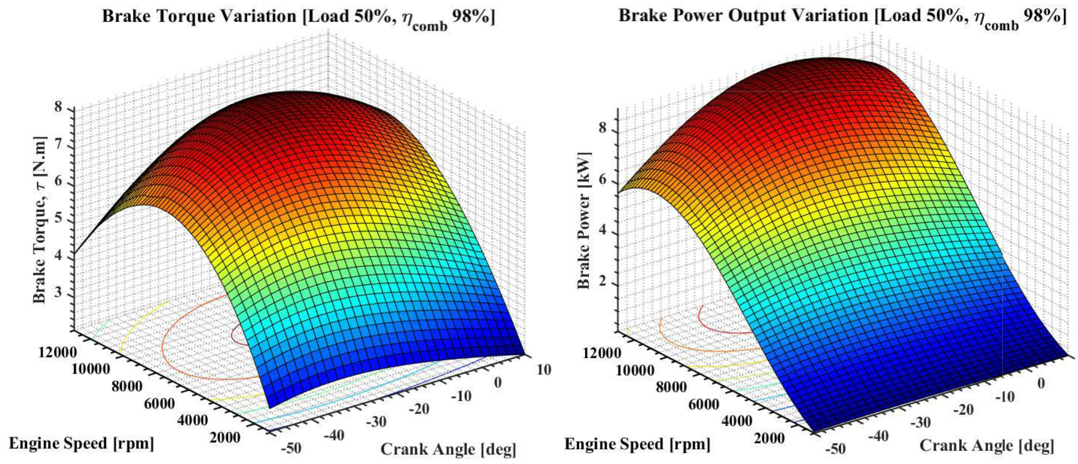

Figure A.3: Optimization Part II - Case scenario (4) - 3D Plot of Brake Torque and Brake Power Variation of The CR Engine

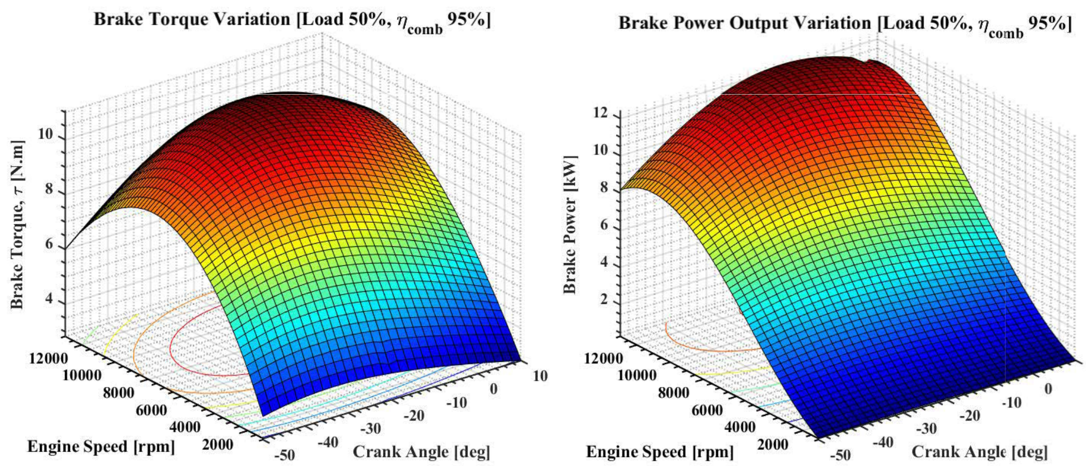

Figure A.4: Optimization Part II - Case scenario (5) - 3D Plot of Brake Torque and Brake Power Variation of The CR Engine

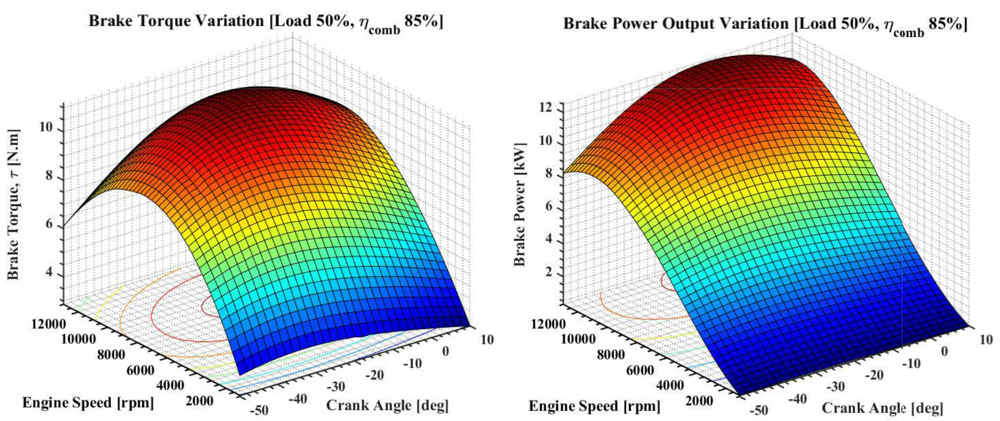

Figure A.5: Optimization Part II - Case scenario (6) - 3D Plot of Brake Torque and Brake Power Variation of The CR Engine

A.2 Brake Torque Variation Using Contour Representation

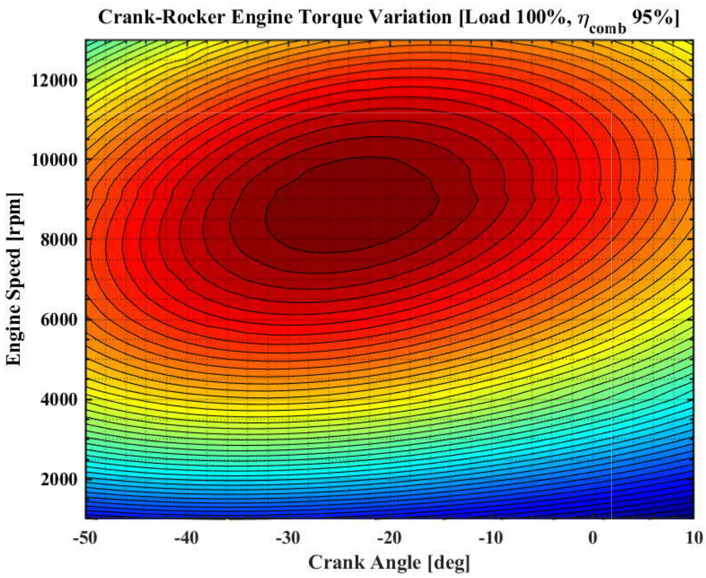

Figure A.6: Optimization Part II - Case scenario (2) - A Contour Representation of Brake Torque Variation of The CR Engine

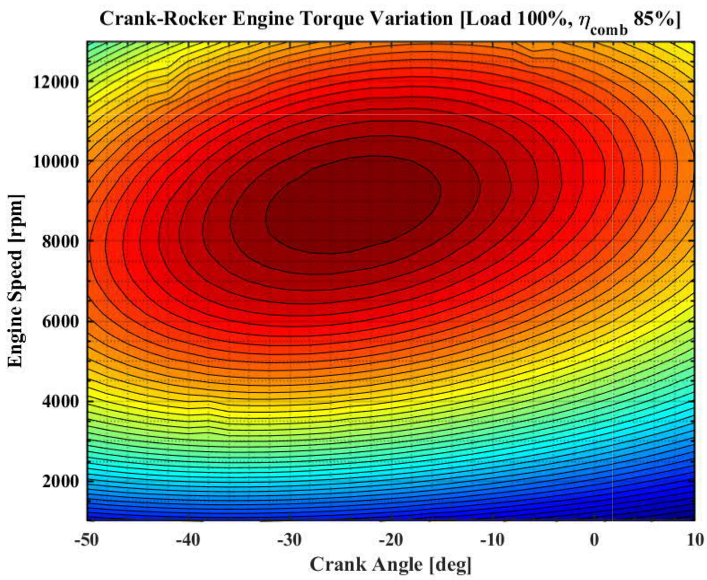

Figure A.7: Optimization Part II - Case scenario (3) - A Contour Representation of Brake Torque Variation of The CR Engine

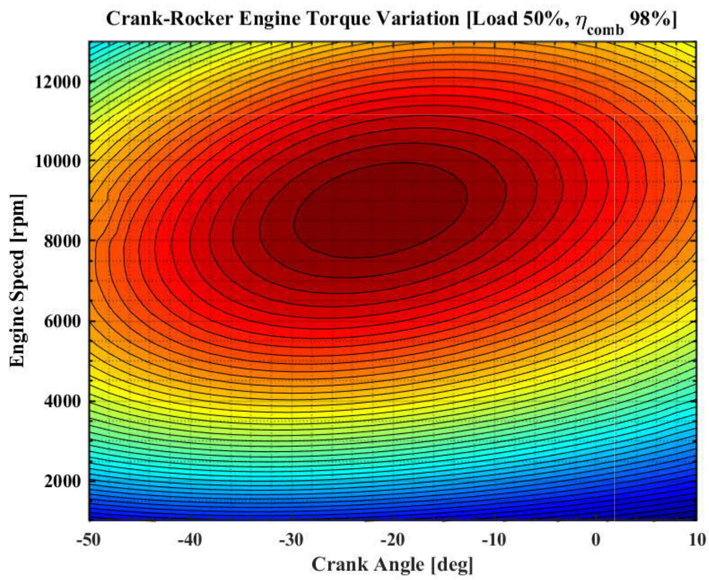

Figure A.8: Optimization Part II - Case scenario (4) - A Contour Representation of Brake Torque Variation of The CR Engine

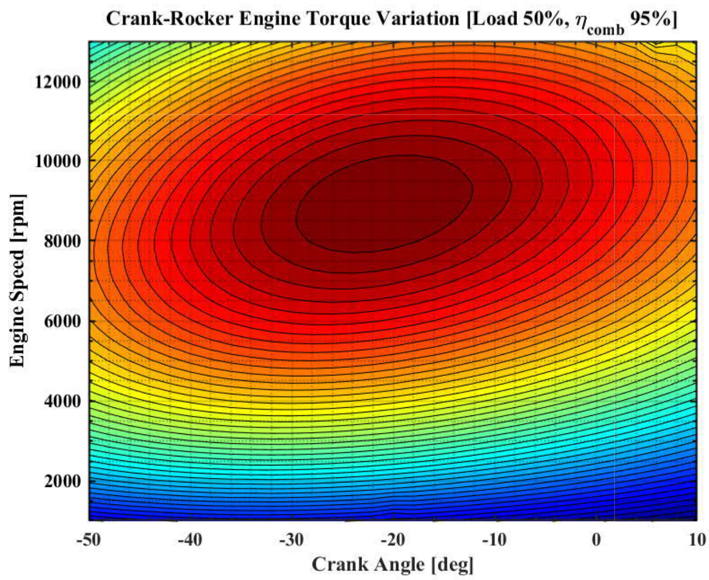

Figure A.9: Optimization Part II - Case scenario (5) - A Contour Representation of Brake Torque Variation of The CR Engine

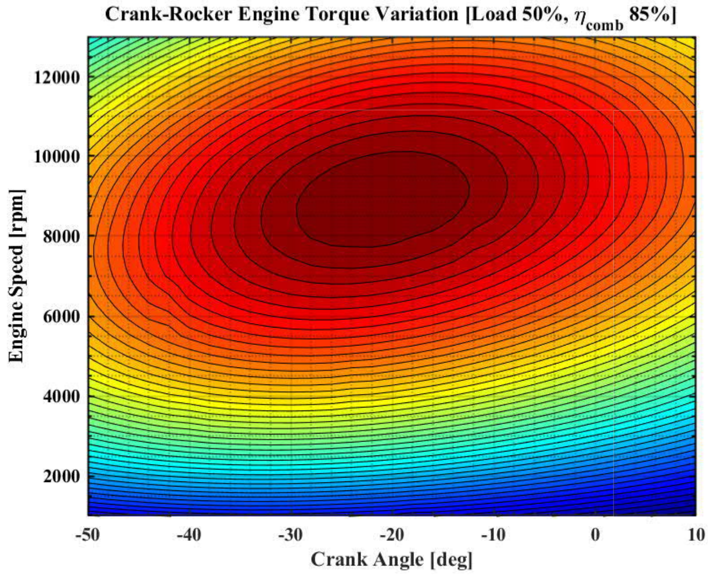

Figure A.10: Optimization Part II - Case scenario (6) - A Contour Representation of Brake Torque Variation of The CR Engine

A.3 Brake Torque, Brake Power, BSFC, and BTE Variation at Optimum Ignition Timing

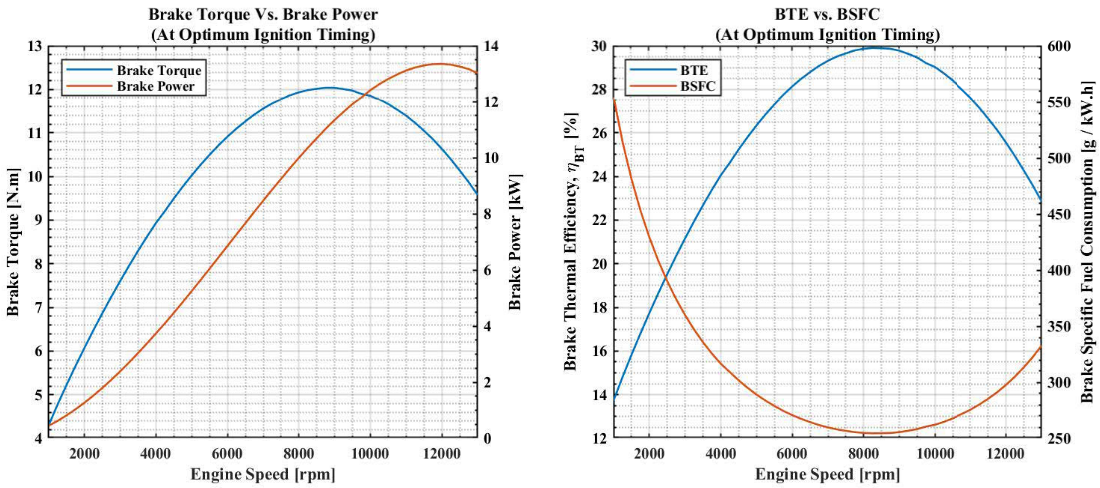

Figure A.11: Optimization Part II - Case scenario (2) - (left-side) Brake Torque and Brake Power Vs Engine Speed at Optimum Ignition timing - (right-side) BSFC and BTE Vs Engine Speed at Optimum Ignition timing

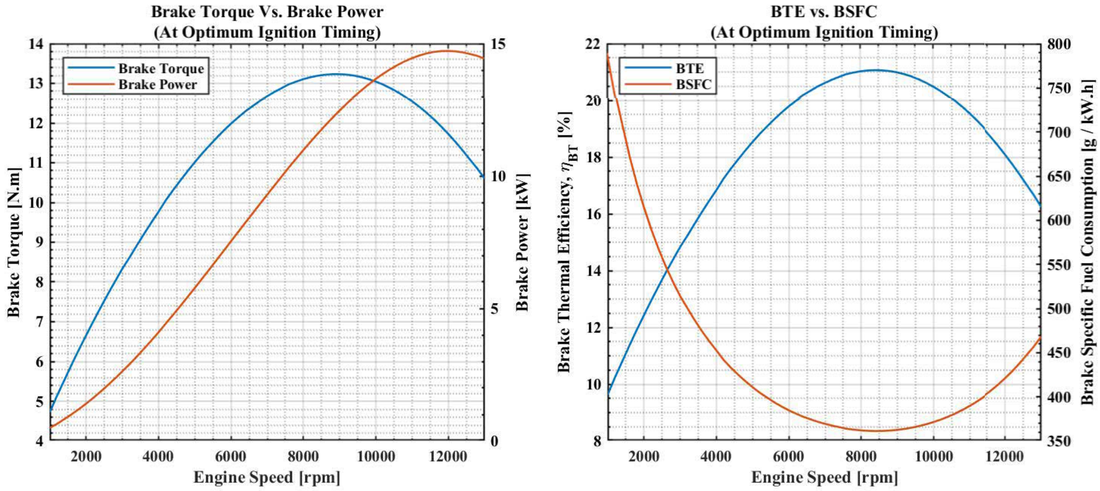

Figure A.12: Optimization Part II - Case scenario (3) - (left-side) Brake Torque and Brake Power Vs Engine Speed at Optimum Ignition timing - (right-side) BSFC and BTE Vs Engine Speed at Optimum Ignition timing

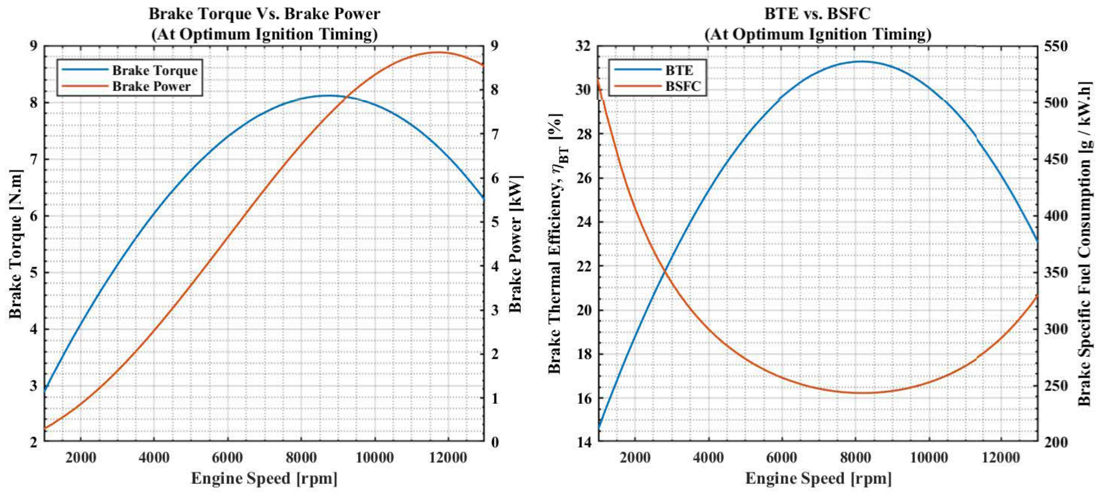

Figure A.13: Optimization Part II - Case scenario (4) - (left-side) Brake Torque and Brake Power Vs Engine Speed at Optimum Ignition timing - (right-side) BSFC and BTE Vs Engine Speed at Optimum Ignition timing

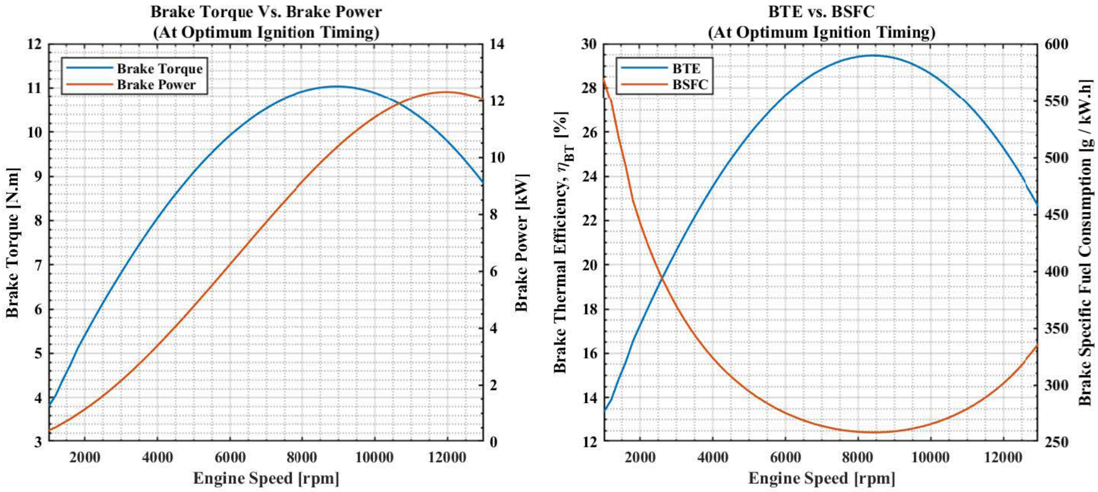

Figure A.14: Optimization Part II - Case scenario (5) - (left-side) Brake Torque and Brake Power Vs Engine Speed at Optimum Ignition timing - (right-side) BSFC and BTE Vs Engine Speed at Optimum Ignition timing

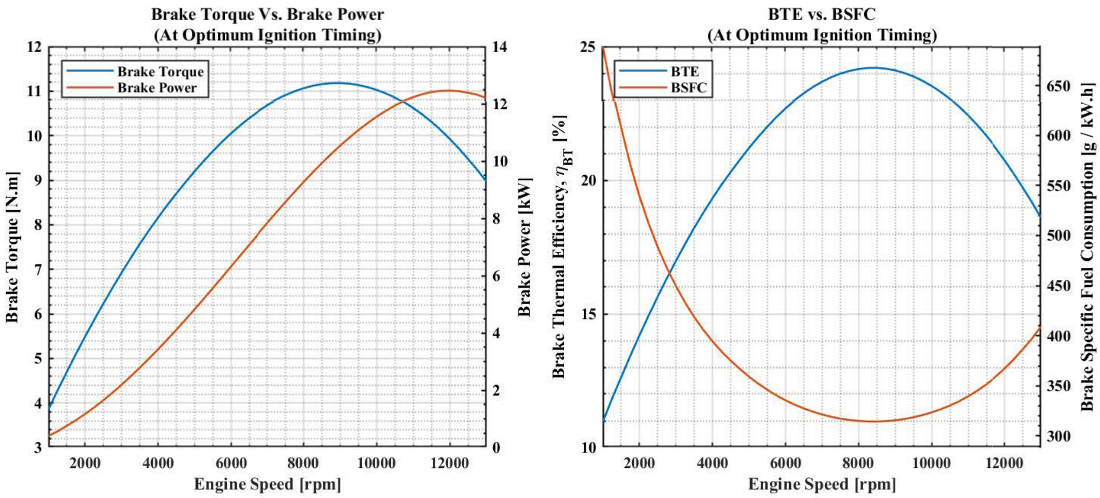

Figure A.15: Optimization Part II - Case scenario (6) - (left-side) Brake Torque and Brake Power Vs Engine Speed at Optimum Ignition timing - (right-side) BSFC and BTE Vs Engine Speed at Optimum Ignition timing

A.4 Brake Specific Fuel Consumption and Brake Thermal Efficiency Variation

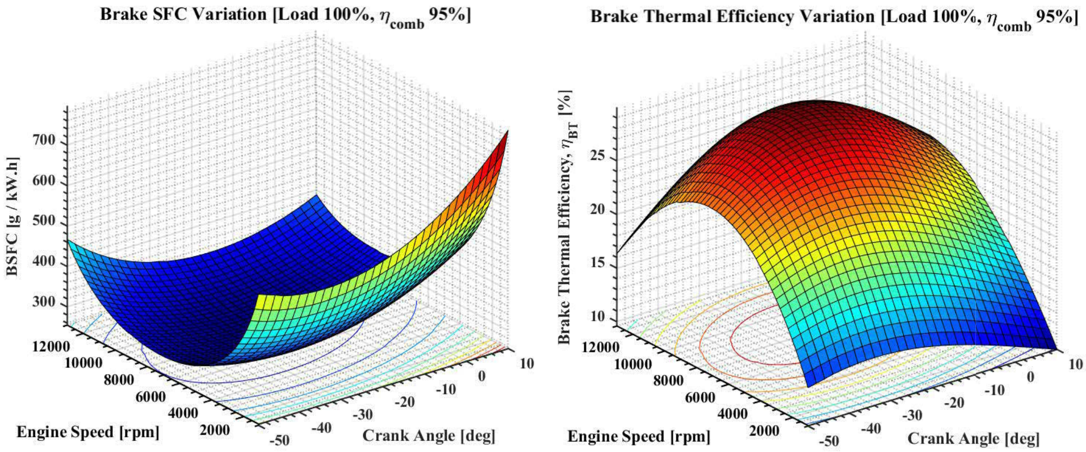

Figure A.16: Optimization Part II - Case scenario (2) - 3D Plot of BSFC and BTE Variation of The CR Engine

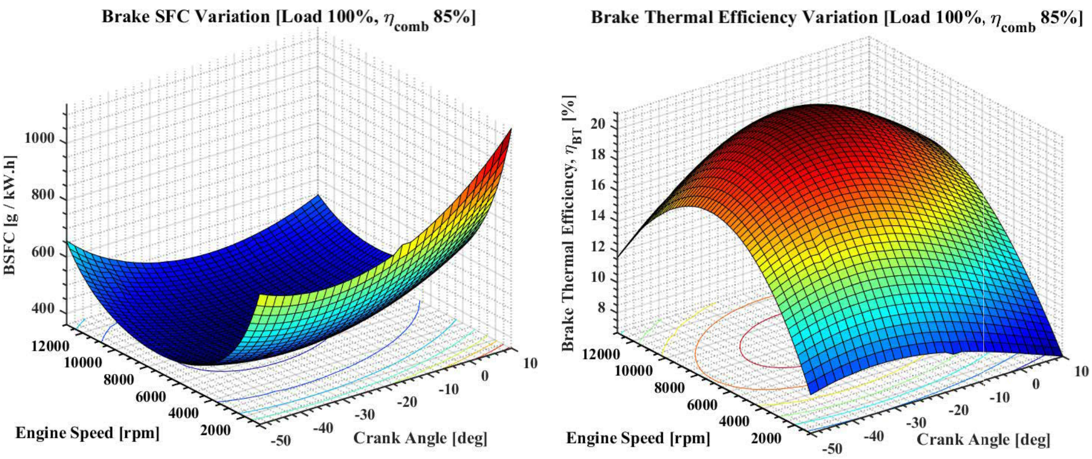

Figure A.17: Optimization Part II - Case scenario (3) - 3D Plot of BSFC and BTE Variation of The CR Engine

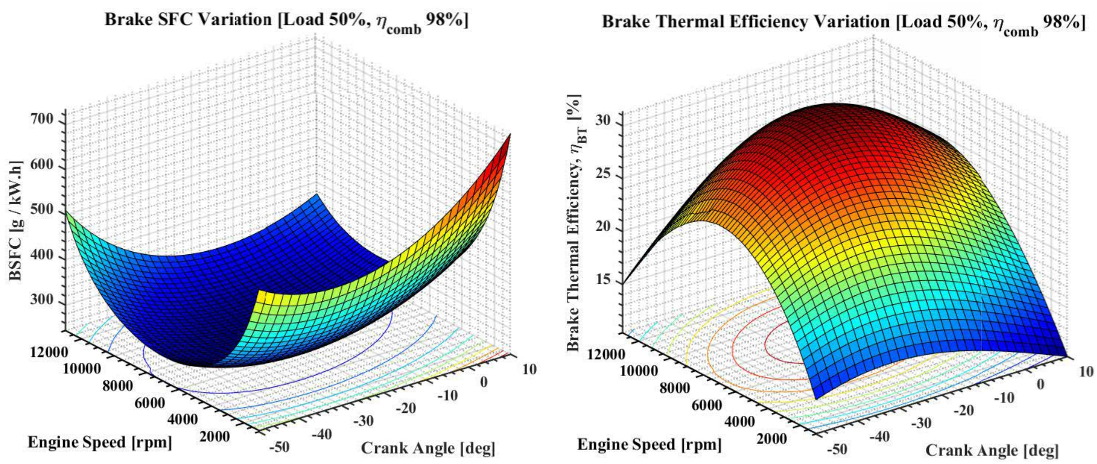

Figure A.18: Optimization Part II - Case scenario (4) - 3D Plot of BSFC and BTE Variation of The CR Engine

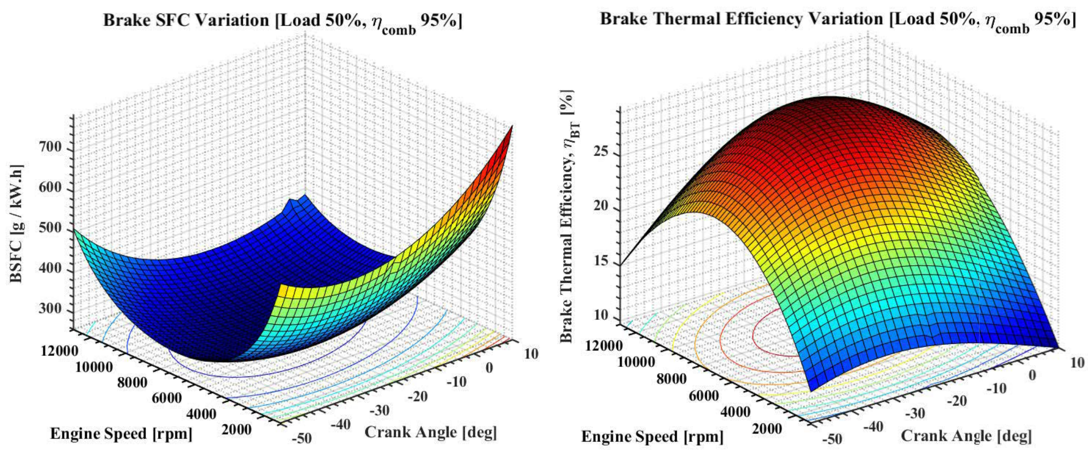

Figure A.19: Optimization Part II - Case scenario (5) - 3D Plot of BSFC and BTE Variation of The CR Engine

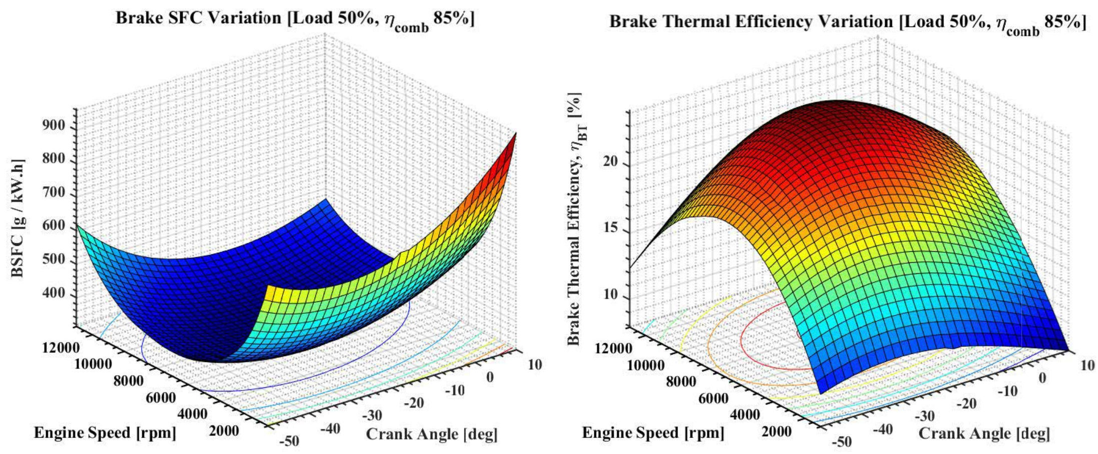

Figure A.20: Optimization Part II - Case scenario (6) - 3D Plot of BSFC and BTE Variation of The CR Engine

A.5 The Combustion Characteristics

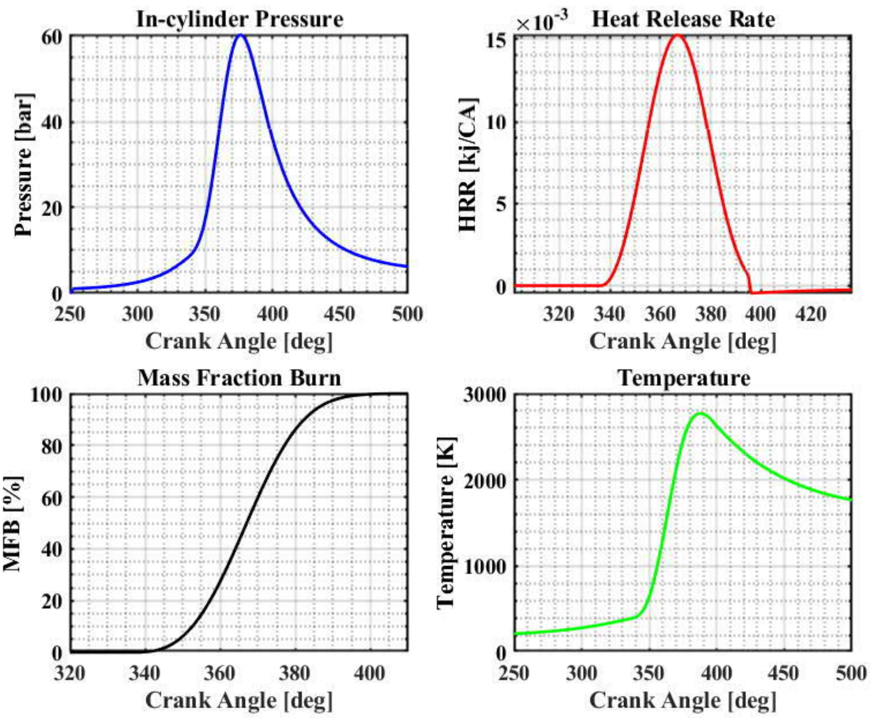

Figure A.21: Optimization Part II - Case scenario (2) - The Combustion Characteristics of The CR Engine at Optimum Speed and Ignition Timing

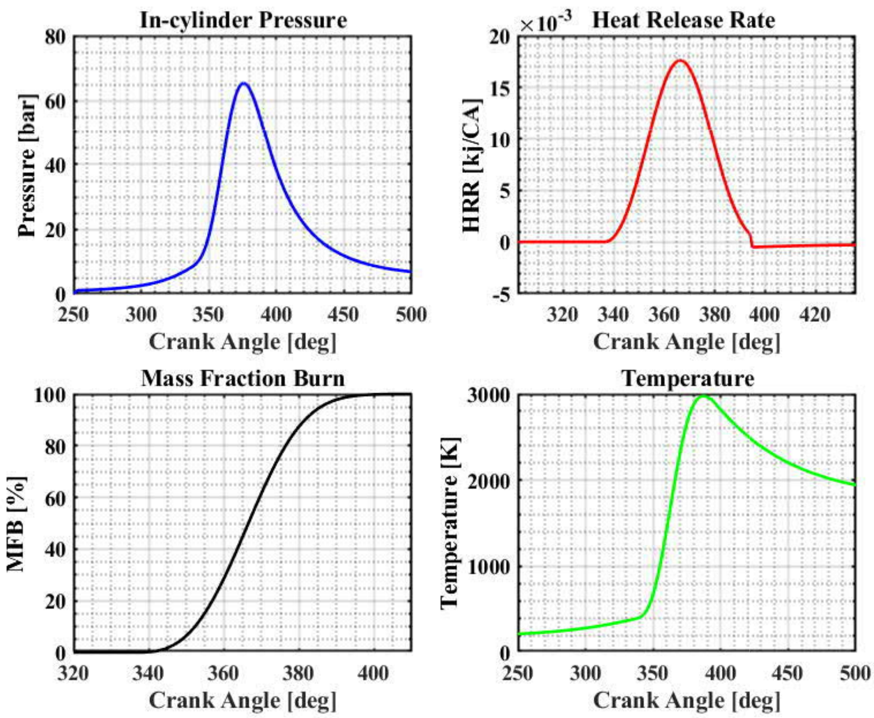

Figure A.22: Optimization Part II - Case scenario (3) - The Combustion Characteristics of The CR Engine at Optimum Speed and Ignition Timing

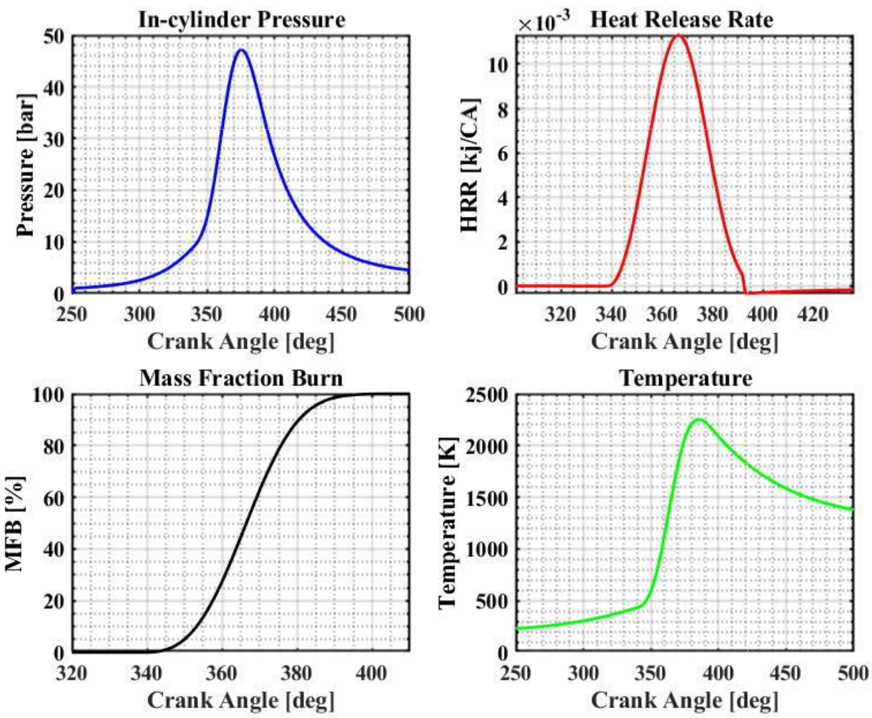

Figure A.23: Optimization Part II - Case scenario (4) - The Combustion Characteristics of The CR Engine at Optimum Speed and Ignition Timing

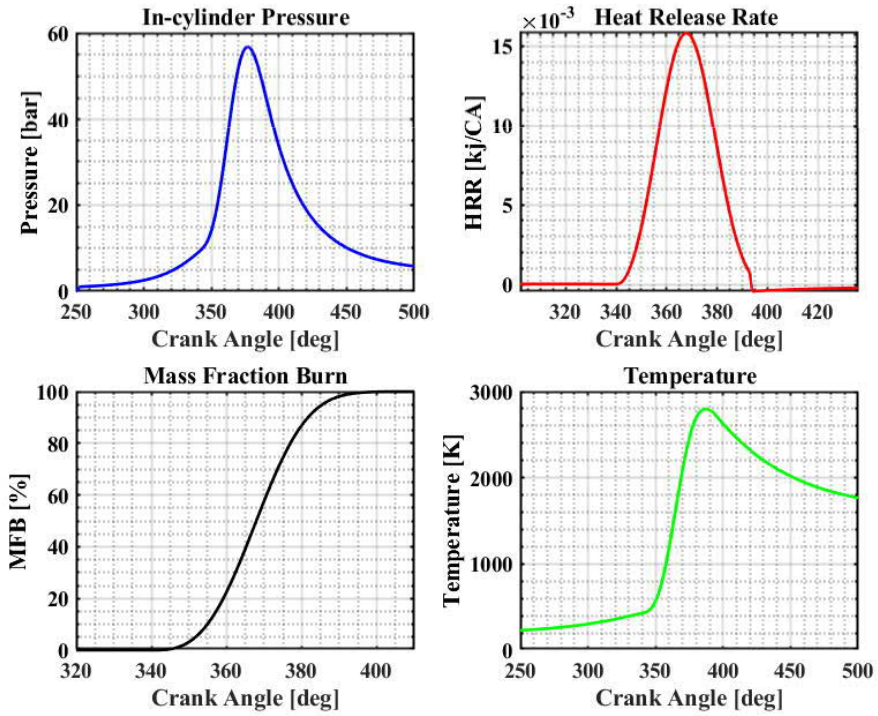

Figure A.24: Optimization Part II - Case scenario (5) - The Combustion Characteristics of The CR Engine at Optimum Speed and Ignition Timing

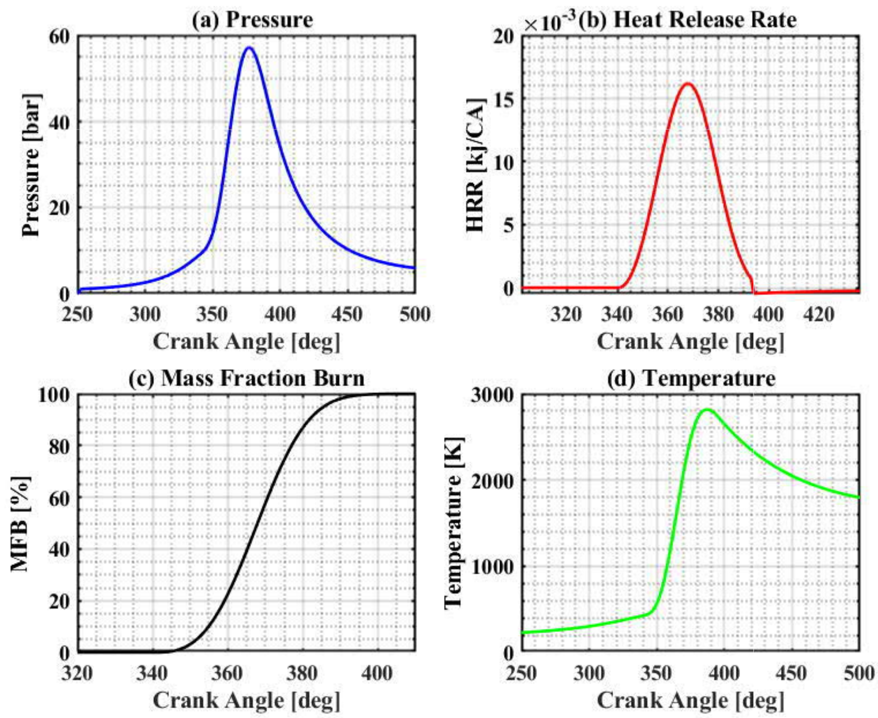

Figure A.25: Optimization Part II - Case scenario (6) - The Combustion Characteristics of The CR Engine at Optimum Speed and Ignition Timing

APPENDIX B

MATLAB CODE: STAGE I AND II

B.1 Modified Combustion and Heat Transfer Model

```
%Universiti Teknologi PETRONAS
%Project: Numerical Investigation and Optimization
%         of The Crank-Rocker Engine Ignition Timing
%         Based on Performance and Combustion Characteristics
%Methodology Stage: STAGE I and II
%Section: Crank-Rocker Engine Modified Combustion Model
%         and Heat Trasnfer Evaluation
%~~~~~~~~~~~~~~~~~~~~~~~~~~~~~~~~~~~~~~~~~~~~~~~~~~~~~~~~~~~~~~~~~~~~~~~~~~
clear;
close all;
clc;
%~~~~~~~~~~~~~~~~~~~~~~~~~~~~~~~~~~~~~~~~~~~~~~~~~~~~~~~~~~~~~~~~~~~~~~~~~~
% INPUT SECTIONS
% THIS SECTION CONTAINS SEVERAL SUB-SECTIONS
% INCLUDING ALL THE REQUIRED INPUTS
% FOR THE MODEL AND SIMULATION.
%~~~~~~~~~~~~~~~~~~~~~~~~~~~~~~~~~~~~~~~~~~~~~~~~~~~~~~~~~~~~~~~~~~~~~~~~~~
% INPUT #1 Crank-Rocker Engine Geometry and Specification Data
%~~~~~~~~~~~~~~~~~~~~~~~~~~~~~~~~~~~~~~~~~~~~~~~~~~~~~~~~~~~~~~~~~~~~~~~~~~
% Length
L2 = 0.0253;   %input('Enter The Crank Radius Length [m]')
L3 = 0.1;      %input('Enter The Connecting Rod Length [m]')
L4 = 0.1388;   %input('Enter The Rocker Length [m]')
L41 = 0.1381;  %input('Enter The Extended Rocker Length [m]')
% Engine Spicification
PHI = 21;      % Swing Angle [degree]
B = 0.055;     % Engine Bore [m]
N_cyl = 1;     % Number of Cylinders
N_r = 2;       % Number of Revolutions Per Power Stroke
C_r = 9;       % Compression ratio
% Speed and Load
RPM = 2000;    % input('Enter The Engine Speed [1/min] =')
Load = 1;      % Engine Load (Load = 1 = FUll Load)
% Valves
IVC = 0;       % Time [degrees], Intake Valve Closes
EVO = 540;     % Time [degrees], Exhaust Valve Opens
% Timing
theta_b = 57;  % Combustion Duration [degree]
theta_0 = 356; % CA at Start of Combustion [degree]/ Ignition timing
%~~~~~~~~~~~~~~~~~~~~~~~~~~~~~~~~~~~~~~~~~~~~~~~~~~~~~~~~~~~~~~~~~~~~~~~~~~
% INPUT #2 Fuel Input Data
%~~~~~~~~~~~~~~~~~~~~~~~~~~~~~~~~~~~~~~~~~~~~~~~~~~~~~~~~~~~~~~~~~~~~~~~~~~
AF_ratio_stoich = 15.09;    % Gravimetric Air Fuel Ratio (Stoich)
AF_ratio_mol_sotich = 14.7; % Molar Air_Fuel Ratio (Stoich)
lambda = 1;                 % Excess Air Coefficient
LHV = 46e6;                 % Lower Heating Value Of Fuel Mixture [J/kg]
R_air = 287;                % Gas Constant For Air [J/kg-K]
%~~~~~~~~~~~~~~~~~~~~~~~~~~~~~~~~~~~~~~~~~~~~~~~~~~~~~~~~~~~~~~~~~~~~~~~~~~
% INPUT #3 Ambient Conditions
%~~~~~~~~~~~~~~~~~~~~~~~~~~~~~~~~~~~~~~~~~~~~~~~~~~~~~~~~~~~~~~~~~~~~~~~~~~
P_atm = 101325;      % Atmospheric Inputs
T_atm = 290;         % Atmospheric Temp Inputs
%~~~~~~~~~~~~~~~~~~~~~~~~~~~~~~~~~~~~~~~~~~~~~~~~~~~~~~~~~~~~~~~~~~~~~~~~~~
% INPUT #4 Assumptions
%~~~~~~~~~~~~~~~~~~~~~~~~~~~~~~~~~~~~~~~~~~~~~~~~~~~~~~~~~~~~~~~~~~~~~~~~~~
eta_combmaX = 0.55;            % Assumed MAX Comb. Efficiency
T_W =490;                      % Assumed Wall Temperature [K]
gamma(1:720) = 1.34;           % Preallocate Gamma Array
```

```
%~~~~~~~~~~~~~~~~~~~~~~~~~~~~~~~~~~~~~~~~~~~~~~~~~~~~~~~~~~~~~~~~~~~~~~~~~
% INITIAL CALCULATION
%~~~~~~~~~~~~~~~~~~~~~~~~~~~~~~~~~~~~~~~~~~~~~~~~~~~~~~~~~~~~~~~~~~~~~~~~~
% Engine Calculations Based On INPUT #1
%~~~~~~~~~~~~~~~~~~~~~~~~~~~~~~~~~~~~~~~~~~~~~~~~~~~~~~~~~~~~~~~~~~~~~~~~~
% Geometry
%~~~~~~~~~~~~~~~~~~~~~~~~~~~~~~~~~~~~~~~~~~~~~~~~~~~~~~~~~~~~~~~~~~~~~~~~~
S = L41*PHI*pi()/180;        % Calculates the Engine Stroke [m]
DD1 = L4*cos(PHI/2*pi()/180);% Calculates the Length DD1 [m]
L1 = sqrt((L3)^2+(DD1)^2);   % Calculates the Engine framelength [m]
%~~~~~~~~~~~~~~~~~~~~~~~~~~~~~~~~~~~~~~~~~~~~~~~~~~~~~~~~~~~~~~~~~~~~~~~~~
% Theta
%~~~~~~~~~~~~~~~~~~~~~~~~~~~~~~~~~~~~~~~~~~~~~~~~~~~~~~~~~~~~~~~~~~~~~~~~~
theta1 = asin(DD1/L1)*180/pi();% Calculates Ineital angle theta1  [degrees]
theta_f = theta_0 + theta_b;   % Crank Angle at End of Combustion [degree]
%~~~~~~~~~~~~~~~~~~~~~~~~~~~~~~~~~~~~~~~~~~~~~~~~~~~~~~~~~~~~~~~~~~~~~~~~~
% Area
%~~~~~~~~~~~~~~~~~~~~~~~~~~~~~~~~~~~~~~~~~~~~~~~~~~~~~~~~~~~~~~~~~~~~~~~~~
A_p = (pi/4)*B^2;   % Calculates Cross Sectional Piston Area [m^2]
A_ch = 2*A_p;       % Calculates Cylinder Head Surface Area (in chamber)
%~~~~~~~~~~~~~~~~~~~~~~~~~~~~~~~~~~~~~~~~~~~~~~~~~~~~~~~~~~~~~~~~~~~~~~~~~
% Volumes
%~~~~~~~~~~~~~~~~~~~~~~~~~~~~~~~~~~~~~~~~~~~~~~~~~~~~~~~~~~~~~~~~~~~~~~~~~
V_d = N_cyl*A_p*S;           % Calculates Displaced Volume Of Engine [m^3]
V_TDC = (V_d/(C_r-1))/N_cyl; % Calculates Clearance Volume [m^3]
V_BDC = (V_d/N_cyl)+V_TDC;   % Calculates Cyl. Volume At BDC [m^3]
%~~~~~~~~~~~~~~~~~~~~~~~~~~~~~~~~~~~~~~~~~~~~~~~~~~~~~~~~~~~~~~~~~~~~~~~~~
% General
%~~~~~~~~~~~~~~~~~~~~~~~~~~~~~~~~~~~~~~~~~~~~~~~~~~~~~~~~~~~~~~~~~~~~~~~~~
N = RPM/60;                  % Converts RPM to RPS [1/s]
S_bar_p = 2*S*N;             % Calculates Mean Piston Speed [m/s]
%~~~~~~~~~~~~~~~~~~~~~~~~~~~~~~~~~~~~~~~~~~~~~~~~~~~~~~~~~~~~~~~~~~~~~~~~~
% Calculateing Losses Due to Friction
%~~~~~~~~~~~~~~~~~~~~~~~~~~~~~~~~~~~~~~~~~~~~~~~~~~~~~~~~~~~~~~~~~~~~~~~~~
fmep = (250*S*RPM)*10^-3;   % Calculating Losses Due To Friction, fmep
%~~~~~~~~~~~~~~~~~~~~~~~~~~~~~~~~~~~~~~~~~~~~~~~~~~~~~~~~~~~~~~~~~~~~~~~~~
%Volumetric Efficiency correction Factor
%~~~~~~~~~~~~~~~~~~~~~~~~~~~~~~~~~~~~~~~~~~~~~~~~~~~~~~~~~~~~~~~~~~~~~~~~~
CF=-8*10^(-9)*RPM^2+.000135*RPM+.31944;   % CF = correction(Load,RPM)
%~~~~~~~~~~~~~~~~~~~~~~~~~~~~~~~~~~~~~~~~~~~~~~~~~~~~~~~~~~~~~~~~~~~~~~~~~
% Engine Calculations Based On INPUT #2
%~~~~~~~~~~~~~~~~~~~~~~~~~~~~~~~~~~~~~~~~~~~~~~~~~~~~~~~~~~~~~~~~~~~~~~~~~
AF_ratio_ac = lambda*AF_ratio_stoich;     % Actual Air Fuel Ratio
AF_ratio_mol=lambda*AF_ratio_mol_sotich;
%~~~~~~~~~~~~~~~~~~~~~~~~~~~~~~~~~~~~~~~~~~~~~~~~~~~~~~~~~~~~~~~~~~~~~~~~~
%Predicts Combustion Efficiency (Reference To Blair)
%~~~~~~~~~~~~~~~~~~~~~~~~~~~~~~~~~~~~~~~~~~~~~~~~~~~~~~~~~~~~~~~~~~~~~~~~~
eta_comb1=eta_combmaX*(-1.6082+4.6509*lambda-2.0764*lambda^2);
P_BDC = Load*P_atm;                       % Inlet Pressure[Pa] Moscow,ID
%~~~~~~~~~~~~~~~~~~~~~~~~~~~~~~~~~~~~~~~~~~~~~~~~~~~~~~~~~~~~~~~~~~~~~~~~~
%Polynomials Used To Calculate Gamma As A Function Of RPM
%~~~~~~~~~~~~~~~~~~~~~~~~~~~~~~~~~~~~~~~~~~~~~~~~~~~~~~~~~~~~~~~~~~~~~~~~~
a_1 = .692; a_2 = 39.17e-06; a_3 = 52.9e-09; a_4 = -228.62e-13;
a_5 = 277.58e-17;b_0 = 3049.33; b_1 = -5.7e-02; b_2 = -9.5e-05;
b_3 = 21.53e-09;b_4 = -200.26e-14;c_u = 2.32584; c_r = 4.186e-03;
d_0 = 10.41066; d_1 = 7.85125; d_3 = -3.71257;e_0 = -15.001e03;
e_1 = -15.838e03; e_3 = 9.613e03;f_0 = -.10329; f_1 = -.38656;
f_3 = .154226; f_4 = -14.763; f_5 = 118.27; f_6 = 14.503;
```

```
r_0 = -.2977; r_1 = 11.98; r_2 = -25442; r_3 = -.4354;
%~~~~~~~~~~~~~~~~~~~~~~~~~~~~~~~~~~~~~~~~~~~~~~~~~~~~~~~~~~~~~~~~~~~~~~~~~
% Initial Preallocation of Matrices
V(1:720)=zeros;          DV(1:720)=zeros;         rho(1:720)=zeros;
mu(1:720)=zeros;         C_k(1:720)=zeros;        C_R(1:720)=zeros;
X(1:720)=zeros;          M_F(1:720)=zeros;        DX(1:720)=zeros;
Re(1:720)=zeros;         Nus(1:720)=zeros;        h_g(1:720)=zeros;
DT(1:720)=zeros;         DP(1:720)=zeros;         P(1:720)=zeros;
T(1:720)=zeros;          W_doT(1:720)=zeros;      W(1:720)=zeros;
u(1:720)=zeros;          m_u(1:720)=zeros;        T_indicated(1:720)=zeros;
du(1:720)=zeros;         cV(1:720)=zeros;         m_b(1:720)=zeros;
V_u(1:720)=zeros;        V_b(1:720)=zeros;        T_u(1:720)=zeros;
T_b(1:720)=zeros;        A_u(1:720)=zeros;        A_b(1:720)=zeros;
DT_u(1:720)=zeros;       gamma_u(1:720)=zeros;    u_u(1:720)=zeros;
du_u(1:720)=zeros;       cv_u(1:720)=zeros;       Throw(1:720)=zeros;
x(1:720)=zeros;          Thrad(1:720)=zeros;      BD(1:720)=zeros;
T4(1:720)=0;             DT_b(1:720)=zeros;       P_m(1:720)=zeros;
w(1:720)=zeros;          h_w(1:720)=zeros;        h_h(1:720)=zeros;
DQ_w_A(1:720)=zeros;     DQ_w2_A(1:720)=zeros;    DQ_w_W(1:720)=zeros;
DQ_w2_W(1:720)=zeros;    DQ_w_H(1:720)=zeros;     DQ_w2_H(1:720)=zeros;
DQ_A(1:720)=zeros;       DQ2_A(1:720)=zeros;      DQ_W(1:720)=zeros;
DQ2_W(1:720)=zeros;      DQ_H(1:720)=zeros;       DQ2_H(1:720)=zeros;
Q_A(1:720)=zeros;        Q2_A(1:720)=zeros;       Q_W(1:720)=zeros;
Q2_W(1:720)=zeros;       Q_H(1:720)=zeros;        Q2_H(1:720)=zeros;
Q_doT_A(1:720)=zeros;    Q_doT_W(1:720)=zeros;    Q_doT_H(1:720)=zeros;
A(1:720)=zeros;          h_a(1:720)=zeros;        h_s(1:720)=zeros;
DQ_w_S(1:720)=zeros;     DQ_w2_S(1:720)=zeros;    DQ_S(1:720)=zeros;
DQ2_S(1:720)=zeros;      Q_S(1:720)=zeros;        Q2_S(1:720)=zeros;
Q_doT_S(1:720)=zeros;    DQ(1:720)=zeros;
% Index (k = 1:2) Serve as the EGR simulation,
% Functionality of the EGR simulation required the script to run two times
% with only the gas temperature and fluid properties changing during the
% second iteration.
% Index (i = 2:360)calculated instantaneous engine features
%~~~~~~~~~~~~~~~~~~~~~~~~~~~~~~~~~~~~~~~~~~~~~~~~~~~~~~~~~~~~~~~~~~~~~~~~~
% Exhaust Gas Residual (EGR) Simulation
%~~~~~~~~~~~~~~~~~~~~~~~~~~~~~~~~~~~~~~~~~~~~~~~~~~~~~~~~~~~~~~~~~~~~~~~~~
R=R_air/1000;
for k = 1:2
% corrects Temperature Based On Exhaust Gas Residuals
if k==1
T_BDC = T_atm;          % Assumed Inlet Temperature [K]
else
T_BDC = T_corr;
end
%~~~~~~~~~~~~~~~~~~~~~~~~~~~~~~~~~~~~~~~~~~~~~~~~~~~~~~~~~~~~~~~~~~~~~~~~~
% Calculate Mass of Air In Cylinder/ Mass Of Fuel Based On AFR
%~~~~~~~~~~~~~~~~~~~~~~~~~~~~~~~~~~~~~~~~~~~~~~~~~~~~~~~~~~~~~~~~~~~~~~~~~
rho_a = P_BDC/(R_air*T_BDC);     % Air Density kg/m^3
m_a = rho_a*V_d;                 % Mass of Air In Cylinder [kg]
m_f = m_a/AF_ratio_ac;           % Mass Of Fuel In Cylinder [kg]
m_c1 = m_a + m_f;                % Mass In Cylinder
%~~~~~~~~~~~~~~~~~~~~~~~~~~~~~~~~~~~~~~~~~~~~~~~~~~~~~~~~~~~~~~~~~~~~~~~~~
% Specifying Initial Conditions For Loops
%~~~~~~~~~~~~~~~~~~~~~~~~~~~~~~~~~~~~~~~~~~~~~~~~~~~~~~~~~~~~~~~~~~~~~~~~~
BD(1:720)=zeros;
theta(1:720)=zeros;            % Starting Crank Angle [degree]
BD(1)=sqrt ((L1)^2+(L2)^2-2*(L1)*(L2)*cosd(theta(1)+theta1));
```

```
T4(1:720)=zeros;
T4(1) = 180-acosd(((L1)^2-(L2)^2+(BD(1))^2)/(2*L1*BD(1)))..
-acosd(((L4)^2-(L3)^2+(BD(1))^2)/(2*L4*BD(1)));
if(i>(180-theta1))
T4(1) = 180+acosd(((L1)^2-(L2)^2+(BD(1))^2)/(2*L1*BD(1)))..
-acosd(((L4)^2-(L3)^2+(BD(1))^2)/(2*L4*BD(1)));
end
if(i>(360-theta1))
T4(1) = 180-acosd(((L1)^2-(L2)^2+(BD(1))^2)/(2*L1*BD(1)))..
-acosd(((L4)^2-(L3)^2+(BD(1))^2)/(2*L4*BD(1)));
end
if(i>(540-theta1))
T4(1) = 180+acosd(((L1)^2-(L2)^2+(BD(1))^2)/(2*L1*BD(1)))..
-acosd(((L4)^2-(L3)^2+(BD(1))^2)/(2*L4*BD(1)));
end
if(i>(720-theta1))
T4(1) = 180-acosd(((L1)^2-(L2)^2+(BD(1))^2)/(2*L1*BD(1)))..
-acosd(((L4)^2-(L3)^2+(BD(1))^2)/(2*L4*BD(1)));
end
%~~~~~~~~~~~~~~~~~~~~~~~~~~~~~~~~~~~~~~~~~~~~~~~~~~~~~~~~~~~~~~~~~~~~~~~~~
V(1:720)=zeros;          % Preallocate Volume Array
V(1)=V_TDC;              % Starting Combustion Chamber Volume [m^3]
G(1:720)=zeros;
DV(1:720)=zeros;         % Preallocate Change In Volume Array
DV(1)=0;                 % Specifying Initial Change In Volume
P(1:720)=P_BDC;          % Preallocate Pressure Array
DP(1:720)=zeros;         % Specifying Initial Change In Pressure
T(1:720)=zeros;          % Preallocate Temperature Array
T(1)=T_BDC;              % Inlet Temperature [K]
DT(1:720)=zeros;         % Specifying Initial Change In Temperature
T_u(1:720)=zeros;        % Preallocate Unburned Temperature Array
T_u(1)=T_BDC;            % Initial Unburned Temperature[K]
DT_u(1:720)=zeros;       % Preallocate Change In Unburned Temperature
gamma(1:720)=zeros;
gamma(1)=1.34;           % Initial Gamma Input
gamma_u(1:720)=zeros; gamma_u(1)=1.34; % Initial Gamma Input
X(1:720)=zeros;          % Preallocate Mass Burn Array
DX(1:720)=zeros;         % Preallocate Change In Mass Burn Fraction
Q(1:720)=zeros;          % Preallocate Heat Array
M_F(1:720)=zeros;        % Preallocate Mass In Comubstion Chamber Array
mu(1:720)=zeros;         % Preallocate Viscosity Array
mu(1)=7.457*10^(-6)+4.1547*10^(-8)*T_BDC-7.4793*10^(-12)*T_BDC^(2);
rho(1:720)=zeros;              % Preallocates Ideal Gas Law array
rho(1)=P(1)/(R_air*T(1));      % Initial Value Ideal Gas Array
C_k(1:720)=zeros;              % Preallocate Thermal Conductivity Array
C_k(1)=6.1944*10^(-3)+7.3814*10^(-5)*T_BDC-1.2491*10^(-8)*T_BDC^(2);
C_R(1:720)=zeros;              % Preallocate Radiation Coefficient Array
C_R(1)=4.25*10^(-09)*((T(1)^4-T_W^4)/(T(1)-T_W));
Re(1:720)=zeros;              % Preallocate Reynolds Value Array
Re(1)=rho(1)*S_bar_p*B/mu(1); % Initial Reynolds Value
Nus(1:720)=zeros;             % Preallocating Nusselt Number Array
Nus(1)=.49*Re(1)^(.7);      % Initial Nusselt Number
h_g(1:720)=zeros;           % Preallocate Heat Transfer Coefficient Array
h_g(1)=C_k(1)*Nus(1)/B;     % Initial Heat Transfer Coefficient (720-THETA)
Throw(1:720)=zeros;         % Preallocates angle Crank/rocker Axes Array
Throw(1)=(T4(1)-T4(1));     % Initial swing angle poistion [Degree]
Thrad(1:720)=zeros
Thrad(1)= Throw(1)*pi/180; % Initial swing angle poistion[Radin]
```

```
x(1:720)=zeros;            % Preallocates Distance Crank/Piston Axes Array
x(1)=L41*Thrad(1);         % Initial piston Distance [m]
W(1:720)=zeros;            % Preallocate Work Array
W_doT(1:720)=zeros;        % Preallocate Power Array
T_indicated(1:720)=zeros;  % Preallocate Torque Array
u(1:720)=zeros;            % Preallocate Internal Energy Array
du(1:720)=zeros;           % Preallocates Change In Internal Energy Array
cV(1:720)=zeros;              % Preallocates Heat Capacity Array
m_b(1:720)=zeros;              % Preallocate mass burned array
m_u(1:720)=m_c1;               % Preallocate unburned mass array
V_u(1:720)=zeros;              % Preallocate unburned Volume Array
V_u(1)=V(1);                   % Initial Unburned Volume
%~~~~~~~~~~~~~~~~~~~~~~~~~~~~~~~~~~~~~~~~~~~~~~~~~~~~~~~~~~~~~~~~~~~~~~~~~~
DQ_w_A(1:720)=zeros;     DQ_w2_A(1:720)=zeros;     DQ_w_W(1:720)=zeros;
DQ_w2_W(1:720)=zeros;    DQ_w_H(1:720)=zeros;      DQ_w2_H(1:720)=zeros;
DQ_A(1:720)=zeros;       DQ2_A(1:720)=zeros;       DQ_W(1:720)=zeros;
DQ2_W(1:720)=zeros;      DQ_H(1:720)=zeros;        DQ2_H(1:720)=zeros;
Q_A(1:720)=zeros;        Q2_A(1:720)=zeros;        Q_W(1:720)=zeros;
Q2_W(1:720)=zeros;       Q_H(1:720)=zeros;         Q2_H(1:720)=zeros;
Q_doT_A(1:720)=zeros;    Q_doT_W(1:720)=zeros;     Q_doT_H(1:720)=zeros;
A(1:720)=zeros;          h_a(1:720)=zeros;         h_s(1:720)=zeros;
DQ_w_S(1:720)=zeros;     DQ_w2_S(1:720)=zeros;     DQ_S(1:720)=zeros;
DQ2_S(1:720)=zeros;      Q_S(1:720)=zeros;         Q2_S(1:720)=zeros;
Q_doT_S(1:720)=zeros;    DQ(1:720)=zeros;          DT_b(1:720)=zeros;
%~~~~~~~~~~~~~~~~~~~~~~~~~~~~~~~~~~~~~~~~~~~~~~~~~~~~~~~~~~~~~~~~~~~~~~~~~~
% Instantaneous Engine Features Simulation
%~~~~~~~~~~~~~~~~~~~~~~~~~~~~~~~~~~~~~~~~~~~~~~~~~~~~~~~~~~~~~~~~~~~~~~~~~~
theta=1:720;
for i=2:720
%~~~~~~~~~~~~~~~~~~~~~~~~~~~~~~~~~~~~~~~~~~~~~~~~~~~~~~~~~~~~~~~~~~~~~~~~~~
BD(i)=sqrt((L1)^2+(L2)^2-2*(L1)*(L2)*cosd(theta(i)+theta1));
% Calculates length BD [m]
G(i)=acosd(((L3)^2+(L4)^2-(BD(i))^2)/(2*L3*L4));
% Calculates Transmission angle [Degree]
T4(i)=180-acosd(((L1)^2-(L2)^2+(BD(i))^2)/(2*L1*BD(i)))-...
acosd(((L4)^2-(L3)^2+(BD(i))^2)/(2*L4*BD(i)));
% Calculates Theta4 [Degree]
if(i>(180-theta1))
T4(i) = 180+acosd(((L1)^2-(L2)^2+(BD(i))^2)/(2*L1*BD(i)))...
-acosd(((L4)^2-(L3)^2+(BD(i))^2)/(2*L4*BD(i)));
end
if(i>(360-theta1))
T4(i) = 180-acosd(((L1)^2-(L2)^2+(BD(i))^2)/(2*L1*BD(i)))...
-acosd(((L4)^2-(L3)^2+(BD(i))^2)/(2*L4*BD(i)));
end
if(i>(540-theta1))
T4(i) = 180+acosd(((L1)^2-(L2)^2+(BD(i))^2)/(2*L1*BD(i)))...
-acosd(((L4)^2-(L3)^2+(BD(i))^2)/(2*L4*BD(i)));
end
if(i>(720-theta1))
T4(i) = 180-acosd(((L1)^2-(L2)^2+(BD(i))^2)/(2*L1*BD(i)))...
-acosd(((L4)^2-(L3)^2+(BD(i))^2)/(2*L4*BD(i)));
end
%~~~~~~~~~~~~~~~~~~~~~~~~~~~~~~~~~~~~~~~~~~~~~~~~~~~~~~~~~~~~~~~~~~~~~~~~~~
Throw(i)=(T4(i)-T4(1));
% Calculates Swing Angle position as a Function of Crank  Angle [Degree]
Thrad(i)=Throw(i)*pi/180;
% Calculates Swing Angle position as a Function of Crank  Angle [Radian]
```

```
x(i)=L41*Thrad(i);
% Calculates Piston Displacement as a Function of Crank  Angle [m]
V(i)=V_TDC + (pi/4)*(B^2)*x(i);
% Calculates Total Cyl. Volume as a Function of Crank  Angle [m3]
DV(i)=V(i)-V(i-1);
%~~~~~~~~~~~~~~~~~~~~~~~~~~~~~~~~~~~~~~~~~~~~~~~~~~~~~~~~~~~~~~~~~~~~~~~~~~
%Calculates Density As A Function Of Crank Angle
rho(i)=P(i-1)/(R_air*T(i-1));
%Calculates Viscosity As A Function Of Temperature
mu(i)=7.457*10^(-6)+4.1547*10^(-8)*T(i-1)-7.4793*10^(-12)*T(i-1)^(2);
%Calculating Instantaneous Thermal Conductivity of Cylinder Gas
C_k(i)=6.1944*10^(-3)+7.3814*10^(-5)*T(i-1)-1.2491*10^(-8)*T(i-1)^(2);
%Calculating The Radiation Heat Transfer Coefficient
C_R(i)=(4.25*10^(-9))*((T(i-1)^4-T_W^4)/(T(i-1)-T_W));
%Instantaneous Suface Area (For Heat Transfer);
A(i) = A_ch + A_p + pi*B*x(i) ;
if i<=2
A_u=A;
end
%~~~~~~~~~~~~~~~~~~~~~~~~~~~~~~~~~~~~~~~~~~~~~~~~~~~~~~~~~~~~~~~~~~~~~~~~~~
%Specifies Mass Fraction Burn As A Function Of Crank Angle (Weibe Fcn.)
%Also Specifies Mass Of Fuel In Combustion Chamber As A Function Of Theta
if theta(i)<theta_0
X(i)=0;
else
X(i) = 1-exp(-5*((theta(i)-theta_0)/theta_b)^3);
if theta(i) < theta_f
M_F(i) = V(theta_0-1)*rho(theta_0-1)/(lambda*AF_ratio_mol);
end
end
%Specifies Change In Mass Fraction Burn As A Function Of Crank Angle
DX(i) = X(i) - X(i-1);
%~~~~~~~~~~~~~~~~~~~~~~~~~~~~~~~~~~~~~~~~~~~~~~~~~~~~~~~~~~~~~~~~~~~~~~~~~~
% Heat Transfer Prediction
%~~~~~~~~~~~~~~~~~~~~~~~~~~~~~~~~~~~~~~~~~~~~~~~~~~~~~~~~~~~~~~~~~~~~~~~~~~
% Using ANNAND METHOD CAlCULATION
%~~~~~~~~~~~~~~~~~~~~~~~~~~~~~~~~~~~~~~~~~~~~~~~~~~~~~~~~~~~~~~~~~~~~~~~~~~
% Calculating Reynolds Number
Re(i)=(rho(i)*S_bar_p*B)/(mu(i));
% Calculating Nusselt Number (constant=.26 two stroke, .49 4 stroke)
Nus(i)=0.49*(Re(i)^(0.7));
% Heat Transfer Coefficient Using Annand Method (convection part)
h_g(i)=(C_k(i)*Nus(i))/B;
% Calculate Heat Transfer Coefficient Using Annand Method
h_a(i)=(h_g(i)+C_R(i));
% Calculates Convective Losses Into Wall As A Function Of Crank Angle
DQ_w_A(i)=(h_g(i)+C_R(i))*A(i)*(T(i-1)-T_W)*(60/(720*RPM));
DQ_w2_A(i)=((h_g(i)+C_R(i))*A_b(i-1)/N_cyl*(T_b(i-1)-T_W)+...
(h_g(i)+C_R(i))*A_u(i-1)/N_cyl*(T_u(i-1)-T_W))*(60/(720*RPM));
%~~~~~~~~~~~~~~~~~~~~~~~~~~~~~~~~~~~~~~~~~~~~~~~~~~~~~~~~~~~~~~~~~~~~~~~~~~
%Using WOSCHNI METHOD
%~~~~~~~~~~~~~~~~~~~~~~~~~~~~~~~~~~~~~~~~~~~~~~~~~~~~~~~~~~~~~~~~~~~~~~~~~~
if IVC >= theta(i) && theta(i)>theta_0      %(compression)
c_1=2.28;
c_2=0;
elseif theta_0>=theta(i)&& theta(i)>EVO     %(Combustion & Expantion)
c_1=2.28;
c_2=3.24*10^-3;
```

```
else                                        %(Intake and Exhaust)
c_1=6.18;
c_2=0;
end
%The working-fluid pressure, volume, and temperature at some
%reference state (say inlet valve closing or start of combustion)
P_r = P(IVC+1);
V_r = V(IVC+1);
T_r = T(IVC+1);
b=0.8;
%P_r = P(theta_0+1);
%V_r = V(theta_0+1);
%T_r = T(theta_0+1);
P_m(i)=(P_r)*((V_r/V(i))^gamma(i));
% the average gas velocity [m/s]
w(i)=((c_1*S_bar_p)+(c_2)*((V_d*T_r)/(P_r*V_r))*((P(i))-P_m(i)));
% the convective heat transfer coefficient
h_w(i)=130*(B^(b-1))*((P(i-1)/100000)^b)...
*((T(i-1))^(0.75-1.62*b))*(w(i-1))^0.8;
% Calculates Convective Losses Into Wall As A Function Of Crank Angle
DQ_w_W(i)=(h_w(i))*A(i)*(T(i-1)-T_W)*(60/(720*RPM));
DQ_w2_W(i)=((h_w(i))*A_u(i-1)/N_cyl*(T_u(i-1)-T_W)...
+(h_w(i))*A_b(i-1)/N_cyl*(T_b(i-1)-T_W))*(60/(720*RPM));
%~~~~~~~~~~~~~~~~~~~~~~~~~~~~~~~~~~~~~~~~~~~~~~~~~~~~~~~~~~~~~~~~~~~~~~~~~~
%Using HOHENBERG METHOD
%~~~~~~~~~~~~~~~~~~~~~~~~~~~~~~~~~~~~~~~~~~~~~~~~~~~~~~~~~~~~~~~~~~~~~~~~~~
h_h(i)= (130*(V_d^(-0.06))*((P(i-1)/100000)^(0.8))...
*((T(i-1))^(-0.4))*((1.4+S_bar_p)^(0.8)));
DQ_w_H(i)=(h_h(i))*A(i)*(T(i-1)-T_W)*(60/(720*RPM));
DQ_w2_H(i)=((h_h(i))*A_u(i-1)/N_cyl*(T_u(i-1)-T_W)...
+(h_h(i))*A_b(i-1)/N_cyl*(T_b(i-1)-T_W))*(60/(720*RPM));
%~~~~~~~~~~~~~~~~~~~~~~~~~~~~~~~~~~~~~~~~~~~~~~~~~~~~~~~~~~~~~~~~~~~~~~~~~~
%Using SITKEI METHOD
%~~~~~~~~~~~~~~~~~~~~~~~~~~~~~~~~~~~~~~~~~~~~~~~~~~~~~~~~~~~~~~~~~~~~~~~~~~
% For different types of combustion chambers, b was found to vary
% Direction combustion chamber (Hesselmann type) (0 - 0.03)
% Piston Chamber (0.05 - 0.1 )
% Swirl Chamber  (0.15 - 0.25)
% Precombustion Chamber (0.25 - 0.35)
% equivalent diameter
d_e = (4*(V_d)/(A(i)));
h_s(i)= 0.01455*(1+0.1)*((((P(i-1))^0.7)...
*(S_bar_p^0.7))/(((T(i-1))^0.2)*(d_e^0.3)))+C_R(i);
DQ_w_S(i)=(h_s(i))*A(i)*(T(i-1)-T_W)*(60/(720*RPM));
DQ_w2_S(i)=((h_s(i))*A_u(i-1)/N_cyl*(T_u(i-1)-T_W)...
+(h_s(i))*A_b(i-1)/N_cyl*(T_b(i-1)-T_W))*(60/(720*RPM));
%~~~~~~~~~~~~~~~~~~~~~~~~~~~~~~~~~~~~~~~~~~~~~~~~~~~~~~~~~~~~~~~~~~~~~~~~~~
%Calculates Total Heat Transfer (Per Cycle)
%~~~~~~~~~~~~~~~~~~~~~~~~~~~~~~~~~~~~~~~~~~~~~~~~~~~~~~~~~~~~~~~~~~~~~~~~~~
%Annand's Correlation
DQ_A(i) = eta_comb1*LHV*M_F(i)*DX(i)-DQ_w_A(i);
%Change In Heat Transfer (total) As A Function Of Crank Angle
DQ2_A(i)= eta_comb1*LHV*M_F(i)*DX(i)-DQ_w2_A(i);
%Change In Heat Transfer (total) As A Function Of Crank Angle Two-Zone
%~~~~~~~~~~~~~~~~~~~~~~~~~~~~~~~~~~~~~~~~~~~~~~~~~~~~~~~~~~~~~~~~~~~~~~~~~~
%Woschni's Correlation
DQ_W(i) = eta_comb1*LHV*M_F(i)*DX(i)-DQ_w_W(i);
%Change In Heat Transfer (total) As A Function Of Crank Angle
```

```
DQ2_W(i)= eta_comb1*LHV*M_F(i)*DX(i)-DQ_w2_W(i);
%Change In Heat Transfer (total) As A Function Of Crank Angle Two-Zone
%~~~~~~~~~~~~~~~~~~~~~~~~~~~~~~~~~~~~~~~~~~~~~~~~~~~~~~~~~~~~~~~~~~~~~~~~~~
%Hohenberg's Correlation
DQ_H(i) = eta_comb1*LHV*M_F(i)*DX(i)-DQ_w_H(i);
%Change In Heat Transfer (total) As A Function Of Crank Angle
DQ2_H(i)= eta_comb1*LHV*M_F(i)*DX(i)-DQ_w2_H(i);
%Change In Heat Transfer (total) As A Function Of Crank Angle Two-Zone
%~~~~~~~~~~~~~~~~~~~~~~~~~~~~~~~~~~~~~~~~~~~~~~~~~~~~~~~~~~~~~~~~~~~~~~~~~~
% Sitkei's Correlation
DQ_S(i) = eta_comb1*LHV*M_F(i)*DX(i)-DQ_w_S(i);
%Change In Heat Transfer (total) As A Function Of Crank Angle
DQ2_S(i)= eta_comb1*LHV*M_F(i)*DX(i)-DQ_w2_S(i);
%Change In Heat Transfer (total) As A Function Of Crank Angle Two-Zone
%~~~~~~~~~~~~~~~~~~~~~~~~~~~~~~~~~~~~~~~~~~~~~~~~~~~~~~~~~~~~~~~~~~~~~~~~~~
%Annand
Q_A(i)  = Q_A(i-1) + DQ_A(i);
Q2_A(i) = Q2_A(i-1)+ DQ2_A(i);
%~~~~~~~~~~~~~~~~~~~~~~~~~~~~~~~~~~~~~~~~~~~~~~~~~~~~~~~~~~~~~~~~~~~~~~~~~~
%Woschni
Q_W(i)  = Q_W(i-1) + DQ_W(i);
Q2_W(i) = Q2_W(i-1)+ DQ2_W(i);
%~~~~~~~~~~~~~~~~~~~~~~~~~~~~~~~~~~~~~~~~~~~~~~~~~~~~~~~~~~~~~~~~~~~~~~~~~~
%Hohenberg
Q_H(i)  = Q_H(i-1) + DQ_H(i);
Q2_H(i) = Q2_H(i-1)+ DQ2_H(i);
%~~~~~~~~~~~~~~~~~~~~~~~~~~~~~~~~~~~~~~~~~~~~~~~~~~~~~~~~~~~~~~~~~~~~~~~~~~
%Sitkei
Q_S(i)  = Q_S(i-1) + DQ_S(i);
Q2_S(i) = Q2_S(i-1)+ DQ2_S(i);
%~~~~~~~~~~~~~~~~~~~~~~~~~~~~~~~~~~~~~~~~~~~~~~~~~~~~~~~~~~~~~~~~~~~~~~~~~~
% To be used on Modified combustion model
DQ(i)=DQ_A(i);    %Annand
%DQ(i)=DQ_W(i);   %Woschni
%DQ(i)=DQ_H(i);   %Hohenberg
%DQ(i)=DQ_S(i);   %Sitkei
%~~~~~~~~~~~~~~~~~~~~~~~~~~~~~~~~~~~~~~~~~~~~~~~~~~~~~~~~~~~~~~~~~~~~~~~~~~
% Specifies Pressure and Temperature Increases Between Intake Valve
% Closing and Exhaust Valve Opening...50
if  IVC < theta(i)
DT(i)=T(i-1)*(gamma(i-1)-1)*((1/(P(i-1)*V(i-1)))*DQ(i)-(1/V(i-1))*DV(i));
DP(i)=(-P(i-1)/V(i-1))*DV(i)+(P(i-1)/T(i-1))*DT(i);
P(i)=P(i-1)+DP(i);
end
if 256<= theta(i)
if P(i)<=P_atm
P(i)=P_atm;
end
end
if EVO < theta(i)
P(i)=0.3086*100000; %this value is based on experimental observation
%P(i)=P(i);         %uncommand this under normal condition
end
%~~~~~~~~~~~~~~~~~~~~~~~~~~~~~~~~~~~~~~~~~~~~~~~~~~~~~~~~~~~~~~~~~~~~~~~~~~
%QUASI-DIMENTIONAL CRANK-ROCKER MODEL (TWO ZONE)
%Calculate Burned, Unburned Mass Fractions (TWO ZONE)
m_b(i) = m_b(i-1)+DX(i)*m_c1;   % Burned zone Mass
m_u(i) = m_u(i-1)-DX(i)*m_c1;   % Unburned zone Mass
```

```
%~~~~~~~~~~~~~~~~~~~~~~~~~~~~~~~~~~~~~~~~~~~~~~~~~~~~~~~~~~~~~~~~~~~~~~~~~~
% Calculating Burned and Unburned Volumes
if theta(i)<=theta_0
V_u(i)=N_cyl*V(i);
elseif theta(i)>theta_0
V_u(i)=((m_u(i)*V_u(i-1))/m_u(i-1))*(P(i)/P(i-1))^(-1/gamma_u(i-1));
end
V_b(i)=N_cyl*V(i)-V_u(i);
if V_b(i)<0
V_b(i)=0;
end
%~~~~~~~~~~~~~~~~~~~~~~~~~~~~~~~~~~~~~~~~~~~~~~~~~~~~~~~~~~~~~~~~~~~~~~~~~~
%Calculating Burned, Unburned Temperatures
T_u(i)=P(i)*V_u(i)/(m_u(i)*R*1000);
if theta(i) <= theta_0+4
T_b(i)=0;
end
if theta(i)>theta_0+4
T_b(i)=P(i)*V_b(i)/(m_b(i)*R*1000);
end
DT_u(i)=T_u(i)-T_u(i-1);
DT_b(i)=T_b(i)-T_b(i-1);
%~~~~~~~~~~~~~~~~~~~~~~~~~~~~~~~~~~~~~~~~~~~~~~~~~~~~~~~~~~~~~~~~~~~~~~~~~~
%Calculate Unburned, Burned Areas Based On Volume Ratio
A_u(i)=A(i)*(1-sqrt(X(i)));
A_b(i)=A(i)*(X(i)/sqrt(X(i)));
%~~~~~~~~~~~~~~~~~~~~~~~~~~~~~~~~~~~~~~~~~~~~~~~~~~~~~~~~~~~~~~~~~~~~~~~~~~
%Returns Temperature Values To Beginning Of Loop
%Assumes Temperature Drops Back To ATM Temp After Exhaust Is Extracted
T(i) = T(i-1)+DT(i);
% Returns Temperature Values To Beginning Of Loop
% Assume A Polytropic Constant Of 1.3
R_frac = (1/C_r)*(P_BDC/P_atm)^(1/1.3)*(1/lambda);
% Calculate The Residual Gas Fraction
% Treats Atmospheric Pressure As Reference State
W(i) = W(i-1)+(P(i)-P_atm)*DV(i);
% Calculates Cylinder Work [J] As A Function Of Crank Angle
W_doT(i)=(N_cyl*W(i)*N/N_r)/1000;
% Calculates Power [kW] As A Function Of Crank Angle
imep = CF*W_doT(720)*N_r*1000/(V_d*1000*N);
% Indicated Mean Effective Pressure
T_indicated(i) = (W_doT(i)*1000)/(2*pi*N);
% Calculates Torque[N*m] As A Function Of Crank Angle
%~~~~~~~~~~~~~~~~~~~~~~~~~~~~~~~~~~~~~~~~~~~~~~~~~~~~~~~~~~~~~~~~~~~~~~~~~~
Q_doT_A(i) = (N_cyl*Q_A(i)*N/N_r)/1000;
% Calculates Heat Loss [kW] As A Function Of Crank Angle Annand
Q_doT_W(i) = (N_cyl*Q_W(i)*N/N_r)/1000;
% Calculates Heat Loss [kW] As A Function Of Crank Angle Woschni
Q_doT_H(i) = (N_cyl*Q_H(i)*N/N_r)/1000;
% Calculates Heat Loss [kW] As A Function Of Crank Angle Hohenberg
Q_doT_S(i) = (N_cyl*Q_S(i)*N/N_r)/1000;
% Calculates Heat Loss [kW] As A Function Of Crank Angle Sitk
%~~~~~~~~~~~~~~~~~~~~~~~~~~~~~~~~~~~~~~~~~~~~~~~~~~~~~~~~~~~~~~~~~~~~~~~~~~
%The Following Section Of Code Calculates An Updated Value Of Gamma
%Using The "Polynomial Method" Developed By Krieger-Borman
%User Of This Code Must Be Careful Because Accuracy Of This Method
%Drops As The Fuel Mixture Becomes Increasingly Rich
%~~~~~~~~~~~~~~~~~~~~~~~~~~~~~~~~~~~~~~~~~~~~~~~~~~~~~~~~~~~~~~~~~~~~~~~~~~
```

```
%Calculates A,B Factors For Following Block Of Code
A_T  = a_1*T(i)+a_2*T(i)^2+a_3*T(i)^3+a_4*T(i)^4+a_5*T(i)^5;
A_tu = a_1*T_u(i)+a_2*T_u(i)^2+a_3*T_u(i)^3+a_4*T_u(i)^4+a_5*T_u(i)^5;
B_T  = b_0+b_1*T(i)+b_2*T(i)^2+b_3*T(i)^3+b_4*T(i)^4;
B_tu = b_0+b_1*T_u(i)+b_2*T_u(i)^2+b_3*T_u(i)^3+b_4*T_u(i)^4;
%Calculates Factor "D" As A Function Of lambda
D_lambda = d_0 + d_1*lambda^(-1)+ d_3*lambda^(-3);
%Calculates Factor "F" As A Function Of Temperature,lambda
E_Tlambda = (e_0+e_1*lambda^(-1)+e_3*lambda^(-3))/T(i);
E_TLambdau =(e_0+e_1*lambda^(-1)+e_3*lambda^(-3))/T_u(i);
F_TPlambda =(f_0+f_1*lambda^(-1)+f_3*lambda^(-3)+...
((f_4 + f_5*lambda^(-1))/T(i)))*log(f_6*P(i));
F_TPLambdau=(f_0+f_1*lambda^(-1)+f_3*lambda^(-3)+...
((f_4 + f_5*lambda^(-1))/T_u(i)))*log(f_6*P(i));
%~~~~~~~~~~~~~~~~~~~~~~~~~~~~~~~~~~~~~~~~~~~~~~~~~~~~~~~~~~~~~~~~~~~~~~~~~~
%Calculates correction Factor For Internal Energy
u_corr = c_u*exp(D_lambda +E_Tlambda + F_TPlambda);
u_corr_u=c_u*exp(D_lambda +E_TLambdau+ F_TPLambdau);
%~~~~~~~~~~~~~~~~~~~~~~~~~~~~~~~~~~~~~~~~~~~~~~~~~~~~~~~~~~~~~~~~~~~~~~~~~~
%Calculates Internal Energy As A Function Of Crank Angle
u(i) = A_T - B_T/lambda + u_corr;
u_u(i) = A_tu - B_tu/lambda + u_corr_u;
%~~~~~~~~~~~~~~~~~~~~~~~~~~~~~~~~~~~~~~~~~~~~~~~~~~~~~~~~~~~~~~~~~~~~~~~~~~
%Calculates Change In Internal Energy
du(i) = u(i) - u(i-1);
du_u(i) = u_u(i) - u_u(i-1);
%~~~~~~~~~~~~~~~~~~~~~~~~~~~~~~~~~~~~~~~~~~~~~~~~~~~~~~~~~~~~~~~~~~~~~~~~~~
%Calculates Heat Capacity "C_v" As A Function Of Crank Angle
cV(i) = du(i)/DT(i);
cv_u(i)=du_u(i)/DT_u(i);
%~~~~~~~~~~~~~~~~~~~~~~~~~~~~~~~~~~~~~~~~~~~~~~~~~~~~~~~~~~~~~~~~~~~~~~~~~~
%Calculates correction Factor For "R" Value As A Function Of Crank Angle
R_corr=c_r*exp(r_0*log(lambda)+...
(r_1+r_2/T(i)+r_3*log(f_6*P(i)))/lambda);
R_corr_u=c_r*exp(r_0*log(lambda)+...
(r_1+r_2/T_u(i-1)+r_3*log(f_6*P(i)))/lambda);
%~~~~~~~~~~~~~~~~~~~~~~~~~~~~~~~~~~~~~~~~~~~~~~~~~~~~~~~~~~~~~~~~~~~~~~~~~~
%Calculates Actual "R" Value
R = .287 + .020/lambda + R_corr;
R_u = .287 + .020/lambda + R_corr_u;
%~~~~~~~~~~~~~~~~~~~~~~~~~~~~~~~~~~~~~~~~~~~~~~~~~~~~~~~~~~~~~~~~~~~~~~~~~~
%Calculates Actual Gamma Value And Returns To Beginning Of Code
gamma_u(i)=1+R_u/cv_u(i);
gamma(i) = 1 + R/cV(i);
if gamma(i)<1.2
gamma(i)=1.34;
gamma_u(i)=1.34;
end
if theta(i)>=EVO
gamma(i)=1.34;
gamma_u(i)=1.34;
end
%~~~~~~~~~~~~~~~~~~~~~~~~~~~~~~~~~~~~~~~~~~~~~~~~~~~~~~~~~~~~~~~~~~~~~~~~~~
%Calculate Temperature Of Exhaust Based On Polytropic Relations
if EVO < theta(i)
T(i)=T(EVO)*(P_BDC/P(EVO))^((gamma(i)-1)/gamma(i));
T_b(i)=T_b(EVO)*(P_BDC/P(EVO))^((gamma(i)-1)/gamma(i));
end
```

```
end
%~~~~~~~~~~~~~~~~~~~~~~~~~~~~~~~~~~~~~~~~~~~~~~~~~~~~~~~~~~~~~~~~~~~~~~~~~~~
%Calculates A corrected Inlet Temperature Based On EGR
%T_corr = R_frac*T(720)+(1-R_frac)*T_BDC;
T_corr = T_BDC;
end
%~~~~~~~~~~~~~~~~~~~~~~~~~~~~~~~~~~~~~~~~~~~~~~~~~~~~~~~~~~~~~~~~~~~~~~~~~~~
%Specified Outputs (On Matlab Screen)
W_doT_indicated=W_doT(720);
bmep = imep-fmep;
W_dot_ac=(bmep*V_d*1000*N/(N_r*1000));
T_ac1 = W_dot_ac/(2*pi*N*10^(-3));
%~~~~~~~~~~~~~~~~~~~~~~~~~~~~~~~~~~~~~~~~~~~~~~~~~~~~~~~~~~~~~~~~~~~~~~~~~~~
%Calculated Mechanical Efficiency (Based On Previous Inputs)
eta_m=bmep/imep;        %Calculates Mechanical Efficiency
%~~~~~~~~~~~~~~~~~~~~~~~~~~~~~~~~~~~~~~~~~~~~~~~~~~~~~~~~~~~~~~~~~~~~~~~~~~~
%Calculates Brake Specific Fuel Consumption (BSFC)
m_ta = P_BDC*V_d/(R_air*T_BDC);      %Calculate Trapped Air In Cylinder
eta_V = CF*((m_ta)/(rho_a*V_d));     %corrected Volumetric Efficiency
m_dot_f = N_cyl*M_F(theta_0)*(N/N_r);%Mass Flow Rate Of Fuel
m_dot_a= AF_ratio_ac*m_dot_f;        %Mass Flow Rate Of Air
BSFC= (m_dot_f*1000*3600)/(W_dot_ac);%BSFC [g/kW*h]
eta_f=3600/(BSFC*(LHV*10^(-6)));
%% Specifies Conditions For Minimum and Maximum Plot Values
x_min = min(x); x_max = max(x);
v_min = min(V); v_max = max(V);
p_min = min(P); p_max = max(P);
w_miN = min(W_doT); w_maX = max(W_doT);
T_miN = min(T); T_maX = max(T);
Q_miN_A = min(Q_doT_A); Q_maX_A = max(Q_doT_A);
Q_miN_W = min(Q_doT_W); Q_maX_W = max(Q_doT_W);
Q_miN_H = min(Q_doT_H); Q_maX_H = max(Q_doT_H);
Q_miN_S = min(Q_doT_S); Q_maX_S = max(Q_doT_S);
h_miN_a = min(h_a); h_maX_a = max(h_a);
h_miN_w = min(h_w); h_maX_w = max(h_w);
h_miN_h = min(h_h); h_maX_h = max(h_h);
h_miN_s = min(h_s); h_maX_s = max(h_s);
%~~~~~~~~~~~~~~~~~~~~~~~~~~~~~~~~~~~~~~~~~~~~~~~~~~~~~~~~~~~~~~~~~~~~~~~~~~~
% for saving the workbench (Use the saved workbench for plotting and
% comparison with experimental data)
% if Load==1
%  save HeatTransfer_100_S
% elseif Load==0.75
%     save HeatTransfer_75_S
% elseif Load==0.5
%     save HeatTransfer_50_S
% elseif Load==0.25
%     save HeatTransfer_25_S
% end
```

B.2 Stage I and II Plotting 1 (Matlab Code)

```
%Universiti Teknologi PETRONAS
%Project: Numerical Investigation and Optimization
%          of The Crank-Rocker Engine Ignition Timing
%          Based on Performance and Combustion Characteristics
%Methodology Stage: STAGE I and II
%Section: Crank-Rocker Engine Modified Combustion Model
%          and Heat Trasnfer Evaluation Plotting
% These codes are for plotting the combustion parameters
%~~~~~~~~~~~~~~~~~~~~~~~~~~~~~~~~~~~~~~~~~~~~~~~~~~~~~~~~~~~~~~~~~~~~~~
clear;
clc;
dd=dir();
%~~~~~~~~~~~~~~~~~~~~~~~~~~~~~~~~~~~~~~~~~~~~~~~~~~~~~~~~~~~~~~~~~~~~~~
%(HeatTransfer_Evaluation) Pressure
%H(parameter)(engine load)=[] -----> Preallocation
HP100=[];
HP75=[];
HP50=[];
HP25=[];
%~~~~~~~~~~~~~~~~~~~~~~~~~~~~~~~~~~~~~~~~~~~~~~~~~~~~~~~~~~~~~~~~~~~~~~
%(HeatTransfer_Evaluation) MFB
HX100=[];
HX75=[];
HX50=[];
HX25=[];
%~~~~~~~~~~~~~~~~~~~~~~~~~~~~~~~~~~~~~~~~~~~~~~~~~~~~~~~~~~~~~~~~~~~~~~
%(HeatTransfer_Evaluation) Volume
HV100=[];
HV75=[];
HV50=[];
HV25=[];
%~~~~~~~~~~~~~~~~~~~~~~~~~~~~~~~~~~~~~~~~~~~~~~~~~~~~~~~~~~~~~~~~~~~~~~
%(HeatTransfer_Evaluation) Temperature
HT100=[];
HT75=[];
HT50=[];
HT25=[];
%~~~~~~~~~~~~~~~~~~~~~~~~~~~~~~~~~~~~~~~~~~~~~~~~~~~~~~~~~~~~~~~~~~~~~~
%(HeatTransfer_Evaluation) Volume variation
HDV100=[];
HDV75=[];
HDV50=[];
HDV25=[];
%~~~~~~~~~~~~~~~~~~~~~~~~~~~~~~~~~~~~~~~~~~~~~~~~~~~~~~~~~~~~~~~~~~~~~~
for i=1:size(dd,1)
    name=dd(i).name;
    if size(name,2)>12
        if isequal(name(1:13),'HeatTransfer_')
            nE=name(14:end);%100_W.mat
            numE=str2num(nE(1:end-6));
            Lname=name(end-4);
            load(name)
            %==================================
            if numE==100
                [HP100,HX100,HV100,HT100,HDV100]=rec1..
                (name,HP100,HX100,HV100,HT100,HDV100);
            elseif numE==75
                [HP75,HX75,HV75,HT75,HDV75]=rec1..
```

```
                (name,HP75,HX75,HV75,HT75,HDV75);
            elseif numE==50
                [HP50,HX50,HV50,HT50,HDV50]=rec1..
                (name,HP50,HX50,HV50,HT50,HDV50);
            elseif numE==25
                [HP25,HX25,HV25,HT25,HDV25]=rec1..
                (name,HP25,HX25,HV25,HT25,HDV25);
            end
            %==================================
        end
    end
end
%~~~~~~~~~~~~~~~~~~~~~~~~~~~~~~~~~~~~~~~~~~~~~~~~~~~~~~~~~~~~~~~~~~~~~~~
%Load Experimental DATA
load V_Exp.csv
load P_Exp.csv
load theta_Exp.csv

%%
figure (1)
plot (theta_Exp,P_Exp,...
     'LineWidth',1.5)
hold on
plot((HP100(1,:)'/100000),'--','LineWidth',1.25)
plot((HP100(2,:)'/100000),':' ,'LineWidth',2)
plot((HP100(3,:)'/100000),'.-','LineWidth',1,...
     'MarkerIndice',1:15:720,'MarkerSize',13)
plot((HP100(4,:)'/100000),'-.','LineWidth',1.5)
legend({'Experimental','Annand','Hohenberg','Sitkei','Woschni'},...
        'Location','northeast',...
        'FontSize',6,...
        'NumColumns',1);
title('Indicated Cylinder Pressure Vs. Crank Angle [100%Load]',...
      'FontSize',5,...
      'position',[400,30.25,0])
xlabel('Crank Angle [deg]',...
       'position',[400,-2,0])
ylabel('Pressure [bar]',...
       'position',[265,15,-1])
axis([280 520 0 30])
hold off
set(gcf,'color','w',...
    'position',[77,57,357.12,265.89])
set(gca,'XMinorTick','on',...
        'YMinorTick','on',...
        'FontSize',7,...
        'FontWeight','bold',...
        'LineWidth',1)
PA100=gcf;
res=800;
print(PA100,'PA[100%].tiff','-dtiff',['-r' sprintf('%.of',res)]);
%~~~~~~~~~~~~~~~~~~~~~~~~~~~~~~~~~~~~~~~~~~~~~~~~~~~~~~~~~~~~~~~~~~~~~~~
figure (2)
plot((HP75(1,:)'/100000),'--','LineWidth',1.25)
hold on
plot((HP75(2,:)'/100000),':' ,'LineWidth',2)
plot((HP75(3,:)'/100000),'.-','LineWidth',1,...
    'MarkerIndice',1:15:720,'MarkerSize',13)
```

```
plot((HP75(4,:)'/100000),'-.','LineWidth',1.5)
legend({'Annand','Hohenberg','Sitkei','Woschni'},...
        'Location','northeast',...
        'FontSize',6,...
        'NumColumns',1);
title('Indicated Cylinder Pressure Vs. Crank Angle [75%Load]',...
      'FontSize',5,...
      'position',[400,30.25,0])
xlabel('Crank Angle [deg]',...
       'position',[400,-2,0])
ylabel('Pressure [bar]',...
       'position',[265,15,-1])
axis([280 520 0 30])
hold off
set(gcf,'color','w',...
    'position',[77,57,357.12,265.89])
set(gca,'XMinorTick','on',...
        'YMinorTick','on',...
        'FontSize',7,...
        'FontWeight','bold',...
        'LineWidth',1)
PA75=gcf;
res=800;
print(PA75,'PA[75%].tiff','-dtiff',['-r' sprintf('%.of',res)]);
%~~~~~~~~~~~~~~~~~~~~~~~~~~~~~~~~~~~~~~~~~~~~~~~~~~~~~~~~~~~~~~~~~~~~~~
figure (3)
plot((HP50(1,:)'/100000),'--','LineWidth',1.25)
hold on
plot((HP50(2,:)'/100000),':' ,'LineWidth',2)
plot((HP50(3,:)'/100000),'.-','LineWidth',1,...
    'MarkerIndice',1:15:720,'MarkerSize',13)
plot((HP50(4,:)'/100000),'-.','LineWidth',1.5)
legend({'Annand','Hohenberg','Sitkei','Woschni'},...
        'Location','northeast',...
        'FontSize',6,...
        'NumColumns',1);
title('Indicated Cylinder Pressure Vs. Crank Angle [50%Load]',...
      'FontSize',5,...
      'position',[400,30.25,0])
xlabel('Crank Angle [deg]',...
       'position',[400,-2,0])
ylabel('Pressure [bar]',...
       'position',[265,15,-1])
axis([280 520 0 30])
hold off
set(gcf,'color','w',...
    'position',[77,57,357.12,265.89])
set(gca,'XMinorTick','on',...
        'YMinorTick','on',...
        'FontSize',7,...
        'FontWeight','bold',...
        'LineWidth',1)
PA50=gcf;
res=800;
print(PA50,'PA[50%].tiff','-dtiff',['-r' sprintf('%.of',res)]);
%~~~~~~~~~~~~~~~~~~~~~~~~~~~~~~~~~~~~~~~~~~~~~~~~~~~~~~~~~~~~~~~~~~~~~~
figure (4)
plot((HP25(1,:)'/100000),'--','LineWidth',1.25)
```

```
hold on
plot((HP25(2,:)'/100000),':' ,'LineWidth',2)
plot((HP25(3,:)'/100000),'.-','LineWidth',1,...
    'MarkerIndice',1:15:720,'MarkerSize',13)
plot((HP25(4,:)'/100000),'-.','LineWidth',1.5)
legend({'Annand','Hohenberg','Sitkei','Woschni'},...
        'Location','northeast',...
        'FontSize',6,...
        'NumColumns',1);
title('Indicated Cylinder Pressure Vs. Crank Angle [25%Load]',...
      'FontSize',5,...
      'position',[400,30.25,0])
xlabel('Crank Angle [deg]',...
       'position',[400,-2,0])
ylabel('Pressure [bar]',...
       'position',[265,15,-1])
axis([280 520 0 30])
hold off
set(gcf,'color','w',...
    'position',[77,57,357.12,265.89])
set(gca,'XMinorTick','on',...
        'YMinorTick','on',...
        'FontSize',7,...
        'FontWeight','bold',...
        'LineWidth',1)
PA25=gcf;
res=800;
print(PA25,'PA[25%].tiff','-dtiff',['-r' sprintf('%.of',res)]);
%~~~~~~~~~~~~~~~~~~~~~~~~~~~~~~~~~~~~~~~~~~~~~~~~~~~~~~~~~~~~~~~~~~~~~~
%BAR CHARTS
%Max Pressure @100 Load
Peak_E_100=21.6876971;
Peak_A_100=21.67;
Peak_H_100=28.331;
Peak_S_100=25.693;
Peak_W_100=25.368;
%~~~~~~~~~~~~~~~~~
%Max Pressure @75 Load
Peak_A_75=21.016;
Peak_H_75=27.974;
Peak_S_75=25.013;
Peak_W_75=24.966;
%~~~~~~~~~~~~~~~~~
%Max Pressure @50 Load
Peak_A_50=20.098;
Peak_H_50=27.456;
Peak_S_50=24.01;
Peak_W_50=24.393;
%~~~~~~~~~~~~~~~~~
%Max Pressure @25 Load
Peak_A_25=18.552;
Peak_H_25=26.535;
Peak_S_25=22.186;
Peak_W_25=23.404;
%~~~~~~~~~~~~~~~~~
%Max Temperature @100 Load
Peak_TA_100=1735.1;
Peak_TH_100=1680.3;
```

```
Peak_TS_100=1699.2;
Peak_TW_100=1704.9;
%~~~~~~~~~~~~~~~~~
%Max Temperature @75 Load
Peak_TA_75=1743;
Peak_TH_75=1683;
Peak_TS_75=1705.5;
Peak_TW_75=1708.6;
%~~~~~~~~~~~~~~~~~
%Max Temperature @50 Load
Peak_TA_50=1754.9;
Peak_TH_50=1687;
Peak_TS_50=1715.5;
Peak_TW_50=1714;
%~~~~~~~~~~~~~~~~~
%Max Temperature @25 Load
Peak_TA_25=1776;
Peak_TH_25=1694.6;
Peak_TS_25=1736.2;
Peak_TW_25=1724.1;
%~~~~~~~~~~~~~~~~~~~~~~~~~~~~~~~~~~~~~~~~~~~~~~~~~~~~~~~~~~~~~~~~~~~~~
figure (5)
y_bar100=[Peak_E_100;Peak_A_100;Peak_H_100;Peak_S_100;Peak_W_100];
bar_PeakPressure_100=bar(y_bar100,0.6,'FaceColor','flat');
bar_PeakPressure_100.CData(1,:) = [0 0.4470 0.7410];
bar_PeakPressure_100.CData(2,:) = [0.6350 0.0780 0.1840];
bar_PeakPressure_100.CData(3,:) = [0.9290 0.6940 0.1250];
bar_PeakPressure_100.CData(4,:) = [0.4940 0.1840 0.5560];
bar_PeakPressure_100.CData(5,:) = [0.4660 0.6740 0.1880];
title('Maximum Pressure [100%Load]')
ylabel('Pressure [bar]',...
       'position',[-0.5,15,-1])
set(gcf,'color','w',...
        'position',[77,57,357.12,265.89])
set(gca,'xticklabel',...
   {'Experiment','Annand','Hohenberg','Sitkei','Woschni'},...
        'YMinorTick','on',...
        'ygrid','on',...
        'yMinorgrid','on',...
        'FontSize',7,...
        'FontWeight','bold',...
        'LineWidth',1)
Peak_P100=gcf;
res=800;
print(Peak_P100,...
     'Peak_P[100%].tiff','-dtiff',['-r' sprintf('%.of',res)]);
%~~~~~~~~~~~~~~~~~~~~~~~~~~~~~~~~~~~~~~~~~~~~~~~~~~~~~~~~~~~~~~~~~~~~~
figure (6)
y_bar75=[Peak_A_75;Peak_H_75;Peak_S_75;Peak_W_75];
bar_PeakPressure_75=bar(y_bar75,0.7,'FaceColor','flat');
bar_PeakPressure_75.CData(1,:) = [0.6350 0.0780 0.1840];
bar_PeakPressure_75.CData(2,:) = [0.9290 0.6940 0.1250];
bar_PeakPressure_75.CData(3,:) = [0.4940 0.1840 0.5560];
bar_PeakPressure_75.CData(4,:) = [0.4660 0.6740 0.1880];
title('Maximum Pressure [75%Load]')
ylabel('Pressure [bar]',...
       'position',[-0.5,15,-1])
set(gcf,'color','w',...
```

```
        'position',[77,57,357.12,265.89])
set(gca,'xticklabel',{'Annand','Hohenberg','Sitkei','Woschni'},...
        'YMinorTick','on',...
        'ygrid','on',...
        'yMinorgrid','on',...
        'FontSize',7,...
        'FontWeight','bold',...
        'LineWidth',1)
Peak_P75=gcf;
res=800;
print(Peak_P75,...
     'Peak_P[75%].tiff','-dtiff',['-r' sprintf('%.of',res)]);
%~~~~~~~~~~~~~~~~~~~~~~~~~~~~~~~~~~~~~~~~~~~~~~~~~~~~~~~~~~~~~~~~~~~~~~~
figure (7)
y_bar50=[Peak_A_50;Peak_H_50;Peak_S_50;Peak_W_50];
bar_PeakPressure_50=bar(y_bar50,0.7,'FaceColor','flat');
bar_PeakPressure_50.CData(1,:) = [0.6350 0.0780 0.1840];
bar_PeakPressure_50.CData(2,:) = [0.9290 0.6940 0.1250];
bar_PeakPressure_50.CData(3,:) = [0.4940 0.1840 0.5560];
bar_PeakPressure_50.CData(4,:) = [0.4660 0.6740 0.1880];
title('Maximum Pressure [50%Load]')
ylabel('Pressure [bar]',...
       'position',[-0.5,15,-1])
set(gcf,'color','w',...
        'position',[77,57,357.12,265.89])
set(gca,'xticklabel',{'Annand','Hohenberg','Sitkei','Woschni'},...
        'YMinorTick','on',...
        'ygrid','on',...
        'yMinorgrid','on',...
        'FontSize',7,...
        'FontWeight','bold',...
        'LineWidth',1)
Peak_P50=gcf;
res=800;
print(Peak_P50,...
     'Peak_P[50%].tiff','-dtiff',['-r' sprintf('%.of',res)]);
%~~~~~~~~~~~~~~~~~~~~~~~~~~~~~~~~~~~~~~~~~~~~~~~~~~~~~~~~~~~~~~~~~~~~~~~
figure (8)
y_bar25=[Peak_A_25;Peak_H_25;Peak_S_25;Peak_W_25];
bar_PeakPressure_25=bar(y_bar25,0.7,'FaceColor','flat');
bar_PeakPressure_25.CData(1,:) = [0.6350 0.0780 0.1840];
bar_PeakPressure_25.CData(2,:) = [0.9290 0.6940 0.1250];
bar_PeakPressure_25.CData(3,:) = [0.4940 0.1840 0.5560];
bar_PeakPressure_25.CData(4,:) = [0.4660 0.6740 0.1880];
title('Maximum Pressure [25%Load]')
ylabel('Pressure [bar]',...
       'position',[-0.5,15,-1])
set(gcf,'color','w',...
        'position',[77,57,357.12,265.89])
set(gca,'xticklabel',{'Annand','Hohenberg','Sitkei','Woschni'},...
        'YMinorTick','on',...
        'ygrid','on',...
        'yMinorgrid','on',...
        'FontSize',7,...
        'FontWeight','bold',...
        'LineWidth',1)
Peak_P25=gcf;
res=800;
```

```
print(Peak_P25,...
     'Peak_P[25%].tiff','-dtiff',['-r' sprintf('%.of',res)]);
%~~~~~~~~~~~~~~~~~~~~~~~~~~~~~~~~~~~~~~~~~~~~~~~~~~~~~~~~~~~~~~~~~~~~~~
figure (9)
y_bar_T100=[Peak_TA_100;Peak_TH_100;Peak_TS_100;Peak_TW_100];
bar_PeakTemperature_100=bar(y_bar_T100,0.7,'FaceColor','flat');
bar_PeakTemperature_100.CData(1,:) = [0.6350 0.0780 0.1840];
bar_PeakTemperature_100.CData(2,:) = [0.9290 0.6940 0.1250];
bar_PeakTemperature_100.CData(3,:) = [0.4940 0.1840 0.5560];
bar_PeakTemperature_100.CData(4,:) = [0.4660 0.6740 0.1880];
title('Maximum Temperature [100%Load]')
ylabel('Temperature [K]',...
       'position',[-0.65,1700,-1])
ylim([1650 1740]);
set(gcf,'color','w',...
        'position',[77,57,357.12,265.89])
set(gca,'xticklabel',{'Annand','Hohenberg','Sitkei','Woschni'},...
        'YMinorTick','on',...
        'ygrid','on',...
        'yMinorgrid','on',...
        'FontSize',7,...
        'FontWeight','bold',...
        'LineWidth',1)
Peak_T100=gcf;
res=800;
print(Peak_T100,...
     'Peak_T[100%].tiff','-dtiff',['-r' sprintf('%.of',res)]);
%~~~~~~~~~~~~~~~~~~~~~~~~~~~~~~~~~~~~~~~~~~~~~~~~~~~~~~~~~~~~~~~~~~~~~~
figure (10)
y_bar_T75=[Peak_TA_75;Peak_TH_75;Peak_TS_75;Peak_TW_75];
bar_PeakTemperature_75=bar(y_bar_T75,0.7,'FaceColor','flat');
bar_PeakTemperature_75.CData(1,:) = [0.6350 0.0780 0.1840];
bar_PeakTemperature_75.CData(2,:) = [0.9290 0.6940 0.1250];
bar_PeakTemperature_75.CData(3,:) = [0.4940 0.1840 0.5560];
bar_PeakTemperature_75.CData(4,:) = [0.4660 0.6740 0.1880];
title('Maximum Temperature [75%Load]')
ylabel('Temperature [K]',...
       'position',[-0.65,1700,-1])
ylim([1640 1750]);
set(gcf,'color','w',...
        'position',[77,57,357.12,265.89])
set(gca,'xticklabel',{'Annand','Hohenberg','Sitkei','Woschni'},...
        'YMinorTick','on',...
        'ygrid','on',...
        'yMinorgrid','on',...
        'FontSize',7,...
        'FontWeight','bold',...
        'LineWidth',1)
Peak_T75=gcf;
res=800;
print(Peak_T75,...
     'Peak_T[75%].tiff','-dtiff',['-r' sprintf('%.of',res)]);
%~~~~~~~~~~~~~~~~~~~~~~~~~~~~~~~~~~~~~~~~~~~~~~~~~~~~~~~~~~~~~~~~~~~~~~
figure (11)
y_bar_T50=[Peak_TA_50;Peak_TH_50;Peak_TS_50;Peak_TW_50];
bar_PeakTemperature_50=bar(y_bar_T50,0.7,'FaceColor','flat');
bar_PeakTemperature_50.CData(1,:) = [0.6350 0.0780 0.1840];
bar_PeakTemperature_50.CData(2,:) = [0.9290 0.6940 0.1250];
```

```
bar_PeakTemperature_50.CData(3,:) = [0.4940 0.1840 0.5560];
bar_PeakTemperature_50.CData(4,:) = [0.4660 0.6740 0.1880];
title('Maximum Temperature [50%Load]')
ylabel('Temperature [K]',...
       'position',[-0.65,1700,-1])
ylim([1640 1760]);
set(gcf,'color','w',...
        'position',[77,57,357.12,265.89])
set(gca,'xticklabel',{'Annand','Hohenberg','Sitkei','Woschni'},...
        'YMinorTick','on',...
        'ygrid','on',...
        'yMinorgrid','on',...
        'FontSize',7,...
        'FontWeight','bold',...
        'LineWidth',1)
Peak_T50=gcf;
res=800;
print(Peak_T50,...
     'Peak_T[50%].tiff','-dtiff',['-r' sprintf('%.of',res)]);
%~~~~~~~~~~~~~~~~~~~~~~~~~~~~~~~~~~~~~~~~~~~~~~~~~~~~~~~~~~~~~~~~~~~~~~
figure (12)
y_bar_T25=[Peak_TA_25;Peak_TH_25;Peak_TS_25;Peak_TW_25];
bar_PeakTemperature_25=bar(y_bar_T25,0.7,'FaceColor','flat');
bar_PeakTemperature_25.CData(1,:) = [0.6350 0.0780 0.1840];
bar_PeakTemperature_25.CData(2,:) = [0.9290 0.6940 0.1250];
bar_PeakTemperature_25.CData(3,:) = [0.4940 0.1840 0.5560];
bar_PeakTemperature_25.CData(4,:) = [0.4660 0.6740 0.1880];
title('Maximum Temperature [25%Load]')
ylabel('Temperature [K]',...
       'position',[-0.65,1720,-1])
ylim([1640 1780]);
set(gcf,'color','w',...
        'position',[77,57,357.12,265.89])
set(gca,'xticklabel',{'Annand','Hohenberg','Sitkei','Woschni'},...
        'YMinorTick','on',...
        'ygrid','on',...
        'yMinorgrid','on',...
        'FontSize',7,...
        'FontWeight','bold',...
        'LineWidth',1)
Peak_T25=gcf;
res=800;
print(Peak_T25,...
     'Peak_T[25%].tiff','-dtiff',['-r' sprintf('%.of',res)]);
%~~~~~~~~~~~~~~~~~~~~~~~~~~~~~~~~~~~~~~~~~~~~~~~~~~~~~~~~~~~~~~~~~~~~~~
%
function [HP,HX,HV,HT,HDV]=rec1(name,HP,HX,HV,HT,HDV)
    Lname=name(end-4);
    load(name)
    if isequal(Lname,'A')
        HP=[HP;P];
        HX=[HX;X];
        HV=[HV;V];
        HT=[HT;T];
        HDV=[HDV;DV];
    end
    if isequal(Lname,'W')
        HP=[HP;P];
```

```
        HX=[HX;X];
        HV=[HV;V];
        HT=[HT;T];
        HDV=[HDV;DV];
    end
    if isequal(Lname,'S')
        HP=[HP;P];
        HX=[HX;X];
        HV=[HV;V];
        HT=[HT;T];
        HDV=[HDV;DV];
    end
    if isequal(Lname,'H')
        HP=[HP;P];
        HX=[HX;X];
        HV=[HV;V];
        HT=[HT;T];
        HDV=[HDV;DV];
    end
end
%~~~~~~~~~~~~~~~~~~~~~~~~~~~~~~~~~~~~~~~~~~~~~~~~~~~~~~~~~~~~~~~~~~~~~~
```

B.3 Stage I and II Plotting 2 (Matlab Code)

```
%Universiti Teknologi PETRONAS
%Project: Numerical Investigation and Optimization
%          of The Crank-Rocker Engine Ignition Timing
%          Based on Performance and Combustion Characteristics
%Methodology Stage: STAGE I and II
%Section: Crank-Rocker Engine Modified Combustion Model
%          and Heat Trasnfer Evaluation Plotting
% These codes are for plotting the heat trasnfer evaluation
%~~~~~~~~~~~~~~~~~~~~~~~~~~~~~~~~~~~~~~~~~~~~~~~~~~~~~~~~~~~~~~~~~~~~~~~
clear;
clc;
%~~~~~~~~~~~~~~~~~~~~~~~~~~~~~~~~~~~~~~~~~~~~~~~~~~~~~~~~~~~~~~~~~~~~~~~
dd=dir();
%a='HeatTransfer_100_W.mat'
HH100=[]; DDQ2100=[]; DDQW100=[];DDQ100=[];DDDQ100=[];DDDQ_doT100=[];
HH75=[];  DDQ275=[];  DDQW75=[]; DDQ75=[]; DDDQ75=[]; DDDQ_doT75=[];
HH50=[];  DDQ250=[];  DDQW50=[]; DDQ50=[]; DDDQ50=[]; DDDQ_doT50=[];
HH25=[];  DDQ225=[];  DDQW25=[]; DDQ25=[]; DDDQ25=[]; DDDQ_doT25=[];
%~~~~~~~~~~~~~~~~~~~~~~~~~~~~~~~~~~~~~~~~~~~~~~~~~~~~~~~~~~~~~~~~~~~~~~~
for i=1:size(dd,1)
name=dd(i).name;
if size(name,2)>12
    %disp('me')
    if isequal(name(1:13),'HeatTransfer_')
        nE=name(14:end);%100_W.mat
        numE=str2num(nE(1:end-6));
        Lname=name(end-4);
        load(name)
        if numE==100
            [HH100,DDQ2100,DDQW100,DDQ100,DDDQ100,DDDQ_doT100]=rec1..
            (name,HH100,DDQ2100,DDQW100,DDQ100,DDDQ100,DDDQ_doT100);
        elseif numE==75
            [HH75,DDQ275,DDQW75,DDQ75,DDDQ75,DDDQ_doT75]=rec1..
            (name,HH75,DDQ275,DDQW75,DDQ75,DDDQ75,DDDQ_doT75);
        elseif numE==50
            [HH50,DDQ250,DDQW50,DDQ50,DDDQ50,DDDQ_doT50]=rec1..
            (name,HH50,DDQ250,DDQW50,DDQ50,DDDQ50,DDDQ_doT50);
        elseif numE==25
            [HH25,DDQ225,DDQW25,DDQ25,DDDQ25,DDDQ_doT25]=rec1..
            (name,HH25,DDQ225,DDQW25,DDQ25,DDDQ25,DDDQ_doT25);
        end
%~~~~~~~~~~~~~~~~~~~~~~~~~~~~~~~~~~~~~~~~~~~~~~~~~~~~~~~~~~~~~~~~~~~~~~~
    end
end
end
%~~~~~~~~~~~~~~~~~~~~~~~~~~~~~~~~~~~~~~~~~~~~~~~~~~~~~~~~~~~~~~~~~~~~~~~
% Plotting for Heat Transfer Analysis
%~~~~~~~~~~~~~~~~~~~~~~~~~~~~~~~~~~~~~~~~~~~~~~~~~~~~~~~~~~~~~~~~~~~~~~~
figure (1)
plot((HH100(1,:)'),'d-','LineWidth',1,'color',...
     '#0072BD','MarkerIndice',1:15:720,'MarkerSize',5)
hold on
plot((HH100(2,:)'),'o-','LineWidth',1,'color',...
    '#D95319','MarkerIndice',1:15:720,'MarkerSize',5)
```

```
plot((HH100(3,:)'),'+-','LineWidth',1,'color',....
    '#EDB120','MarkerIndice',1:15:720,'MarkerSize',5)
plot((HH100(4,:)'),'s-','LineWidth',1,'color',...
    '#7E2F8E','MarkerIndice',1:15:720,'MarkerSize',5)
grid on
grid minor
legend({'Annand','Hohenberg','Sitkei','Woschni'},...
    'Location','northeast',...
    'FontSize',6,...
    'NumColumns',1);
title('The Heat Transfer Coefficients Vs. Crank Angle [100%Load]',...
    'FontSize',5,...
    'position',[400,855,0])
xlabel('Crank Angle [deg]',...
    'position',[400,5,0])
ylabel('Heat Transfer Coefficients [W/m^2 - K]',...
    'position',[235,450,-1])
axis([257 540 50 850])
hold off
set(gcf,'color','w',...
    'position',[77,57,357.12,265.89])
set(gca,'XMinorTick','on',...
    'YMinorTick','on',...
    'FontSize',7,...
    'FontWeight','bold',...
    'LineWidth',1)
HT_Coe_100=gcf;
res=800;
print(HT_Coe_100,'HT_COE[100%].tiff',...
      '-dtiff',['-r' sprintf('%.of',res)]);
%~~~~~~~~~~~~~~~~~~~~~~~~~~~~~~~~~~~~~~~~~~~~~~~~~~~~~~~~~~~~~~~~~~~~~~
figure (2)
plot((HH50(1,:)'),'d-','LineWidth',1,...
     'color','#0072BD','MarkerIndice',1:15:720,'MarkerSize',5)
hold on
plot((HH50(2,:)'),'o-','LineWidth',1,...
     'color','#D95319','MarkerIndice',1:15:720,'MarkerSize',5)
plot((HH50(3,:)'),'+-','LineWidth',1,...
     'color','#EDB120','MarkerIndice',1:15:720,'MarkerSize',5)
plot((HH50(4,:)'),'s-','LineWidth',1,...
     'color','#7E2F8E','MarkerIndice',1:15:720,'MarkerSize',5)
grid on
grid minor
legend({'Annand','Hohenberg','Sitkei','Woschni'},...
    'Location','northeast',...
    'FontSize',6,...
    'NumColumns',1);
title('The Heat Transfer Coefficients Vs. Crank Angle [50%Load]',...
    'FontSize',5,...
    'position',[400,855,0])
xlabel('Crank Angle [deg]',...
    'position',[400,5,0])
ylabel('Heat Transfer Coefficients [W/m^2 - K]',...
    'position',[235,450,-1])
```

```
axis([257 540 50 850])
hold off
set(gcf,'color','w',...
    'position',[77,57,357.12,265.89])
set(gca,'XMinorTick','on',...
    'YMinorTick','on',...
    'FontSize',7,...
    'FontWeight','bold',...
    'LineWidth',1)
HT_Coe_50=gcf;
res=800;
print(HT_Coe_50,'HT_COE[50].tiff','-dtiff',['-r' sprintf('%.of',res)]);
%~~~~~~~~~~~~~~~~~~~~~~~~~~~~~~~~~~~~~~~~~~~~~~~~~~~~~~~~~~~~~~~~~~~~~~~
figure (3)
plot((DDQW100(1,:)'),'d-','LineWidth',1,...
     'color','#0072BD','MarkerIndice',1:15:720,'MarkerSize',5)
hold on
plot((DDQW100(2,:)'),'o-','LineWidth',1,...
     'color','#D95319','MarkerIndice',1:15:720,'MarkerSize',5)
plot((DDQW100(3,:)'),'+-','LineWidth',1,...
     'color','#EDB120','MarkerIndice',1:15:720,'MarkerSize',5)
plot((DDQW100(4,:)'),'s-','LineWidth',1,...
     'color','#7E2F8E','MarkerIndice',1:15:720,'MarkerSize',5)
grid on
grid minor
legend({'Annand','Hohenberg','Sitkei','Woschni'},...
    'Location','northeast',...
    'FontSize',6,...
    'NumColumns',1);
xlabel('Crank Angle [deg]',...
    'position',[450,-0.02,0])
ylabel('Changes in Heat Loss [J/power strock]',...
    'position',[345,0.15,-1])
axis([360 540 0 0.3])
hold off
set(gcf,'color','w',...
    'position',[77,57,357.12,265.89])
set(gca,'XMinorTick','on',...
    'YMinorTick','on',...
    'FontSize',7,...
    'FontWeight','bold',...
    'LineWidth',1)
title('Instantaneous Changes in Heat Transfer to The Wall [100%Load]',...
    'FontSize',6.25,...
    'position',[450,0.308,0])
HT_Ins_100=gcf;
res=800;
print(HT_Ins_100,'HT_Ins[100].tiff','-dtiff',['-r' sprintf('%.of',res)]);
%~~~~~~~~~~~~~~~~~~~~~~~~~~~~~~~~~~~~~~~~~~~~~~~~~~~~~~~~~~~~~~~~~~~~~~~
figure (4)
plot((DDQW50(1,:)'),'d-','LineWidth',1,...
     'color','#0072BD','MarkerIndice',1:15:720,'MarkerSize',5)
hold on
plot((DDQW50(2,:)'),'o-','LineWidth',1,...
```

```
     'color','#D95319','MarkerIndice',1:15:720,'MarkerSize',5)
plot((DDQW50(3,:)'),'+-','LineWidth',1,...
     'color','#EDB120','MarkerIndice',1:15:720,'MarkerSize',5)
plot((DDQW50(4,:)'),'s-','LineWidth',1,...
     'color','#7E2F8E','MarkerIndice',1:15:720,'MarkerSize',5)
grid on
grid minor
legend({'Annand','Hohenberg','Sitkei','Woschni'},...
    'Location','northeast',...
    'FontSize',6,...
    'NumColumns',1);
xlabel('Crank Angle [deg]',...
    'position',[450,-0.02,0])
ylabel('Changes in Heat Loss [J/power strock]',...
    'position',[345,0.15,-1])
axis([360 540 0 0.3])
hold off
set(gcf,'color','w',...
    'position',[77,57,357.12,265.89])
set(gca,'XMinorTick','on',...
    'YMinorTick','on',...
    'FontSize',7,...
    'FontWeight','bold',...
    'LineWidth',1)
title('Instantaneous Changes in Heat Transfer to The Wall[50%Load]',...
    'FontSize',6.25,...
    'position',[450,0.308,0])
HT_Ins_50=gcf;
res=800;
print(HT_Ins_50,'HT_Ins[50].tiff','-dtiff',['-r' sprintf('%.of',res)]);
%~~~~~~~~~~~~~~~~~~~~~~~~~~~~~~~~~~~~~~~~~~~~~~~~~~~~~~~~~~~~~~~~~~~~~~
figure(5)
plot((DDDQ100(1,:)'),'--','LineWidth',1.25,...
     'color','#0072BD','MarkerIndice',1:15:720)
hold on
plot((DDDQ100(2,:)'),'-.','LineWidth',1.5,...
     'color','#D95319','MarkerIndice',1:15:720)
plot((DDDQ100(3,:)'),':','LineWidth',2.5,...
     'color','#EDB120','MarkerIndice',1:15:720)
plot((DDDQ100(4,:)'),'.-','LineWidth',1.5,...
     'color','#7E2F8E','MarkerIndice',1:15:720,'MarkerSize',10)
grid on
grid minor
xlabel('Crank Angle [deg]',...
    'position',[350,-18,0])
ylabel('Net Heat Transfer [J/power strock]',...
    'position',[170,150,-1])
legend({'Annand','Hohenberg','Sitkei','Woschni'},...
    'Location','southeast',...
    'FontSize',6,...
    'NumColumns',1);
axis([200 540 -0.1 300])
hold off
set(gcf,'color','w',...
```

```
    'position',[77,57,357.12,265.89])
set(gca,'XMinorTick','on',...
    'YMinorTick','on',...
    'FontSize',8,...
    'FontWeight','bold',...
    'LineWidth',1)
title('Net Heat Transfer Vs. Crank Angle [100% Load]',...
    'FontSize',8,...
    'position',[375,305,0])
HT_Net_100=gcf;
res=800;
print(HT_Net_100,'HT_Net[100].tiff','-dtiff',['-r' sprintf('%.of',res)]);
%~~~~~~~~~~~~~~~~~~~~~~~~~~~~~~~~~~~~~~~~~~~~~~~~~~~~~~~~~~~~~~~~~~~~~~~
figure(6)
plot((DDDQ50(1,:)'),'--','LineWidth',1.25,...
     'color','#0072BD','MarkerIndice',1:15:720)
hold on
plot((DDDQ50(2,:)'),'-.','LineWidth',1.5,...
     'color','#D95319','MarkerIndice',1:15:720)
plot((DDDQ50(3,:)'),':','LineWidth',2.5,...
     'color','#EDB120','MarkerIndice',1:15:720)
plot((DDDQ50(4,:)'),'.-','LineWidth',1.5,...
     'color','#7E2F8E','MarkerIndice',1:15:720,'MarkerSize',10)
grid on
grid minor
xlabel('Crank Angle [deg]',...
    'position',[350,-18,0])
ylabel('Net Heat Transfer [J/power strock]',...
    'position',[170,150,-1])
legend({'Annand','Hohenberg','Sitkei','Woschni'},...
    'Location','southeast',...
    'FontSize',6,...
    'NumColumns',1);
axis([200 540 -0.1 300])
hold off
set(gcf,'color','w',...
    'position',[77,57,357.12,265.89])
set(gca,'XMinorTick','on',...
    'YMinorTick','on',...
    'FontSize',8,...
    'FontWeight','bold',...
    'LineWidth',1)
title('Net Heat Transfer Vs. Crank Angle [50% Load]',...
    'FontSize',8,...
    'position',[375,305,0])
HT_Net_50=gcf;
res=800;
print(HT_Net_50,'HT_Net[50].tiff','-dtiff',['-r' sprintf('%.of',res)]);
%~~~~~~~~~~~~~~~~~~~~~~~~~~~~~~~~~~~~~~~~~~~~~~~~~~~~~~~~~~~~~~~~~~~~~~~
figure(7)
plot((DDDQ_doT100(1,:)'),'--','LineWidth',1.25,...
     'color','#0072BD','MarkerIndice',1:15:720)
hold on
plot((DDDQ_doT100(2,:)'),'-.','LineWidth',1.5,...
```

```
     'color','#D95319','MarkerIndice',1:15:720)
plot((DDDQ_doT100(3,:)'),':','LineWidth',2.5,...
     'color','#EDB120','MarkerIndice',1:15:720)
plot((DDDQ_doT100(4,:)'),'.-','LineWidth',1.5,...
     'color','#7E2F8E','MarkerIndice',1:15:720,'MarkerSize',10)
grid on
grid minor
legend ({'Annand','Hohenberg','Sitkei','Woschni'},...
    'Location','southeast',...
    'FontSize',6,...
    'NumColumns',1);
xlabel ('Crank Angle [deg]',...
    'position',[350,-0.43,0])
ylabel ('Heat Loss [kW]',...
    'position',[185,2.5,-1])
hold off
axis([200 540 -0.1 5])
set(gcf,'color','w',...
    'position',[77,57,357.12,265.89])
set(gca,'XMinorTick','on',...
    'YMinorTick','on',...
    'FontSize',8,...
    'FontWeight','bold',...
    'LineWidth',1)
title('Heat Loss Vs. Crank Angle [100% Load]',...
    'FontSize',8,...
    'position',[368,5.1,0])
HT_Loss_100=gcf;
res=800;
print(HT_Loss_100,'HT_Loss[100].tiff',...
     '-dtiff',['-r' sprintf('%.of',res)]);
%~~~~~~~~~~~~~~~~~~~~~~~~~~~~~~~~~~~~~~~~~~~~~~~~~~~~~~~~~~~~~~~~~~~~~~
figure(8)
plot((DDDQ_doT50(1,:)'),'--','LineWidth',1.25,...
     'color','#0072BD','MarkerIndice',1:15:720)
hold on
plot((DDDQ_doT50(2,:)'),'-.','LineWidth',1.5,...
     'color','#D95319','MarkerIndice',1:15:720)
plot((DDDQ_doT50(3,:)'),':','LineWidth',2.5,...
     'color','#EDB120','MarkerIndice',1:15:720)
plot((DDDQ_doT50(4,:)'),'.-','LineWidth',1.5,...
     'color','#7E2F8E','MarkerIndice',1:15:720,'MarkerSize',10)
grid on
grid minor
legend ({'Annand','Hohenberg','Sitkei','Woschni'},...
    'Location','southeast',...
    'FontSize',6,...
    'NumColumns',1);
xlabel ('Crank Angle [deg]',...
    'position',[350,-0.43,0])
ylabel ('Heat Loss [kW]',...
    'position',[185,2.5,-1])
axis([200 540 -0.1 5])
set(gcf,'color','w',...
```

```
    'position',[77,57,357.12,265.89])
set(gca,'XMinorTick','on',...
    'YMinorTick','on',...
    'FontSize',8,...
    'FontWeight','bold',...
    'LineWidth',1)
title('Heat Loss Vs. Crank Angle [50% Load]',...
    'FontSize',8,...
    'position',[368,5.1,0])
HT_Loss_50=gcf;
res=800;
print(HT_Loss_50,'HT_Loss[50].tiff','-dtiff',['-r' sprintf('%.of',res)]);
%~~~~~~~~~~~~~~~~~~~~~~~~~~~~~~~~~~~~~~~~~~~~~~~~~~~~~~~~~~~~~~~~~~~~~~~
function [HH,DDQ2,DDQW,DDQ,DDDQ,DDDQ_doT]=rec1..
         (name,HH,DDQ2,DDQW,DDQ,DDDQ,DDDQ_doT)
Lname=name(end-4);
load(name)
if isequal(Lname,'A')
    HH=[HH;h_a];
    DDQ2=[DDQ2;DQ2_A];
    DDQW=[DDQW;DQ_w_A];
    DDQ=[DDQ;DQ_A];
    DDDQ=[DDDQ;Q_A];
    DDDQ_doT=[DDDQ_doT;Q_doT_A];
end
%~~~~~~~~~~~~~~~~~~~~~~~~~~~~~~~~~~~~~~~~~~~~~~~~~~~~~~~~~~~~~~~~~~~~~~~
if isequal(Lname,'W')
    HH=[HH;h_w];
    DDQ2=[DDQ2;DQ2_W];
    DDQW=[DDQW;DQ_w_W];
    DDQ=[DDQ;DQ_W];
    DDDQ=[DDDQ;Q_W];
    DDDQ_doT=[DDDQ_doT;Q_doT_W];
end
%~~~~~~~~~~~~~~~~~~~~~~~~~~~~~~~~~~~~~~~~~~~~~~~~~~~~~~~~~~~~~~~~~~~~~~~
if isequal(Lname,'S')
    HH=[HH;h_s];
    DDQ2=[DDQ2;DQ2_S];
    DDQW=[DDQW;DQ_w_S];
    DDQ=[DDQ;DQ_S];
    DDDQ=[DDDQ;Q_S];
    DDDQ_doT=[DDDQ_doT;Q_doT_S];
end
%~~~~~~~~~~~~~~~~~~~~~~~~~~~~~~~~~~~~~~~~~~~~~~~~~~~~~~~~~~~~~~~~~~~~~~~
if isequal(Lname,'H')
    HH=[HH;h_h];
    DDQ2=[DDQ2;DQ2_H];
    DDQW=[DDQW;DQ_w_H];
    DDQ=[DDQ;DQ_H];
    DDDQ=[DDDQ;Q_H];
    DDDQ_doT=[DDDQ_doT;Q_doT_H];
end
%~~~~~~~~~~~~~~~~~~~~~~~~~~~~~~~~~~~~~~~~~~~~~~~~~~~~~~~~~~~~~~~~~~~~~~~
end
```

APPENDIX C

MATLAB CODE: STAGE III

C.1 MATLAB Function for Three Case Scenarios

```
function [W_dot_ac,T_ac1,Torque_1]=timingfunc_senarios..
         (eta_combmaX,theta_0,theta_b)
% Universiti Teknologi PETRONAS
% Project: Numerical Investigation and Optimization
%          of The Crank-Rocker Engine Ignition Timing
%          Based on Performance and Combustion Characteristics
% Methodology Stage: STAGE III
% Section: Function of Three Case scenarios (Combined CR Model)
%~~~~~~~~~~~~~~~~~~~~~~~~~~~~~~~~~~~~~~~~~~~~~~~~~~~~~~~~~~~~~~~~~~~~~~
% NOTE: Apply the following on the function file and calling function
% Stage III-Case Scenario 1: remove theta_b (line 2)
% Stage III-Case Scenario 2: remove eta_combmaX (line 2)
% Stage III-Case Scenario 3: keep both theta_b and eta_combmaX (line 2)
%~~~~~~~~~~~~~~~~~~~~~~~~~~~~~~~~~~~~~~~~~~~~~~~~~~~~~~~~~~~~~~~~~~~~~~
% INPUT SECTIONS
% THIS SECTION CONTAINS SEVERAL SUB-SECTIONS
% INCLUDING ALL THE REQUIRED INPUTS FOR THE MODEL AND SIMULATION.
%~~~~~~~~~~~~~~~~~~~~~~~~~~~~~~~~~~~~~~~~~~~~~~~~~~~~~~~~~~~~~~~~~~~~~~
% INPUT #1 Crank-Rocker Engine Geometry and Specification Data
%~~~~~~~~~~~~~~~~~~~~~~~~~~~~~~~~~~~~~~~~~~~~~~~~~~~~~~~~~~~~~~~~~~~~~~
% Length
L2 = 0.0253;   %input('Enter The Crank Radius Length [m]')
L3 = 0.1;      %input('Enter The Connecting Rod Length [m]')
L4 = 0.1388;   %input('Enter The Rocker Length [m]')
L41 = 0.1381;  %input('Enter The Extended Rocker Length [m]')
% Engine Spicification
PHI = 21;      % Swing Angle [degree]
B = 0.055;     % Engine Bore [m]
N_cyl = 1;     % Number of Cylinders
N_r = 2;       % Number of Revolutions Per Power Stroke
C_r = 8.5;     % Compression ratio
% Speed and Load
RPM = 2000;    % input('Enter The Engine Speed [1/min] =')
Load = 1;      % Engine Load (Load = 1 = FUll Load)
% Valves
IVC = 0;       % Time [degrees], Intake Valve Closes
EVO = 540;     % Time [degrees], Exhaust Valve Opens
% Timing
%theta_b = 74;  % Combustion Duration [degree]
%theta_0 = 356; % CA at Start of Combustion [degree]/ Ignition timing
%~~~~~~~~~~~~~~~~~~~~~~~~~~~~~~~~~~~~~~~~~~~~~~~~~~~~~~~~~~~~~~~~~~~~~~
% INPUT #2 Fuel Input Data
%~~~~~~~~~~~~~~~~~~~~~~~~~~~~~~~~~~~~~~~~~~~~~~~~~~~~~~~~~~~~~~~~~~~~~~
AF_ratio_stoich = 15.09;      % Gravimetric Air Fuel Ratio (Stoich)
AF_ratio_mol_sotich = 14.7;   % Molar Air_Fuel Ratio (Stoich)
lambda = 1;                   % Excess Air Coefficient
LHV = 46e6;                   % Lower Heating Value Of Fuel Mixture
R_air = 287;                  % Gas Constant For Air [J/kg-K]
%~~~~~~~~~~~~~~~~~~~~~~~~~~~~~~~~~~~~~~~~~~~~~~~~~~~~~~~~~~~~~~~~~~~~~~
% INPUT #3 Ambient Conditions
%~~~~~~~~~~~~~~~~~~~~~~~~~~~~~~~~~~~~~~~~~~~~~~~~~~~~~~~~~~~~~~~~~~~~~~
%Ambient Conditions
```

```
P_atm = 101325;      % Atmospheric Inputs
T_atm = 290;         % Atmospheric Temp Inputs          290;
%~~~~~~~~~~~~~~~~~~~~~~~~~~~~~~~~~~~~~~~~~~~~~~~~~~~~~~~~~~~~~~~~~~~~~~
% INPUT #4 Assumptions
%~~~~~~~~~~~~~~~~~~~~~~~~~~~~~~~~~~~~~~~~~~~~~~~~~~~~~~~~~~~~~~~~~~~~~~
%eta_combmaX = 0.80;   % Assumed MAX Comb. Efficiency
T_W =490;              % Assumed Wall Temperature [K]
gamma(1:720) = 1.34;   % Preallocate Gamma Array (sets initial value)
%~~~~~~~~~~~~~~~~~~~~~~~~~~~~~~~~~~~~~~~~~~~~~~~~~~~~~~~~~~~~~~~~~~~~~~
% INITIAL CALCULATION
%~~~~~~~~~~~~~~~~~~~~~~~~~~~~~~~~~~~~~~~~~~~~~~~~~~~~~~~~~~~~~~~~~~~~~~
% Engine Calculations Based On INPUT #1
%~~~~~~~~~~~~~~~~~~~~~~~~~~~~~~~~~~~~~~~~~~~~~~~~~~~~~~~~~~~~~~~~~~~~~~
% Geometry
%~~~~~~~~~~~~~~~~~~~~~~~~~~~~~~~~~~~~~~~~~~~~~~~~~~~~~~~~~~~~~~~~~~~~~~
S = L41*PHI*pi()/180;         % Calculates the Engine Stroke [m]
DD1 = L4*cos(PHI/2*pi()/180); % Calculates the Length DD1 [m]
L1 = sqrt((L3)^2+(DD1)^2);    % Calculates the Engine framelength [m]
%~~~~~~~~~~~~~~~~~~~~~~~~~~~~~~~~~~~~~~~~~~~~~~~~~~~~~~~~~~~~~~~~~~~~~~
% Theta
%~~~~~~~~~~~~~~~~~~~~~~~~~~~~~~~~~~~~~~~~~~~~~~~~~~~~~~~~~~~~~~~~~~~~~~
theta1 = asin(DD1/L1)*180/pi(); % Calculates Initial angle theta1
theta_f = theta_0 + theta_b;    % CA at End of Combustion
%~~~~~~~~~~~~~~~~~~~~~~~~~~~~~~~~~~~~~~~~~~~~~~~~~~~~~~~~~~~~~~~~~~~~~~
% Area
%~~~~~~~~~~~~~~~~~~~~~~~~~~~~~~~~~~~~~~~~~~~~~~~~~~~~~~~~~~~~~~~~~~~~~~
A_p = (pi/4)*B^2; % Calculates Cross Sectional Piston Area [m^2]
A_ch = 2*A_p;% Calculates Cylinder Head Surface Area (in chamber)
%~~~~~~~~~~~~~~~~~~~~~~~~~~~~~~~~~~~~~~~~~~~~~~~~~~~~~~~~~~~~~~~~~~~~~~
% Volumes
%~~~~~~~~~~~~~~~~~~~~~~~~~~~~~~~~~~~~~~~~~~~~~~~~~~~~~~~~~~~~~~~~~~~~~~
V_d = N_cyl*A_p*S;% Calculates Displaced Volume Of Engine [m^3]
V_TDC = (V_d/(C_r-1))/N_cyl;% Calculates Clearance Volume [m^3]
%~~~~~~~~~~~~~~~~~~~~~~~~~~~~~~~~~~~~~~~~~~~~~~~~~~~~~~~~~~~~~~~~~~~~~~
% General
%~~~~~~~~~~~~~~~~~~~~~~~~~~~~~~~~~~~~~~~~~~~~~~~~~~~~~~~~~~~~~~~~~~~~~~
N = RPM/60;   % Converts RPM to RPS [1/s]
S_bar_p = 2*S*N; % Calculates Mean Piston Speed [m/s]
%~~~~~~~~~~~~~~~~~~~~~~~~~~~~~~~~~~~~~~~~~~~~~~~~~~~~~~~~~~~~~~~~~~~~~~
% Calculateing Losses Due to Friction
%~~~~~~~~~~~~~~~~~~~~~~~~~~~~~~~~~~~~~~~~~~~~~~~~~~~~~~~~~~~~~~~~~~~~~~
fmep = (250*S*RPM)*10^-3; % Calculating Losses Due To Friction
%~~~~~~~~~~~~~~~~~~~~~~~~~~~~~~~~~~~~~~~~~~~~~~~~~~~~~~~~~~~~~~~~~~~~~~
%Volumetric Efficiency correction Factor
%~~~~~~~~~~~~~~~~~~~~~~~~~~~~~~~~~~~~~~~~~~~~~~~~~~~~~~~~~~~~~~~~~~~~~~
CF=-8*10^(-9)*RPM^2+.000135*RPM+.31944;
%~~~~~~~~~~~~~~~~~~~~~~~~~~~~~~~~~~~~~~~~~~~~~~~~~~~~~~~~~~~~~~~~~~~~~~
% Engine Calculations Based On INPUT #2
%~~~~~~~~~~~~~~~~~~~~~~~~~~~~~~~~~~~~~~~~~~~~~~~~~~~~~~~~~~~~~~~~~~~~~~
AF_ratio_ac = lambda*AF_ratio_stoich; % Actual Air Fuel Ratio
AF_ratio_mol=lambda*AF_ratio_mol_sotich;
%~~~~~~~~~~~~~~~~~~~~~~~~~~~~~~~~~~~~~~~~~~~~~~~~~~~~~~~~~~~~~~~~~~~~~~
```

```
%Predicts Combustion Efficiency (Reference To Blair)
%~~~~~~~~~~~~~~~~~~~~~~~~~~~~~~~~~~~~~~~~~~~~~~~~~~~~~~~~~~~~~~~~~~~~~~
eta_comb1=eta_combmaX*(-1.6082+4.6509*lambda-2.0764*lambda^2);
P_BDC = Load*P_atm;    % Inlet Pressure[Pa] Moscow,ID
%~~~~~~~~~~~~~~~~~~~~~~~~~~~~~~~~~~~~~~~~~~~~~~~~~~~~~~~~~~~~~~~~~~~~~~
%Polynomials Used To Calculate Gamma As A Function Of RPM
%~~~~~~~~~~~~~~~~~~~~~~~~~~~~~~~~~~~~~~~~~~~~~~~~~~~~~~~~~~~~~~~~~~~~~~
a_1 = .692; a_2 = 39.17e-06; a_3 = 52.9e-09; a_4 = -228.62e-13;
a_5 = 277.58e-17;b_0 = 3049.33; b_1 = -5.7e-02; b_2 = -9.5e-05;
b_3 = 21.53e-09;b_4 = -200.26e-14;c_u = 2.32584; c_r = 4.186e-03;
d_0 = 10.41066; d_1 = 7.85125; d_3 = -3.71257;e_0 = -15.001e03;
e_1 = -15.838e03; e_3 = 9.613e03;f_0 = -.10329; f_1 = -.38656;
f_3 = .154226; f_4 = -14.763; f_5 = 118.27; f_6 = 14.503;
r_0 = -.2977; r_1 = 11.98; r_2 = -25442; r_3 = -.4354;
%~~~~~~~~~~~~~~~~~~~~~~~~~~~~~~~~~~~~~~~~~~~~~~~~~~~~~~~~~~~~~~~~~~~~~~
% Initial Preallocation of Matrices
%~~~~~~~~~~~~~~~~~~~~~~~~~~~~~~~~~~~~~~~~~~~~~~~~~~~~~~~~~~~~~~~~~~~~~~
V(1:720)=zeros;        DV(1:720)=zeros;      rho(1:720)=zeros;
mu(1:720)=zeros;       M_F(1:720)=zeros;     h_g(1:720)=zeros;
C_k(1:720)=zeros;      C_R(1:720)=zeros;     X(1:720)=zeros;
DX(1:720)=zeros;       Re(1:720)=zeros;      Nus(1:720)=zeros;
DQ_w_A(1:720)=zeros;   DQ(1:720)=zeros;      Q(1:720)=zeros;
DT(1:720)=zeros;       W_doT(1:720)=zeros;   T_indicated(1:720)=zeros;
DP(1:720)=zeros;       P(1:720)=zeros;       T(1:720)=zeros;
W(1:720)=zeros;        Q_doT(1:720)=zeros;   u(1:720)=zeros;
du(1:720)=zeros;       cV(1:720)=zeros;      m_b(1:720)=zeros;
m_u(1:720)=zeros;      T_b(1:720)=zeros;     gamma_u(1:720)=zeros;
V_u(1:720)=zeros;      V_b(1:720)=zeros;     T_u(1:720)=zeros;
A_u(1:720)=zeros;      A_b(1:720)=zeros;     DT_u(1:720)=zeros;
u_u(1:720)=zeros;      du_u(1:720)=zeros;    cv_u(1:720)=zeros;
DQ2(1:720)=zeros;      x(1:720)=zeros;       DT_b(1:720)=zeros;
DQ_w2_A(1:720)=zeros;  Q2(1:720)=zeros;      Throw(1:720)=zeros;
Thrad(1:720)=zeros;    BD(1:720)=zeros;      T4(1:720)=0;
ROHR(1:720)=zeros;     A(1:720)=zeros;
%~~~~~~~~~~~~~~~~~~~~~~~~~~~~~~~~~~~~~~~~~~~~~~~~~~~~~~~~~~~~~~~~~~~~~~
% Index (k = 1:2) Serve as the EGR simulation,
% Functionality of the EGR simulation required the script
% to run two times with only the gas temperature ...
% and fluid properties changing during the second iteration.
% Index (i = 2:720)calculated instantaneous engine features
%~~~~~~~~~~~~~~~~~~~~~~~~~~~~~~~~~~~~~~~~~~~~~~~~~~~~~~~~~~~~~~~~~~~~~~
% Exhaust Gas Residual (EGR) Simulation
%~~~~~~~~~~~~~~~~~~~~~~~~~~~~~~~~~~~~~~~~~~~~~~~~~~~~~~~~~~~~~~~~~~~~~~
R=R_air/1000;
for k = 1:2
%~~~~~~~~~~~~~~~~~~~~~~~~~~~~~~~~~~~~~~~~~~~~~~~~~~~~~~~~~~~~~~~~~~~~~~
% corrects Temperature Based On Exhaust Gas Residuals
%~~~~~~~~~~~~~~~~~~~~~~~~~~~~~~~~~~~~~~~~~~~~~~~~~~~~~~~~~~~~~~~~~~~~~~
if k==1
T_BDC = T_atm;          % Assumed Inlet Temperature [K]
else
T_BDC = T_corr;
```

```
end
%~~~~~~~~~~~~~~~~~~~~~~~~~~~~~~~~~~~~~~~~~~~~~~~~~~~~~~~~~~~~~~~~~~~~~~
% Calculate Mass of Air In Cylinder/ Mass Of Fuel Based On AFR
%~~~~~~~~~~~~~~~~~~~~~~~~~~~~~~~~~~~~~~~~~~~~~~~~~~~~~~~~~~~~~~~~~~~~~~
rho_a = P_BDC/(R_air*T_BDC);     % Air Density kg/m^3
m_a = rho_a*V_d;                 % Mass of Air In Cylinder [kg]
m_f = m_a/AF_ratio_ac;           % Mass Of Fuel In Cylinder [kg]
m_c1 = m_a + m_f;                % Mass In Cylinder
%~~~~~~~~~~~~~~~~~~~~~~~~~~~~~~~~~~~~~~~~~~~~~~~~~~~~~~~~~~~~~~~~~~~~~~
% Specifying Initial Conditions For Loops
%~~~~~~~~~~~~~~~~~~~~~~~~~~~~~~~~~~~~~~~~~~~~~~~~~~~~~~~~~~~~~~~~~~~~~~
BD(1:720)=zeros;
theta(1:720)=zeros;            % Starting Crank Angle [degree]
BD(1)=sqrt ((L1)^2+(L2)^2-2*(L1)*(L2)*cosd(theta(1)+theta1));
T4(1:720)=zeros;
T4(1) = 180-acosd(((L1)^2-(L2)^2+(BD(1))^2)/(2*L1*BD(1)))..
        -acosd(((L4)^2-(L3)^2+(BD(1))^2)/(2*L4*BD(1)));
%~~~~~~~~~~~~~~~~~~~~~~~~~~~~~~~~~~~~~~~~~~~~~~~~~~~~~~~~~~~~~~~~~~~~~~
V(1:720)=zeros;% Preallocate Volume Array
V(1)=V_TDC; % Starting Combustion Chamber Volume [m^3]
G(1:720)=zeros;
DV(1:720)=zeros;% Preallocate Change In Volume Array
DV(1)=0; % Specifying Initial Change In Volume [m^3}-5.72*10^-7
P(1:720)=P(1);
P(1)=P_BDC;
DP(1:720)=zeros;   % Specifying Initial Change In Pressure
T(1:720)=zeros;    % Preallocate Temperature Array
T(1)=T_BDC;        % Inlet Temperature [K]
DT(1:720)=zeros;   % Specifying Initial Change In Temperature
T_u(1:720)=zeros;  % Preallocate Unburned Temperature Array
T_u(1)=T_BDC;      % Initial Unburned Temperature[K]
DT_u(1:720)=zeros; % Preallocate Change In Unburned Temperature
gamma(1:720)=zeros;
gamma(1)=1.4;     % Initial Gamma Input
gamma_u(1:720)=zeros;
gamma_u(1)=1.4;      % Initial Gamma Input
X(1:720)=zeros;    % Preallocate Mass Burn Array
DX(1:720)=zeros;   % Preallocate Change In Mass Burn Fraction
DQ(1:720)=zeros;   % Preallocate Heat Release Array
DQ2(1:720)=zeros;  % Preallocate Two Zone Heat Release Array
Q(1:720)=zeros;    % Preallocate Heat Array
Q2(1:720)=zeros;   % Preallocate two-zone Heat release Array
M_F(1:720)=zeros;  % Preallocate Mass In Comubstion Chamber Array
mu(1:720)=zeros;   % Preallocate Viscosity Array
mu(1)=7.457*10^(-6)+4.1547*10^(-8)*T_BDC-7.4793*10^(-12)*T_BDC^(2);
rho(1:720)=zeros;   % Preallocates Ideal Gas Law array
rho(1)=P(1)/(R_air*T(1));  % Initial Value Ideal Gas Array
C_k(1:720)=zeros;      % Preallocate Thermal Conductivity Array
C_k(1)=6.1944*10^(-3)+7.3814*10^(-5)*T_BDC-1.2491*10^(-8)*T_BDC^(2);
C_R(1:720)=zeros;  % Preallocate Radiation Coefficient Array
C_R(1)=4.25*10^(-09)*((T(1)^4-T_W^4)/(T(1)-T_W));
Re(1:720)=zeros;  % Preallocate Reynolds Value Array
```

```
Re(1)=rho(1)*S_bar_p*B/mu(1);  % Initial Reynolds Value
Nus(1:720)=zeros;   % Preallocating Nusselt Number Array
Nus(1)=.49*Re(1)^(.7); % Initial Nusselt Number
h_g(1:720)=zeros; % Preallocate Heat Transfer Coefficient Array
h_g(1)=C_k(1)*Nus(1)/B;% Initial Heat Transfer Coefficient (720-THETA)
A(1:720)=zeros;
Throw(1:720)=zeros;% Preallocates angle Crank/rocker Axes Array
Throw(1)=(T4(1)-T4(1));% Initial swing angle poistion [Degree]
Thrad(1:720)=zeros;
Thrad(1)= Throw(1)*pi/180;% Initial swing angle poistion[Radin]
x(1:720)=zeros;   % Distance Crank/Piston Axes Array
x(1)=L41*Thrad(1);% Initial piston Distance [m]
W(1:720)=zeros; % Preallocate Work Array
W_doT(1:720)=zeros;  % Preallocate Power Array
T_indicated(1:720)=zeros; % Preallocate Torque Array
Q_doT(1:720)=zeros;   % Preallocate Heat Transfer Array
u(1:720)=zeros;    % Preallocate Internal Energy Array
du(1:720)=zeros;  % Preallocates Change In Internal Energy Array
cV(1:720)=zeros; % Preallocates Heat Capacity Array
DQ_w_A(1:720)=zeros;   % Preallocate Convective Heat Loss Annand
DQ_w2_A(1:720)=zeros;  % Preallocate Convective Heat Loss Annand 2 zone
m_b(1:720)=zeros; % Preallocate mass burned array
m_u(1:720)=m_c1;   % Preallocate unburned mass array
V_u(1:720)=zeros; % Preallocate unburned Volume Array
V_u(1)=V(1);      % Initial Unburned Volume
DT_b(1:720)=zeros;
ROHR(1:720)=zeros;
%~~~~~~~~~~~~~~~~~~~~~~~~~~~~~~~~~~~~~~~~~~~~~~~~~~~~~~~~~~~~~~~~~~~~~~~
% Instantaneous Engine Features Simulation
%~~~~~~~~~~~~~~~~~~~~~~~~~~~~~~~~~~~~~~~~~~~~~~~~~~~~~~~~~~~~~~~~~~~~~~~
theta=1:720;
for i=2:720
%~~~~~~~~~~~~~~~~~~~~~~~~~~~~~~~~~~~~~~~~~~~~~~~~~~~~~~~~~~~~~~~~~~~~~~~
BD(i)=sqrt((L1)^2+(L2)^2-2*(L1)*(L2)*cosd(theta(i)+theta1));
% Calculates length BD [m]
G(i)=acosd(((L3)^2+(L4)^2-(BD(i))^2)/(2*L3*L4));
% Calculates Transmission angle [Degree]
T4(i)=180-acosd(((L1)^2-(L2)^2+(BD(i))^2)/(2*L1*BD(i)))-...
      acosd(((L4)^2-(L3)^2+(BD(i))^2)/(2*L4*BD(i)));
% Calculates Theta4 [Degree]
if(i>(180-theta1))
T4(i) = 180+acosd(((L1)^2-(L2)^2+(BD(i))^2)/(2*L1*BD(i)))..
        -acosd(((L4)^2-(L3)^2+(BD(i))^2)/(2*L4*BD(i)));
end
if(i>(360-theta1))
T4(i) = 180-acosd(((L1)^2-(L2)^2+(BD(i))^2)/(2*L1*BD(i)))..
           -acosd(((L4)^2-(L3)^2+(BD(i))^2)/(2*L4*BD(i)));
end
if(i>(540-theta1))
T4(i) = 180+acosd(((L1)^2-(L2)^2+(BD(i))^2)/(2*L1*BD(i)))..
           -acosd(((L4)^2-(L3)^2+(BD(i))^2)/(2*L4*BD(i)));
end
```

```
if(i>(720-theta1))
T4(i) = 180-acosd(((L1)^2-(L2)^2+(BD(i))^2)/(2*L1*BD(i)))..
        -acosd(((L4)^2-(L3)^2+(BD(i))^2)/(2*L4*BD(i)));
end
%~~~~~~~~~~~~~~~~~~~~~~~~~~~~~~~~~~~~~~~~~~~~~~~~~~~~~~~~~~~~~~~~~~~~~~
Throw(i)=(T4(i)-T4(1));
% Calculates Swing Angle position as a Function of Crank Angle
Thrad(i)=Throw(i)*pi/180;
% Calculates Swing Angle position as a Function of Crank Angle
x(i)=L41*Thrad(i);
% Calculates Piston Displacement as a Function of Crank  Angle [m]
V(i)=V_TDC + (pi/4)*(B^2)*x(i);
% Calculates Total Cyl. Volume as a Function of Crank  Angle [m3]
DV(i)=V(i)-V(i-1);
%~~~~~~~~~~~~~~~~~~~~~~~~~~~~~~~~~~~~~~~~~~~~~~~~~~~~~~~~~~~~~~~~~~~~~~
%Calculates Density As A Function Of Crank Angle
rho(i)=P(i-1)/(R_air*T(i-1));
%Calculates Viscosity As A Function Of Temperature
mu(i)=7.457*10^(-6)+4.1547*10^(-8)*T(i-1)-7.4793*10^(-12)*T(i-1)^(2);
%Calculating Instantaneous Thermal Conductivity of Cylinder Gas
C_k(i)=6.1944*10^(-3)+7.3814*10^(-5)*T(i-1)-1.2491*10^(-8)*T(i-1)^(2);
%Calculating The Radiation Heat Transfer Coefficient
C_R(i)=(4.25*10^(-09))*((T(i-1)^4-T_W^4)/(T(i-1)-T_W));
%~~~~~~~~~~~~~~~~~~~~~~~~~~~~~~~~~~~~~~~~~~~~~~~~~~~~~~~~~~~~~~~~~~~~~~
%Instantaneous Suface Area (For Heat Transfer);
A(i)= A_ch + A_p + pi*B*x(i) ;
%~~~~~~~~~~~~~~~~~~~~~~~~~~~~~~~~~~~~~~~~~~~~~~~~~~~~~~~~~~~~~~~~~~~~~~
%Specifies Mass Fraction Burn As A Function Of Crank Angle
%~~~~~~~~~~~~~~~~~~~~~~~~~~~~~~~~~~~~~~~~~~~~~~~~~~~~~~~~~~~~~~~~~~~~~~
if theta(i)<theta_0
X(i)=0;
else
X(i) = 1-exp(-5*((theta(i)-theta_0)/theta_b)^3);
if theta(i) < theta_f
M_F(i) = V(theta_0-1)*rho(theta_0-1)/(lambda*AF_ratio_mol);
end
end
%~~~~~~~~~~~~~~~~~~~~~~~~~~~~~~~~~~~~~~~~~~~~~~~~~~~~~~~~~~~~~~~~~~~~~~
%Specifies Change In Mass Fraction Burn As A Function Of Crank Angle
%~~~~~~~~~~~~~~~~~~~~~~~~~~~~~~~~~~~~~~~~~~~~~~~~~~~~~~~~~~~~~~~~~~~~~~
DX(i) = X(i) - X(i-1);
%~~~~~~~~~~~~~~~~~~~~~~~~~~~~~~~~~~~~~~~~~~~~~~~~~~~~~~~~~~~~~~~~~~~~~~
% Heat Transfer Prediction
%~~~~~~~~~~~~~~~~~~~~~~~~~~~~~~~~~~~~~~~~~~~~~~~~~~~~~~~~~~~~~~~~~~~~~~
%Using ANNAND METHOD
%CACULATION
Re(i)=(rho(i)*S_bar_p*B)/(mu(i));
% Calculating Reynolds Number
Nus(i)=0.49*(Re(i)^(0.7));
% Calculating Nusselt Number (constant=.26 two stroke, .49 4 stroke)
h_g(i)=(C_k(i)*Nus(i))/B;
% HT Coefficient Using Annand Method (convection part)
```

```
DQ_w_A(i)=(h_g(i)+C_R(i))*A(i)*(T(i-1)-T_W)*(60/(720*RPM));
% Calculates Convective Losses Into Wall As A Function Of Crank Angle
DQ_w2_A(i)=((h_g(i)+C_R(i))*A_b(i-1)/N_cyl*(T_b(i-1)-T_W)..
+(h_g(i)+C_R(i))*A_u(i-1)/N_cyl*(T_u(i-1)-T_W))*(60/(720*RPM));
%Calculates Total Heat Transfer (Per Cycle)
DQ(i) = eta_comb1*LHV*M_F(i)*DX(i)-DQ_w_A(i);
% Calculates Change In Heat Transfer (total)
DQ2(i)= eta_comb1*LHV*M_F(i)*DX(i)-DQ_w2_A(i);
% Calculates Change In Heat Transfer (total) Two-Zone
Q(i)  = Q(i-1) + DQ(i);
Q2(i) = Q2(i-1)+ DQ2(i);
%~~~~~~~~~~~~~~~~~~~~~~~~~~~~~~~~~~~~~~~~~~~~~~~~~~~~~~~~~~~~~~~~~~~~~~
% Specifies Pressure and Temperature Increases Between Intake Valve
%~~~~~~~~~~~~~~~~~~~~~~~~~~~~~~~~~~~~~~~~~~~~~~~~~~~~~~~~~~~~~~~~~~~~~~
% Closing and Exhaust Valve Opening...50
if  IVC <= theta(i)
DT(i)=T(i-1)*(gamma(i-1)-1)*((1/(P(i-1)*V(i-1)))*DQ(i)-(1/V(i-1))*DV
(i));
DP(i)=(-P(i-1)/V(i-1))*DV(i)+(P(i-1)/T(i-1))*DT(i);
P(i)=P(i-1)+DP(i);
end
if 252<= theta(i)
if P(i)<=P_atm
P(i)=P_atm;
end
end
if EVO < theta(i)
P(i)=0.3086*100000;
%P(i)=P(i);
%P(i)=P_atm;
end
%~~~~~~~~~~~~~~~~~~~~~~~~~~~~~~~~~~~~~~~~~~~~~~~~~~~~~~~~~~~~~~~~~~~~~~
%Returns Temperature Values To Beginning Of Loop
%Assumes Temperature Drops Back To ATM Temp After Exhaust Is Extracted
%~~~~~~~~~~~~~~~~~~~~~~~~~~~~~~~~~~~~~~~~~~~~~~~~~~~~~~~~~~~~~~~~~~~~~~
T(i) = T(i-1)+DT(i);
% Returns Temperature Values To Beginning Of Loop
% Treats Atmospheric Pressure As Reference State
W(i) = W(i-1)+(P(i)-P_atm)*DV(i);
% Calculates Cylinder Work [J] As A Function Of Crank Angle
W_doT(i)=(N_cyl*W(i)*N/N_r)/1000;
% Calculates Power [kW] As A Function Of Crank Angle
imep = CF*W_doT(720)*N_r*1000/(V_d*1000*N);
% Indicated Mean Effective Pressure
T_indicated(i) = (W_doT(i)*1000)/(2*pi*N);
% Calculates Torque[N*m] As A Function Of Crank Angle
Q_doT(i) = (N_cyl*Q(i)*N/N_r)/1000;
% Calculates Heat Loss [kW] As A Function Of Crank Angle
%~~~~~~~~~~~~~~~~~~~~~~~~~~~~~~~~~~~~~~~~~~~~~~~~~~~~~~~~~~~~~~~~~~~~~~
%The Following Section Of Code Calculates An Updated Value Of Gamma
%Using The "Polynomial Method" Developed By Krieger-Borman
%User Of This Code Must Be Careful Because Accuracy Of This Method
```

```
%Drops As The Fuel Mixture Becomes Increasingly Rich
%~~~~~~~~~~~~~~~~~~~~~~~~~~~~~~~~~~~~~~~~~~~~~~~~~~~~~~~~~~~~~~~~~~~~~~
%Calculates A,B Factors For Following Block Of Code
A_T  = a_1*T(i)+a_2*T(i)^2+a_3*T(i)^3+a_4*T(i)^4+a_5*T(i)^5;
A_tu = a_1*T_u(i)+a_2*T_u(i)^2+a_3*T_u(i)^3+a_4*T_u(i)^4+a_5*T_u(i)^5;
B_T  = b_0+b_1*T(i)+b_2*T(i)^2+b_3*T(i)^3+b_4*T(i)^4;
B_tu = b_0+b_1*T_u(i)+b_2*T_u(i)^2+b_3*T_u(i)^3+b_4*T_u(i)^4;
%Calculates Factor "D" As A Function Of lambda
D_lambda = d_0 + d_1*lambda^(-1)+ d_3*lambda^(-3);
%Calculates Factor "F" As A Function Of Temperature,lambda
E_Tlambda = (e_0+e_1*lambda^(-1)+e_3*lambda^(-3))/T(i);
E_TLambdau =(e_0+e_1*lambda^(-1)+e_3*lambda^(-3))/T_u(i);
F_TPlambda =(f_0+f_1*lambda^(-1)+f_3*lambda^(-3)+...
           ((f_4 + f_5*lambda^(-1))/T(i)))*log(f_6*P(i));
F_TPLambdau=(f_0+f_1*lambda^(-1)+f_3*lambda^(-3)+...
           ((f_4 + f_5*lambda^(-1))/T_u(i)))*log(f_6*P(i));
%~~~~~~~~~~~~~~~~~~~~~~~~~~~~~~~~~~~~~~~~~~~~~~~~~~~~~~~~~~~~~~~~~~~~~~
%Calculates correction Factor For Internal Energy
u_corr = c_u*exp(D_lambda +E_Tlambda + F_TPlambda);
u_corr_u=c_u*exp(D_lambda +E_TLambdau+ F_TPLambdau);
%~~~~~~~~~~~~~~~~~~~~~~~~~~~~~~~~~~~~~~~~~~~~~~~~~~~~~~~~~~~~~~~~~~~~~~
%Calculates Internal Energy As A Function Of Crank Angle
u(i) = A_T - B_T/lambda + u_corr;
u_u(i) = A_tu - B_tu/lambda + u_corr_u;
%~~~~~~~~~~~~~~~~~~~~~~~~~~~~~~~~~~~~~~~~~~~~~~~~~~~~~~~~~~~~~~~~~~~~~~
%Calculates Change In Internal Energy
du(i) = u(i) - u(i-1);
du_u(i) = u_u(i) - u_u(i-1);
%~~~~~~~~~~~~~~~~~~~~~~~~~~~~~~~~~~~~~~~~~~~~~~~~~~~~~~~~~~~~~~~~~~~~~~
%Calculates Heat Capacity "C_v" As A Function Of Crank Angle
cV(i) = du(i)/DT(i);
cv_u(i)=du_u(i)/DT_u(i);
%~~~~~~~~~~~~~~~~~~~~~~~~~~~~~~~~~~~~~~~~~~~~~~~~~~~~~~~~~~~~~~~~~~~~~~
%Calculates correction Factor For "R" Value As A
R_corr=c_r*exp(r_0*log(lambda)...
       +(r_1+r_2/T(i)+ r_3*log(f_6*P(i)))/lambda);
R_corr_u = c_r*exp(r_0*log(lambda)...
         + (r_1+r_2/T_u(i-1) + r_3*log(f_6*P(i)))/lambda);
%~~~~~~~~~~~~~~~~~~~~~~~~~~~~~~~~~~~~~~~~~~~~~~~~~~~~~~~~~~~~~~~~~~~~~~
%Calculates Actual "R" Value
R = .287 + .020/lambda + R_corr;
R_u = .287 + .020/lambda + R_corr_u;
%~~~~~~~~~~~~~~~~~~~~~~~~~~~~~~~~~~~~~~~~~~~~~~~~~~~~~~~~~~~~~~~~~~~~~~
%Calculates Actual Gamma Value And Returns To Beginning Of Code
%~~~~~~~~~~~~~~~~~~~~~~~~~~~~~~~~~~~~~~~~~~~~~~~~~~~~~~~~~~~~~~~~~~~~~~
gamma_u(i)=1+R_u/cv_u(i);
gamma(i) = 1 + R/cV(i);
if gamma(i)<1.2
gamma(i)=1.34;
gamma_u(i)=1.34;
end
if theta(i)>=EVO
```

```
gamma(i)=1.34;
gamma_u(i)=1.34;
end
%~~~~~~~~~~~~~~~~~~~~~~~~~~~~~~~~~~~~~~~~~~~~~~~~~~~~~~~~~~~~~~~~~~~~~~
%Calculate Temperature Of Exhaust Based On Polytropic Relations
if EVO < theta(i)
T(i)=T(EVO)*(P_BDC/P(EVO))^((gamma(i)-1)/gamma(i));
T_b(i)=T_b(EVO)*(P_BDC/P(EVO))^((gamma(i)-1)/gamma(i));
end
%~~~~~~~~~~~~~~~~~~~~~~~~~~~~~~~~~~~~~~~~~~~~~~~~~~~~~~~~~~~~~~~~~~~~~~
end
%Calculates A corrected Inlet Temperature Based On EGR
%T_corr = R_frac*T(720)+(1-R_frac)*T_BDC;
T_corr = T_BDC;
end
%% Specified Outputs (On Matlab Screen)
bmep = imep-fmep;
W_dot_ac=(bmep*V_d*1000*N/(N_r*1000)); %Brake Power
T_ac1 = W_dot_ac/(2*pi*N*10^(-3)); %Brake Torque
Torque_1=(1*bmep*V_d*1000)/(4*pi); %Brake Torque
end
```

C.2 MATLAB Call Function for Three Case Scenarios

```
% Universiti Teknologi PETRONAS
% Project: Numerical Investigation and Optimization
%          of The Crank-Rocker Engine Ignition Timing
%          Based on Performance and Combustion Characteristics
% Methodology Stage: STAGE III
% Section: Call Function of Case Scenarios
%~~~~~~~~~~~~~~~~~~~~~~~~~~~~~~~~~~~~~~~~~~~~~~~~~~~~~~~~~~~~~~~~~~~~~~~
% NOTE: Apply the following on the file and calling function
% Stage III-Case Scenario 1: remove or comment theta_b
% Stage III-Case Scenario 2: remove or comment eta_combmaX
% Stage III-Case Scenario 3: keep both theta_b and eta_combmaX
%~~~~~~~~~~~~~~~~~~~~~~~~~~~~~~~~~~~~~~~~~~~~~~~~~~~~~~~~~~~~~~~~~~~~~~~
clear
clc;
%~~~~~~~~~~~~~~~~~~~~~~~~~~~~~~~~~~~~~~~~~~~~~~~~~~~~~~~~~~~~~~~~~~~~~~~
%Set Spark Angle Bounds
theta_st_1 = 309;
theta_fin= 360;
%~~~~~~~~~~~~~~~~~~~~~~~~~~~~~~~~~~~~~~~~~~~~~~~~~~~~~~~~~~~~~~~~~~~~~~~
%Set Assumed Efficiency range
eta_combmaX_st=25;
eta_combmaX_fin=80;
%~~~~~~~~~~~~~~~~~~~~~~~~~~~~~~~~~~~~~~~~~~~~~~~~~~~~~~~~~~~~~~~~~~~~~~~
%Set Assumed Combustion Duration
theta_b_st_1=25;
theta_b_fin=80;
%~~~~~~~~~~~~~~~~~~~~~~~~~~~~~~~~~~~~~~~~~~~~~~~~~~~~~~~~~~~~~~~~~~~~~~~
%Set Bound
N_theta=theta_fin-theta_st_1;
eta_combmaX_Increment=5;
N_eta_combmaX=(eta_combmaX_fin-eta_combmaX_st)/eta_combmaX_Increment;
%(divide by the decrement rate )
theta_b_Increment=5;
N_theta_b=(theta_b_fin-theta_b_st_1)/theta_b_Increment;
%~~~~~~~~~~~~~~~~~~~~~~~~~~~~~~~~~~~~~~~~~~~~~~~~~~~~~~~~~~~~~~~~~~~~~~~
%Preallocations
%Case Senario 3
W_dot_ac(1:N_theta,1:N_theta_b,1:N_eta_combmaX)=zeros;
T_ac1(1:N_theta,1:N_theta_b,1:N_eta_combmaX)=zeros;
Torque_1(1:N_theta,1:N_theta_b,1:N_eta_combmaX)=zeros;
theta_o(1:N_theta)=zeros;
eta_combmaX_o(1:N_eta_combmaX)=zeros;
theta_b_o(1:N_theta_b)=zeros;
%~~~~~~~~~~~~~~~~~~~~~~~~~~~~~~~~~~~~~~~~~~~~~~~~~~~~~~~~~~~~~~~~~~~~~~~
% Changes Spark Angle As A Function Of (i)
% changes efficiency as a function of (j)
% changes combustion duration as a function of (z)
eta_combmaX=eta_combmaX_st/100;
eta_combmaX_o(1)=eta_combmaX;
for z=1:N_eta_combmaX
    eta_combmaX=(eta_combmaX+(eta_combmaX_Increment/100));
    eta_combmaX_o(z)=eta_combmaX;
```

```
    %Return to the initial condition
    theta_b_st=theta_b_st_1;
    theta_b=theta_b_st;
    theta_b_o(1)=theta_b;
    for j=1:N_theta_b
        theta_b=(theta_b+(theta_b_Increment));
        theta_b_o(j)=theta_b;
        %Return to the initial condition
        theta_st=theta_st_1;
        theta_0=theta_st;
        theta_o(1)=theta_0;
        for i=1:N_theta
            theta_0=theta_0+1;
            [W_dot_ac(i,j,z),T_ac1(i,j,z),Torque_1(i,j,z)]..
            =timingfunc_senarios(eta_combmaX,theta_0,theta_b);
            theta_o(i)=theta_0;
            Sim=[eta_combmaX theta_b theta_0];
            disp=(Sim)
        end
    end
end
%~~~~~~~~~~~~~~~~~~~~~~~~~~~~~~~~~~~~~~~~~~~~~~~~~~~~~~~~~~~~~~~~~~~~~~
%Data Categorization
A=Torque_1(:,:,1);
Aa=A';
A1=(Aa(1,:));A2=(Aa(2,:));A3=(Aa(3,:));
A4=(Aa(4,:));A5=(Aa(5,:));A6=(Aa(6,:));
A7=(Aa(7,:));A8=(Aa(8,:));A9=(Aa(9,:));
A10=(Aa(10,:));A11=(Aa(11,:));
%~~~~~~~~~~~~~~~~~~~~~~~~~~~~~~~~~~~~~~~~~~~~~~~~~~~~~~~~~~~~~~~~~~~~~~
B=Torque_1(:,:,2);
Bb=B';
B1=(Bb(1,1:51));B2=(Bb(2,1:51));B3=(Bb(3,1:51));
B4=(Bb(4,1:51));B5=(Bb(5,1:51));B6=(Bb(6,1:51));
B7=(Bb(7,1:51));B8=(Bb(8,1:51));B9=(Bb(9,1:51));
B10=(Bb(10,1:51));B11=(Bb(11,1:51));
%~~~~~~~~~~~~~~~~~~~~~~~~~~~~~~~~~~~~~~~~~~~~~~~~~~~~~~~~~~~~~~~~~~~~~~
C=Torque_1(:,:,3);
Cc=C';
C1=(Cc(1,1:51));C2=(Cc(2,1:51));C3=(Cc(3,1:51));
C4=(Cc(4,1:51));C5=(Cc(5,1:51));C6=(Cc(6,1:51));
C7=(Cc(7,1:51));C8=(Cc(8,1:51));C9=(Cc(9,1:51));
C10=(Cc(10,1:51));C11=(Cc(11,1:51));
%~~~~~~~~~~~~~~~~~~~~~~~~~~~~~~~~~~~~~~~~~~~~~~~~~~~~~~~~~~~~~~~~~~~~~~
D=Torque_1(:,:,4);
Dd=D';
D1=(Dd(1,1:51));D2=(Dd(2,1:51));D3=(Dd(3,1:51));
D4=(Dd(4,1:51));D5=(Dd(5,1:51));D6=(Dd(6,1:51));
D7=(Dd(7,1:51));D8=(Dd(8,1:51));D9=(Dd(9,1:51));
D10=(Dd(10,1:51));D11=(Dd(11,1:51));
%~~~~~~~~~~~~~~~~~~~~~~~~~~~~~~~~~~~~~~~~~~~~~~~~~~~~~~~~~~~~~~~~~~~~~~
E=Torque_1(:,:,5);
```

```
Ee=E';
E1=(Ee(1,1:51));E2=(Ee(2,1:51));E3=(Ee(3,1:51));
E4=(Ee(4,1:51));E5=(Ee(5,1:51));E6=(Ee(6,1:51));
E7=(Ee(7,1:51));E8=(Ee(8,1:51));E9=(Ee(9,1:51));
E10=(Ee(10,1:51));E11=(Ee(11,1:51));
%~~~~~~~~~~~~~~~~~~~~~~~~~~~~~~~~~~~~~~~~~~~~~~~~~~~~~~~~~~~~~~~~~~~~~~
F=Torque_1(:,:,6);
Ff=F';
F1=(Ff(1,1:51));F2=(Ff(2,1:51));F3=(Ff(3,1:51));
F4=(Ff(4,1:51));F5=(Ff(5,1:51));F6=(Ff(6,1:51));
F7=(Ff(7,1:51));F8=(Ff(8,1:51));F9=(Ff(9,1:51));
F10=(Ff(10,1:51));F11=(Ff(11,1:51));
%~~~~~~~~~~~~~~~~~~~~~~~~~~~~~~~~~~~~~~~~~~~~~~~~~~~~~~~~~~~~~~~~~~~~~~
G=Torque_1(:,:,7);
Gg=G';
G1=(Gg(1,1:51));G2=(Gg(2,1:51));G3=(Gg(3,1:51));
G4=(Gg(4,1:51));G5=(Gg(5,1:51));G6=(Gg(6,1:51));
G7=(Gg(7,1:51));G8=(Gg(8,1:51));G9=(Gg(9,1:51));
G10=(Gg(10,1:51));G11=(Gg(11,1:51));
%~~~~~~~~~~~~~~~~~~~~~~~~~~~~~~~~~~~~~~~~~~~~~~~~~~~~~~~~~~~~~~~~~~~~~~
H=Torque_1(:,:,8);
Hh=H';
H1=(Hh(1,1:51));H2=(Hh(2,1:51));H3=(Hh(3,1:51));
H4=(Hh(4,1:51));H5=(Hh(5,1:51));H6=(Hh(6,1:51));
H7=(Hh(7,1:51));H8=(Hh(8,1:51));H9=(Hh(9,1:51));
H10=(Hh(10,1:51));H11=(Hh(11,1:51));
%~~~~~~~~~~~~~~~~~~~~~~~~~~~~~~~~~~~~~~~~~~~~~~~~~~~~~~~~~~~~~~~~~~~~~~
I=Torque_1(:,:,9);
Ii=I';
I1=(Ii(1,1:51));I2=(Ii(2,1:51));I3=(Ii(3,1:51));
I4=(Ii(4,1:51));I5=(Ii(5,1:51));I6=(Ii(6,1:51));
I7=(Ii(7,1:51));I8=(Ii(8,1:51));I9=(Ii(9,1:51));
I10=(Ii(10,1:51));I11=(Ii(11,1:51));
%~~~~~~~~~~~~~~~~~~~~~~~~~~~~~~~~~~~~~~~~~~~~~~~~~~~~~~~~~~~~~~~~~~~~~~
J=Torque_1(:,:,10);
Jj=J';
J1=(Jj(1,1:51));J2=(Jj(2,1:51));J3=(Jj(3,1:51));
J4=(Jj(4,1:51));J5=(Jj(5,1:51));J6=(Jj(6,1:51));
J7=(Jj(7,1:51));J8=(Jj(8,1:51));J9=(Jj(9,1:51));
J10=(Jj(10,1:51));J11=(Jj(11,1:51));
%~~~~~~~~~~~~~~~~~~~~~~~~~~~~~~~~~~~~~~~~~~~~~~~~~~~~~~~~~~~~~~~~~~~~~~
K=Torque_1(:,:,11);
Kk=K';
K1=(Kk(1,1:51));K2=(Kk(2,1:51));K3=(Kk(3,1:51));
K4=(Kk(4,1:51));K5=(Kk(5,1:51));K6=(Kk(6,1:51));
K7=(Kk(7,1:51));K8=(Kk(8,1:51));K9=(Kk(9,1:51));
K10=(Kk(10,1:51));K11=(Kk(11,1:51));
%~~~~~~~~~~~~~~~~~~~~~~~~~~~~~~~~~~~~~~~~~~~~~~~~~~~~~~~~~~~~~~~~~~~~~~
PoW=W_dot_ac;
L=PoW(:,:,1);
Ll=L';
L1=(Ll(1,1:51));L2=(Ll(2,1:51));L3=(Ll(3,1:51));
```

```
L4=(Ll(4,1:51));L5=(Ll(5,1:51));L6=(Ll(6,1:51));
L7=(Ll(7,1:51));L8=(Ll(8,1:51));L9=(Ll(9,1:51));
L10=(Ll(10,1:51));L11=(Ll(11,1:51));
%~~~~~~~~~~~~~~~~~~~~~~~~~~~~~~~~~~~~~~~~~~~~~~~~~~~~~~~~~~~~~~~~~~~~~~~~
M=PoW(:,:,2);
Mm=M';
M1=(Mm(1,1:51));M2=(Mm(2,1:51));M3=(Mm(3,1:51));
M4=(Mm(4,1:51));M5=(Mm(5,1:51));M6=(Mm(6,1:51));
M7=(Mm(7,1:51));M8=(Mm(8,1:51));M9=(Mm(9,1:51));
M10=(Mm(10,1:51));M11=(Mm(11,1:51));
%~~~~~~~~~~~~~~~~~~~~~~~~~~~~~~~~~~~~~~~~~~~~~~~~~~~~~~~~~~~~~~~~~~~~~~~~
N=PoW(:,:,3);
Nn=N';
N1=(Nn(1,1:51));N2=(Nn(2,1:51));N3=(Nn(3,1:51));
N4=(Nn(4,1:51));N5=(Nn(5,1:51));N6=(Nn(6,1:51));
N7=(Nn(7,1:51));N8=(Nn(8,1:51));N9=(Nn(9,1:51));
N10=(Nn(10,1:51));N11=(Nn(11,1:51));
%~~~~~~~~~~~~~~~~~~~~~~~~~~~~~~~~~~~~~~~~~~~~~~~~~~~~~~~~~~~~~~~~~~~~~~~~
O=PoW(:,:,4);
Oo=O';
O1=(Oo(1,1:51));O2=(Oo(2,1:51));O3=(Oo(3,1:51));
O4=(Oo(4,1:51));O5=(Oo(5,1:51));O6=(Oo(6,1:51));
O7=(Oo(7,1:51));O8=(Oo(8,1:51));O9=(Oo(9,1:51));
O10=(Oo(10,1:51));O11=(Oo(11,1:51));
%~~~~~~~~~~~~~~~~~~~~~~~~~~~~~~~~~~~~~~~~~~~~~~~~~~~~~~~~~~~~~~~~~~~~~~~~
P=PoW(:,:,5);
Pp=P';
P1=(Pp(1,1:51));P2=(Pp(2,1:51));P3=(Pp(3,1:51));
P4=(Pp(4,1:51));P5=(Pp(5,1:51));P6=(Pp(6,1:51));
P7=(Pp(7,1:51));P8=(Pp(8,1:51));P9=(Pp(9,1:51));
P10=(Pp(10,1:51));P11=(Pp(11,1:51));
%~~~~~~~~~~~~~~~~~~~~~~~~~~~~~~~~~~~~~~~~~~~~~~~~~~~~~~~~~~~~~~~~~~~~~~~~
Q=PoW(:,:,6);
Qq=Q';
Q1=(Qq(1,1:51));Q2=(Qq(2,1:51));Q3=(Qq(3,1:51));
Q4=(Qq(4,1:51));Q5=(Qq(5,1:51));Q6=(Qq(6,1:51));
Q7=(Qq(7,1:51));Q8=(Qq(8,1:51));Q9=(Qq(9,1:51));
Q10=(Qq(10,1:51));Q11=(Qq(11,1:51));
%~~~~~~~~~~~~~~~~~~~~~~~~~~~~~~~~~~~~~~~~~~~~~~~~~~~~~~~~~~~~~~~~~~~~~~~~
R=PoW(:,:,7);
Rr=R';
R1=(Rr(1,1:51));R2=(Rr(2,1:51));R3=(Rr(3,1:51));
R4=(Rr(4,1:51));R5=(Rr(5,1:51));R6=(Rr(6,1:51));
R7=(Rr(7,1:51));R8=(Rr(8,1:51));R9=(Rr(9,1:51));
R10=(Rr(10,1:51));R11=(Rr(11,1:51));
%~~~~~~~~~~~~~~~~~~~~~~~~~~~~~~~~~~~~~~~~~~~~~~~~~~~~~~~~~~~~~~~~~~~~~~~~
S=PoW(:,:,8);
Ss=S';
S1=(Ss(1,1:51));S2=(Ss(2,1:51));S3=(Ss(3,1:51));
S4=(Ss(4,1:51));S5=(Ss(5,1:51));S6=(Ss(6,1:51));
S7=(Ss(7,1:51));S8=(Ss(8,1:51));S9=(Ss(9,1:51));
S10=(Ss(10,1:51));S11=(Ss(11,1:51));
```

```
%~~~~~~~~~~~~~~~~~~~~~~~~~~~~~~~~~~~~~~~~~~~~~~~~~~~~~~~~~~~~~~~~~~~~~~
T=PoW(:,:,9);
Tt=T';
T1=(Tt(1,1:51));T2=(Tt(2,1:51));T3=(Tt(3,1:51));
T4=(Tt(4,1:51));T5=(Tt(5,1:51));T6=(Tt(6,1:51));
T7=(Tt(7,1:51));T8=(Tt(8,1:51));T9=(Tt(9,1:51));
T10=(Tt(10,1:51));T11=(Tt(11,1:51));
%~~~~~~~~~~~~~~~~~~~~~~~~~~~~~~~~~~~~~~~~~~~~~~~~~~~~~~~~~~~~~~~~~~~~~~
U=PoW(:,:,10);
Uu=U';
U1=(Uu(1,1:51));U2=(Uu(2,1:51));U3=(Uu(3,1:51));
U4=(Uu(4,1:51));U5=(Uu(5,1:51));U6=(Uu(6,1:51));
U7=(Uu(7,1:51));U8=(Uu(8,1:51));U9=(Uu(9,1:51));
U10=(Uu(10,1:51));U11=(Uu(11,1:51));
%~~~~~~~~~~~~~~~~~~~~~~~~~~~~~~~~~~~~~~~~~~~~~~~~~~~~~~~~~~~~~~~~~~~~~~
V=PoW(:,:,11);
Vv=V';
V1=(Vv(1,1:51));V2=(Vv(2,1:51));V3=(Vv(3,1:51));
V4=(Vv(4,1:51));V5=(Vv(5,1:51));V6=(Vv(6,1:51));
V7=(Vv(7,1:51));V8=(Vv(8,1:51));V9=(Vv(9,1:51));
V10=(Vv(10,1:51));V11=(Vv(11,1:51));
%~~~~~~~~~~~~~~~~~~~~~~~~~~~~~~~~~~~~~~~~~~~~~~~~~~~~~~~~~~~~~~~~~~~~~~
% Ploting
figure(1)
subplot(1,2,1)
%~~~~~~~~~~~~~~~~~~~~~~~~~~~~~~~~~~~~~~~~~~~~~~~~~~~~~~~~~~~~~~~~~~~~~~
%30
Torque_Exp=[3.97,4.12,5.067,4.954,4.87];
Theta_Exp=[353.5,351.5,349.5,347.5,345.5];
EXP1=plot(Theta_Exp,Torque_Exp,'k*','MarkerSize',10);
hold on;
Theo1=plot(theta_o,A1,'linestyle','--','color','r');
plot(theta_o,A2,'linestyle','--','color','r');
plot(theta_o,A3,'linestyle','--','color','r');
plot(theta_o,A4,'linestyle','--','color','r');
plot(theta_o,A5,'linestyle','--','color','r');
plot(theta_o,A6,'linestyle','--','color','r');
plot(theta_o,A7,'linestyle','--','color','r');
plot(theta_o,A8,'linestyle','--','color','r');
plot(theta_o,A9,'linestyle','--','color','r');
plot(theta_o,A10,'linestyle','--','color','r');
plot(theta_o,A11,'linestyle','--','color','r');
%~~~~~~~~~~~~~~~~~~~~~~~~~~~~~~~~~~~~~~~~~~~~~~~~~~~~~~~~~~~~~~~~~~~~~~
%40
Theo2=plot(theta_o,C1,'linestyle','--','color','g');
plot(theta_o,C2,'linestyle','--','color','b');
plot(theta_o,C3,'linestyle','--','color','b');
plot(theta_o,C4,'linestyle','--','color','b');
plot(theta_o,C5,'linestyle','--','color','b');
plot(theta_o,C6,'linestyle','--','color','b');
plot(theta_o,C7,'linestyle','--','color','b');
plot(theta_o,C8,'linestyle','--','color','b');
```

```
plot(theta_o,C9,'linestyle','--','color','b');
plot(theta_o,C10,'linestyle','--','color','b');
plot(theta_o,C11,'linestyle','--','color','b');
%~~~~~~~~~~~~~~~~~~~~~~~~~~~~~~~~~~~~~~~~~~~~~~~~~~~~~~~~~~~~~~~~~~~~~~~~~
%50
Theo3=plot(theta_o,E1,'linestyle','--','color','k');
plot(theta_o,E2,'linestyle','--','color','k');
plot(theta_o,E3,'linestyle','--','color','k');
plot(theta_o,E4,'linestyle','--','color','k');
plot(theta_o,E5,'linestyle','--','color','k');
plot(theta_o,E6,'linestyle','--','color','k');
plot(theta_o,E7,'linestyle','--','color','k');
plot(theta_o,E8,'linestyle','--','color','k');
plot(theta_o,E9,'linestyle','--','color','k');
plot(theta_o,E10,'linestyle','--','color','k');
plot(theta_o,E11,'linestyle','--','color','k');
%~~~~~~~~~~~~~~~~~~~~~~~~~~~~~~~~~~~~~~~~~~~~~~~~~~~~~~~~~~~~~~~~~~~~~~~~~
%60
Theo4=plot(theta_o,G1,'linestyle','--','color','g');
plot(theta_o,G2,'linestyle','--','color','g');
plot(theta_o,G3,'linestyle','--','color','g');
plot(theta_o,G4,'linestyle','--','color','g');
plot(theta_o,G5,'linestyle','--','color','g');
plot(theta_o,G6,'linestyle','--','color','g');
plot(theta_o,G7,'linestyle','--','color','g');
plot(theta_o,G8,'linestyle','--','color','g');
plot(theta_o,G9,'linestyle','--','color','g');
plot(theta_o,G10,'linestyle','--','color','g');
plot(theta_o,G11,'linestyle','--','color','g');
%~~~~~~~~~~~~~~~~~~~~~~~~~~~~~~~~~~~~~~~~~~~~~~~~~~~~~~~~~~~~~~~~~~~~~~~~~
%70
Theo5=plot(theta_o,I1,'linestyle','--','color','c');
plot(theta_o,I2,'linestyle','--','color','c');
plot(theta_o,I3,'linestyle','--','color','c');
plot(theta_o,I4,'linestyle','--','color','c');
plot(theta_o,I5,'linestyle','--','color','c');
plot(theta_o,I6,'linestyle','--','color','c');
plot(theta_o,I7,'linestyle','--','color','c');
plot(theta_o,I8,'linestyle','--','color','c');
plot(theta_o,I9,'linestyle','--','color','c');
plot(theta_o,I10,'linestyle','--','color','c');
plot(theta_o,I11,'linestyle','--','color','c');
%~~~~~~~~~~~~~~~~~~~~~~~~~~~~~~~~~~~~~~~~~~~~~~~~~~~~~~~~~~~~~~~~~~~~~~~~~
%80
Theo6=plot(theta_o,K1,'linestyle','--','color','m');
plot(theta_o,K2,'linestyle','--','color','m');
plot(theta_o,K3,'linestyle','--','color','m');
plot(theta_o,K4,'linestyle','--','color','m');
plot(theta_o,K5,'linestyle','--','color','m');
plot(theta_o,K6,'linestyle','--','color','m');
plot(theta_o,K7,'linestyle','--','color','m');
plot(theta_o,K8,'linestyle','--','color','m');
```

```
plot(theta_o,K9,'linestyle','--','color','m');
plot(theta_o,K10,'linestyle','--','color','m');
plot(theta_o,K11,'linestyle','--','color','m');
%~~~~~~~~~~~~~~~~~~~~~~~~~~~~~~~~~~~~~~~~~~~~~~~~~~~~~~~~~~~~~~~~~~~~~~
hold off
set(gca,...
    'Ycolor','k',...
    'XMinorTick','on',...
    'YMinorTick','on',...
    'FontName','Times',...
    'FontWeight','bold',...
    'LineWidth',1)
set(gcf,'color','w')
grid on;
grid minor;
legend([EXP1,Theo1,Theo2,Theo3,Theo4,Theo5,Theo6],...
    {'Experimental',...
     '30%\eta','40%\eta','50%\eta','60%\eta','70%\eta','80%\eta'},...
     'Location','southoutside',...
     'Numcolumns',3);
title('Spark Ignition Vs. Brake Torque')
xlabel('Spark Ignition[deg]')
ylabel('Brake Torque [N.m]')
%~~~~~~~~~~~~~~~~~~~~~~~~~~~~~~~~~~~~~~~~~~~~~~~~~~~~~~~~~~~~~~~~~~~~~~
subplot(1,2,2)
Power_Exp=↙
[0.831474856,0.862890782,1.061229998,1.037563334,1.019970415];
EXP2=plot(Theta_Exp,Power_Exp,'k*','MarkerSize',10);
hold on;
%~~~~~~~~~~~~~~~~~~~~~~~~~~~~~~~~~~~~~~~~~~~~~~~~~~~~~~~~~~~~~~~~~~~~~~
%30
Theo11=plot(theta_o,L1,'linestyle','--','color','r');
plot(theta_o,L2,'linestyle','--','color','r');
plot(theta_o,L3,'linestyle','--','color','r');
plot(theta_o,L4,'linestyle','--','color','r');
plot(theta_o,L5,'linestyle','--','color','r');
plot(theta_o,L6,'linestyle','--','color','r');
plot(theta_o,L7,'linestyle','--','color','r');
plot(theta_o,L8,'linestyle','--','color','r');
plot(theta_o,L9,'linestyle','--','color','r');
plot(theta_o,L10,'linestyle','--','color','r');
plot(theta_o,L11,'linestyle','--','color','r');
%~~~~~~~~~~~~~~~~~~~~~~~~~~~~~~~~~~~~~~~~~~~~~~~~~~~~~~~~~~~~~~~~~~~~~~
% %40
Theo22=plot(theta_o,N1,'linestyle','--','color','b');
plot(theta_o,N2,'linestyle','--','color','b');
plot(theta_o,N3,'linestyle','--','color','b');
plot(theta_o,N4,'linestyle','--','color','b');
plot(theta_o,N5,'linestyle','--','color','b');
plot(theta_o,N6,'linestyle','--','color','b');
plot(theta_o,N7,'linestyle','--','color','b');
plot(theta_o,N8,'linestyle','--','color','b');
```

```
plot(theta_o,N9,'linestyle','--','color','b');
plot(theta_o,N10,'linestyle','--','color','b');
plot(theta_o,N11,'linestyle','--','color','b');
%~~~~~~~~~~~~~~~~~~~~~~~~~~~~~~~~~~~~~~~~~~~~~~~~~~~~~~~~~~~~~~~~~~~~~~~
% %50
Theo33=plot(theta_o,P1,'linestyle','--','color','k');
plot(theta_o,P2,'linestyle','--','color','k');
plot(theta_o,P3,'linestyle','--','color','k');
plot(theta_o,P4,'linestyle','--','color','k');
plot(theta_o,P5,'linestyle','--','color','k');
plot(theta_o,P6,'linestyle','--','color','k');
plot(theta_o,P7,'linestyle','--','color','k');
plot(theta_o,P8,'linestyle','--','color','k');
plot(theta_o,P9,'linestyle','--','color','k');
plot(theta_o,P10,'linestyle','--','color','k');
plot(theta_o,P11,'linestyle','--','color','k');
%~~~~~~~~~~~~~~~~~~~~~~~~~~~~~~~~~~~~~~~~~~~~~~~~~~~~~~~~~~~~~~~~~~~~~~~
%60
Theo44=plot(theta_o,R1,'linestyle','--','color','g');
plot(theta_o,R2,'linestyle','--','color','g');
plot(theta_o,R3,'linestyle','--','color','g');
plot(theta_o,R4,'linestyle','--','color','g');
plot(theta_o,R5,'linestyle','--','color','g');
plot(theta_o,R6,'linestyle','--','color','g');
plot(theta_o,R7,'linestyle','--','color','g');
plot(theta_o,R8,'linestyle','--','color','g');
plot(theta_o,R9,'linestyle','--','color','g');
plot(theta_o,R10,'linestyle','--','color','g');
plot(theta_o,R11,'linestyle','--','color','g');
%~~~~~~~~~~~~~~~~~~~~~~~~~~~~~~~~~~~~~~~~~~~~~~~~~~~~~~~~~~~~~~~~~~~~~~~
%70
Theo55=plot(theta_o,T1,'linestyle','--','color','c');
plot(theta_o,T2,'linestyle','--','color','c');
plot(theta_o,T3,'linestyle','--','color','c');
plot(theta_o,T4,'linestyle','--','color','c');
plot(theta_o,T5,'linestyle','--','color','c');
plot(theta_o,T6,'linestyle','--','color','c');
plot(theta_o,T7,'linestyle','--','color','c');
plot(theta_o,T8,'linestyle','--','color','c');
plot(theta_o,T9,'linestyle','--','color','c');
plot(theta_o,T10,'linestyle','--','color','c');
plot(theta_o,T11,'linestyle','--','color','c');
%~~~~~~~~~~~~~~~~~~~~~~~~~~~~~~~~~~~~~~~~~~~~~~~~~~~~~~~~~~~~~~~~~~~~~~~
%80
Theo66=plot(theta_o,V1,'linestyle','--','color','m');
plot(theta_o,V2,'linestyle','--','color','m');
plot(theta_o,V3,'linestyle','--','color','m');
plot(theta_o,V4,'linestyle','--','color','m');
plot(theta_o,V5,'linestyle','--','color','m');
plot(theta_o,V6,'linestyle','--','color','m');
plot(theta_o,V7,'linestyle','--','color','m');
plot(theta_o,V8,'linestyle','--','color','m');
```

```
plot(theta_o,V9,'linestyle','--','color','m');
plot(theta_o,V10,'linestyle','--','color','m');
plot(theta_o,V11,'linestyle','--','color','m');
%~~~~~~~~~~~~~~~~~~~~~~~~~~~~~~~~~~~~~~~~~~~~~~~~~~~~~~~~~~~~~~~~~~~~~~
hold off
set(gca,...
    'Ycolor','k',...
    'XMinorTick','on',...
    'YMinorTick','on',...
    'FontName','Times',...
    'FontWeight','bold',...
    'LineWidth',1)
set(gcf,'color','w')  %357.12,265.89
grid on;
grid minor;
legend([EXP2,Theo11,Theo22,Theo33,Theo44,Theo55,Theo66],...
    {'Experimental',...
     '30%\eta','40%\eta','50%\eta','60%\eta','70%\eta','80%\eta'},...
     'Location','southoutside',...
     'Numcolumns',3);
title('Spark Ignition Vs. Brake Power')
xlabel('Spark Ignition[deg]')
ylabel('Brake Power [kW]')
```

APPENDIX D

MATLAB CODE: STAGE IV

D.1 MATLAB Function

```
function [W_dot_ac,T_ac1,Torque_1,eta_m,eta_V...
,BTE,BSFC,P,DQ,X,T,m_dot_f]=StageIVFunction..
(RPM,theta_0,eta_combmaX,theta_b,Load)
% Universiti Teknologi PETRONAS
% Project: Numerical Investigation and Optimization
%          of The Crank-Rocker Engine Ignition Timing
%          Based on Performance and Combustion Characteristics
% Methodology Stage: STAGE IV
% Section: Function of Optimization Part II
%~~~~~~~~~~~~~~~~~~~~~~~~~~~~~~~~~~~~~~~~~~~~~~~~~~~~~~~~~~~~~~~~~~~~~~
% INPUT SECTIONS
% THIS SECTION CONTAINS SEVERAL SUB-SECTIONS
% INCLUDING ALL THE REQUIRED INPUTS FOR THE MODEL AND SIMULATION.
%~~~~~~~~~~~~~~~~~~~~~~~~~~~~~~~~~~~~~~~~~~~~~~~~~~~~~~~~~~~~~~~~~~~~~~
% INPUT #1 Crank-Rocker Engine Geometry and Specification Data
%~~~~~~~~~~~~~~~~~~~~~~~~~~~~~~~~~~~~~~~~~~~~~~~~~~~~~~~~~~~~~~~~~~~~~~
% Length
L2 = 0.0253;   %input('Enter The Crank Radius Length [m]')
L3 = 0.1;      %input('Enter The Connecting Rod Length [m]')
L4 = 0.1388;   %input('Enter The Rocker Length [m]')
L41 = 0.1381;  %input('Enter The Extended Rocker Length [m]')
%~~~~~~~~~~~~~~~~~~~~~~~~~~~~~~~~~~~~~~~~~~~~~~~~~~~~~~~~~~~~~~~~~~~~~~
% Engine Spicification
PHI = 21;      % Swing Angle [degree]
B = 0.055;     % Engine Bore [m]
N_cyl = 1;     % Number of Cylinders
N_r = 2;       % Number of Revolutions Per Power Stroke
C_r = 8.5;     % Compression ratio
%~~~~~~~~~~~~~~~~~~~~~~~~~~~~~~~~~~~~~~~~~~~~~~~~~~~~~~~~~~~~~~~~~~~~~~
% Speed and Load
%RPM = 2000;    % input('Enter The Engine Speed [1/min] =')
%Load = 1;      % Engine Load (Load = 1 = FUll Load)
%~~~~~~~~~~~~~~~~~~~~~~~~~~~~~~~~~~~~~~~~~~~~~~~~~~~~~~~~~~~~~~~~~~~~~~
% Valves
IVC = 0;       % Time [degrees], Intake Valve Closes
EVO = 540;     % Time [degrees], Exhaust Valve Opens
%~~~~~~~~~~~~~~~~~~~~~~~~~~~~~~~~~~~~~~~~~~~~~~~~~~~~~~~~~~~~~~~~~~~~~~
% Timing
%theta_b = 74;  % Combustion Duration [degree]
%theta_0 = 356; % CA at Start of Combustion [degree]/ Ignition timing
%~~~~~~~~~~~~~~~~~~~~~~~~~~~~~~~~~~~~~~~~~~~~~~~~~~~~~~~~~~~~~~~~~~~~~~
% INPUT #2 Fuel Input Data
%~~~~~~~~~~~~~~~~~~~~~~~~~~~~~~~~~~~~~~~~~~~~~~~~~~~~~~~~~~~~~~~~~~~~~~
AF_ratio_stoich = 15.09;    % Gravimetric Air Fuel Ratio (Stoich)
AF_ratio_mol_sotich = 14.7; % Molar Air_Fuel Ratio (Stoich)
lambda = 0.9;         % Excess Air Coefficient
LHV =47.3e6;          % Lower Heating Value Of Fuel Mixture [J/kg]
R_air = 287;          % Gas Constant For Air [J/kg-K]
%~~~~~~~~~~~~~~~~~~~~~~~~~~~~~~~~~~~~~~~~~~~~~~~~~~~~~~~~~~~~~~~~~~~~~~
% INPUT #3 Ambient Conditions
%~~~~~~~~~~~~~~~~~~~~~~~~~~~~~~~~~~~~~~~~~~~~~~~~~~~~~~~~~~~~~~~~~~~~~~
%Ambient Conditions
```

```
P_atm = 101325;      % Atmospheric Inputs
T_atm = 290;         % Atmospheric Temp Inputs
%~~~~~~~~~~~~~~~~~~~~~~~~~~~~~~~~~~~~~~~~~~~~~~~~~~~~~~~~~~~~~~~~~~~~~~
% INPUT #4 Assumptions
%~~~~~~~~~~~~~~~~~~~~~~~~~~~~~~~~~~~~~~~~~~~~~~~~~~~~~~~~~~~~~~~~~~~~~~
%eta_combmaX = 0.85;  % Assumed MAX Comb. Efficiency
T_W =490;             % Assumed Wall Temperature [K]
gamma(1:720) = 1.34;  % Preallocate Gamma Array (sets initial value)
%~~~~~~~~~~~~~~~~~~~~~~~~~~~~~~~~~~~~~~~~~~~~~~~~~~~~~~~~~~~~~~~~~~~~~~
% INITIAL CALCULATION
%~~~~~~~~~~~~~~~~~~~~~~~~~~~~~~~~~~~~~~~~~~~~~~~~~~~~~~~~~~~~~~~~~~~~~~
% Engine Calculations Based On INPUT #1
%~~~~~~~~~~~~~~~~~~~~~~~~~~~~~~~~~~~~~~~~~~~~~~~~~~~~~~~~~~~~~~~~~~~~~~
% Geometry
%~~~~~~~~~~~~~~~~~~~~~~~~~~~~~~~~~~~~~~~~~~~~~~~~~~~~~~~~~~~~~~~~~~~~~~
S = L41*PHI*pi()/180;       % Calculates the Engine Stroke [m]
DD1 = L4*cos(PHI/2*pi()/180);% Calculates the Length DD1 [m]
L1 = sqrt((L3)^2+(DD1)^2);   % Calculates the Engine framelength [m]
%~~~~~~~~~~~~~~~~~~~~~~~~~~~~~~~~~~~~~~~~~~~~~~~~~~~~~~~~~~~~~~~~~~~~~~
% Theta
%~~~~~~~~~~~~~~~~~~~~~~~~~~~~~~~~~~~~~~~~~~~~~~~~~~~~~~~~~~~~~~~~~~~~~~
theta1 = asin(DD1/L1)*180/pi();
% Calculates Ineital angle theta1  [degrees]
theta_f = theta_0 + theta_b;
% Crank Angle at End of Combustion [degree]
%~~~~~~~~~~~~~~~~~~~~~~~~~~~~~~~~~~~~~~~~~~~~~~~~~~~~~~~~~~~~~~~~~~~~~~
% Area
%~~~~~~~~~~~~~~~~~~~~~~~~~~~~~~~~~~~~~~~~~~~~~~~~~~~~~~~~~~~~~~~~~~~~~~
A_p = (pi/4)*B^2;
% Calculates Cross Sectional Piston Area [m^2]
A_ch = 2*A_p;
% Calculates Cylinder Head Surface Area (in chamber)
%~~~~~~~~~~~~~~~~~~~~~~~~~~~~~~~~~~~~~~~~~~~~~~~~~~~~~~~~~~~~~~~~~~~~~~
% Volumes
%~~~~~~~~~~~~~~~~~~~~~~~~~~~~~~~~~~~~~~~~~~~~~~~~~~~~~~~~~~~~~~~~~~~~~~
V_d = N_cyl*A_p*S;
% Calculates Displaced Volume Of Engine [m^3]
V_TDC = (V_d/(C_r-1))/N_cyl;
% Calculates Clearance Volume [m^3]
%~~~~~~~~~~~~~~~~~~~~~~~~~~~~~~~~~~~~~~~~~~~~~~~~~~~~~~~~~~~~~~~~~~~~~~
% General
%~~~~~~~~~~~~~~~~~~~~~~~~~~~~~~~~~~~~~~~~~~~~~~~~~~~~~~~~~~~~~~~~~~~~~~
N = RPM/60;         % Converts RPM to RPS [1/s]
S_bar_p = 2*S*N;    % Calculates Mean Piston Speed [m/s]
%~~~~~~~~~~~~~~~~~~~~~~~~~~~~~~~~~~~~~~~~~~~~~~~~~~~~~~~~~~~~~~~~~~~~~~
% Calculateing Losses Due to Friction
%~~~~~~~~~~~~~~~~~~~~~~~~~~~~~~~~~~~~~~~~~~~~~~~~~~~~~~~~~~~~~~~~~~~~~~
fmep = (250*S*RPM)*10^-3; % Calculating Losses Due To Friction
%Volumetric Efficiency correction Factor
CF=-8*10^(-9)*RPM^2+.000135*RPM+.31944;
%~~~~~~~~~~~~~~~~~~~~~~~~~~~~~~~~~~~~~~~~~~~~~~~~~~~~~~~~~~~~~~~~~~~~~~
% Engine Calculations Based On INPUT #2
```

```
%~~~~~~~~~~~~~~~~~~~~~~~~~~~~~~~~~~~~~~~~~~~~~~~~~~~~~~~~~~~~~~~~~~~~~~
AF_ratio_ac = lambda*AF_ratio_stoich; % Actual Air Fuel Ratio
AF_ratio_mol=lambda*AF_ratio_mol_sotich;
%Predicts Combustion Efficiency (Reference To Blair)
eta_comb1=eta_combmaX*(-1.6082+4.6509*lambda-2.0764*lambda^2);
P_BDC = Load*P_atm; % Inlet Pressure[Pa] Moscow,ID
%~~~~~~~~~~~~~~~~~~~~~~~~~~~~~~~~~~~~~~~~~~~~~~~~~~~~~~~~~~~~~~~~~~~~~~
%Polynomials Used To Calculate Gamma As A Function Of RPM
%~~~~~~~~~~~~~~~~~~~~~~~~~~~~~~~~~~~~~~~~~~~~~~~~~~~~~~~~~~~~~~~~~~~~~~
a_1 = .692; a_2 = 39.17e-06; a_3 = 52.9e-09; a_4 = -228.62e-13;
a_5 = 277.58e-17;b_0 = 3049.33; b_1 = -5.7e-02; b_2 = -9.5e-05;
b_3 = 21.53e-09;b_4 = -200.26e-14;c_u = 2.32584; c_r = 4.186e-03;
d_0 = 10.41066; d_1 = 7.85125; d_3 = -3.71257;e_0 = -15.001e03;
e_1 = -15.838e03; e_3 = 9.613e03;f_0 = -.10329; f_1 = -.38656;
f_3 = .154226; f_4 = -14.763; f_5 = 118.27; f_6 = 14.503;
r_0 = -.2977; r_1 = 11.98; r_2 = -25442; r_3 = -.4354;
%~~~~~~~~~~~~~~~~~~~~~~~~~~~~~~~~~~~~~~~~~~~~~~~~~~~~~~~~~~~~~~~~~~~~~~
% Initial Preallocation of Matrices
V(1:720)=zeros;         DV(1:720)=zeros;      rho(1:720)=zeros;
mu(1:720)=zeros;        M_F(1:720)=zeros;     h_g(1:720)=zeros;
C_k(1:720)=zeros;       C_R(1:720)=zeros;     X(1:720)=zeros;
DX(1:720)=zeros;        Re(1:720)=zeros;      Nus(1:720)=zeros;
DQ_w_A(1:720)=zeros;    DQ(1:720)=zeros;      Q(1:720)=zeros;
DT(1:720)=zeros;        W_doT(1:720)=zeros;   T_indicated(1:720)=zeros;
DP(1:720)=zeros;        P(1:720)=zeros;       T(1:720)=zeros;
W(1:720)=zeros;         Q_doT(1:720)=zeros;   u(1:720)=zeros;
du(1:720)=zeros;        cV(1:720)=zeros;      m_b(1:720)=zeros;
m_u(1:720)=zeros;       gamma_u(1:720)=zeros; DQ2(1:720)=zeros;
V_u(1:720)=zeros;       %V_b(1:720)=zeros;
T_u(1:720)=zeros;       T_b(1:720)=zeros;     x(1:720)=zeros;
A_u(1:720)=zeros;       A_b(1:720)=zeros;     DT_u(1:720)=zeros;
u_u(1:720)=zeros;       du_u(1:720)=zeros;    cv_u(1:720)=zeros;
DQ_w2_A(1:720)=zeros;   Q2(1:720)=zeros;      Throw(1:720)=zeros;
Thrad(1:720)=zeros;     BD(1:720)=zeros;      T4(1:720)=0;
A(1:720)=zeros;         DT_b(1:720)=zeros;
%~~~~~~~~~~~~~~~~~~~~~~~~~~~~~~~~~~~~~~~~~~~~~~~~~~~~~~~~~~~~~~~~~~~~~~
% Index (k = 1:2) Serve as the EGR simulation,
% Functionality of the EGR simulation required
% the script to run two times with only the gas temperature ...
% and fluid properties changing during the second iteration.
% Index (i = 2:720)calculated instantaneous engine features
%~~~~~~~~~~~~~~~~~~~~~~~~~~~~~~~~~~~~~~~~~~~~~~~~~~~~~~~~~~~~~~~~~~~~~~
% Exhaust Gas Residual (EGR) Simulation
%~~~~~~~~~~~~~~~~~~~~~~~~~~~~~~~~~~~~~~~~~~~~~~~~~~~~~~~~~~~~~~~~~~~~~~
for k = 1:2
%~~~~~~~~~~~~~~~~~~~~~~~~~~~~~~~~~~~~~~~~~~~~~~~~~~~~~~~~~~~~~~~~~~~~~~
% corrects Temperature Based On Exhaust Gas Residuals
if k==1
T_BDC = T_atm; % Assumed Inlet Temperature [K]
else
T_BDC = T_corr;
end
```

```matlab
% Calculate Mass of Air In Cylinder/ Mass Of Fuel Based On AFR
rho_a = P_BDC/(R_air*T_BDC);     % Air Density kg/m^3
m_a = rho_a*V_d;                 % Mass of Air In Cylinder [kg]
m_f = m_a/AF_ratio_ac;           % Mass Of Fuel In Cylinder [kg]
m_c1 = m_a + m_f;                % Mass In Cylinder
%~~~~~~~~~~~~~~~~~~~~~~~~~~~~~~~~~~~~~~~~~~~~~~~~~~~~~~~~~~~~~~~~~~~~~~~~
%Specifying Initial Conditions For Loops
BD(1:720)=zeros;
theta(1:720)=zeros; % Starting Crank Angle [degree]
BD(1)=sqrt ((L1)^2+(L2)^2-2*(L1)*(L2)*cosd(theta(1)+theta1));
T4(1:720)=zeros;
T4(1) = 180-acosd(((L1)^2-(L2)^2+(BD(1))^2)/(2*L1*BD(1)))...
        -acosd(((L4)^2-(L3)^2+(BD(1))^2)/(2*L4*BD(1)));
V(1:720)=zeros;  % Preallocate Volume Array
V(1)=V_TDC;      % Starting Combustion Chamber Volume [m^3]
G(1:720)=zeros;
DV(1:720)=zeros; % Preallocate Change In Volume Array
DV(1)=0;         % Specifying Initial Change In Volume
P(1:720)=P(1);
P(1)=P_BDC;
DP(1:720)=zeros; % Specifying Initial Change In Pressure
T(1:720)=zeros;  % Preallocate Temperature Array
T(1)=T_BDC;      % Inlet Temperature [K]
DT(1:720)=zeros; % Specifying Initial Change In Temperature
T_u(1:720)=zeros;% Preallocate Unburned Temperature Array
T_u(1)=T_BDC;    % Initial Unburned Temperature[K]
DT_u(1:720)=zeros;% Preallocate Change In Unburned Temperature
gamma(1:720)=zeros;
gamma(1)=1.4;   % Initial Gamma Input
gamma_u(1:720)=zeros;
gamma_u(1)=1.4; % Initial Gamma Input
X(1:720)=zeros; % Preallocate Mass Burn Array
DX(1:720)=zeros; % Preallocate Change In Mass Burn Fraction
DQ(1:720)=zeros; % Preallocate Heat Release Array
DQ2(1:720)=zeros;% Preallocate Two Zone Heat Release Array
Q(1:720)=zeros;  % Preallocate Heat Array
Q2(1:720)=zeros; % Preallocate two-zone Heat release Array
M_F(1:720)=zeros; % Preallocate Mass In Comubstion Chamber Array
mu(1:720)=zeros;  % Preallocate Viscosity Array
mu(1)=7.457*10^(-6)+4.1547*10^(-8)*T_BDC-7.4793*10^(-12)*T_BDC^(2);
rho(1:720)=zeros;  % Preallocates Ideal Gas Law array
rho(1)=P(1)/(R_air*T(1));% Initial Value Ideal Gas Array
C_k(1:720)=zeros;  % Preallocate Thermal Conductivity Array
C_k(1)=6.1944*10^(-3)+7.3814*10^(-5)*T_BDC-1.2491*10^(-8)*T_BDC^(2);
C_R(1:720)=zeros;  % Preallocate Radiation Coefficient Array
C_R(1)=4.25*10^(-09)*((T(1)^4-T_W^4)/(T(1)-T_W));
% Initial Rad. Coeff heat trasnfer coeeficient for radiation part
Re(1:720)=zeros;  % Preallocate Reynolds Value Array
Re(1)=rho(1)*S_bar_p*B/mu(1);% Initial Reynolds Value
Nus(1:720)=zeros; % Preallocating Nusselt Number Array
Nus(1)=.49*Re(1)^(.7);% Initial Nusselt Number
h_g(1:720)=zeros;% Preallocate Heat Transfer Coefficient Array
```

```
h_g(1)=C_k(1)*Nus(1)/B; % Initial Heat Transfer Coefficient
A(1:720)=zeros;
Throw(1:720)=zeros;% Preallocates angle Crank/rocker Axes Array
Throw(1)=(T4(1)-T4(1));% Initial swing angle poistion [Degree]
Thrad(1:720)=zeros;
Thrad(1)= Throw(1)*pi/180;% Initial swing angle poistion[Radin]
x(1:720)=zeros;   % Preallocates Distance Crank/Piston Axes Array
x(1)=L41*Thrad(1);% Initial piston Distance [m]
W(1:720)=zeros;   % Preallocate Work Array
W_doT(1:720)=zeros; % Preallocate Power Array
T_indicated(1:720)=zeros;% Preallocate Torque Array
Q_doT(1:720)=zeros;% Preallocate Heat Transfer Array
u(1:720)=zeros;   % Preallocate Internal Energy Array
du(1:720)=zeros;  % Preallocates Change In Internal Energy Array
cV(1:720)=zeros;  % Preallocates Heat Capacity Array
DQ_w_A(1:720)=zeros; % Preallocate Convective Heat Loss
DQ_w2_A(1:720)=zeros;% Preallocate Convective Heat Loss 2 zone
m_b(1:720)=zeros; % Preallocate mass burned array
m_u(1:720)=m_c1;  % Preallocate unburned mass array
V_u(1:720)=zeros; % Preallocate unburned Volume Array
V_u(1)=V(1);      % Initial Unburned Volume
DT_b(1:720)=zeros;
%~~~~~~~~~~~~~~~~~~~~~~~~~~~~~~~~~~~~~~~~~~~~~~~~~~~~~~~~~~~~~~~~~~~~~~
% Instantaneous Engine Features Simulation
%~~~~~~~~~~~~~~~~~~~~~~~~~~~~~~~~~~~~~~~~~~~~~~~~~~~~~~~~~~~~~~~~~~~~~~
theta=1:720;
for i=2:720
%~~~~~~~~~~~~~~~~~~~~~~~~~~~~~~~~~~~~~~~~~~~~~~~~~~~~~~~~~~~~~~~~~~~~~~
BD(i)=sqrt((L1)^2+(L2)^2-2*(L1)*(L2)*cosd(theta(i)+theta1));
% Calculates length BD [m]
G(i)=acosd(((L3)^2+(L4)^2-(BD(i))^2)/(2*L3*L4));
% Calculates Transmission angle [Degree]
T4(i)=180-acosd(((L1)^2-(L2)^2+(BD(i))^2)/(2*L1*BD(i)))-...
      acosd(((L4)^2-(L3)^2+(BD(i))^2)/(2*L4*BD(i)));
% Calculates Theta4 [Degree]
if(i>(180-theta1))
T4(i) = 180+acosd(((L1)^2-(L2)^2+(BD(i))^2)/(2*L1*BD(i)))..
       -acosd(((L4)^2-(L3)^2+(BD(i))^2)/(2*L4*BD(i)));
end
if(i>(360-theta1))
T4(i) = 180-acosd(((L1)^2-(L2)^2+(BD(i))^2)/(2*L1*BD(i)))..
       -acosd(((L4)^2-(L3)^2+(BD(i))^2)/(2*L4*BD(i)));
end
if(i>(540-theta1))
T4(i) = 180+acosd(((L1)^2-(L2)^2+(BD(i))^2)/(2*L1*BD(i)))..
       -acosd(((L4)^2-(L3)^2+(BD(i))^2)/(2*L4*BD(i)));
end
if(i>(720-theta1))
T4(i) = 180-acosd(((L1)^2-(L2)^2+(BD(i))^2)/(2*L1*BD(i)))..
       -acosd(((L4)^2-(L3)^2+(BD(i))^2)/(2*L4*BD(i)));
end
%%↙
```

```
~~~~~~~~~~~~~~~~~~~~~~~~~~~~~~~~~~~~~~~~~~~~~~~~~~~~~~~~~~~~~~~~~~~~~~
Throw(i)=(T4(i)-T4(1));
% Calculates Swing Angle position as a Function of Crank Angle [Degree]
Thrad(i)=Throw(i)*pi/180;
% Calculates Swing Angle position as a Function of Crank Angle [Radian]
x(i)=L41*Thrad(i);
% Calculates Piston Displacement as a Function of Crank  Angle [m]
V(i)=V_TDC + (pi/4)*(B^2)*x(i);
% Calculates Total Cyl. Volume as a Function of Crank  Angle [m3]
DV(i)=V(i)-V(i-1);
%~~~~~~~~~~~~~~~~~~~~~~~~~~~~~~~~~~~~~~~~~~~~~~~~~~~~~~~~~~~~~~~~~~~~~~
%Calculates Density As A Function Of Crank Angle
rho(i)=P(i-1)/(R_air*T(i-1));
%Calculates Viscosity As A Function Of Temperature
mu(i)=7.457*10^(-6)+4.1547*10^(-8)*T(i-1)-7.4793*10^(-12)*T(i-1)^(2);
%Calculating Instantaneous Thermal Conductivity of Cylinder Gas
C_k(i)=6.1944*10^(-3)+7.3814*10^(-5)*T(i-1)-1.2491*10^(-8)*T(i-1)^(2);
%Calculating The Radiation Heat Transfer Coefficient
C_R(i)=(4.25*10^(-09))*((T(i-1)^4-T_W^4)/(T(i-1)-T_W));
%~~~~~~~~~~~~~~~~~~~~~~~~~~~~~~~~~~~~~~~~~~~~~~~~~~~~~~~~~~~~~~~~~~~~~~
%Instantaneous Suface Area (For Heat Transfer);
A(i)= A_ch + A_p + pi*B*x(i) ;
%~~~~~~~~~~~~~~~~~~~~~~~~~~~~~~~~~~~~~~~~~~~~~~~~~~~~~~~~~~~~~~~~~~~~~~
%Specifies Mass Fraction Burn As A Function Of Crank Angle (Weibe Fcn.)
if theta(i)<theta_0
X(i)=0;
else
X(i) = 1-exp(-5*((theta(i)-theta_0)/theta_b)^3);
if theta(i) < theta_f
M_F(i) = V(theta_0-1)*rho(theta_0-1)/(lambda*AF_ratio_mol);
end
end
%~~~~~~~~~~~~~~~~~~~~~~~~~~~~~~~~~~~~~~~~~~~~~~~~~~~~~~~~~~~~~~~~~~~~~~
%Specifies Change In Mass Fraction Burn As A Function Of Crank Angle
DX(i) = X(i) - X(i-1);
%~~~~~~~~~~~~~~~~~~~~~~~~~~~~~~~~~~~~~~~~~~~~~~~~~~~~~~~~~~~~~~~~~~~~~~
% Heat Transfer Prediction
%~~~~~~~~~~~~~~~~~~~~~~~~~~~~~~~~~~~~~~~~~~~~~~~~~~~~~~~~~~~~~~~~~~~~~~
%Using ANNAND METHOD
%CACULATION
Re(i)=(rho(i)*S_bar_p*B)/(mu(i));
% Calculating Reynolds Number
Nus(i)=0.49*(Re(i)^(0.7));
% Calculating Nusselt Number
h_g(i)=(C_k(i)*Nus(i))/B;
% Calculating Heat Transfer Coefficient(convection part)
DQ_w_A(i)=(h_g(i)+C_R(i))*A(i)*(T(i-1)-T_W)*(60/(720*RPM));
% Calculates Convective Losses Into Wall
DQ_w2_A(i)=((h_g(i)+C_R(i))*A_b(i-1)/N_cyl*(T_b(i-1)-T_W)...
+(h_g(i)+C_R(i))*A_u(i-1)/N_cyl*(T_u(i-1)-T_W))*(60/(720*RPM));
%Calculates Total Heat Transfer (Per Cycle)
DQ(i) = eta_comb1*LHV*M_F(i)*DX(i)-DQ_w_A(i);
```

```
% Calculates Change In Heat Transfer (total)
DQ2(i)= eta_comb1*LHV*M_F(i)*DX(i)-DQ_w2_A(i);
% Calculates Change In Heat Transfer (total)Two-Zone
Q(i)  = Q(i-1) + DQ(i);
Q2(i) = Q2(i-1)+ DQ2(i);
%~~~~~~~~~~~~~~~~~~~~~~~~~~~~~~~~~~~~~~~~~~~~~~~~~~~~~~~~~~~~~~~~~~~~~~
% Specifies Pressure and Temperature Increases Between Intake Valve
%~~~~~~~~~~~~~~~~~~~~~~~~~~~~~~~~~~~~~~~~~~~~~~~~~~~~~~~~~~~~~~~~~~~~~~
% Closing and Exhaust Valve Opening...50
if  IVC <= theta(i)
DT(i)=T(i-1)*(gamma(i-1)-1)...
      *((1/(P(i-1)*V(i-1)))*DQ(i)-(1/V(i-1))*DV(i));
DP(i)=(-P(i-1)/V(i-1))*DV(i)+(P(i-1)/T(i-1))*DT(i);
P(i)=P(i-1)+DP(i);
end
if 252<= theta(i)              %256
if P(i)<=P_atm
P(i)=P_atm;
end
end
if EVO < theta(i)
P(i)=0.3086*100000;
%P(i)=P(i);
%P(i)=P_atm;
end
%~~~~~~~~~~~~~~~~~~~~~~~~~~~~~~~~~~~~~~~~~~~~~~~~~~~~~~~~~~~~~~~~~~~~~~
%Returns Temperature Values To Beginning Of Loop
%Assumes Temperature Drops Back To ATM Temp After Exhaust Is Extracted
T(i) = T(i-1)+DT(i);
% Returns Temperature Values To Beginning Of Loop
% Assume A Polytropic Constant Of 1.3
% Treats Atmospheric Pressure As Reference State
W(i) = W(i-1)+(P(i)-P_atm)*DV(i);
% Calculates Cylinder Work [J] As A Function Of Crank Angle
W_doT(i)=(N_cyl*W(i)*N/N_r)/1000;
% Calculates Power [kW] As A Function Of Crank Angle
imep = CF*W_doT(720)*N_r*1000/(V_d*1000*N);
% Indicated Mean Effective Pressure
T_indicated(i) = (W_doT(i)*1000)/(2*pi*N);
% Calculates Torque[N*m] As A Function Of Crank Angle
Q_doT(i) = (N_cyl*Q(i)*N/N_r)/1000;
% Calculates Heat Loss [kW] As A Function Of Crank Angle
%~~~~~~~~~~~~~~~~~~~~~~~~~~~~~~~~~~~~~~~~~~~~~~~~~~~~~~~~~~~~~~~~~~~~~~
%The Following Section Of Code Calculates An Updated Value Of Gamma
%Using The "Polynomial Method" Developed By Krieger-Borman
%User Of This Code Must Be Careful Because Accuracy Of This Method
%Drops As The Fuel Mixture Becomes Increasingly Rich
%~~~~~~~~~~~~~~~~~~~~~~~~~~~~~~~~~~~~~~~~~~~~~~~~~~~~~~~~~~~~~~~~~~~~~~
%Calculates A,B Factors For Following Block Of Code
A_T  = a_1*T(i)+a_2*T(i)^2+a_3*T(i)^3+a_4*T(i)^4+a_5*T(i)^5;
A_tu = a_1*T_u(i)+a_2*T_u(i)^2+a_3*T_u(i)^3+a_4*T_u(i)^4+a_5*T_u(i)^5;
B_T  = b_0+b_1*T(i)+b_2*T(i)^2+b_3*T(i)^3+b_4*T(i)^4;
```

```
B_tu = b_0+b_1*T_u(i)+b_2*T_u(i)^2+b_3*T_u(i)^3+b_4*T_u(i)^4;
%Calculates Factor "D" As A Function Of lambda
D_lambda = d_0 + d_1*lambda^(-1)+ d_3*lambda^(-3);
%Calculates Factor "F" As A Function Of Temperature,lambda
E_Tlambda = (e_0+e_1*lambda^(-1)+e_3*lambda^(-3))/T(i);
E_TLambdau =(e_0+e_1*lambda^(-1)+e_3*lambda^(-3))/T_u(i);
F_TPlambda =(f_0+f_1*lambda^(-1)+f_3*lambda^(-3)...
            +((f_4 + f_5*lambda^(-1))/T(i)))*log(f_6*P(i));
F_TPLambdau=(f_0+f_1*lambda^(-1)+f_3*lambda^(-3)...
            +((f_4 + f_5*lambda^(-1))/T_u(i)))*log(f_6*P(i));
%~~~~~~~~~~~~~~~~~~~~~~~~~~~~~~~~~~~~~~~~~~~~~~~~~~~~~~~~~~~~~~~~~~~~~~~
%Calculates correction Factor For Internal Energy
u_corr = c_u*exp(D_lambda +E_Tlambda + F_TPlambda);
u_corr_u=c_u*exp(D_lambda +E_TLambdau+ F_TPLambdau);
%~~~~~~~~~~~~~~~~~~~~~~~~~~~~~~~~~~~~~~~~~~~~~~~~~~~~~~~~~~~~~~~~~~~~~~~
%Calculates Internal Energy As A Function Of Crank Angle
u(i) = A_T - B_T/lambda + u_corr;
u_u(i) = A_tu - B_tu/lambda + u_corr_u;
%~~~~~~~~~~~~~~~~~~~~~~~~~~~~~~~~~~~~~~~~~~~~~~~~~~~~~~~~~~~~~~~~~~~~~~~
%Calculates Change In Internal Energy
du(i) = u(i) - u(i-1);
du_u(i) = u_u(i) - u_u(i-1);
%~~~~~~~~~~~~~~~~~~~~~~~~~~~~~~~~~~~~~~~~~~~~~~~~~~~~~~~~~~~~~~~~~~~~~~~
%Calculates Heat Capacity "C_v" As A Function Of Crank Angle
cV(i) = du(i)/DT(i);
cv_u(i)=du_u(i)/DT_u(i);
%~~~~~~~~~~~~~~~~~~~~~~~~~~~~~~~~~~~~~~~~~~~~~~~~~~~~~~~~~~~~~~~~~~~~~~~
%Calculates correction Factor For "R" Value
R_corr=c_r*exp(r_0*log(lambda)+...
      (r_1+r_2/T(i)+r_3*log(f_6*P(i)))/lambda);
R_corr_u =c_r*exp(r_0*log(lambda)...
     +(r_1+r_2/T_u(i-1)+r_3*log(f_6*P(i)))/lambda);
%~~~~~~~~~~~~~~~~~~~~~~~~~~~~~~~~~~~~~~~~~~~~~~~~~~~~~~~~~~~~~~~~~~~~~~~
%Calculates Actual "R" Value
R = .287 + .020/lambda + R_corr;
R_u = .287 + .020/lambda + R_corr_u;
%~~~~~~~~~~~~~~~~~~~~~~~~~~~~~~~~~~~~~~~~~~~~~~~~~~~~~~~~~~~~~~~~~~~~~~~
%Calculates Actual Gamma Value And Returns To Beginning Of Code
gamma_u(i)=1+R_u/cv_u(i);
gamma(i) = 1 + R/cV(i);
if gamma(i)<1.2
gamma(i)=1.34;
gamma_u(i)=1.34;
end
if theta(i)>=EVO
gamma(i)=1.34;
gamma_u(i)=1.34;
end
%~~~~~~~~~~~~~~~~~~~~~~~~~~~~~~~~~~~~~~~~~~~~~~~~~~~~~~~~~~~~~~~~~~~~~~~
%Calculate Temperature Of Exhaust Based On Polytropic Relations
if EVO < theta(i)
T(i)=T(EVO)*(P_BDC/P(EVO))^((gamma(i)-1)/gamma(i));
```

```
T_b(i)=T_b(EVO)*(P_BDC/P(EVO))^((gamma(i)-1)/gamma(i));
end
end
%~~~~~~~~~~~~~~~~~~~~~~~~~~~~~~~~~~~~~~~~~~~~~~~~~~~~~~~~~~~~~~~~~~~~~~
% Calculates A corrected Inlet Temperature Based On EGR
%T_corr = R_frac*T(720)+(1-R_frac)*T_BDC;
T_corr = T_BDC;
end
%~~~~~~~~~~~~~~~~~~~~~~~~~~~~~~~~~~~~~~~~~~~~~~~~~~~~~~~~~~~~~~~~~~~~~~
% Specified Outputs (On Matlab Screen)
bmep = imep-fmep;
W_dot_ac=(bmep*V_d*1000*N/(N_r*1000)); %Brake Power
T_ac1 = W_dot_ac/(2*pi*N*10^(-3)); %Brake Torque
Torque_1=(1*bmep*V_d*1000)/(4*pi); %Brake Torque
eta_m=bmep/imep;
%~~~~~~~~~~~~~~~~~~~~~~~~~~~~~~~~~~~~~~~~~~~~~~~~~~~~~~~~~~~~~~~~~~~~~~
% Calcualtes Brake Specific Fuel Consumption
m_ta = P_BDC*V_d/(R_air*T_BDC);
%Calculate Trapped Air In Cylinder
eta_V = CF*((m_ta)/(rho_a*V_d));
%corrected Volumetric Efficiency
m_dot_f = N_cyl*M_F(theta_0)*(N/N_r);
%Mass Flow Rate Of Fuel [kg/s]
BSFC= ((m_dot_f*1000*3600)/(W_dot_ac));
%BSFC [g/kW*h]
BTE=((W_dot_ac)/(m_dot_f*47300))*100;
%[kW]/[kg/s]*[kJ/kg]= [kW/(kJ/s)]= Unit less *100%=percentage
end
```

D.2 MATLAB Call Function

```
% Universiti Teknologi PETRONAS
% Project: Numerical Investigation and Optimization
%          of The Crank-Rocker Engine Ignition Timing
%          Based on Performance and Combustion Characteristics
% Methodology Stage: STAGE IV
% Section: Call Function of Optimization Part II
%
~~~~~~~~~~~~~~~~~~~~~~~~~~~~~~~~~~~~~~~~~~~~~~~~~~~~~~~~~~~~~~~~~~~~~~
~~~
clc
clear
close all
%
~~~~~~~~~~~~~~~~~~~~~~~~~~~~~~~~~~~~~~~~~~~~~~~~~~~~~~~~~~~~~~~~~~~~~~
~~~
%Input Section
Load1 = input...
('Enter The Engine Load value in [%]:');
eta_combmaX1=input...
('Enter The Engine Assumed Max Combustion Efficiency value in [%]:');
RPM_st1=input...
('Enter The Starting Engine Speed value in [RPM]:');
RPM_fin=input...
('Enter The Finishing Engine Speed value in [RPM]:');
RPM_Increment=input...
('Enter The Increment of Engine Speed value in [RPM]:');
theta_st_11=input...
('Enter The Lower Range of Your Guessed Ignition Timing value in
[deg]:');
theta_fin=input...
('Enter The Upper Range of Your Guessed Ignition Timing value in
[deg]:');
theta_increment=input...
('Enter The Increment of Crank Angle For Ignition Timing value in
[deg]:');
theta_b_Input=input...
('Does Combustion Duration Increase ?? [Yes/No]?? :','s');
if isempty(theta_b_Input)
    error('Please type "Yes" or "No"');
end
%
~~~~~~~~~~~~~~~~~~~~~~~~~~~~~~~~~~~~~~~~~~~~~~~~~~~~~~~~~~~~~~~~~~~~~~
~~~
% Initial Calculation
RPM_st=RPM_st1-RPM_Increment;
N_RPM=(RPM_fin-RPM_st)/RPM_Increment;
theta_st_1=theta_st_11-theta_increment;
N_theta=(theta_fin-theta_st_1)/theta_increment;
eta_combmaX=eta_combmaX1/100;
%
~~~~~~~~~~~~~~~~~~~~~~~~~~~~~~~~~~~~~~~~~~~~~~~~~~~~~~~~~~~~~~~~~~~~~~
~~~
```

```
% Preallocations
W_dot_ac(1:N_RPM,1:N_theta)=zeros;  Torque_1(1:N_RPM,1:N_theta)=zeros;
T_ac1(1:N_RPM,1:N_theta)=zeros;     eta_m(1:N_RPM,1:N_theta)=zeros;
eta_V(1:N_RPM,1:N_theta)=zeros;     BTE(1:N_RPM,1:N_theta)=zeros;
BSFC(1:N_RPM,1:N_theta)=zeros;      P(1:N_theta,1:720,1:N_RPM)=zeros;
DQ(1:N_theta,1:720,1:N_RPM)=zeros;  X(1:N_theta,1:720,1:N_RPM)=zeros;
T(1:N_theta,1:720,1:N_RPM)=zeros;   m_dot_f(1:N_RPM,1:N_theta)=zeros;
RPM_o(1:N_RPM)=zeros;               theta_b1(1:N_RPM)=zeros;
theta_b11(1:N_RPM)=zeros;           theta_b2(1:N_RPM)=zeros;
theta_b_o(1:N_RPM)=zeros;           theta_o(1:N_theta)=zeros;
theta_o_TC(1:N_theta)=zeros;
%↙
~~~~~~~~~~~~~~~~~~~~~~~~~~~~~~~~~~~~~~~~~~~~~~~~~~~~~~~~~~~~~~~~~~~~~~~↙
~~~
for zz=1:N_RPM  %%For loop if combustion duration is decreasing
    Load=Load1/100;
    MPR=(RPM_st1:RPM_Increment:RPM_fin);
    if Load==1
        theta_b1(zz)=ceil(.0038*MPR(zz)+40);
        theta_b2=flip(theta_b1);
    end
    if Load<1
        theta_b1(zz)=ceil(.0038*MPR(zz)+40)-(10-Load*10);
        theta_b2=flip(theta_b1);
    end
end
%↙
~~~~~~~~~~~~~~~~~~~~~~~~~~~~~~~~~~~~~~~~~~~~~~~~~~~~~~~~~~~~~~~~~~~~~~~↙
~~~
for nn=1:N_RPM %For loop if combustion duration is increasing
    Load=Load1/100;
    MPR=(RPM_st1:RPM_Increment:RPM_fin);
    if Load==1
        theta_b11(nn)=ceil(.0038*MPR(nn)+40);
    end
    if Load<1
        theta_b11(nn)=ceil(.0038*MPR(nn)+40)-(10-Load*10);
    end
end
%↙
~~~~~~~~~~~~~~~~~~~~~~~~~~~~~~~~~~~~~~~~~~~~~~~~~~~~~~~~~~~~~~~~~~~~~~~↙
~~~
% define the combustion duration varation
if strcmpi(theta_b_Input, 'Yes')
    theta_b_o(1)=theta_b11(1);
elseif strcmpi(theta_b_Input, 'No')
    theta_b_o(1)=theta_b2(1);
else
    error('Please type "Yes" or "No"');
end
%↙
~~~~~~~~~~~~~~~~~~~~~~~~~~~~~~~~~~~~~~~~~~~~~~~~~~~~~~~~~~~~~~~~~~~~~~~↙
```

```
~~~
% The main loop starting point
RPM=RPM_st;
RPM_o(1)=RPM;
for z=1:N_RPM % vary the engine speed
    RPM=(RPM+(RPM_Increment));
    RPM_o(z)=RPM;
    %define the combustion duration varation
    if strcmpi(theta_b_Input, 'Yes')
        theta_b=theta_b11(z);
        theta_b_o(z)=theta_b;
    elseif strcmpi(theta_b_Input, 'No')
        theta_b=theta_b2(z);
        theta_b_o(z)=theta_b;
    else
        error('Please type "Yes" as yes or "No" as no');
    end
    %Return to the initial condition for ignition timing
    theta_st=theta_st_1;
    theta_0=theta_st;
    theta_o(1)=theta_0;
    theta_o_TC(1)=theta_0-360;
    for i=1:N_theta
        theta_0=theta_0+theta_increment;
        [W_dot_ac(z,i),T_ac1(z,i),Torque_1(z,i),eta_m(z,i),eta_V(z↙
i)...
        ,BTE(z,i),BSFC(z,i),P(i,1:720,z),DQ(i,1:720,z)...
        ,X(i,1:720,z),T(i,1:720,z),m_dot_f(z,i)]=StageIVFunction...
        (RPM,theta_0,eta_combmaX,theta_b,Load);
        theta_o(i)=theta_0;
        theta_o_TC(i)=theta_0-360;
        Sim=[num2str(RPM),'[RPM],'...
            ,num2str(theta_0),'[deg],'...
            ,num2str(theta_b),'[deg]'];
        disp(Sim)
    end
end
%↙
~~~~~~~~~~~~~~~~~~~~~~~~~~~~~~~~~~~~~~~~~~~~~~~~~~~~~~~~~~~~~~~~~~~~~~~↙
~~~
% Maximum values
% For maximum values the most important parameters are Torque and Power
% which they are 2-dimentional matrix that rows are different speeds &
% columns are different ignition timing)
%↙
~~~~~~~~~~~~~~~~~~~~~~~~~~~~~~~~~~~~~~~~~~~~~~~~~~~~~~~~~~~~~~~~~~~~~~~↙
~~~
%finds the maximum over all elements of A.
[MaxNum_TorQ_OA,MaxIndex_Torq_OA]=max(Torque_1,[],'all','linear');
[MaxNum_PoWr_OA,MaxIndex_PoWr_OA]=max(W_dot_ac,[],'all','linear');
%finds the row and column of the maximum value
[MaxTorQ_row,MaxToQ_column] = find(Torque_1 == MaxNum_TorQ_OA);
```

```
[MaxPoW_row,MaxPoW_column] = find(W_dot_ac == MaxNum_PoWr_OA);
%
~~~~~~~~~~~~~~~~~~~~~~~~~~~~~~~~~~~~~~~~~~~~~~~~~~~~~~~~~~~~~~~~~~~~~~~
~~~
% Display the Optimum ignition timing and engine speed
Optimum_IG1=['The maximum brake torque value is equal to ',...
             num2str(MaxNum_TorQ_OA),' [N.m]'];
Optimum_IG2=['The optimum ignition timing have been selected at ',...
             num2str(theta_o(MaxToQ_column)),' [deg]'];
Optimum_IG3=['The selected optimum ignition timing is equivalent to
',...
             num2str(abs(theta_o(MaxToQ_column)-360)),' [deg] BTDC'];
Optimum_IG4=['The optimum speed for crank-rocker engine have been
selected at ',...
             num2str(RPM_o(MaxTorQ_row)),' [rpm]'];
disp(Optimum_IG1)
disp(Optimum_IG2)
disp(Optimum_IG3)
disp(Optimum_IG4)
%
~~~~~~~~~~~~~~~~~~~~~~~~~~~~~~~~~~~~~~~~~~~~~~~~~~~~~~~~~~~~~~~~~~~~~~~
~~~
% Plotting for a quick checking
%
~~~~~~~~~~~~~~~~~~~~~~~~~~~~~~~~~~~~~~~~~~~~~~~~~~~~~~~~~~~~~~~~~~~~~~~
~~~
% Figure(1) 3D Torque
%
~~~~~~~~~~~~~~~~~~~~~~~~~~~~~~~~~~~~~~~~~~~~~~~~~~~~~~~~~~~~~~~~~~~~~~~
~~~
Fig(1)=figure (1);
surfc(theta_o_TC,RPM_o,Torque_1)
colormap('jet');
set(gca,...
    'Ycolor','k',...
    'XMinorTick','on',...
    'YMinorTick','on',...
    'ZMinorTick','on',...
    'FontName','Times',...
    'FontSize',10,...
    'FontWeight','bold',...
    'LineWidth',1)
% set x limits
xfig1=theta_o_TC(mod(theta_o_TC,10)==0);
xticks(xfig1);
xticklabels(xfig1)
xlim([min(xfig1) max(xfig1)])
% set
set(gcf,'color','w')
grid on;
grid minor;
title('Crank-Rocker Engine Brake Torque Variation',...
```

```
    'FontSize',12)
xlabel('Crank Angle [deg]')
ylabel('Engine Speed [rpm]')
zlabel('Brake Torque, \tau [N.m]')
OPT_TorQ_3D=gcf;
%↙
~~~~~~~~~~~~~~~~~~~~~~~~~~~~~~~~~~~~~~~~~~~~~~~~~~~~~~~~~~~~~~~~~~~~~~~~↙
~~~
% Figure(2) 3D Power
%↙
~~~~~~~~~~~~~~~~~~~~~~~~~~~~~~~~~~~~~~~~~~~~~~~~~~~~~~~~~~~~~~~~~~~~~~~~↙
~~~
Fig(2)=figure (2);
surfc(theta_o_TC,RPM_o,W_dot_ac)
colormap('jet');
% set x limits
xfig2=theta_o_TC(mod(theta_o_TC,10)==0);
xticks(xfig2);
xticklabels(xfig2)
xlim([min(xfig2) max(xfig2)])
% set
set(gcf,'color','w')
grid on;
grid minor;
xlabel('Crank Angle [deg]')
ylabel('Engine Speed [rpm]')
zlabel('Brake Power [kW]')
set(gca,...
    'Ycolor','k',...
    'XMinorTick','on',...
    'YMinorTick','on',...
    'ZMinorTick','on',...
    'FontName','Times',...
    'FontSize',10,...
    'FontWeight','bold',...
    'LineWidth',1)
title('Crank-Rocker Engine Brake Power Output Variation',...
    'FontSize',12)
OPT_Pow_3D=gcf;
%↙
~~~~~~~~~~~~~~~~~~~~~~~~~~~~~~~~~~~~~~~~~~~~~~~~~~~~~~~~~~~~~~~~~~~~~~~~↙
~~~
% Figure 3 3D BSFC
%↙
~~~~~~~~~~~~~~~~~~~~~~~~~~~~~~~~~~~~~~~~~~~~~~~~~~~~~~~~~~~~~~~~~~~~~~~~↙
~~~
Fig(3)=figure (3);
surfc(theta_o_TC,RPM_o,BSFC)
colormap('jet');
% set x limits
xfig3=theta_o_TC(mod(theta_o_TC,10)==0);
xticks(xfig3);
```

```
xticklabels(xfig3)
xlim([min(xfig3) max(xfig3)])
% set
set(gcf,'color','w')
grid on;
grid minor;
xlabel('Crank Angle [deg]')
ylabel('Engine Speed [rpm]')
zlabel('Brake SFC [g / kW.h]')
set(gca,...
    'Ycolor','k',...
    'XMinorTick','on',...
    'YMinorTick','on',...
    'ZMinorTick','on',...
    'FontName','Times',...
    'FontSize',10,...
    'FontWeight','bold',...
    'LineWidth',1)
title('Crank-Rocker Engine Brake Specific Fuel Consumption
Variation',...
    'FontSize',12)
OPT_BSFC_3D=gcf;
%
~~~~~~~~~~~~~~~~~~~~~~~~~~~~~~~~~~~~~~~~~~~~~~~~~~~~~~~~~~~~~~~~~~~~~~~
~~~
% Figure 4 3D BTE
%
~~~~~~~~~~~~~~~~~~~~~~~~~~~~~~~~~~~~~~~~~~~~~~~~~~~~~~~~~~~~~~~~~~~~~~~
~~~
Fig(4)=figure (4);
surfc(theta_o_TC,RPM_o,BTE)
colormap('jet');
% set x limits
xfig4=theta_o_TC(mod(theta_o_TC,10)==0);
xticks(xfig4);
xticklabels(xfig4)
xlim([min(xfig4) max(xfig4)])
% set
set(gcf,'color','w')
grid on;
grid minor;
xlabel('Crank Angle [deg]')
ylabel('Engine Speed [rpm]')
zlabel('Brake Thermal Efficiency, \eta_{BT} [%]')
set(gca,...
    'Ycolor','k',...
    'XMinorTick','on',...
    'YMinorTick','on',...
    'ZMinorTick','on',...
    'FontName','Times',...
    'FontSize',10,...
    'FontWeight','bold',...
```

```
    'LineWidth',1)
title('Crank-Rocker Engine Brake Thermal Efficiency Variation',...
    'FontSize',12)
OPT_BTE_3D=gcf;
%↙
~~~~~~~~~~~~~~~~~~~~~~~~~~~~~~~~~~~~~~~~~~~~~~~~~~~~~~~~~~~~~~~~~~~~~~~↙
~~~
% Figure 5 3D Mechanical Efficiency
%↙
~~~~~~~~~~~~~~~~~~~~~~~~~~~~~~~~~~~~~~~~~~~~~~~~~~~~~~~~~~~~~~~~~~~~~~~↙
~~~
Fig(5)=figure (5);
surfc(theta_o_TC,RPM_o,eta_m*100)
colormap('jet');
% set x limits
xfig5=theta_o_TC(mod(theta_o_TC,10)==0);
xticks(xfig5);
xticklabels(xfig5)
xlim([min(xfig5) max(xfig5)])
% set
set(gcf,'color','w')
grid on;
grid minor;
xlabel('Crank Angle [deg]')
ylabel('Engine Speed [rpm]')
zlabel('Mechanical Efficiency, \eta_{M} [%]')
set(gca,...
    'Ycolor','k',...
    'XMinorTick','on',...
    'YMinorTick','on',...
    'ZMinorTick','on',...
    'FontName','Times',...
    'FontSize',10,...
    'FontWeight','bold',...
    'LineWidth',1)
title('Crank-Rocker Engine Mechanical Efficiency Variation',...
    'FontSize',12)
OPT_etaM_3D=gcf;
%↙
~~~~~~~~~~~~~~~~~~~~~~~~~~~~~~~~~~~~~~~~~~~~~~~~~~~~~~~~~~~~~~~~~~~~~~~↙
~~~
% Figure 6 3D Volumetric Efficiency
%↙
~~~~~~~~~~~~~~~~~~~~~~~~~~~~~~~~~~~~~~~~~~~~~~~~~~~~~~~~~~~~~~~~~~~~~~~↙
~~~
Fig(6)=figure (6);
surfc(theta_o_TC,RPM_o,eta_V*100)
colormap('jet');
% set x limits
xfig6=theta_o_TC(mod(theta_o_TC,10)==0);
xticks(xfig6);
xticklabels(xfig6)
```

```
xlim([min(xfig6) max(xfig6)])
% set
set(gcf,'color','w')
grid on;
grid minor;
xlabel('Crank Angle [deg]')
ylabel('Engine Speed [rpm]')
zlabel('Volumetric Efficiency, \eta_{V} [%]')
set(gca,...
    'Ycolor','k',...
    'XMinorTick','on',...
    'YMinorTick','on',...
    'ZMinorTick','on',...
    'FontName','Times',...
    'FontSize',10,...
    'FontWeight','bold',...
    'LineWidth',1)
title('Crank-Rocker Engine Volumetric Efficiency Variation',...
    'FontSize',12)
OPT_etaV_3D=gcf;
%↙
~~~~~~~~~~~~~~~~~~~~~~~~~~~~~~~~~~~~~~~~~~~~~~~~~~~~~~~~~~~~~~~~~~~~~~~~↙
~~~
% Figure 7 contour Torque
%↙
~~~~~~~~~~~~~~~~~~~~~~~~~~~~~~~~~~~~~~~~~~~~~~~~~~~~~~~~~~~~~~~~~~~~~~~~↙
~~~
Fig(7)=figure (7);
set(gcf,'color','w')
contourf(theta_o_TC,RPM_o,Torque_1,45)
colormap('jet');
% set x limits
xfig7=theta_o_TC(mod(theta_o_TC,10)==0);
xticks(xfig7);
xticklabels(xfig7)
xlim([min(xfig7) max(xfig7)])
grid on;
grid minor;
xlabel('Crank Angle [deg]')
ylabel('Engine Speed [rpm]')
set(gca,...
    'Ycolor','k',...
    'XMinorTick','on',...
    'YMinorTick','on',...
    'FontName','Times',...
    'FontSize',10,...
    'FontWeight','bold',...
    'LineWidth',1)
title('Crank-Rocker Engine Torque Variation',...
    'FontSize',12)
OPT_TorQ_contour=gcf;
%↙
```

```
~~~~~~~~~~~~~~~~~~~~~~~~~~~~~~~~~~~~~~~~~~~~~~~~~~~~~~~~~~~~~~~~~~~~~~~~↙
~~~
% Figure(8) Brake Torque & Brake Power
%↙
~~~~~~~~~~~~~~~~~~~~~~~~~~~~~~~~~~~~~~~~~~~~~~~~~~~~~~~~~~~~~~~~~~~~~~~~↙
~~~
Fig(8)=figure (8);
set(gcf,'color','w')
%your data
X_fig8 = RPM_o;
Y1_fig8 = (Torque_1(:,MaxToQ_column))';
Y2_fig8 = (W_dot_ac(:,MaxToQ_column))';
%set X limitis
xfig8=RPM_o(mod(RPM_o,1000)==0);
xlim([min(xfig8) max(xfig8)])
%Set x label
xlabel('Engine Speed [rpm]',...
    'FontSize',11)
%set yaxis left
yyaxis left
fig8_1=plot(X_fig8,Y1_fig8,...
    'LineWidth',1.25);
ylabel('Brake Torque, \tau [N.m]',...
    'FontSize',11)
set(gca,...
    'Ycolor','k',...
    'XMinorTick','on',...
    'YMinorTick','on',...
    'ZMinorTick','on',...
    'FontName','Times',...
    'FontWeight','bold',...
    'LineWidth',1)
%set yaxis right
yyaxis right
fig8_2=plot(X_fig8,Y2_fig8,...
    'LineWidth',1.25);
ylabel('Brake Power [kW]',...
    'FontSize',11)
grid on;
grid minor;
set(gca,...
    'Ycolor','k',...
    'XMinorTick','on',...
    'YMinorTick','on',...
    'ZMinorTick','on',...
    'FontName','Times',...
    'FontWeight','bold',...
    'LineWidth',1)
legend([fig8_1,fig8_2],...
    {'Brake Torque','Brake Power'},'Location','northwest');
title({'Brake Torque Vs. Brake Power',...
    '(@ Optimum Ignition Timing)'},...
```

```
    'FontSize',12)
OPT_BTBP_2D=gcf;
%↙
~~~~~~~~~~~~~~~~~~~~~~~~~~~~~~~~~~~~~~~~~~~~~~~~~~~~~~~~~~~~~~~~~~~~~~~~~↙
~~~
% Figure 9 BSFC & Brake thermal Efficiency
%↙
~~~~~~~~~~~~~~~~~~~~~~~~~~~~~~~~~~~~~~~~~~~~~~~~~~~~~~~~~~~~~~~~~~~~~~~~~↙
~~~
Fig(9)=figure (9);
set(gcf,'color','w')
%your data
X_fig9 = RPM_o;
Y1_fig9 = (BTE(:,MaxToQ_column))';
Y2_fig9 = (BSFC(:,MaxToQ_column))';
%set X limitis
xfig9=RPM_o(mod(RPM_o,1000)==0);
xlim([min(xfig9) max(xfig9)])
%Set x label
xlabel('Engine Speed [rpm]',...
    'FontSize',11)
%set yaxis left
yyaxis left
fig9_1=plot(X_fig9,Y1_fig9,...
    'LineWidth',1.25);
ylabel('Brake Thermal Efficiency, \eta_{BT} [%]',...
    'FontSize',11)
set(gca,...
    'Ycolor','k',...
    'XMinorTick','on',...
    'YMinorTick','on',...
    'ZMinorTick','on',...
    'FontName','Times',...
    'FontWeight','bold',...
    'LineWidth',1)
%set yaxis right
yyaxis right
fig9_2=plot(X_fig9,Y2_fig9,...
    'LineWidth',1.25);
ylabel('Brake Specific Fuel Consumption [g / kW.h]',...
    'FontSize',11)
grid on;
grid minor;
set(gca,...
    'Ycolor','k',...
    'XMinorTick','on',...
    'YMinorTick','on',...
    'ZMinorTick','on',...
    'FontName','Times',...
    'FontWeight','bold',...
    'LineWidth',1)
legend([fig9_1,fig9_2],...
```

```
    {'Brake Thermal Efficiency','Brake SFC'},'Location','northwest');
title({'Brake Thermal Efficiency Vs. Brake Specific Fuel
Consumption',...
    '(@ Optimum Ignition Timing)'},...
    'FontSize',12)
OPT_BSFCBTE_2D=gcf;
%
~~~~~~~~~~~~~~~~~~~~~~~~~~~~~~~~~~~~~~~~~~~~~~~~~~~~~~~~~~~~~~~~~~~~~~~
~~~
% Plotting Combustion parameters
% based on the optimum speed and optimum ignition
%
~~~~~~~~~~~~~~~~~~~~~~~~~~~~~~~~~~~~~~~~~~~~~~~~~~~~~~~~~~~~~~~~~~~~~~~
~~~
% Figure 10
%
~~~~~~~~~~~~~~~~~~~~~~~~~~~~~~~~~~~~~~~~~~~~~~~~~~~~~~~~~~~~~~~~~~~~~~~
~~~
Fig(10)=figure(10);
set(gcf,'color','w')
%Plotting data
X_fig10=(1:720);
Y_fig10_s1=(P(MaxToQ_column,1:720,MaxTorQ_row)/10^5);
Y_fig10_s2=(DQ(MaxToQ_column,1:720,MaxTorQ_row)/1000);
Y_fig10_s3=(X(MaxToQ_column,1:720,MaxTorQ_row)*100);
Y_fig10_s4=(T(MaxToQ_column,1:720,MaxTorQ_row));
%
~~~~~~~~~~~~~~~~~~~~~~~~~~~~~~~~~~~~~~~~~~~~~~~~~~~~~~~~~~~~~~~~~~~~~~~
~~~
%subplot one : HRR
subplot(2,2,1);
plot(X_fig10,Y_fig10_s1,'b',...
    'LineWidth',1.25);
title('  (a) Pressure')
%set X & Y limitis
xlim([250 500])
%set GCA
grid on;
grid minor;
set(gca,...
    'Ycolor','k',...
    'XMinorTick','on',...
    'YMinorTick','on',...
    'ZMinorTick','on',...
    'FontName','Times',...
    'FontWeight','bold',...
    'LineWidth',1)
%Set labels
xlabel('Crank Angle [deg]')
ylabel('Pressure [bar]')
%
~~~~~~~~~~~~~~~~~~~~~~~~~~~~~~~~~~~~~~~~~~~~~~~~~~~~~~~~~~~~~~~~~~~~~~~
```

```
~~~
%subplot two : MFB
subplot(2,2,2);
plot(X_fig10,Y_fig10_s2,'r',...
    'LineWidth',1.25);
title('(b) Heat Release Rate ')
%set X & Y limitis
xlim([302 436])
%ylim([-1/1000 16/1000])
%set GCA
grid on;
grid minor;
set(gca,...
    'Ycolor','k',...
    'XMinorTick','on',...
    'YMinorTick','on',...
    'ZMinorTick','on',...
    'FontName','Times',...
    'FontWeight','bold',...
    'LineWidth',1)
%Set labels
xlabel('Crank Angle [deg]')
ylabel('HRR [kj/CA]')
%↙
~~~~~~~~~~~~~~~~~~~~~~~~~~~~~~~~~~~~~~~~~~~~~~~~~~~~~~~~~~~~~~~~~~~~~~~↙
~~~
%subplot three temperature
subplot(2,2,3);
plot(X_fig10,Y_fig10_s3,'k',...
    'LineWidth',1.25);
title('(c) Mass Fraction Burn')
%set X limitis
xlim([320 410])
% ylim([-0.05 1.05])
%set GCA
grid on;
grid minor;
set(gca,...
    'Ycolor','k',...
    'XMinorTick','on',...
    'YMinorTick','on',...
    'ZMinorTick','on',...
    'FontName','Times',...
    'FontWeight','bold',...
    'LineWidth',1)
%Set labels
xlabel('Crank Angle [deg]')
ylabel('MFB [%]')
%↙
~~~~~~~~~~~~~~~~~~~~~~~~~~~~~~~~~~~~~~~~~~~~~~~~~~~~~~~~~~~~~~~~~~~~~~~↙
~~~
%subplot four Pressure
```

```
subplot(2,2,4);
plot(X_fig10,Y_fig10_s4,'g',...
    'LineWidth',1.25);
title('(d) Temperature')
%set X limitis
xlim([250 500])
%set GCA
grid on;
grid minor;
set(gca,...
    'Ycolor','k',...
    'XMinorTick','on',...
    'YMinorTick','on',...
    'ZMinorTick','on',...
    'FontName','Times',...
    'FontWeight','bold',...
    'LineWidth',1)
%Set labels
xlabel('Crank Angle [deg]')
ylabel('Temperature [K]')
OPT_COMBUSTION_4f=gcf;
%↙
~~~~~~~~~~~~~~~~~~~~~~~~~~~~~~~~~~~~~~~~~~~~~~~~~~~~~~~~~~~~~~~~~~~~~~~↙
~~~
% Save the figures from plotting section
%↙
~~~~~~~~~~~~~~~~~~~~~~~~~~~~~~~~~~~~~~~~~~~~~~~~~~~~~~~~~~~~~~~~~~~~~~~↙
~~~
 SaveFig_Option=input...
         ('Would you like to save the figures [Yes/No]?? :¦,'s');
if strcmpi(SaveFig_Option,'Yes')
 param2=Load1;
 param3=eta_combmaX1;
 if strcmpi(theta_b_Input, 'Yes') %according to the optimization
     param1=3; %optimization 3 if combustion duration is increased
 elseif strcmpi(theta_b_Input, 'No')
     param1=2; %optimization 2 if combustion duration is decreased
 end
 filename=sprintf('FiguresFile_Optimization[%d]_Load[%d]_Eff[%d].↙
fig',...
                 param1, param2, param3);
 savefig(Fig,filename);
end
%↙
~~~~~~~~~~~~~~~~~~~~~~~~~~~~~~~~~~~~~~~~~~~~~~~~~~~~~~~~~~~~~~~~~~~~~~~↙
~~~
% Save the workspace and data based on the given input
%↙
~~~~~~~~~~~~~~~~~~~~~~~~~~~~~~~~~~~~~~~~~~~~~~~~~~~~~~~~~~~~~~~~~~~~~~~↙
~~~
Save_Option=input...
    ('Would you like to save the Data (.mat)format?[Yes/No]?? :¦,'s');
```

```
if strcmpi(Save_Option,'Yes')
    param2=Load1;
    param3=eta_combmaX1;
    if strcmpi(theta_b_Input, 'Yes') %according to the optimization
        param1=3; %optimization 3 if combustion duration is increased
    elseif strcmpi(theta_b_Input, 'No')
        param1=2; %optimization 2 if combustion duration is decreased
    end
    filename1=sprintf('Optimization[%d]_Load[%d]_Eff[%d].mat',...
        param1, param2, param3);
    save(filename1)
end
```

APPENDIX E

NUMERICAL MODELS DESCRIPTION

E.1 Overview

Internal combustion engine modeling has been a continuing effort over the years, and many models have been developed to predict engine performance parameters. Computer models of engine processes are valuable tools for analysis and optimization of engine performance and allow exploration of many engine alternative designs in an inexpensive way. These models allow researchers to vary and investigate numerous parameters to predict engine performances under different operating conditions. The accuracy of any model depends on its structure, availability of the information, and the assumptions made.Based on the past literatures, there are several techniques and models to adopt for CR engine modeling. These models are either being implemented or investigated for their suitability for the CR engine modeling. The purpose of this chapter is to provide a numerical description and governing equations of the models that are not covered in the literature review.

This chapter covers the CR engine geometry (section E.2) including the calculation of kinematic and positioning (E.2.1), stroke length (E.2.2), piston displacement (E.2.3), and CR engine volume (E.2.4). In section E.3.4, the main components of the CR engine heat release model is provided that includes assumptions (E.3.5), calculations of In-cylinder pressure (E.3.7), and mass fraction burn profile (E.3.8). Other components are described in a separate sections, for instance, section E.4 described the heat transfer modeling, and the specific heat ratio modeling can be found in section E.6. It should be noted that the numerical method used to solve the differential equations in this study is based on backward Euler method known as implicit Euler method.

E.2 The CR Engine Geometry Description

This section presents the theoretical formula for mechanism and kinematic properties. The CR engine geometry calculation focuses on the kinetic calculation by analyzing the positioning of the links, stroke length, piston displacement, and volume calculation. In terms, of transmission angle calculation and other important parameters please refer to the given references.

E.2.1 Kinematic and Positioning Calculation

Figure E.1 shows a CR mechanism with its links and joints. To obtain an analytical solution for the position prediction in terms of kinetic calculation, a new parameter is introduced and the cosine law has been utilized. The internal angles of γ, α, β, θ_3 and θ can be estimated using the following set of equations at a particular crank position θ_2 for given link dimensions of L_1, L_2, L_3, and L_4 [22].

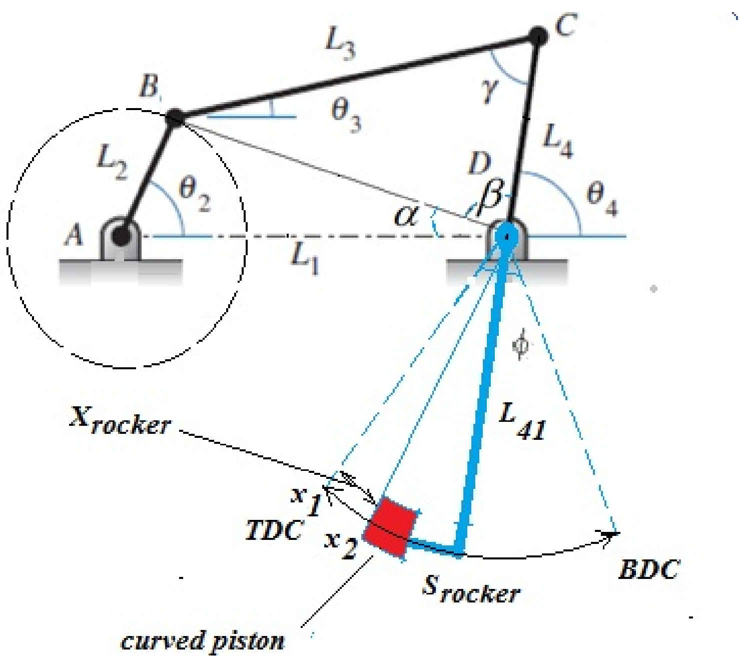

Figure E.1: Crank-Rocker Engine Mechanism [22].

$$BD = \sqrt{L_1^2 + L_2^2 - 2L_1L_2\cos\theta_2} \tag{E.1}$$

$$\gamma = \cos^{-1}\left(\frac{L_3^2 + L_4^2 - {L_1}^2 - {L_2}^2 + 2L_1L_2\cos\left(\theta_2\right)}{2L_3L_4}\right) \tag{E.2}$$

$$\alpha = \cos^{-1}\left(\frac{\left(L_1 - L_2\cos\left(\theta_2\right)\right)}{\left({L_1}^2 + {L_2}^2 - 2L_1L_2\cos\left(\theta_2\right)\right)^{0.5}}\right) \tag{E.3}$$

$$\beta = \cos^{-1}\left(\frac{L_3^2 - L_4^2 + {L_1}^2 + {L_2}^2 - 2L_1L_2\cos\left(\theta_2\right)}{2L_4\left({L_1}^2 + {L_2}^2 - 2L_1L_2\cos\left(\theta_2\right)\right)^{0.5}}\right) \tag{E.4}$$

$$\theta_4 = 180 - \alpha - \beta \tag{E.5}$$

If $\theta_2 > 180$ then:

$$\theta_4 = 180 + \alpha - \beta \tag{E.6}$$

$$\theta_3 = \tan^{-1}\left(\frac{L_4\sin\left(\theta_4\right) - L_2\sin\left(\theta_2\right)}{L_1 + L_4\cos\left(\theta_4\right) - L_2\cos\left(\theta_2\right)}\right) \tag{E.7}$$

The oscillating angle between the top and bottom-dead-center position of the extended rocker arm is known as the swing angle; it is denoted by ϕ and measured in radian [22].

E.2.2 Stroke Length Calculation

Unlike the conventional engines, the stroke of the CR engine does not depend on the crankshaft radius; The length of the stroke can be altered without changing the crank radius. The stroke length of the CR engine, S_{rocker} can be obtained through the length of the extended rocker arm L_{41}, the crank length L_2, and the rocker length L_4 [22].

$$S_{\text{rocker}} = L_{41}\frac{\pi}{180}\left(2\sin^{-1}\left(\frac{L_2}{L_4}\right)\right) \tag{E.8}$$

E.2.3 Piston Displacement Calculation

The piston displacement for the slider-crank and crank-rocker engines differs in the motions. In the CR engine moves in curve linear motion, unlike the slider-crank that moves in translational motion. As illustrated in Figure E.1, the piston has an arcuate motion from point x_1 to point x_2 at a certain crank angle θ_2. Therefore, the piston displacement is a function of the crank angle and denoted by x_{rocker} and calculated as follows [22]:

$$x_{\text{rocker}} = L_{41}\frac{\pi}{180}\left(180 - \partial\alpha - \partial\beta - \partial\theta_4\right) \tag{E.9}$$

E.2.4 Engine Volume Calculation

According to Figure E.2, the CR cylinder has a geometry of a torus; and since the piston moves forward and backward in an arc path within its extreme positions (TDC and BDC), the curve-cylinder volume changes with respect to the crank angle. The following equation can be used to calculate the volume [22].

$$V(\theta) = V_C + \left(\pi r^2\right)\left(\frac{\pi \emptyset R}{180}\right) \tag{E.10}$$

where,

V = the curved-cylinder volume

V_C = the clearance volume

r = small circle radius (mm)

R = big circle radius

θ = the crank angle (in degree)

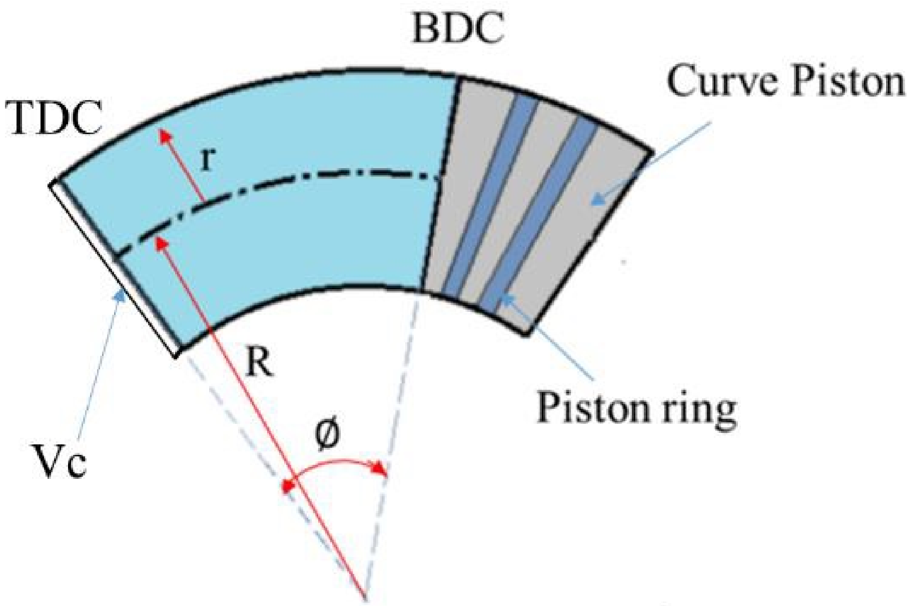

Figure E.2: The torus geometry of the crank-rocker cylinder [22].

E.3 The Heat Release Model Basis and Their Assumptions

The fundamental principle of the majority of the heat-release models has been obtained through utilizing the first law of thermodynamics. In an open cycle system, the energy conservation equation can be expressed as:

$$dU = dQ - dW + \sum_i h_i \, dm_i \tag{E.11}$$

Where the internal energy variation of the mass in the system is denoted by dU, the transported heat to the system is dQ, dW is the produced amount of work by the system, $\sum_i h_i \, dm_i$ is the enthalpy flux across the system boundary. dm_i and h_i are mass flow and the mass specific enthalpy of flow i respectively. The mass specific enthalpy is evaluated based on the given conditions at the zone where the mass element leaves.

There are several possible mass flows within the system (mass in and out); for instance, throughout the valves, the crevice regions, the piston ring blow-by, and the direct injection of the fuel into the combustion chamber. It should be noted that any mass flow entering the system is considered a positive value.

As mentioned earlier, the main focus of this research is single-zone models. Thus, by considering the system to be an open system and a single-zone model, the most frequent assumptions that could be stated are:

1. The gas mixture is an ideal-gas.
2. The combustion is modeled as the release of heat.
3. The heat released due to the combustion occurs uniformly and also the cylinder contents and the state is uniform throughout the entire chamber.
4. The cylinder head, wall, and piston crown of the combustion chamber act as a boundary.

With regard to equation (E.11), the heat variation of the system dQ consists of the heat addition and removal process due to the released chemical energy from the fuel $dQ_{ch,fuel}$, and heat transfer through the cylinder walls dQ_{ht}, respectively. The transported heat is stated as:

$$Q = Q_{ch,fuel} - Q_{ht} \tag{E.12}$$

Now considering the work done by the system is a positive process and produced by the fluid on the piston W_p; thus, $dW = dW_p = pdV$. Therefore, equation (E.11) could be represented as:

$$dQ_{ch,fuel} = dU_s + dW_p - \sum_i h_i dm_i + dQ_{ht} \tag{E.13}$$

Where dU_s is the sensible energy changes for an ideal gas that behaves only as a function of mean charge temperature. Thus, $U_s = m_c u(T)$ which its differentiated form expressed as:

$$dU_s = m_c c_v(T)dT + u(T)dm_c \tag{E.14}$$

By utilizing the ideal gas law, the mean temperature and its differentiated form could often be found as equations (E.15) and (E.16), respectively.

$$T = \frac{pV}{m_c R} \tag{E.15}$$

$$dT = \frac{1}{m_c R} \left(V dp + p dV - RT dm_c \right) \tag{E.16}$$

The mass of charge and mass specific heat at constant volume are denoted by m_c and c_v, respectively. The value of R is assumed to be constant; equation (E.13) is rewritten using equations (E.14) and (E.16).

$$dQ_{ch,f} = \frac{c_v}{R} V dp + \frac{c_v + R}{R} p dV + (u - c_v T)\, dm_c - \sum_i h_i dm_i + dQ_{ht} \tag{E.17}$$

Hence, assuming the gas mixture is an ideal gas, the mass-specific gas constant R can be defined as $R = c_p - c_v$ and specific heat ratio as $\gamma = \frac{c_p}{c_v}$. Therefore, the mass-specific heat at constant volume is specified as:

$$c_v = \frac{R}{\gamma - 1} \tag{E.18}$$

Inserting equation (E.18) into equation (E.17) results in:

$$dQ_{ch,f} = \frac{1}{\gamma - 1} V dp + \frac{\gamma}{\gamma - 1} p dV + \left(u - \frac{RT}{\gamma - 1} \right) dm_c - \sum_i h_i dm_i \tag{E.19}$$

From the above equation, different models have been derived, and each has its complexity such as Rassweiler and Withrow [82], Krieger and Borman [83], and Gatowski et al. [84] models.

E.3.1 Rassweiler - Withrow Model

The developed model is considered to be one of the simplest and computationally efficient models for MFB calculation (denoted by $x_b(\theta)$) by normalizing the burned mass $m_b(\theta)$ using the total charge mass m_c.

$$x_b(\theta) = \frac{m_b(\theta)}{m_c} \tag{E.20}$$

$$pV^n = \text{ constant} \tag{E.21}$$

In the above polytropic relation, the pressure and volume are represented by their first letter, while the variable n is a polytropic index. Theoretically, equation (E.21) can be developed based on the first thermodynamics law equation in the previous subsection (see sub-section E.3, equation (E.19)). However, few assumptions are required to be made.

First of all, the crevices effects and crank-case leakages (known as blow-by) are assumed as negligible parameters (i.e. $dm_c = dm_i = 0$). Second, no explicit account should be considered for heat transfer $(dQ_{ht} = 0)$. Third, the specific heat ratio parameter (denoted by $\gamma(T)$) is a temperature-dependent value, and it should be assumed as a constant value. This value is captured by the polytropic index $(\gamma(T) = n)$. Lastly, based on the previous assumption, there would not be any chemical energy release during compression, combustion, and expansion strokes; therefore, $dQ = 0$. Thus, these assumptions yield the following equation:

$$dp = -\frac{np}{V}dV \tag{E.22}$$

Equation (E.22) could be rewritten as equation (E.23) by considering $dQ = dQ_{ch} \neq 0$.

$$dp = -\frac{n-1}{V}dQ - \frac{np}{V}dV = dp_c + dp_v \tag{E.23}$$

- dp_c = The pressure change (due to the combustion)
- dp_v = The pressure change (due to the volume changes)

Rassweiler and Withrow [82], stated that the pressure variation is a result of the rise in combustion and volumetric pressure, which can be illustrated below:

$$\Delta P = \Delta P_c + \Delta P_v \tag{E.24}$$

E.3.2 Krieger – Borman Model

This approach takes neither crevice nor heat transfer into account. Thus, the equation (E.19) can be expressed as:

$$\frac{dQ}{dt} = \frac{\gamma}{\gamma - 1}p\frac{dV}{dt} + \frac{1}{\gamma - 1}V\frac{dp}{dt} \tag{E.25}$$

By considering the crank angle (θ) and replacing time with it, equation (E.25) can be rewritten as:

$$\frac{dQ}{d\theta} = \frac{\gamma}{\gamma - 1}p\frac{dV}{d\theta} + \frac{1}{\gamma - 1}V\frac{dp}{d\theta} \tag{E.26}$$

E.3.3 Gatowski et al. Model

In terms of heat release models, there is a more complex model that has been developed by Gatowski et al. [84]. This model incorporates various subsidiary models, including heat transfer, crevices effects, and specific heat ratios, into the equation (E.19).

E.3.4 The CR Engine Heat Release Model Main Components

In this section, a single-zone model is developed to form the basis of the heat release model based on the developed model by Krieger and Borman [83], known as Apparent heat release. However, due to the importance of heat transfer in the system mentioned by Gatowskie [84] and Klein [77], the heat transfer model has been included in the modified CR engine model. However, the numerical description of heat transfer and specific heat ratio models are covered separately. Section E.3.4 mainly focuses on the model assumptions, in-cylinder pressure prediction, and the mass fraction burn profile.

E.3.5 Heat Release Model Assumptions

In order to simplify the single-zone model, some assumptions have been made as follows:

- The gases mixture in the system is considered an ideal gas.
- The cylinder contents are assumed uniform that applies throughout the cylinder.
- To simulate the combustion process of the engine, the process is considered as a release of heat.
- The released heat during the combustion is assumed to be uniform.
- The separation between the unburned and burned zones is assumed to be an extremely thin boundary without any heat transfer within the zones.

E.3.6 Zero-dimensional CR Model

The most common approach in modeling an engine is to treat the cylinder contents as a single zone that views the burned and unburned gases, residual gases, as a single ideal gas with uniform pressure through the cylinder. The basis of the single-zone CR engine model is formed using energy conservation first law of thermodynamics and the ideal gas law defined as:

$$PV = mRT \tag{E.27}$$

The instantaneous parameters such as P,V, and T can be obtained relative to the crank angle of the engine by using the differential form of the above equation with respect to $d\theta$.

$$\frac{dP}{d\theta}V + P\left(\frac{dV}{d\theta}\right) = mR\left(\frac{dT}{d\theta}\right) \tag{E.28}$$

and upon rearranging in order to solve for dP equation (E.29) is obtained:

$$\frac{dP}{d\theta} = \left(-\frac{P}{V}\right)\left(\frac{dV}{d\theta}\right) + \left(\frac{P}{T}\right)\left(\frac{dT}{d\theta}\right) \tag{E.29}$$

The same approach can be applied to the first law of thermodynamics and expressed as follows:

$$\Delta U = Q - W \tag{E.30}$$

and,

$$\frac{dU}{d\theta} = \frac{dQ}{d\theta} - \frac{dW}{d\theta} = mc_v\left(\frac{dT}{d\theta}\right) \tag{E.31}$$

where the total change in internal energy of the system is denoted by ΔU, Q is total energy transferred into the system, while W is the work done by the system. The formation of the work can be described as:

$$\frac{dW}{d\theta} = P\left(\frac{dV}{d\theta}\right) \tag{E.32}$$

The instantaneous change in the temperature can be defined by substituting equation (E.32) and (E.33) into equation (E.31) and expressed as equation (E.34) [25]:

$$\frac{c_v}{R} = \frac{c_v}{c_p - c_v} = \frac{1}{\gamma - 1} \tag{E.33}$$

$$\frac{dT}{d\theta} = \mathrm{T}(\gamma - 1)\left[\left(\frac{1}{PV}\right)\left(\frac{dQ}{d\theta}\right) - \left(\frac{1}{V}\right)\left(\frac{dV}{d\theta}\right)\right] \tag{E.34}$$

The heat input $\frac{dQ}{d\theta}$, into the system, can be defined by [73]:

$$\frac{dQ}{d\theta} = Q_{\text{in}}\left(\frac{dX_b}{d\theta}\right) - \left(\frac{dQ_w}{d\theta}\right) \tag{E.35}$$

Where the heat input is denoted by Q_{in}, x_b is the mass fraction burned, and Q_w is the heat loss rate to the cylinder wall. The heat input known as the generated heat by the combustion of an engine can be stated as the following equation [22]:

$$Q_{\text{in}} = \eta_c LHV \left(\frac{1}{AF_{ac}}\right)\left(\frac{P}{R_{gc}T}\right) V_d \tag{E.36}$$

where,

$\eta_c =$ The combustion efficiency

$LHV =$ The lower heating value

$AF_{ac} =$ The actual air to fuel ratio

$R_{gc} =$ The gas constant

$\mathrm{T} =$ The mean gas temperature

$V_d =$ displaced cylinder volume

E.3.7 In-cylinder Pressure Calculation

The differential form of the cylinder pressure as a function of crank angle is obtained using the first law of thermodynamics, and upon substituting (E.30), the in-cylinder pressure can be defined as [22]:

$$\frac{dP}{d\theta} = \left(-\frac{\gamma P}{V}\right)\left(\frac{dV}{d\theta}\right) + \left(\frac{\gamma - 1}{V}\right)\left(\frac{dQ}{d\theta}\right) \tag{E.37}$$

where P is the pressure of the cylinder, γ is the specific heat ratio, V is the volume of the cylinder, and $\dfrac{dQ}{d\theta}$ defined in equation (E.35). After substituting, equation (E.37) can be rewritten as:

$$\frac{dP}{d\theta} = \left(-\frac{\gamma P}{V}\right)\left(\frac{dV}{d\theta}\right) + \left(\frac{\gamma - 1}{V}\right) Q_{\text{in}} \left(\frac{dX_b}{d\theta}\right) - \left(\frac{\gamma - 1}{V}\right)\left(\frac{dQ_w}{d\theta}\right) \tag{E.38}$$

E.3.8 The Combustion Calculation

In order to represent the chemical energy released as a function of the crank angle in single-zone models, the Wiebe function has been selected. The Wiebe function, often used by the researcher to estimate the fuel fraction burning rate [22]. The Wiebe function expressed as [22]:

$$X_b(\theta) = 1 - \exp\left[-a\left(\frac{\theta - \theta_s}{\theta_d}\right)^n\right] \tag{E.39}$$

where,X_b $=$ Mass fraction burn, θ $=$ Crank angle, θ_s $=$ Spark timing (start of energy release), θ_d $=$ Duration of combustion (duration of energy release), a $=$ Weibe efficiency factor, and n $=$ Wiebe form factor. The differentiated form of Wiebe function is stated as [22]:

$$\frac{dX_b(\theta)}{d\theta} = \frac{a(n)}{\theta_d}\left(\frac{\theta - \theta_s}{\theta_d}\right)^{n-1} \exp\left[-a\left(\frac{\theta - \theta_s}{\theta_d}\right)^n\right] \tag{E.40}$$

E.4 Heat Transfer Model

Based on the discussion provided in literature review, Heat transfer analysis are highly required to increase the accuracy of the model. As described in section 2.8, there are various correlations that have been developed to model the instantaneous heat transfer coefficient. In this study, there are four correlations developed by Woschni, Hohenburg, Sitkei, and Annand are adopted to be used in the heat release model for CR engine. However, due to uncertainty of accuracy of each in case of CR engine, it was decided to conduct a comparative study to evaluate each correlation separately.

There are many approaches to utilize heat transfer calculation. It is said that heat transfer analysis is a complicated process with the complexity to appraise. There are two main reasons for this. Firstly, the conditions of heat transfer between gasses and the cylinder walls are non-uniformly as well as unsteady. The second reason is due to considering the type of results that are expected. However, the most commonly used formulation is the Newton relation in zero-dimensional models [68].

$$\dot{Q} = h_g A \left(T_g - T_w\right) \tag{E.41}$$

In the above equation, the convective heat transfer coefficient is represented by h_g, the exposed surface area is denoted by A, and the gas and cylinder wall temperatures are represented by T_g and T_w, respectively. Among these parameters, the heat transfer coefficient represents a precise observation and accurate evaluation of the losses during an engine cycle.

E.4.1 Woschni's Correlation Model

In the following equation (E.42), Woschni's correlation is illustrated [92].

$$h_g = C_0 B^{-0.2} \times P^{0.8} \times w^{0.8} \times T^{-0.53} \tag{E.42}$$

Where the cylinder bore is denoted by B, the instantaneous pressure and temperature of the cylinder are denoted by their first letter (P and T) respectively, and w the burned gas speed (the average gas velocity). A constant variable is visible in the equation, and it is denoted by C_0. The value of this constant varies from 110 to 130.

The gas velocity can be expressed as below equation:

$$w(\theta) = C_1 \bar{U}_p + C_2 \frac{V_d T_r}{p_r V_r} \left(p(\theta) - p_m\right) \tag{E.43}$$

In the above equation, mean piston velocity is shown by $\bar{U}_p$; the reference volume, pressure, and temperature are denoted by V_r, p_r, and T_r, respectively. In terms of reference, it can be considered at the initial stage of combustion or the inlet valve closing (IVC). There are two constants denoted by C_1 and C_2 that their values differ at various phases (please refer to Table E.1). With regard to the motored cylinder pressure p_m, it is modeled as a polytropic process. As suggested [69], this process takes place during compression and expansion strokes.

The motored cylinder pressure is represented as below:

$$p_m = p_r \left(\frac{V_r}{V}\right)^n \tag{E.44}$$

Table E.1: Woschni C_1 and C_2 value [92]

Phases	C_1	$C_2 \left[\frac{m}{sK}\right]$
Intake	6.18	0
Compression	2.28	0
Combustion	2.28	3.24E-03
Expansion	2.28	3.24E-03
Exhaust	6.18	0

E.4.2 Hohenberg's Correlation Model

The numerical description of this correlation has been individually described in section (2.8.2)

E.4.3 Sitkei's Correlation Model

The numerical description of this correlation has been individually described in section (2.8.3)

E.4.4 Annand's Correlation Model

The numerical description of this correlation has been individually described in section (2.8.4)

E.5 Air-Fuel Ratio (AFR) Determination

In general, the air-fuel ratio (AFR) can be measured using the obtained reading of the lambda (λ), the balanced equation, and the stoichiometric reaction between air and fuel. The balanced stoichiometric reaction for hydrocarbons fuel is presented as follows [12]:

$$C_xH_y + a\,(O_2 - 3.76N_2) \rightarrow xCO_2 + \left(\frac{y}{2}\right) H_2O + a\,(3.76N_2) \tag{E.45}$$

In the equation (E.45), the number of carbon and hydrogen atoms in the fuel are denoted by x and y, respectively. To balance the equation, the constant a is dedicated. For instance, the balanced stoichiometric reaction of octane ($\mathrm{C_8H_{18}}$) fuel is defined as:

$$C_8H_{18} + \left(\frac{25}{2}\right)(O_2 - 3.76N_2) \rightarrow 8CO_2 + 9H_2O + \left(\frac{25}{2}\right)(3.76N_2) \tag{E.46}$$

The stoichiometric air-fuel ratio can be found by substituting the values of x, y, and a (see equation E.47) [12]. At last, the actual ratio of air-fuel can be calculated according to the equation (E.48).

$$AF_{\text{stoich}} = \frac{4.76(a)}{1}\left(\frac{\text{Molecular Weight}_{\text{air}}}{\text{Molecular Weight}_{\text{fuel}}}\right) \tag{E.47}$$

$$AF_{\text{actual}} = \lambda AF_{\text{stoich}} \tag{E.48}$$

E.6 Specific Heat Ratio Model

The specific heat ratios are highly desired for modeling an ICE. This is due to the large temperature gradient in them. This particular parameter has been described in the literature section completely. According to the section 2.7, numerous specific heat ratio models have been developed over the years with different complexity. According to [25], the accuracy of these models are highly dependent on the complexity of the corresponding computation. Moreover, the consideration of including such models in the heat release model is highly recommended due to their influence and improvement on the accuracy of simulations. Under such circumstances, it was decided to include the specific heat ratio model in this study to modify the combustion modeling and increase its prediction.

E.6.1 Linear Model by Gatowskie et al.

In Gatowskie et al. [84], the ratio of specific heat (γ) is modeled as a linear function of temperature as shown below.

$$\gamma_{lin}(T) = \gamma_{300} + b(T - 300) \tag{E.49}$$

In equation (E.49), the value of the slope (denoted by b) and γ_{300} have to be adjusted based on the temperature region and the used air-fuel ratio.

E.6.2 Chun and Heywood Model

The following assumptions for gamma have been made by Chun and Heywood [80]; to further expand the accuracy of the heat release models prediction.

- During the compression segment, γ is considered as a linear function of temperature.
- During the combustion segment, γ is considered as a constant value.
- During the post-combustion segment, γ is also considered as a linear function of temperature.

Based on the above assumptions the gamma (γ) model is presented as follow:

$$\gamma_{seg}\left(T, x_b\right) = \begin{cases} \gamma_{300}^{comp} + b^{\text{comp}}\left(T - 300\right) & x_b < 0.01 \\ \gamma_{300}^{\text{comb}} & 0.01 \leq x_b \leq 0.99 \\ \gamma_{300}^{exp} + b^{exp}(T - 300) & x_b > 0.99 \end{cases} \tag{E.50}$$

E.6.3 Krieger and Borman Model

There is a particular equation set that can be presented for those with lower and stoichiometric mixtures ($\lambda \geq 1$), while different sets of equations are introduced for each $\lambda < 1$ [77]. The model for internal energy given in kJ per kg of original air for $\lambda \geq 1$ can be found in equation (E.51).

$$u\left(T,P,\lambda\right) = A\left(T\right) - \frac{B\left(T\right)}{\lambda} + u_{corr}(T,P,\lambda) \tag{E.51}$$

In equation (E.51), $A\left(T\right)$ and $B\left(T\right)$ are constants as function of temperature that can be expressed as equations (E.52) and (E.53), respectively.

$$A\left(T\right) = a_1 T + a_2 T^2 + \ldots + a_5 T^5 \tag{E.52}$$

$$B\left(T\right) = b_0 + b_1 T + \ldots + b_4 T^4 \tag{E.53}$$

To calculate the gas constant, the following equation (E.54) were used, which is given in $\left[\frac{kJ}{(kg\ of\ original\ air).\ K}\right]$.

$$R\left(T,P,\lambda\right) = 0.287 + \frac{0.020}{\lambda} + R_{corr}(T,P,\lambda) \tag{E.54}$$

According to Krieger and Borman [83], it is recommended that there should be some correction terms for variables R and u. The correction terms are denoted as R_{corr} and u_{corr}. These parameters are considered for dissociation as they are non-zero variable for temperature greater than 1450 K. Equations (E.55) and (E.56) express the correction factors for internal energy and gas constant, respectively.

$$u_{\text{corr}}\left(T,p,\lambda\right) = c_u \exp(D(\lambda) + E(T,\lambda) + F(T,p,\lambda)) \tag{E.55}$$

$$R_{\text{corr}}\left(T,P,\lambda\right) = C_r \exp\left(r^{\circ}\ln(\lambda) + \frac{r_1 + \frac{r_2}{T} + r_3\ln\left(f_6 P\right)}{\lambda}\right) \tag{E.56}$$

Take note that the temperature and pressure are calculated in Kelvin (K) and bar accordingly. The values of $D\left(\lambda\right),\ \ E\left(T,\lambda\right),\ \ F(T,P,\lambda)$ can be calculated based on the following expressions.

$$D(\lambda) = d_0 + d_1\lambda^{-1} + d_3\lambda^{-3} \tag{E.57}$$

$$E(T,\lambda) = \frac{e_0 + e_1\lambda^{-1} + e_3\lambda^{-3}}{T} \tag{E.58}$$

$$F(T,P,\lambda) = \left(f_0 + f_1\lambda^{-1} + f_3\lambda^{-3} + \frac{f_4 + f_5\lambda^{-1}}{T}\right)\ln(f_6, P) \tag{E.59}$$

The ratio of specific heats is then modeled as equation (E.60):

$$\gamma = \frac{c_p}{c_v} = 1 + \frac{R}{c_v} \tag{E.60}$$

It is important to note that all the values for the coefficients used in equation (E.51) - (E.60) can be found in Table E.2.

Table E.2: Coefficient values [77]

Coeff	Value	Coeff	Value	Coeff	Value	Coeff	Value
a_1	6.92E-01	b_2	-9.50E-05	d_3	-3.71E+00	f_4	1.48E+01
a_2	3.92E-05	b_3	2.15E-08	e_0	-1.50E+04	f_5	1.18E+02
a_3	5.29E-08	b_4	-2.00E-12	e_1	-1.58E+04	f_6	1.45E+01
a_4	-2.29E-11	c_u	2.33E+00	e_3	9.61E+03	r_0	-2.98E-01
a_5	2.78E-15	c_r	4.19E-03	f_0	-1.03E-01	r_1	1.20E+01
b_0	3.05E+03	d_0	1.04E+01	f_1	-3.87E-01	r_2	-2.54E+04
b_1	-5.70E-02	d_1	7.85E+00	f_3	1.54E-01	r_3	-4.35E-01

Based on the conclusion made in literature review section, a curve-fitted polynomial method developed by Krieger and Borman [83] is selected to compute the specific heat ratio for the CR engine modified combustion model.

E.7 Friction Losses Model

The concerns about mechanical friction losses come to mind when deciding to reduce fuel consumption in an engine while increasing its efficiency. As mentioned by Monaghan [107], a maximum of five percent fuel economy could be obtained by a ten percent reduction in friction losses of the engine. It can be stated that the friction losses and the engine speed are directly correlated; with the increment in the speed, the engine friction rises rapidly. This increment not only reduces the engine power output but also the efficiency drops significantly.

The modeling of friction losses can be significantly burdensome with a lack of engine data. They vary significantly between different types of engines that can be commonly introduced through different components such as bearings, pistons, and other driven accessories [25]. Thus, the modeling of friction losses can be a difficult task without a sufficient amount of engine data. Moreover, friction losses can fluctuate based on engine coolant, oil temperature, ambient conditions, and the throttle setting of an engine [25].

To determine Friction-Mean-Effective-Pressure (FMEP) losses, the approach recommended by Blair [99] was adopted with the assumption setting of rolling bearings. This method is useful to estimate the engine performance on a variety of theoretical or actual engines; regardless of the restriction of the model to any particular application. The general linear equations have been used by several researchers including Blair and Heywood [42, 99] to determine FMEP losses as a function of engine speed in rpm and defined by:

$$fmep = a + b(L)(RPM) \tag{E.61}$$

$$FMEP = 250\,(S_{\text{rocker}})\,(N) \tag{E.62}$$

In equation (E.61), a and b are constants, which vary based on the engine type. The letter L is the stroke calculated in meter and N is engine speed $(\frac{rev}{min})$. Equation (E.62) is based on a SI motorcycle engine with rolling bearings.

E.8 Residual Gas Fraction Model

There are always some burned gases that remain inside the cylinder during the exhaust phase of an ICE. These remaining gases that are trapped in the clearance volume are referred to as residual gas. During the intake stroke of an engine, these remainders will be mixed with the new batch of the air-fuel mixture. The fraction of these gases is often defined as [62]:

$$f = \frac{1}{r_c} \left[\frac{P_i}{P_e} \right]^{\frac{1}{\gamma}} \tag{E.63}$$

The compression ratio in the above term is denoted by r_c while γ is the specific heat ratio. The inlet and exhaust gas pressures are represented by P_i and P_e, respectively. To calculate the gas temperature of a four-stroke Otto cycle at the end of the intake valve (before IVC), the equation below was used.

$$T_1 = (1-f)T_i + T_e f \left[1 - \left(1 - \frac{P_i}{P_e} \right) \left(\frac{\gamma - 1}{\gamma} \right) \right] \tag{E.64}$$

In the above equation, the inlet and the exhaust gas temperatures are denoted by T_i and T_e, respectively. According to [25], an assumption of the initial value of *f* is required to find T_1 and *f*. The iteration should be performed till the approximate error is lower than the specific error. The typical values of *f* are between 0.03 to 0.12.

E.9 Summary

This chapter described the numerical description of those parameters and models that have not been explained previously. For instance, in section E.2 the CR engine geometry calculations are presented that includes kinematic and positioning calculations, stroke length, and piston displacement, along with the volume calculations. The obtained heat release model has been described in a detailed manner (see section E.3.4). Additionally, the AFR, friction losses, and residual gas fractions calculations are described.